1973

# Optimization of oxygen transfer into water in a coarse-bubble, diffused aeration system.

Donald S. Mavinic
*University of Windsor*

# OPTIMIZATION OF OXYGEN TRANSFER INTO WATER IN A COARSE-BUBBLE, DIFFUSED AERATION SYSTEM

A DISSERTATION

Submitted to the Faculty of Graduate Studies in partial fulfillment of the requirements for the Degree of Doctor of Philosophy in Civil Engineering

by

Donald S. Mavinic, B.A.Sc., M.A.Sc.

University of Windsor

Windsor, Ontario, Canada.

1973

ABSTRACT

Several modifications of a conventional diffused aeration system have been studied to optimize the transfer of oxygen so that the increasing oxygen demands in the biological treatment of wastewater can be met. All of these modifications are based on the idea of increasing the contact time of the air bubbles in the liquid and thereby increasing the amount of oxygen transferred.

This study was conducted in a closed-loop, coarse-bubble, diffused aeration system, consisting of a 4 in. internal diameter plexiglass U-Tube of height varying from 3 to 9 feet, in 1 foot intervals, and a 4 1/2 x 2 x 1 1/2 ft water recirculating reservoir at the top, also constructed of plexiglass.

Four separate systems of aeration were investigated using tap water as the oxygen absorbing medium. These systems are such that they can be easily adapted to existing conventional aeration tanks. System I was a simple column of water; System II used only diffused air for water circulation, thereby creating an upward, co-current flow of air and water; System III employed pumping for water circulation, with a control on the water velocity such that counter-current, air-water flow was maintained; and System IV used pumping to

circulate water, with the water velocity made large enough to create a downward, co-current flow of air and water. The operating conditions in each system were varied by changing airflow rates, waterflow rates, and water depth.

A circular ring with multiple openings was used as a coarse-bubble diffuser. This diffuser was located at the bottom of one side of the U-Tube in Systems I, II, and III, and near the top in System IV. Additional tests were carried out using commercially-available porous diffusers and the results compared to that obtained with the coarse-bubble ring.

Aeration efficiencies are reported in terms of $E_o$ and $E_p$, where $E_o$ is the rate of oxygen transferred/rate of oxygen supplied, given in per cent, and $E_p$ is the rate of oxygen transferred/power input, given in lb/kwhr. The values for the Overall Transfer Coefficient, $K_La$, in $hr^{-1}$, and the Liquid Film Coefficient, $K_L$, in ft/sec, have also been calculated for different operating conditions in each of the four systems. In addition, the values of $K_La$ have been correlated to airflow rate and water depth, for the purposes of design.

Results of this study indicate that System III is the most efficient system of aeration, both in terms of $E_o$ and $E_p$. The greatly improved performance under this system of aeration is shown to result from the increased contact time between the air bubbles and water during counter-current flow of air and water. Because the pumping of water in

Systems III and IV adds considerable water power to the total power input used in evaluating $E_p$, the presence of favourable conditions, such as availability of natural head in waste-water flow, would produce even higher values of $E_p$ in these two systems. A complete elimination of the high water power input in System IV may prove this system equally or more efficient than System III. As expected, aeration efficiencies were higher when the porous diffusers were used because of the formation of much smaller bubbles.

ACKNOWLEDGEMENTS

The author is extremely grateful to Dr. J. K. Bewtra for his continuous and patient guidance as well as generous aid and constructive criticism throughout the completion of this work. My deep appreciation for this man goes far beyond words.

The author also wishes to express his sincere gratitude to Mr. George Michalczuk, Mr. Peter Feimer, and Mr. Otto Brudy, lab technicians, for very valuable technical assistance and services rendered.

I would also like to thank Dr. J. A. McCorquodale of the same department, who, on many occasions, inherited the role of secondary supervisor to my work. His assistance became invaluable at times. Special thanks also go to my colleague, Dr. H. Ali for his continuous help and encouragement.

Many thanks also go to my wife, Susanne, and to my friends, who persevered with me throughout the completion of my studies. I deeply appreciate their understanding.

Lastly, the author wishes to express his sincere gratitude to the National Research Council who made this work possible.

TABLE OF CONTENTS

LIST OF FIGURES

List of Figures (continued)

List of Figures (continued)

List of Figures (continued)

List of Figures (continued)

List of Figures (continued)

List of Figures (continued)

List of Figures (continued)

## LIST OF TABLES

LIST OF TABLES (continued)

# I - INTRODUCTION

The growing need for minimizing water pollution has, within the last decade, placed a tremendous burden on waste treatment plants to produce effluents of suitable quality. Because of steadily increasing population, especially in urban areas, the amount of domestic wastewater being produced for treatment has risen sharply year after year. Also, industrial effluents have increased both in quantity and diversity, thereby creating additional load on the waste treatment plants, especially where joint treatment is practiced. On top of this has come increased government and public pressure to produce a high quality effluent, free of as much organic and toxic material as technologically possible, before discharging into local bodies of water.

In many instances, the increased loading on wastewater treatment plants has necessitated a change or at least a redesign of one or more of the unit operations comprising the treatment process. When the overloading has been too great, entire waste treatment plants have had to be redesigned to cope with the additional flow.

One of the unit operations most affected by the increased organic load placed upon it has been the biological reactor

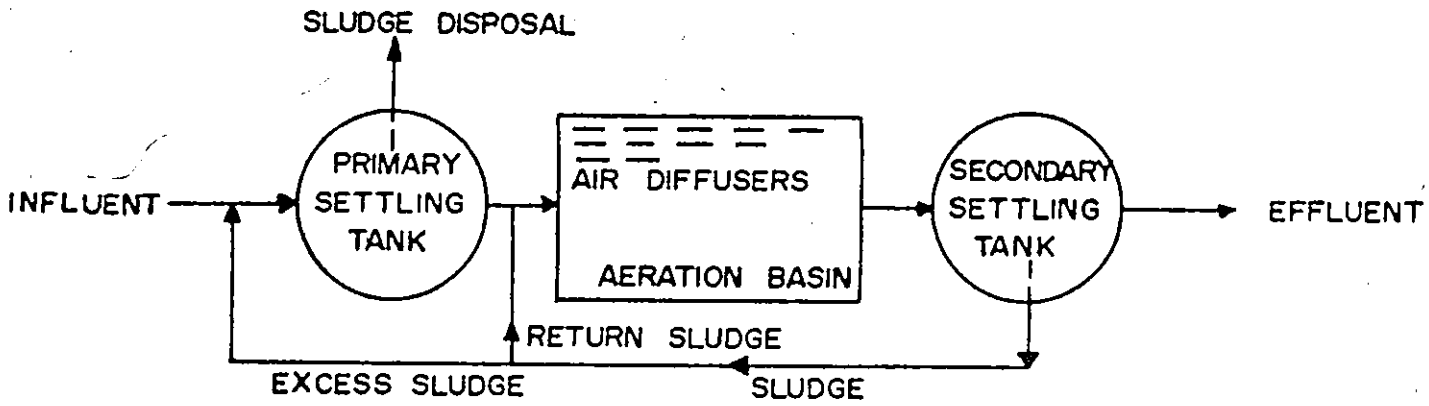


This illustrates the most common use of a typical aeration tank. Aeration of the mixed-liquor supplies oxygen for the aerobic, biological decomposition of organics, production of new bacterial cells, stabilization of certain wastes through oxidation, and mixing of the floc.

FIG. 1 —CONVENTIONAL ACTIVATED—SLUDGE TREATMENT

in the activated sludge process. An important step in this process is to aerate the contents of the reactor, that is, the mixed liquor containing organic matter and bacterial mass, better known as the activated sludge floc. In addition to supplying oxygen for aerobic, biological decomposition of organic matter, aeration also provides mixing to keep the floc in suspension and directly oxidizes certain types of wastes to a more stabilized form. Thus, it is responsible for the production of new bacterial cells to keep the process going. The overall process is illustrated in Figure 1, (1).

There are various methods of supplying oxygen to this aeration basin but two most common means are by mechanical or surface agitation and by diffused bubble aeration. The latter can be further divided into fine-bubble or coarse-bubble diffusion. However, despite higher efficiencies generally associated with fine-bubble diffusers, they have limitations in practice due to their tendency to clog, both internally from the impurities in compressed air and externally from the wastes in the aeration basin.

The coarse-bubble diffusion process, commonly employed in activated sludge treatment plants, has been the object of many extensive investigations with the purpose of improving the transfer of oxygen into wastewater. The process itself involves the diffusion of air, in the form of bubbles, through small openings, into the liquid. These openings or outlets are usually located near the bottom and along one side of the tank, as illustrated in Figure 2, (2), (3). Because of

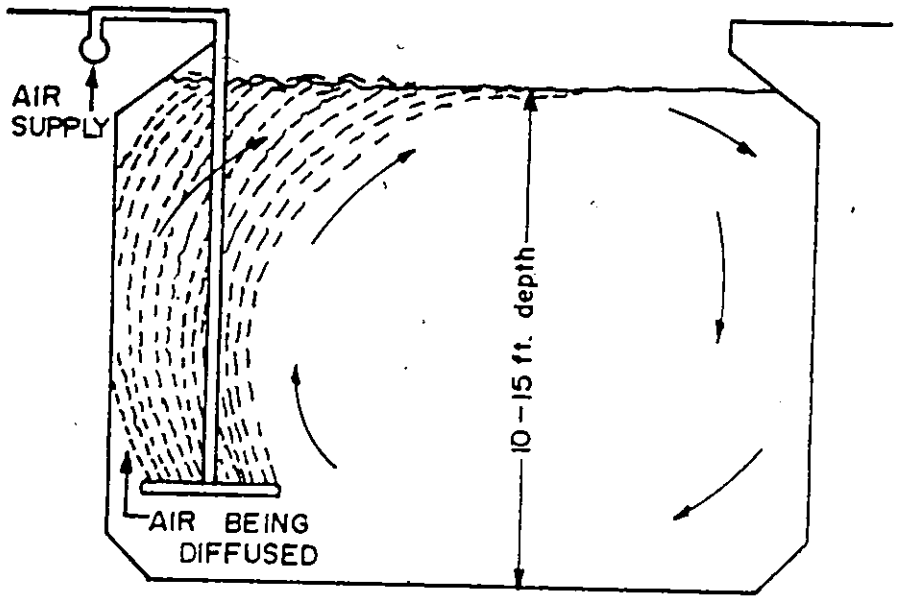


Note: Flow is perpendicular to the cross-section – the moving spiral velocity is in the order of 1/2 ft./min. in a conventional system ∴ very slow longitudinal movement of tank contents.

FIG. 2 – CROSS-SECTION OF A TYPICAL DIFFUSED-AIR, SPIRAL-FLOW, CONVENTIONAL ACTIVATED-SLUDGE "AERATION TANK."

the resulting low density of the air-water mixture above the air-outlets, as well as the direction of liquid flow, a rising, circulating spiral motion of the mixture results throughout the entire tank. This circulating motion keeps the activated sludge floc in suspension and the air bubbles provide the necessary oxygen needed by the biological suspension in the system. However, this type of motion also increases the overall rising velocity of the air bubbles, thereby decreasing their contact time in the liquid.

Although there are many factors or parameters affecting the efficiency of this type of operation, the key to obtaining maximum oxygen transfer efficiency is the contact time of the air bubbles in the liquid. If the air bubbles can be held in contact with the liquid for extended periods of time, then higher efficiencies should be expected from the system. Since the cost of compressing air constitutes the largest portion of operating costs in an activated sludge system, any method that can produce higher transfer efficiencies and thus improve the aeration process would certainly reduce these operating costs.

With this motive in mind, the present study was undertaken to optimize the transfer of oxygen into water, using a coarse-bubble, diffused-aeration system, and to explore the various factors affecting that transfer. Various aeration systems have been investigated and a method for their application to existing aeration basins has been suggested.

# II - LITERATURE REVIEW

## A. "Two Film" Theory of Gas Transfer

The well-known "Two Film" theory of gas transfer was first developed by Lewis and Whitman in 1924 (4). Later, in 1952, it was adapted and revised by Ippen et al. (5) for the computation of oxygen absorption rates in water. This theory can best be described by considering the sketches in Figure 3.

The gas passes through the two films by the slow rate of molecular diffusion. This mass transfer by diffusion occurs between the two phases by a "driving" force, which is a partial pressure gradient in the gas phase and a concentration gradient in the liquid phase. In the case of a gas of low solubility, like oxygen in water, the gas film offers very little resistance as compared to the liquid film. Therefore, $P_i \approx P_g$. Hence, it may be assumed that the concentration of oxygen in solution at the interface is that of saturation and that the entire resistance to the passage of oxygen into the water is due to the liquid film, i.e., $C_i \approx C_s$ = saturation concentration of dissolved oxygen at the partial pressure, $P_g$ (6).

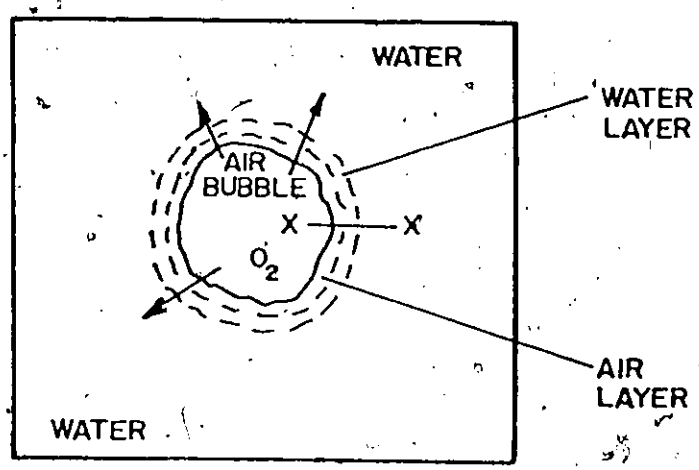


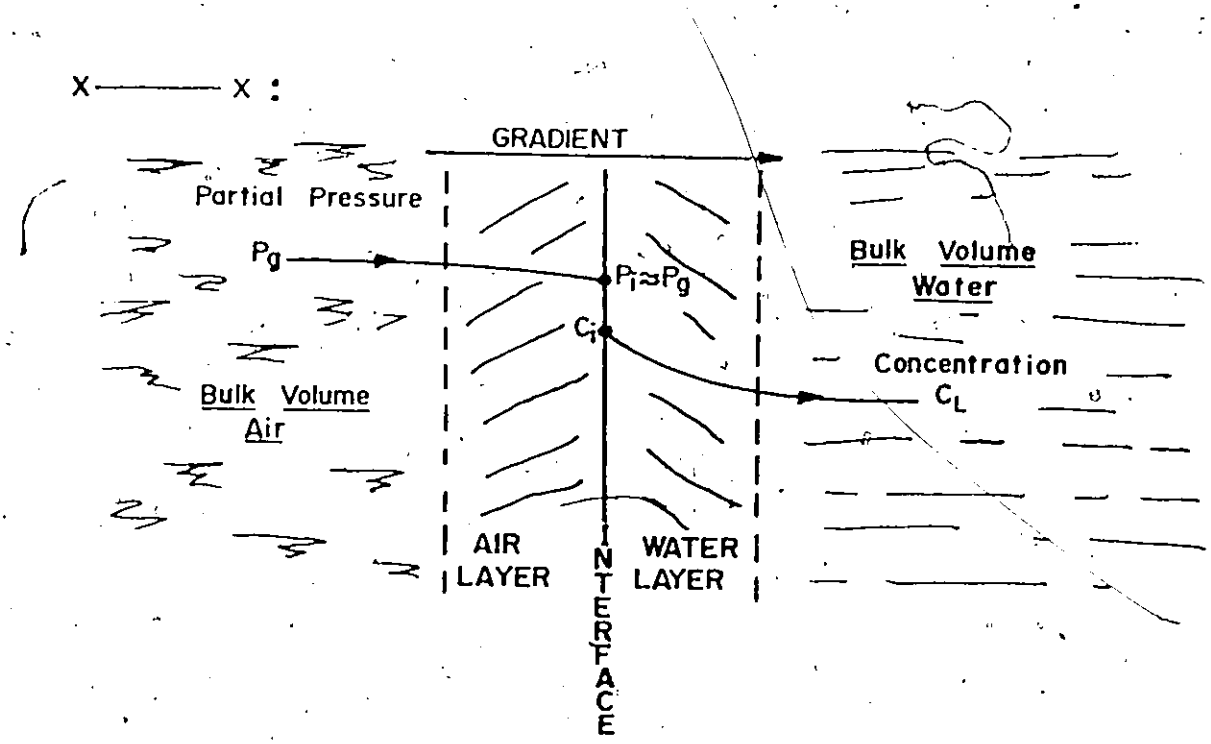


FIG. 3 — MASS TRANSFER OF OXYGEN INTO WATER - "TWO FILM" THEORY

Two assumptions are necessary to justify the use of this theory:

(i) $P_g$ is the same throughout the entire bulk volume of air, i.e., oxygen is completely mixed in the gas stage.

and (ii) Beneath the liquid film, the oxygen in solution is mixed with the main body of the liquid at such a rate that the concentration is constant throughout, i.e., $C_L$ is the same in the bulk water (7).

B. Basic Mathematical Expression of Oxygen Transfer

The relationships developed by Ippen et al. (5), in accordance with the "Two Film" theory, were first presented as:

Rate of mass transfer due to diffusion

$$= \frac{dm}{dt} = \frac{D_L}{y_L} A (C_i - C_L) = \frac{D_g}{y_g} A (P_i - P_g)$$

$$= K_L A (C_i - C_L) \quad \ldots\ldots\ldots\ldots\ldots\ldots\ldots\ldots\ldots\ldots \quad 1$$

(because the resistance in the gas phase is negligible as compared to the liquid phase)

where $\frac{dm}{dt}$ = Time rate of mass transfer by diffusion.

$D_L$ = Diffusion coefficient for oxygen in water or molecular diffusivity of the gas through the

liquid film.

$D_g$ = Molecular diffusivity of the gas through the gas film.

$y_L$ = Hypothetical liquid film thickness.

$y_g$ = Hypothetical gas film thickness.

A = Interfacial or absorbing area.

$K_L$ = Liquid Film Coefficient .

This mass equation may be expressed in concentration units by introducing the volume of liquid, V.

Thus, $$\frac{1}{V}\frac{dm}{dt} = \frac{dc}{dt} = K_L \frac{A}{V}(C_i - C_L)$$

$$= K_L a (C_i - C_L) \quad \ldots\ldots\ldots \quad 2$$

where $K_L a$ is an Overall Transfer Coefficient.

Therefore, $$\frac{dc}{dt} = K_L a (C_i - C_L) \quad \ldots\ldots\ldots\ldots \quad 3$$

Despite many modifications and supplements made to the above theory (8), this form of the equation is still widely recognized and has been a basis for more detailed investigations of modern aeration practices.

## C. Factors Affecting the Rate of Oxygen Transfer

Important factors affecting the rate of oxygen transfer into wastewater in diffused aeration systems are (9), (10), (11), (12):

(i) Oxygen concentration gradient, i.e., the deficit or driving force $(C_i - C_L)$.

(ii) Temperature of the liquid: affects both the oxygen saturation concentration, $C_s$, and the overall transfer coefficient, $K_L a$.

(iii) Turbulence in and around the gas-liquid interface, i.e., the rate of liquid-surface renewal.

(iv) Waste characteristics of the liquid: generally reported in terms of $\alpha$, where

$$\alpha = \frac{(K_L a) \text{ waste}}{(K_L a) \text{ water}}$$

(v) Depth of liquid: the partial pressure increases with depth, thereby affecting both the saturation concentration, $C_s$, and thus the driving force $(C_i - C_L)$ and also the bubble size.

(vi) Contact time of the bubble in the liquid.

(vii) Size of air bubble: governs the amount of interfacial or absorbing area per unit volume through which diffusion occurs.

(viii) Rate of airflow: this directly affects
  (a) the bubble size
  (b) the total interfacial area available for diffusion

(ix) Type of diffuser: this governs the bubble size.

(x) Position of the diffuser: this influences the contact time of the bubble in the liquid.

(xi) Tank geometry: primarily influences mixing conditions and circulating velocities.

## D. Previous Investigations Associated with Oxygen Transfer Efficiency

A voluminous amount of literature exists on aeration and the factors associated with the transfer of oxygen into water. The prime concern of these investigations was the specific attempts to increase the oxygen transfer efficiency, employing diffused aeration to improve the process of oxygen transfer, thereby reducing the high costs associated with this unit operation. Surprisingly, the last fifty years or so have produced only a handful of direct efforts to improve the oxygen transfer operation, even though it continues to be a major expense. Instead, most of the research has been directed toward the theoretical approach to the evaluation of various parameters surrounding the mathematical description of the "Two Film" Theory and its various modifications and

corollaries.

One of the earliest attempts to investigate the factors which influence the efficiency of aeration was made by Eckenfelder (13). Working with an experimental aeration tank and employing an agitator and air sparger ring, he noted that the depth of submergence had a very large effect on the overall efficiency of the aerating system. The transfer efficiency had increased as the depth increased. However, the power required had also increased approximately linearly with increasing depth. He, therefore, concluded that a balance must be arrived at between power saving by increased transfer efficiency and power increase due to increased depth.

Carver (9), also, had observed the influence of depth on transfer efficiency. Employing a Venturi diffuser for discharging bubbles into a six inch lucite column filled with water, he noticed that for a given bubble size, the percentage absorption increased linearly with column height. He attributed this behaviour to the increased retention time of the bubbles in the aeration column.

Morgan and Bewtra (14), while conducting tests in a 4 foot long section of a conventional spiral flow aeration tank, 24 feet in width and 15.5 feet in total depth, concluded that the rate of oxygen transfer for a given airflow rate was proportional to the diffuser submergence and that it made little difference whether the change of submergence was accomplished by changing the depth of water in the tank

or by changing the elevation of the diffusers in the tank. This study was conducted both with Saran tubes, producing fine bubbles, and spargers, producing coarse bubbles.

Bewtra and Nicholas (15), working on the same tank and using the same type of diffusers, also found that the rate of oxygen absorption per unit of power input increased with a decrease in submergence depth, although the differences in values obtained with spargers could be considered negligible. This observation directly supports the earlier suggestion of Eckenfelder (13) on the need for a balance between increased transfer efficiency and power increase as a function of depth.

Since the individual influence of diffuser submergence and bubble retention time is inseparable in most studies, both factors have been considered simultaneously in the development of the U-Tube concept of transferring oxygen to water. In 1958, the first U-Tube operation was reported by Bruijn and Tuinzaad (16) from the Netherlands. The purpose of this system was to dissolve as much oxygen into the water as possible with the least possible energy input. Their concept arose from experiments conducted at an independent Dutch research institute on a U-shaped tube, 3.2 inches in diameter, mounted vertically, with one stem being a 44 foot long downdraft tube and the other stem being 9.5 feet shorter. The diffuser was located at the top of the tube. Since the solubility of oxygen in water increases approximately linearly with the pressure, the oxygen transfer efficiencies obtained

were much higher due to the pressure increase and the longer contact time of the downward travelling bubbles. Bruijn and Tuizaad, noting this two-fold effect on bubbles travelling down a deep column of water, modified the original U-Tube and developed a system whereby an air-water mixture travelled vertically down a central 2 foot pipe and exited at the bottom into an outer 5 foot pipe, with the mixture now travelling upwards. Depths of 14 to 50 feet were studied and, as expected, transfer efficiency improved with an increase in depth. Also, in comparison to three other common aeration systems, the deeptube aerator exhibited the least energy requirements, thus cutting down on power costs. In addition to its higher efficiency, this type of aeration system was considered to require (i) less space, (ii) less supervision, (iii) virtually no maintenance and (iv) low construction cost.

The U-Tube concept was developed further by Speece et al. (17), using tap water, various size bubble dispersers, and a 40 foot deep chamber, separated into downflow and upflow segments by a shorter baffle. The air disperser was located near the top of the system, in the downflow segment. They observed that, in addition to the increased contact time of the downward flowing bubbles, U-Tube aeration is a gas transfer process which provides temporary pressurization of a gas-liquid mixture by means of a temporary hydrostatic head. This pressurization causes an increase in the dissolved gas deficit and thus an increase in rate of gas transfer. In

addition, power requirements for air injection are low because air is injected at shallower depths. Their experimental results indicated that minimum diffuser submergence, increased air-water ratios, and increased U-Tube depths gave maximum oxygen transfer economy within the limits of the study. Speece concluded that the U-Tube aerator, with its capacity to dissolve 3000 lb. oxygen/day/1000 ft.$^3$, as compared to about 500 lb. of oxygen/day/1000 ft.$^3$ for turbine aerators and 250 lb. of oxygen/day/1000 ft.$^3$ for simple diffused-air aerators, provided an attractive alternative means of aerating water and wastewater. Thus, he recommended it as the most economical aeration system available for saturating water. He has also stated that the oxygen transfer economy and the capital cost of U-Tube type oxygenation systems appear to be competitive with conventional aeration systems, which can only transfer oxygen economically to waters with low dissolved oxygen concentrations. However, it must be kept in mind that he used an operating depth of 40 feet, more than twice as large as conventional aeration tanks, and thus not very practical for adaption in existing treatment plants.

Speece (17) has further observed that if sufficient hydraulic head were available, the water could be caused to drop free-fall into the inlet of the U-Tube, thus entraining air bubbles in this fashion and negating the need for any external power requirement. This would be especially desirable for stream reaeration in remote areas with no power available

and would be a more practical application of this system because of the depths involved. In fact, in their recent publications, Speece (18), (19) and Thackston and Speece (20), have recommended the adaption of the U-Tube concept in reaeration of flowing streams, hypoliminions of lakes and reservoirs, and dam impoundment releases. The system would be especially attractive during the summer season when oxygen deficiency is at its most critical stage. Thackston et al. (20) further comment that, since U-Tubes are much more efficient than any other method in use today in flowing streams, this system possibly could be applied to larger streamflows by constructing a deep trench and forcing all or a fraction of the flow to pass under a deep baffle after diffused air has been introduced. This could also be used in aerating wastewater treatment plant effluents and impoundment discharges. Speece (19) also has suggested that, in hypolimnion aeration, oxygen transfer from the bubbles in a U-Tube is about double that for high-pressure air injection at the bottom of an impoundment of equal depth, because the path of the bubbles in contact with the water is doubled. He further supports his contentions by illustrating a proposed installation.

Most recently, the Rocketdyne Corporation (21) and the U.S. Environmental Protection Agency (22) have studied the U-Tube concept and its possible applications and both have given favourable reports on its oxygen transfer ability. The EPA has suggested its use in post-aeration of treatment plant effluents and has determined that, under gravity

conditions where natural head is available, the U-Tube concept is likely to be the cheapest of all aeration devices currently on the market.

From the above-mentioned description, it is evident that the most important factor in improving the oxygen transfer efficiency is the contact time of the air bubble. If the bubble can be kept in contact with the water for a longer period of time, then more oxygen will be transferred to that water. In addition to the studies discussed above, several other investigations also have been directed toward increasing the contact time of the air bubbles. King (23), in 1955, while discussing the mechanics of oxygen transfer in conventional spiral flow aeration tanks, commented that if the velocity of the overturning current is more than what is necessary to produce adequate mixing, then this velocity should be reduced in order to increase the bubble retention time in the liquid and thereby improve the absorption efficiency. Lamb (24) also has mentioned that the velocity of the air bubble, which is the vectorial sum of its terminal velocity of rise and the velocity of the air-water mixture, has an important effect on oxygen transfer. In conventional spiral flow tanks, the velocity of this air-water mixture is appreciably high, and thus the detention time of the air bubbles is reduced. He has suggested that an improvement can be made by spreading the diffusers uniformly over the entire tank bottom, thereby reducing the velocity of the air-water mixture, and consequently increasing the contact time and

oxygen transfer efficiency. Pasveer (25) also has noted that in the conventional systems, the air bubbles enter the water stream, which possesses a rising rate 2-3 times as great as that of the air bubble and as a result, the contact time of the air bubble is reduced to only 1/3 - 1/4 of the expected value. In a tank 10 feet deep, this amounts to only 3-4 seconds instead of 10-12 seconds. Therefore, the oxygen transfer is only 1/3 - 1/4 of what could be achieved otherwise.

This line of reasoning led Pasveer and Sweeris (25), (26) to a totally different approach to increasing the bubble contact time, that of a horizontal-flow, diffused-air system. They reasoned that the conditions for upward flow of the mixed liquor of a conventional system would not prevail in this arrangement. According to them, the time of contact of the air bubble in the horizontal-flow, diffused-air system, is determined by the self-velocity of ascent of the air bubble and the height of the water column and thus would have more or less the same value as if the air bubble ascended in a column of quiescent water. They experimented with a ring-shaped aeration tank (oxidation-ditch type) having diffusers along the bottom, with 272 cm of water above these diffusers and variable horizontal velocity of flow. The results indicated that the efficiency of aeration in the horizontal-flow system was 2 to 2.5 times that of the vertical or spiral-flow system with the same water depth. They concluded that only 40% of the length of the porous tubes and only 40 per cent of the volume of air and of the energy,

needed in the spiral-flow system, must be supplied. Increasing the horizontal flow velocity also showed an increase in oxygen transfer efficiency, since the bubbles were carried downstream further, thereby increasing their contact time. Further work on the horizontal flow concept was carried out by Danjes in Munich, in 1965, (25), using a fine-bubble, horizontal-flow system, strategic baffling to increase relative water velocities, and tap water. Results similar to those of Pasveer and Sweeris were obtained.

More recently, Speece (18), (19), (27) investigated another approach to increasing the transfer efficiency by increasing the detention time of the air bubbles. He employed an aeration chamber with expanding cross-section and water moving downward. The entrance and exit velocities were such that the air bubbles were entrapped in this inverted cone and provided prolonged contact time and subsequently an increase in oxygen transfer. He has called this system the Downflow Bubble Contact Aeration or DBCA system of aeration. The author notes that it has the dual advantage of being able to efficiently absorb oxygen into the water while simultaneously stripping dissolved nitrogen from it. The key to its operation is the fact that the water velocity at the entrance is designed to be higher than the buoyant velocity of the air bubbles to keep them from escaping at the top, while the exit water velocity is designed to be lower than the buoyant velocity of the bubbles so they are not swept out at the bottom. Results of experiments with

pure oxygen rather than air have indicated about 90% of the oxygen is absorbed from the bubbles, before wasting, and that about 1.0 mg/l of dissolved nitrogen is stripped for every 3.5 mg/l of dissolved oxygen absorbed. Speece mentions that although the increase in oxygen transfer efficiency in the DBCA system is primarily due to the indefinite period of bubble contact time with water inside the expanding hood, filling of this chamber with bubbles also provides a high ratio of bubble interfacial area to water volume. Also, there is considerably high turbulence and this results in much higher gas transfer rates. Because of these reasons, Speece has recommended its possible use in the aeration of oxygen deficient rivers, dam impoundment releases, lake hypolimnions, and fish hatchery tanks, as well as conventional activated sludge mixed-liquors. He concludes that the DBCA system offers a very efficient method of transferring oxygen because simplicity and low energy input result in considerable savings toward capital and operating costs.

Another important factor having significant influence on oxygen transfer is the bubble size. Since smaller bubbles have smaller terminal or rising velocities (9), (23), (28), they have increased detention times in the liquid. King (23), in quoting the work of Scouller and Nixon (29), commented that, under the same conditions of temperature and dissolved oxygen content in a water column, the rate of oxygen transfer varies inversely with the diameter of the air bubble. Carver (9) also has stated that bubbles in the range of

0.1 - 0.6 mm. radius and greater than 4.0 mm. radius exhibit increasing terminal velocities with an increase in bubble size. Thus, for a given gas flow rate the rate of absorption decreases not only due to a loss in retention time but also due to a reduction in bubble surface area when larger bubbles are employed. Pasveer (28), while discussing the importance of the rapid rate of surface renewal around the bubble for efficient oxygen transfer, has stated that in the case of smaller air bubbles, the degree of renewal of the interfacial surface is definitely less. However, he has concluded that, because of the high value of interfacial surface area to bubble volume when smaller bubbles are used, the transfer of oxygen is far more rapid than in the case of larger air bubbles. This conclusion has been accepted by most of the people involved with aeration research.

Eckenfelder (12), in his discussion of the various factors affecting the aeration efficiency of sewage and industrial wastes, has mentioned that by dividing the larger bubbles into smaller sizes by tank turbulence alone, the surface area to bubble volume ratio can be increased, thereby increasing the transfer efficiency. Morgan and Bewtra (30), while conducting tests on a full scale aeration tank, observed that better transfer efficiencies were obtained when bubble shearing devices were used along with coarse-bubble spargers. These devices, located near the point of air introduction into the tank, were used to create smaller air bubbles, thereby increasing both the bubble-liquid

interfacial area and the liquid turbulence. This resulted in increased oxygen absorption rates and improved aeration efficiencies. The comparative values of 6% for spargers alone, and 8% for shear box or venturi with spargers were reported.

In his discussion of a paper presented by Dobbins (8), Burrough accepted the improved transfer efficiency commonly associated with fine-bubble or porous diffusers but pointed out the problem of diffuser clogging, when used in conventional activated sludge tanks. He stated that partially clogged porous diffusers could lose up to 20 per cent of their clean-tube diffusion ability and consequently, many plants have changed to coarse-bubble spargers to eliminate clogging and high maintenance cost at some sacrifice in transfer efficiency. Pasveer (25) also expounded on this problem of clogging associated with small-bubble diffusers. He commented that, despite several advantages associated with the use of smaller bubbles, the risk of clogging is very great, inspite of advanced technology in this field. More recently, the U.S. Environmental Protection Agency (22) has stated that the fine-bubble diffuser system is more efficient and cheaper to operate, but represents a greater capital investment and a costlier maintenance problem than a coarse-bubble diffuser system. The costlier maintenance is associated with the periodical removal and cleaning of the clogged fine-bubble diffusers.

Another important factor influencing oxygen transfer efficiency and closely related to bubble size and contact time is the rate of air supply to the system. Carver (9) found that, whether using compressed air or pure oxygen, increasing the gas flow rate caused a decreasing trend of oxygen absorption. This reduction in the oxygen transfer rate with increasing airflow rate was attributed to the production of larger bubbles with greater frequency at higher airflow rates, thus resulting in a greater concentration of bubbles vertically above the diffusers. He has further stated that the entrainment of liquid in the wakes of the ascending bubbles created an upward motion of liquid, or so-called "chimney" effect, which increased in intensity with increasing airflow rate and resulted in a reduction of the lateral diffusion of dissolved oxygen.

Eckenfelder (12) also observed that, for most types of diffusers, the efficienoy decreased as the airflow increased. He has stated that the mean diameter of air bubbles produced at any airflow rate could be shown to be a direct exponential function of that flow rate. However, he also has mentioned that, in cases where nozzle-type spargers are used with high airflow rates, increasing airflow rates and tank turbulence tend to redivide the larger bubbles into smaller sizes, thereby increasing both the surface renewal rate and the bubble surface area to volume relationship (6), (12), (31). Under these conditions, the transfer efficiency actually may increase with increasing gas rate. This phenomenon, however,

was related to tank geometry and the location of the diffuser unit. Therefore, Eckenfelder has emphasized the importance of relating absorption efficiency to actual tank conditions. Bewtra et al. (14), (15), (30), working with a full-scale aeration tank, reported that for Saran porous diffusers, reducing the unit rate of airflow resulted in an improved efficiency, whereas with spargers, only an insignificant difference existed.

In efforts to improve aeration efficiency, the effects of size and spacing of diffusers with respect to the tank have also been investigated. King (23), (32), in his experiments on spiral flow aeration tanks, reported that, for normal working depths, the diffuser plate area should be as large as economical and practical, taking into consideration such factors as costs, the problems involved in the distribution of air to the diffusers, and the limitations of diffuser area as related to the minimum circulating velocities necessary for adequate mixing. He concluded from his tests that the rate of oxygen transfer increased about 8% when the diffuser plate area was increased from 5 to 10 per cent with all other conditions remaining the same. He also indicated that improved absorption efficiency should result if the porous plate diffusers were set in rows further from the wall and also spaced farther apart, instead of setting them in a row along one side close to the tank wall. The reason for the increased efficiency is the decrease in velocity of the rising liquid just above the diffusers and therefore, longer retention time

of the air bubbles.

Bewtra (11), (15), (33) also investigated the effects of diffuser size and spacing in a full-scale aeration tank. Results showed that a wide band of diffusers gave a greater oxygen transfer than a narrow band, for the same airflow rates. Also, an appreciable increase in oxygen transfer values was observed when the diffusers were moved away from the side wall of the tank. He attributed this to full expansion of the air-water mixture stream and hence lower rising velocities. Bewtra and Nicholas (15) further concluded that, as the area covered by air diffusion is increased, the peak efficiency is reached at comparatively lower airflow rates. This again indicates that the uniform distribution of air diffusion over the entire tank bottom reduces the velocity of air bubble rise and thereby increases the oxygen absorption. Pasveer (34) also has suggested that the entire bottom of the aeration tank should be provided with diffusers to improve the transfer efficiency. He has attributed the improvement largely to the absence or decrease of vertical circulation.

Similarly, the effects of tank geometry and bubble entrainment on transfer efficiency have been investigated extensively. The majority of research in this area has been conducted by Morgan, Bewtra and Nicholas (14), (15), using a 4 foot long section of a full-scale aeration tank. However, Morgan and Bewtra (30), also compared oxygen absorption in a two-column aeration tank representing conditions in a conventional spiral flow system, with that in a single-column

tank. They observed that efficiencies in the two-column unit were only about 60% of those in the single-column unit, under otherwise similar conditions. Violent turbulence, bubble breakage, and rapid surface renewal in the confined column were cited as the reasons for the increased transfer efficiency. Although realizing that the single-column efficiency could not be readily duplicated in a large aeration tank, they mentioned that this comparison did indicate the tremendous effect of tank geometry.

Morgan and Bewtra (14) also investigated the effects of tank geometry in the full-scale tank by dividing the 24 foot wide test unit into two 12 foot wide units, so that each half was equivalent to a tank 4 ft x 12 ft x 15 ft deep. To maintain the same ratio of airflow to water volume, one diffuser in the 12 foot tank was compared to two diffusers in the 24 foot tank. Although absorption efficiencies were similar at low air flows, higher airflows showed significantly higher transfer efficiencies due to the greater bubble carry-over or entrainment in the smaller tank. Bewtra (33) later concluded that the number of air bubbles entrained in the downward moving water in the spiral flow tank increases as the ratio of the width of the air-water mixture stream to the effective tank width is increased. This increase in air bubble entrainment results in increased contact time and thus increased oxygen absorption. He has explained that the air bubble is entrained and carried downward by the liquid stream whenever the natural buoyant force acting on the air

bubble is overcome by the drag force due to the circulating velocity of the liquid. This circulating velocity, in turn, is greatly affected by the tank geometry (11).

Bewtra and Nicholas (15) further studied the effect of tank width on oxygen absorption efficiency by testing a wide band diffuser system in tank widths of 8, 12, 16, and 24 feet. The results showed that the per cent oxygen absorption increased as the aeration tank width decreased and the values for the fine-bubble Saran tubes were higher than for the coarse-bubble spargers. They indicated that, as the aeration tank width is decreased, a larger per cent of the air bubbles reach the zone of downward-moving water and are entrained and carried toward the tank bottom. This entrainment prolongs the bubble detention time and thus increases the transfer efficiency.

The influence of circulating velocities within the tank has already been mentioned in the above presentation. However, Bewtra (33) has stated that the overall velocity of an air bubble in the aeration tank is the vectorial sum of its terminal velocity and velocity of the air-water mixture within the aeration chamber. Any attempt to reduce the air-water mixture velocity would certainly increase the bubble detention time and therefore the oxygen absorption. Bewtra and Nicholas (15), in working with a full scale tank, demonstrated mathematically that increasing the velocity of the air-liquid has a two-fold effect in the aeration tank. It not only decreases the transfer of oxygen but also decreases the usable energy induced to the liquid. Therefore, they concluded that, for

effective aeration, the circulating or air-liquid mixture velocity should be maintained at the minimum value required to keep the biological floc in suspension. The authors (15) also quoted Alani's work on a two-column aeration tank, which demonstrated that the percent oxygen absorption was inversely proportional to the circulating velocity throughout the tank, the latter being related to the airflow rate. Alani had admitted that the conditions in a two-column tank were not identical to those in a full-scale aeration tank because of the boundary walls present around the rising air-water stream, but he expected a similar trend for the effect of water velocity on oxygen absorption. More recently, Mavinic (10), (35) verified the work of Alani in a two-column tank and reported that both the oxygen transfer efficiency and unit power efficiency decreased as the circulating velocity through the columns increased.

Agitation, boundary layer turbulence, and high oxygen deficits, although important factors influencing oxygen transfer efficiencies, surprisingly have been given very little consideration. Of course, the effects of turbulence, etc., are indirectly included with many other factors but these variables have not been investigated separately to any great extent. Eckenfelder (13) and Barthelemew (36) have noted that the intensity of agitation and turbulence have a profound effect, both on the aeration efficiency and the process efficiency in general. The sludge cells tend to clump together and this results in a decrease in the quantity of

oxygen transferred to them due to an increase in resistance to oxygen transfer. Higher agitation tends to break up these clumps and therefore increases the oxygen transfer rate to the cells for the metabolism. Pasveer (25) has commented that, for the acceleration of the solution of oxygen in water, not only should there be a boundary layer at the water-air interface as large as possible and an oxygen deficit as large as possible, but also a rapid renewal of that boundary layer by means of a continuous supply of new water layers from the bulk volume of water. Thus, all of these factors are of importance in achieving higher aeration efficiencies. Eckenfelder (12) has also stated that waste treatment aeration tanks should be maintained at about 2.0 ppm dissolved oxygen in the mixed liquor. This, therefore, assures a high oxygen deficit or driving force, which increases the transfer rate, while simultaneously maintaining aerobic conditions in the system.

While reviewing the effect of turbulence and rapid surface renewal, it is also worth mentioning the various attempts made to improve the aerating devices for obtaining better oxygen transfer. Eckenfelder (9), (12) has discussed a number of different aeration devices used to improve transfer efficiencies, through generation of smaller bubbles and larger velocity gradients. These include turbine aerators, jet aerators, disc-type units, and impingement aerators. The impingement aerator employs a liquid stream, air-lifted from the aeration tanks, as a shearing device for air bubbles

discharged from a large orifice and results have shown that transfer efficiencies increase linearly with the quantity of impingement-liquor flow through the air-lift pumps (9).

Morgan and Bewtra (30) conducted experiments with a hydraulic shear box and venturi-diffuser in their full-scale aeration tank. Their results indicated that the increased bubble-liquid interfacial area and liquid turbulence created by these devices resulted in improved oxygen transfer efficiencies. Thackston and Speece (20) have mentioned another possible method of improving aeration, known as "pressure injection", and currently in trial use in Great Britain. In this system, a small amount of the total volume of water is compressed and air is mixed with it until the water is supersaturated. When this supersaturated water rejoins the main flow, the excess air comes out of solution as very small bubbles, which rise through and aerate the rest of the water. It is claimed that this method is more effective than any other means of aeration. Recently, Speece et al. (17) have tried using pure oxygen in conjunction with the U-Tube system and have reported that change in dissolved oxygen levels are about five times as large as when air is used. In the last few years, more consideration is being given to the replacement of compressed air with commercially available pure oxygen.

Most of the research, discussed above, has been conducted either to expound upon the factors affecting oxygen transfer in a diffused aeration system or to improve or

increase the oxygen absorption efficiency in that system. The present study was undertaken to economically optimize the transfer of oxygen into water, in a coarse-bubble, diffused aeration system.

## III - METHOD FOR COMPUTING THE TRANSFER OF OXYGEN INTO WATER

All computations in this study are based on Lewis and Whitman' "Two Film" theory of gas transfer (4). In measuring oxygen transfer rates, a quantity of water was first deoxygenated until the dissolved oxygen was reduced to approximately zero. Then the aeration was started and the rate of oxygen uptake was determined, using the following relationship described earlier:

$$\frac{dc}{dt} = K_L a\ (C_i - C_L) \quad \ldots\ldots\ldots\ldots\ldots\ldots\ 3$$

or

$$\frac{dc}{dt} = \frac{10^6}{W} K_L A\ (C_i - C_L) \quad \ldots\ldots\ldots\ldots\ldots\ 4$$

in which, $\frac{dc}{dt}$ = Rate of change of dissolved oxygen concentration in the liquid, mg/l/hr

$K_L a$ = Overall Transfer Coefficient, $hr^{-1}$.

$K_L$ = Liquid diffusion coefficient, lb. oxygen per hour per $ft^2$ per unit concentration difference in mg/l.

$A$ = Interfacial or absorbing area, $ft^2$.

$W$ = Weight of water in the aeration system, lb.

$C_i$ = Equilibrium concentration of oxygen at the phase interface, mg/l. It is assumed to be the saturation value at mid-depth over diffuser.

$C_L$ = Concentration of oxygen in the liquid at time t, mg/l.

Upon integration, the equation becomes,

$$\log_{10} \frac{C_i - C_o}{C_i - C_L} = \frac{10^6}{2.30W} K_L A t \quad \ldots\ldots\ldots 5$$

where, $C_o$ = Initial concentration of oxygen in the liquid, mg/l. For plotting purposes, the axis is adjusted so that $C_o = 0$ at t=0; thus $(C_i - C_o) = C_i$ = the saturation at mid-depth over diffuser.

and $(C_i - C_L)$ = Oxygen saturation deficit in the liquid, mg/l.

By plotting $\frac{C_i - C_o}{C_i - C_L}$ vs. time on semi-log paper, the value of $\frac{10^6}{2.30W} K_L A$ was found from the slope of the plotted values. This procedure is illustrated in Figure 4.

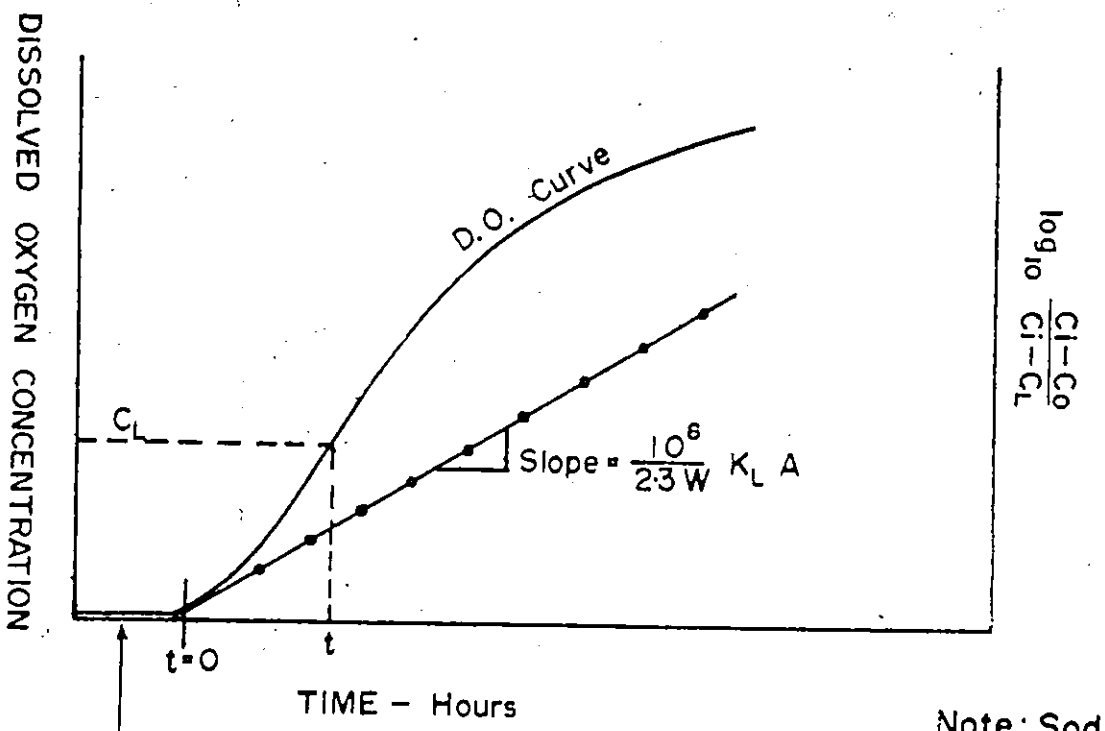


lag portion = $Na_2SO_3$ being used up- then, $[O_2]$ begins to increase

Note: Sodium sulfite, $Na_2SO_3$, used to deoxygenate water initially–

$2Na_2SO_3 + O_2 \longrightarrow 2Na_2SO_4$

FIG. 4 – OXYGEN UPTAKE RATE IN WATER

Therefore, $\frac{dc}{dt} = \text{slope} \times 2.30 \times (C_i - C_L)$ ..... 6

If $C_L$ is taken as zero, then dc/dt is the rate of oxygen absorption into the water in mg/l/hr at zero dissolved oxygen. Then,

$$\frac{dc}{dt} = \text{slope} \times 2.30 \times C_i \quad \text{..... 7}$$

The value of $C_i$, calculated at mid-depth of vertical travel of the bubble from the diffused air outlet, is obtained from $C_s$, the saturation concentration of dissolved oxygen at water temperature and atmospheric pressure, after correcting for actual pressure in water according to the following equation given in STANDARD METHODS (37),

$$C_i = C_s \frac{P - p}{760 - p} \quad \text{..... 8}$$

where $C_s$ is the solubility at 760 mm mercury, P is any other barometric pressure, in mm, and p is the pressure of saturated water vapour, in mm, at the temperature of the water. Since p is small as compared to P and can be ignored (37), the equation becomes,

$$C_i \approx C_s \frac{P}{760} \approx C_s \frac{760 + H_s}{760} \quad \text{..... 9}$$

where $H_s$ is the pressure at mid-depth of vertical travel of the air bubble from the outlet, in mm.

Or, $$C_i \approx C_s \left(1 + \frac{H_s}{34}\right) \quad \text{..... 10}$$

where $H_s$ is in feet.

Because dc/dt is the rate of oxygen absorption into water, in mg/l/hr, therefore the quantitative rate of oxygen transfer, $R_o$, in lb/hr, can be determined from the following equation:

$$R_o = dc/dt \times W \times 10^{-6} \quad \ldots\ldots\ldots\ldots \quad 11$$

where W is the total weight of water aerated, in lb.

The rate of oxygen supplied to the system, $R_s$, in lb/hr, is obtained from the relation:

$$R_s = 1.05\, Q_a \quad \ldots\ldots\ldots\ldots\ldots\ldots \quad 12$$

where $Q_a$ is the rate of airflow in cfm at S.T.P. conditions and 1.05 is a conversion factor determined from the weight of a cubic foot of air and the percentage of oxygen in air, as obtained from the Chemical Engineers' Handbook (38).

Now, the oxygen transfer efficiency, $E_o$, in per cent, can be determined from

$$E_o = \frac{\text{lb. } O_2 \text{ transferred/unit time}}{\text{lb. } O_2 \text{ supplied/unit time}} \times 100$$

$$= \frac{R_o}{R_s} \times 100 \quad \ldots\ldots\ldots\ldots\ldots \quad 13$$

Aeration efficiency can also be reported in terms of rate of oxygen transferred per unit power input, $E_p$, in lb/kwhr,

i.e. $$E_p = \frac{R_o}{P_a + P_w} \quad \ldots\ldots\ldots\ldots\ldots \quad 14$$

where $P_a$ is the theoretical power, in Kw, required to compress

air and $P_w$ is the theoretical input of power required to circulate water, in Kw. The air power is determined from the equation given by Bewtra (11):

$$P_a = 7430\ Q_a \left[\left(\frac{H_T' + 34}{34}\right)^{0.286} - 1\right], \frac{ft - lb}{min.}$$

$$= \frac{7430 \times 0.746}{33,000}\ Q_a \left[\left(\frac{H_T' + 34}{34}\right)^{0.286} - 1\right], Kw$$

$$= 0.168\ Q_a \left[\left(\frac{H_T' + 34}{34}\right)^{0.286} - 1\right] \ldots\ldots 15$$

where $H_T'$ is the corrected water head or submergence of the diffuser, in feet, and $Q_a$ is in scfm.

$P_w$, the water power supplied to the system, is a function of the differential head, $\Delta H$, in feet, on two sides of the partition in the overhead tank, and the water flow rate, $Q_w$, in USGPM (39), (40). It is obtained from the relation:

$$P_w = \frac{(Q_w \times 0.1336) \times \Delta H \times 62.4 \times 0.746}{33,000}, Kw$$

or $$P_w = 1.885 \times 10^{-4}\ Q_w\ \Delta H \ldots\ldots 16$$

Another method of reporting the performance of an aeration system is to give values for the Overall Transfer Coefficient, $K_L a$, in $hr^{-1}$. From the examination of the previous equations and the semi-log plot, it can easily be observed that

$$K_L a = \text{slope} \times 2.30 \ldots\ldots 17$$

However, it must be kept in mind that $K_L a$ is temperature dependent (12), (13), (41), and any comparisons should be made at standard temperatures. For comparative purposes, the $K_L a$ values are corrected to 20° C, using the following equation given by Bewtra et al. (42):

$$\left(K_L a\right)_T = \left(K_L a\right)_{20} 1.02^{(T-20)} \quad \ldots\ldots\ldots\ldots \quad 18$$

where T is the water temperature in °C.

Thus the aeration efficiencies in this study have been reported as

(I) $\left(K_L a\right)_{20}$ , $hr^{-1}$

(II) $E_o = \frac{R_o}{R_s} \times 100$ , %

(III) $E_p = \frac{R_o}{P_a + P_w}$ , lb/kwhr

A typical calculation, employing the above relationships and quantities, is shown in Appendix B.

# IV - APPARATUS AND INSTRUMENTATION

The assembled apparatus, as shown in Figure 5, represents a section through a conventional aeration tank (Figure 2). Although the longitudinal velocity, normally associated with typical, spiral-flow tanks, is not provided in this apparatus, in practice this velocity is only in the order of 1/2 ft/min and its influence on aeration is considered to be negligible.

The holding tank at the top, approximately 4 1/2 ft x 2 ft x 1 1/2 ft, was constructed of plexiglass with 3/8" thick walls and 1/2" thick floor. The entire tank was reinforced with an angle iron frame. There was a removable, centre, plexiglass partition, and two, single-tube manometers, calibrated in feet, were fastened on the outside of the tank. These manometers were connected to two taps at the bottom of the tank, one on either side of the partition, and were used in reading head differentials, where applicable.

Two, 4 1/2" diameter holes were drilled in the bottom of the tank, one on either side, in which 6" long sections of 1/4" thick, 4" diameter plexiglass tubing were permanently fitted as base connections. To these permanent fixtures were fastened the sections of plexiglass tubing, which were easily interchangeable to vary the height. These sections of plexiglass

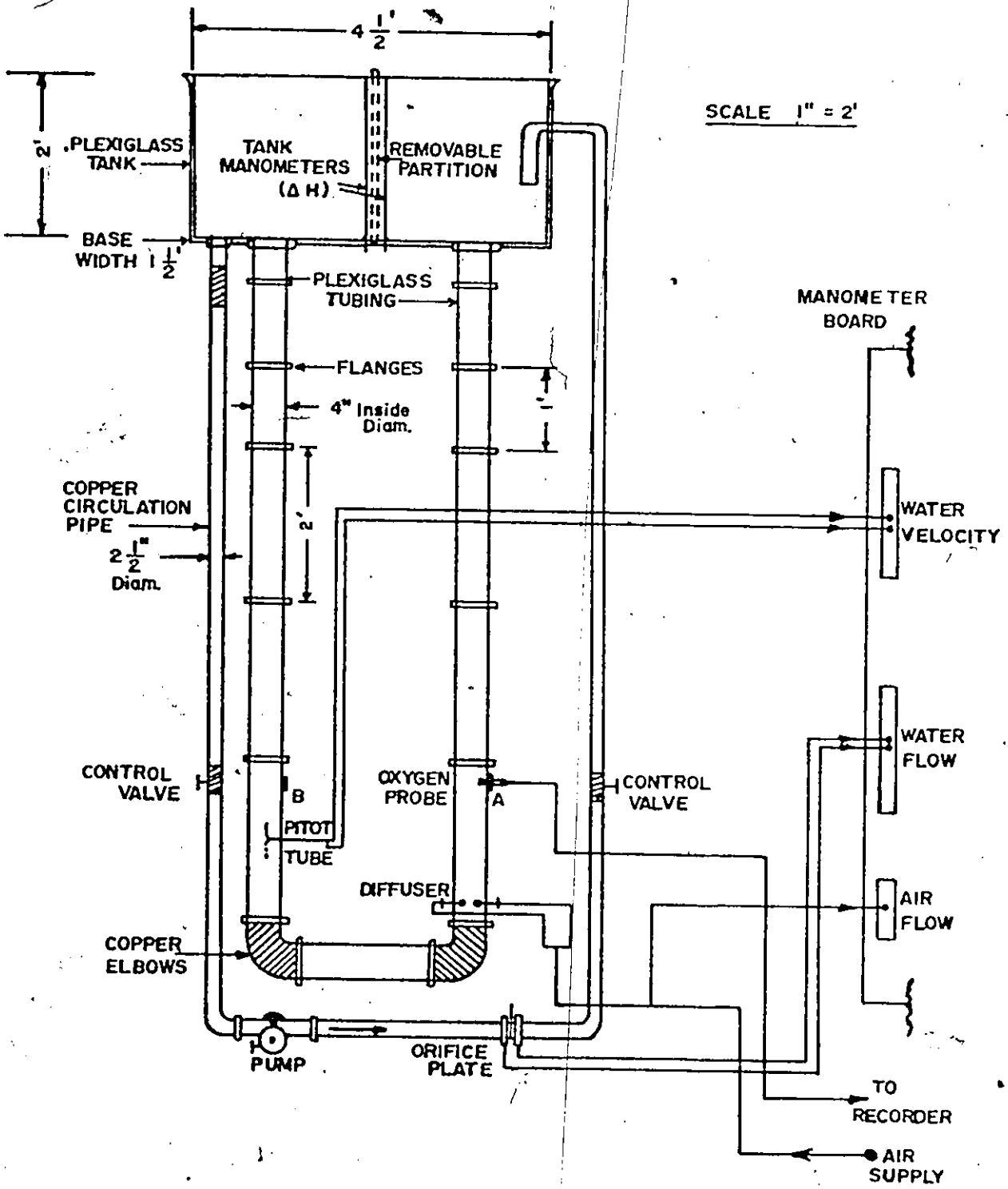


FIG. 5 – CLOSED – LOOP APPARATUS

tubing, were in 1 and 2 foot lengths, 1/4" thick, with a 4" internal diameter, and were fitted with 5/8" plexiglass flanges at either end. Once assembled, these tubes were fitted with either 4" copper elbows at the end, and a horizontal plexiglass base tube in between, or with a special contracting-section, 45° plexiglass bend, depending on the system used. Further details on the assembled apparatus are given in Figures 5 and 6. When completely assembled, the apparatus resembled a closed-loop configuration, consisting of a U-Tube plus water recirculating reservoir at the top. The elbows or bends were fitted with a tap for drainage.

Two piezometric taps were fitted along the lengths of the plexiglass tubing, one at the diffuser level and the other at a certain distance along the column as shown subsequently in Figures 10 to 13 . These taps were used for obtaining pressure-head differentials between these two points while the air-water system was in operation. Recirculation was accomplished by using long sections of 2 1/2" diameter copper pipe, fitted with a Jenkins flow control valve, and with a low-head, circulation pump, having a pumping capacity of 100 USGPM. Where the copper pipe was connected to the base of the tank, the connection was made with a rubber joint and clamps, to reduce vibrations from the pump. Also, the piping was clamped to the supporting steel frame at several locations for added support. Special bolted hooks, connected at the bottom of the plexiglass tubing along with a chain connected at the top of the frame, gave needed support

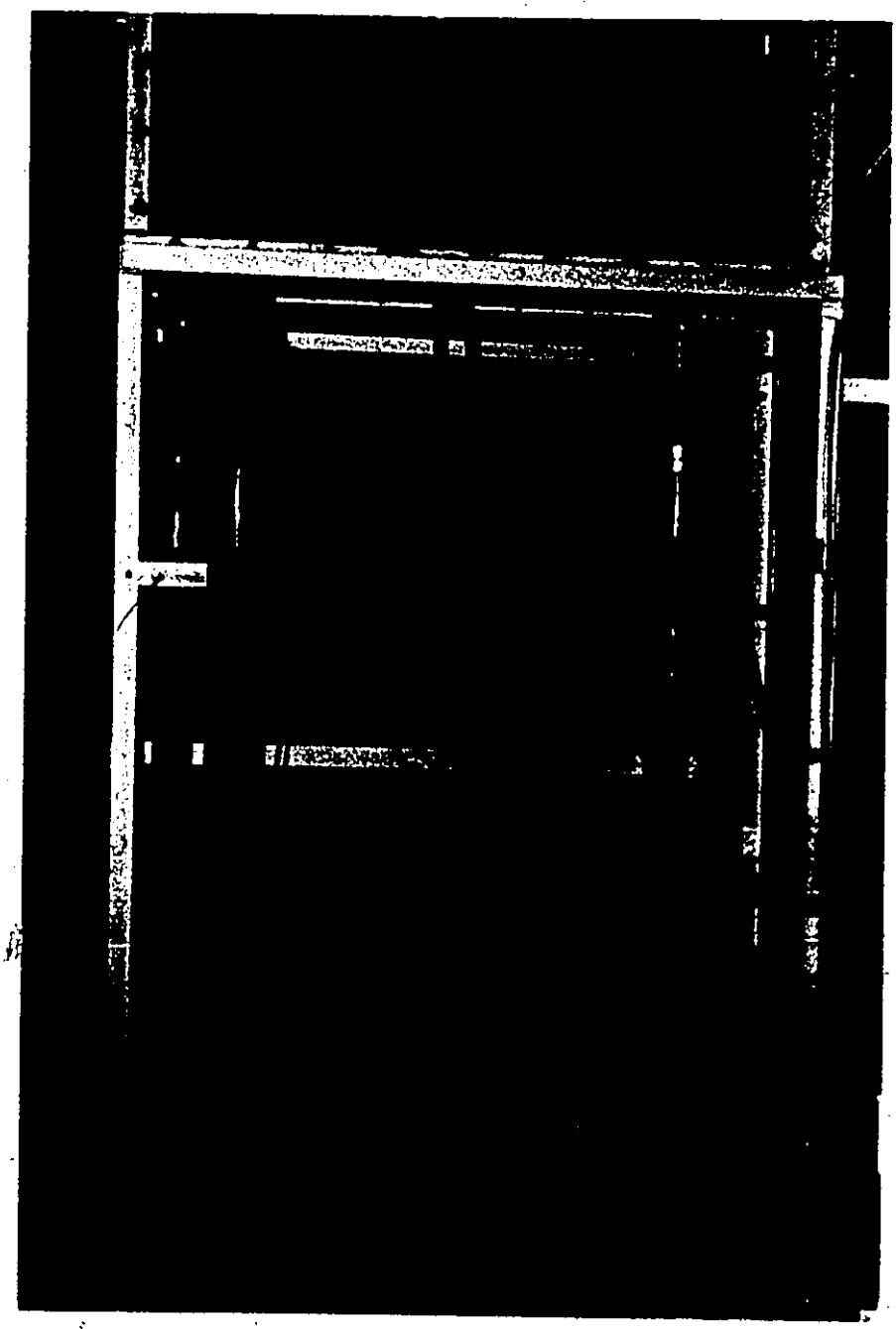

Figure 6 - System IV in Full Operation

to the water-filled U-Tube.

Both the air diffuser and the oxygen probe were fitted into one of the 2 foot plexiglass modules. The diffuser was inserted 3" from the end of the tube and was in the shape of a ring as described on page 53. The feeder tubes to the ring were connected by Tygon flexible tubing to the airflow meter and air supply line. Near the other end of the same plexiglass module, a special reinforced hole was drilled, large enough to accomodate the oxygen probe used in this study. This probe, in turn, was connected by an insulated wire to a Galvanic Cell Oxygen Analyzer and a strip chart recorder. These instruments have been described elsewhere in this chapter.

Another 2 foot module, on the other side of the U-Tube, was fitted with a standard, 1/8" pitot tube at the centre of its cross-section and an additional oxygen probe. The pitot tube, used for measuring water velocities, was connected, through Tygon tubing, to a pre-calibrated, sloping manometer. The manometer was precalibrated for velocities in ft/sec. The additional probe was provided to obtain simultaneous, dissolved oxygen readings on either side of the U-Tube, if desired.

The rate of water circulation through the pump was measured through an orifice plate placed between two tapped flanges. The taps were connected to a pre-calibrated, reservoir-type manometer to give the rate of flow in USGPM.

The specifications of the equipment used in this study

are given below.

RECORDING INSTRUMENTS

Airflow Meter: The feeder tubes of the diffuser were connected through an airflow meter to a constant-pressure, compressed-air, supply line. The airflow meter was a Lab Crest, Mark III model (448-324), distributed by Fisher Scientific Co. It operated on a ball-float system and had a capacity to measure airflows from 900 - 23,400 cc/min, at standard conditions, when using the 1/4" stainless-steel float. The airflow rates were obtained from a calibration curve (#C65816) supplied by the manufacturer.

Dissolved Oxygen Analyzer and Recorder: The Galvanic Cell Oxygen Analyzer, Precision Scientific Co. Model # 68850, was capable of measuring both temperature and dissolved oxygen. It had a temperature measuring capacity of 0 - 50 ° C, via a 50 foot thermistor probe, and an oxygen measuring capacity of 0 - 45 mg/l on two scales. The oxygen probe was a silver cathode-lead anode type and was used exclusively with the above instrument. The strip chart recorder used was an Hitachi-Perkin-Elmer Model, No. 165, with a maximum graph width of 10 inches and a chart speed range of 5 - 240 mm/min. The Dissolved Oxygen Analyzer and recorder are shown in Figure 7.

Water Flow Meter: The two tapped flanges, with the orifice plate inserted between them, were connected to a well-type

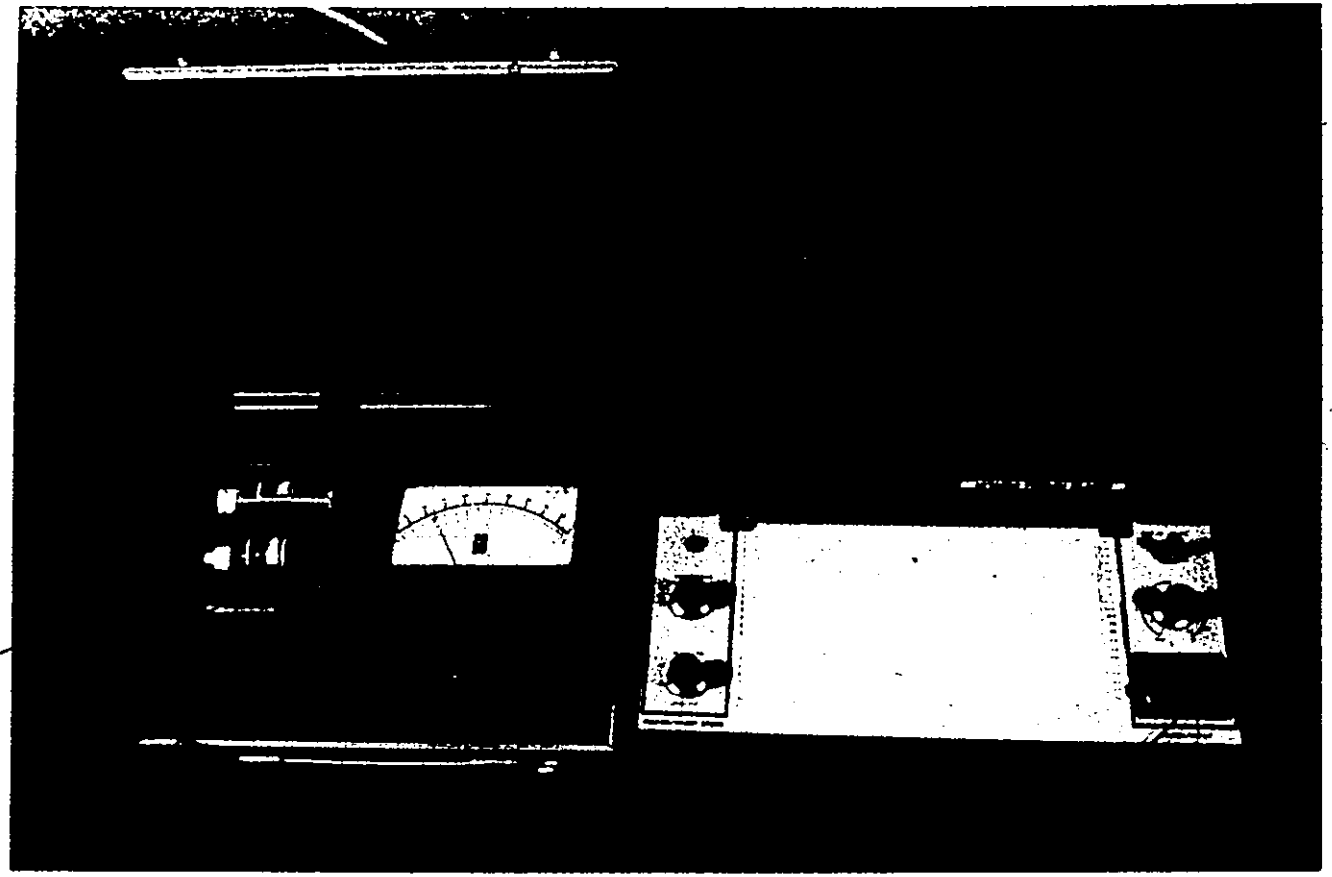

Figure 7 - Dissolved Oxygen Analyzer, Probe and Recorder

manometer, Meriam No. 30 - EA - 15, which used mercury as the indicating fluid. It had a vertical range of 12 inches and was calibrated in USGPM with the following ranges:

(i) 0 - 30 USGPM when using orifice tang plate # D-15562, with a bore of 0.847 inches and pipe diameter of 2 1/2";

(ii) 0 - 102 USGPM when using orifice tang plate # D-15561, with bore of 1.484 inches and pipe diameter of 2 1/2".

Water Velocity Meter: The 1/8" pitot tube, obtained from the United Sensor Corporation, was connected to an inclined tube, type manometer, Meriam No. 40 - GD - 10 - WM - 3, which used a blue fluid of specific gravity 1.75 as the indicating liquid. This manometer was precalibrated and had a measuring capacity of 0 - 3.95 ft/sec.

# V - EXPERIMENTAL PROCEDURE

The following general procedure was employed in all of the experiments conducted:

Before starting actual experimentation in any one run, the oxygen probe was calibrated against titration by the Winkler Method as described in Standard Methods (37). Also, if water flow measurements were to be taken, the proper orifice plate was installed in the return pipe line as shown in Figure 5. Then, the airflow, waterflow, and water velocity lines were connected to their respective manometers. All air lines and manometer connections were checked for leakage before each experimental run.

City water was employed to fill the experimental system up to the desired level. The air supply was opened and the recirculation pump, if called for in the experiment, was turned on. Both air and waterflow rates were adjusted to their desired values and the system was allowed to stabilize. While waiting for this to occur, the water lines leading from the pitot tube and orifice flanges were completely "bled" to remove air bubbles that might have been trapped. Once the air-water system had stabilized, enough sodium sulfite was added to the water to completely deplete

the dissolved oxygen content. Then the oxygen probe was connected to the galvanic-cell, dissolved oxygen analyzer, which in turn was connected to an automatic, strip-chart recorder. The temperature of the water was obtained with the thermistor probe, connected to the galvanometer, and suspended at approximately mid-depth of the system. Temperature readings, with an accuracy of 1/10°C, were taken both at the beginning and at the end of the experimental run. Airflow rates were monitored with the standard airflow rotameter while water velocities and waterflow rates were monitored with standard inclined-tube and well-type manometers, respectively.

With the experiment now in operation, all necessary manometric readings were taken while the recorder was automatically plotting a graph indicating the change in dissolved oxygen concentration with time. The entire study was divided into the following four aeration systems as shown in Figure 8:

SYSTEM I - Simple Water Column

Conditions: (i) Blind flange was inserted 3 inches below the coarse-bubble diffuser in the plexiglass tubing, thus forming a column of water only.

(ii) Using the interchangeable 1 and 2-foot plexiglass tubes, column heights of 2 to 9 feet were used.

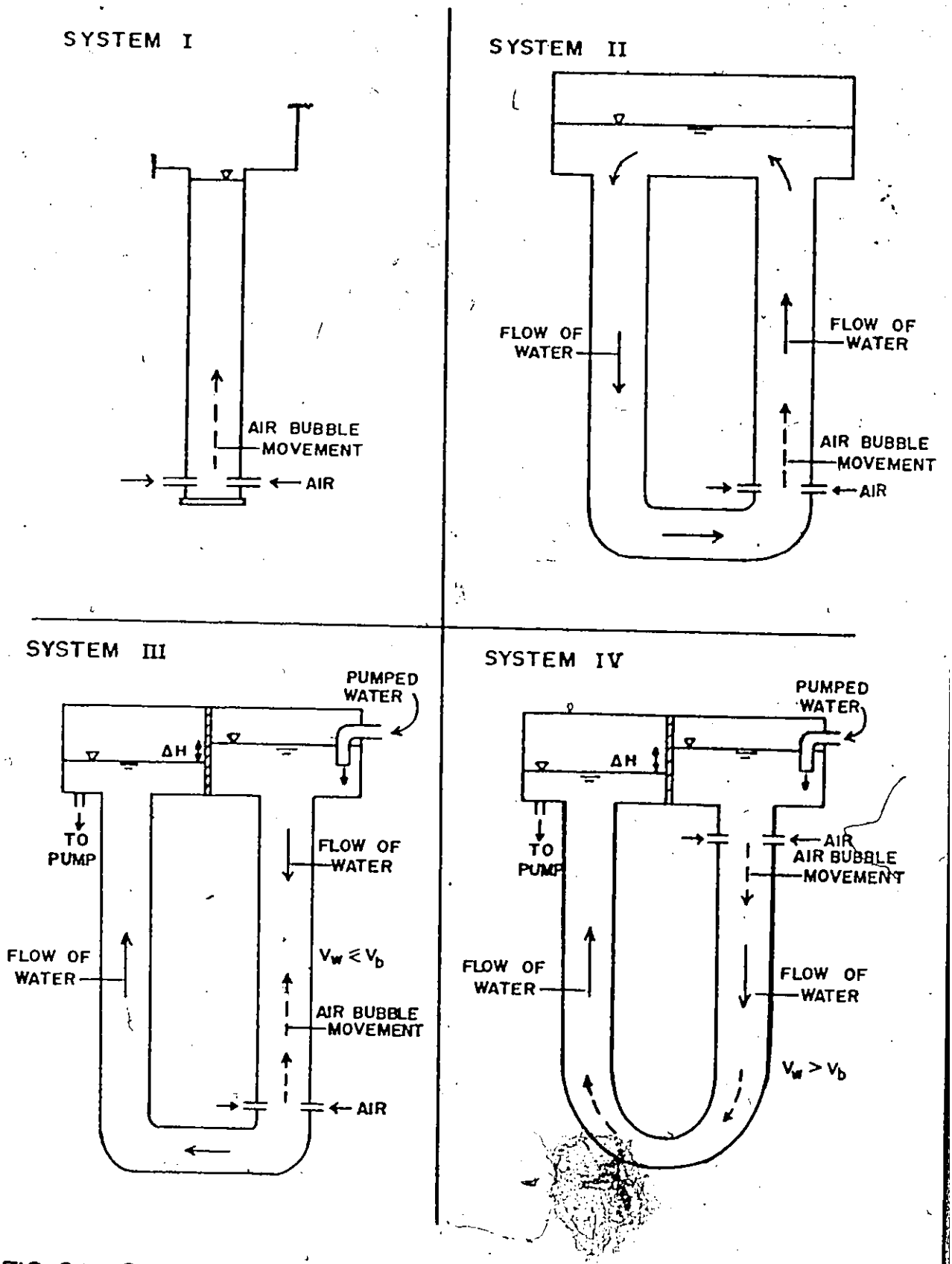


FIG. 8 — SCHEMATIC VIEW OF THE FOUR SYSTEMS USED

(iii) Five airflow rates in the range of 0.10 to 0.38 scfm were employed.

(iv) The coarse-bubble diffuser was located 3 inches above the bottom of the column.

(v) The recirculating tank remained empty.

SYSTEM II - Circulation Without Pumping

Conditions: (i) The central partition was removed from the recirculating tank, thus allowing circulation to occur through the closed loop.

(ii) Heights of column sections ranged between 2 and 8 feet, in 1 foot intervals.

(iii) Five airflow rates in the range of 0.11 to 0.38 scfm were employed.

(iv) The coarse-bubble diffuser was located 3 inches above the bottom of the last plexiglass section and just above the corner elbow.

(v) Depth of water in the recirculating tank was 1 foot.

SYSTEM III - Circulation with Pumping, $V_w \leq V_b$

Conditions: (i) The central partition was in place in the recirculating tank and the water was recirculated, by means of the pump, through the 2 1/2 inch diameter copper pipe.

(ii) Heights of column sections varied from 3 to 8 feet, in 1 foot intervals.

(iii) The coarse-bubble diffuser was located 3 inches above the bottom of the last plexiglass section and just above the elbow.

(iv) Five airflow rates in the range of 0.11 to 0.38 scfm were employed.

(v) Water was pumped against the flow of air bubbles with the average velocity of the water 'equal to' or 'less than' the velocity of the rising bubble (terminal velocity), i.e., $V_w \leq V_b$. This water flow rate, $Q_w$, was called $Q_{max}$.

(vi) The initial depth of water in the recirculating tank was 9 inches.

(vii) Head differential readings were taken from the manometers fixed on the side of the tank.

SYSTEM-IV - Circulation with Pumping, $V_w > V_b$

Conditions: (i) The central partition was in place in the recirculating tank.

(ii) Heights of the column sections varied from 2 to 7 feet, in 1 foot intervals.

(iii) The coarse-bubble diffuser was located 9 inches below the bottom of the tank, near the top of the system.

(iv) Five airflow rates in the range of 0.10 to 0.32 scfm were employed.

(v) Water was pumped so that the air-water mixture moved in the same direction, i.e., the average velocity of the water was just greater than the terminal bubble velocity on the diffuser side of the system. Thus, $V_w > V_b$. This waterflow rate, $Q_w$, was called $Q_{min}$.

(vi) The initial depth of water in the recirculating tank was 9 inches.

(vii) Head differential readings were taken from the manometers fixed on the side of the recirculating tank.

The coarse-bubble diffuser employed in this work was a 3/8" diameter, copper tube, which was formed into a ring. Twelve, evenly-spaced, 1/16" diameter holes were drilled along the inside edge of this copper ring. This arrangement gave a fairly even distribution of air bubbles throughout the cross-section of the plexiglass column. The diffuser ring was fastened on the inside of the column and the air was fed through four, 1/8" diameter, copper tubes which were connected to main air lines.

Some experiments were also conducted with two different types of porous or fine-bubble diffusers. These diffusers were either porous, disc-like plates or porous, cylindrical stones and were commercially available from two different companies, Norton Company of Massachusetts and Fisher Scientific Company, respectively. Only System II was employed for the experiments conducted with porous diffusers and the results were compared to those of the coarse-bubble diffuser, in terms of oxygen transfer efficiency.

From the plotted graph, the readings for the change in dissolved oxygen with time were obtained and the various relationships and values were computed using the equations described in Chapter III. This procedure is illustrated by the typical calculation of Appendix B.

# VI - COMPUTATIONS INVOLVED IN THE DETERMINATION OF BUBBLE CONTACT TIME, BUBBLE SIZE, AND LIQUID FILM COEFFICIENT

## A. CONTACT TIME AND BUBBLE SIZE

### (a) System I - Simple Water Column

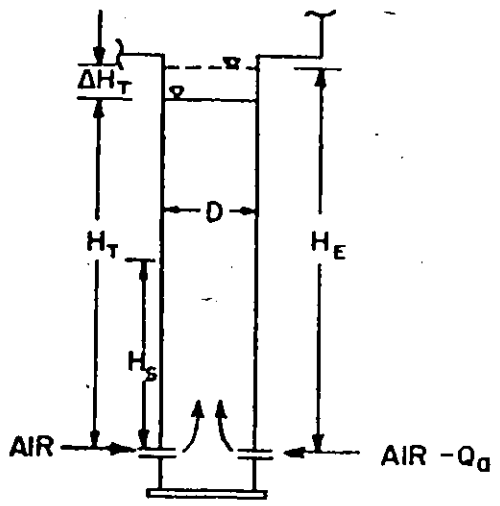


FIG. 9 — DETAILS OF SYSTEM I

where, $H_T$ = Initial diffuser submergence, ft.

$H_E$ = Expanded water depth, ft.

$\Delta H_T$ = Change in water depth due to presence of air = $H_E - H_T$ , ft.

$D$ = Diameter of the column, inches.

The inside cross-sectional area of the column, in $ft^2$, is found from

$$A_n = \pi/4\ (D/12)^2 \quad \ldots\ldots\ldots\ldots\ldots\ldots \quad 19$$

The change in volume of the fluid due to trapped air, in $ft^3$, can be determined from

$$\Delta V = A_n \Delta H_T \quad \ldots\ldots\ldots\ldots\ldots\ldots \quad 20$$

The airflow rate at mid-depth of air bubble travel, $H_s$, i.e., corresponding to the mid-pressure head, and given in cfm, can be found from the relation

$$Q_a' = \frac{Q_a}{1 + \frac{H_s}{34}} \quad \ldots\ldots\ldots\ldots\ldots\ldots \quad 21$$

Therefore, the average bubble contact time, in seconds, becomes equal to

$$t_c = \frac{\Delta V}{Q_a'} \times 60 \quad \ldots\ldots\ldots\ldots\ldots\ldots \quad 22$$

Since the velocity of water in the column, $V_w = 0$, therefore, the average terminal velocity of the air bubble, in ft/sec, is found from

$$V_b = \frac{H_E}{t_c} \quad \ldots\ldots\ldots\ldots\ldots\ldots \quad 23$$

From the plot of terminal velocity vs. bubble radius (9), (25), (43), the average bubble diameter, $d_{ave.}$, in mm, can be obtained.

(b) System II - Circulation Without Pumping

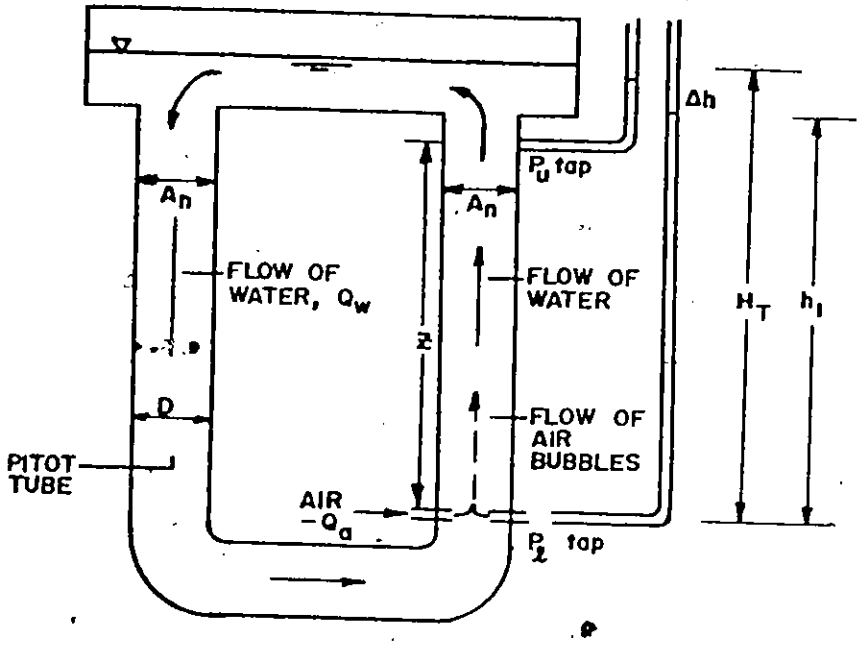


FIG. 10 – DETAILS OF SYSTEM II

where,

$P_u$ = Piezometric reading for the upper tap after air is introduced, ft.

$P_l$ = Piezometric reading for the lower tap after air is introduced, ft.

$Z$ = Distance between piezometric "taps", ft.

$H_T$ = Initial diffuser submergence, ft.

$h_l$ = Lower piezometric head, ft.

$Q_w$ = Waterflow rate, cfs.

The inside cross-sectional area of each column, in $ft^2$

is found from

$$A_n = \pi/4 \ (D/12)^2 \quad \ldots\ldots\ldots\ldots\ldots \quad 19$$

The volume of trapped air between the two taps, in $ft^3$, can be determined from

$$V_a = A_n \ (P_u - P_l)$$

$$= A_n \Delta h \quad \ldots\ldots\ldots\ldots\ldots\ldots \quad 24$$

The pressure-head at mid-depth, in ft, can be found from $(h_1 - Z/2)$ and thus the airflow rate, in cfm, becomes

$$Q_a' = \frac{Q_a}{1 + \frac{h_1 - Z/2}{34}} \quad \ldots\ldots\ldots\ldots \quad 25$$

The detention time, $t_d$, in seconds, of the average air bubble, between the two taps is found from

$$t_d = \frac{V_a}{Q_a'} \times 60 \quad \ldots\ldots\ldots\ldots\ldots \quad 26$$

and the total bubble velocity, in ft/sec, is now equal to:

$$V_T = Z/t_d \quad \ldots\ldots\ldots\ldots\ldots\ldots \quad 27$$

Therefore, the average bubble contact time for the entire depth, in seconds, becomes

$$t_c = H_T/V_T \quad \ldots\ldots\ldots\ldots\ldots\ldots \quad 28$$

The average water velocity on the left-hand side of the system, as recorded by the pitot tube, in ft/sec, is given by

$$V_{Pave.} = \frac{Q_w}{A_n} \quad \ldots\ldots\ldots\ldots\ldots\ldots \quad 29$$

The average water velocity, $V_w$, in ft/sec, in the air-water flow on the right-hand side can be determined from the relation:

$$V_w = \frac{Q_w + Q_a'}{A_n}$$

$$= \frac{Q_w}{A_n} + \frac{Q_a'}{A_n} \quad \ldots\ldots\ldots\ldots\ldots\ldots \quad 30$$

Therefore,

$$V_{w_{right}} = \frac{Q_w}{A_n} + \frac{Q_a'}{A_n}$$

$$= V_{Pave.} + \frac{Q_a'}{A_n \times 60} \quad \ldots\ldots\ldots \quad 31$$

and is given ft/sec.

Since the total bubble velocity is the vectorial sum of the average terminal velocity of the air bubble and the average water velocity on the right-hand side of this system, therefore

$$V_T = V_b + V_{w_{right}}$$

or

$$V_b = V_T - V_{w_{right}} \quad \ldots\ldots\ldots\ldots\ldots\ldots \quad 32$$

Then the average bubble diameter, $d_{ave.}$, in mm, is obtained from the graph of $V_b$ vs. bubble radius (9), (25), (43).

(c) System III - Circulation with Pumping, $V_w \leq V_b$

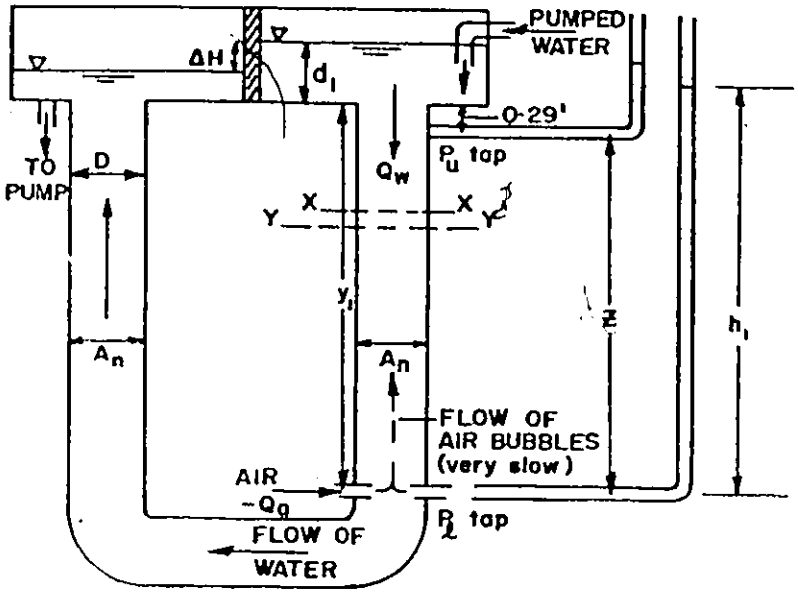


FIG. II – DETAILS OF SYSTEM III

where, $y_1$ = Distance from diffuser to tank bottom, ft.

$d_1$ = Water depth in right side of recirculating tank, ft.

$\Delta H$ = Head loss in the recirculating tank, ft.

All other variables are as defined in System II.

The inside cross-sectional area of each column, in $ft^2$, is found from:

$$A_n = \pi/4 \ (D/12)^2 \quad \ldots\ldots\ldots\ldots\ldots\ldots \quad 19$$

The volume of air trapped between the two piezometric, in $ft^3$, can be determined from

$$V_a = A_n \ (P_u - P_l) \quad \ldots\ldots\ldots\ldots\ldots \quad 33$$

The pressure-head at mid-depth, in ft, can be found from $(h_1 - \ell/2)$ and thus the airflow rate $Q_a'$, in cfm, becomes

$$Q_a' = \frac{Q_a}{1 + \frac{h_1 - \ell/2}{34}} \quad \ldots\ldots\ldots\ldots \quad 35$$

The detention time, $t_d$, in seconds, of the air bubble in distance $\ell$ is found from

$$t_d = \frac{V_a}{Q_a'} \times 60 \quad \ldots\ldots\ldots\ldots \quad 36$$

and the total bubble velocity, in ft per sec, is found from the relation,

$$V_T = \ell/t_d \quad \ldots\ldots\ldots\ldots \quad 37$$

By closely examining a unit element in the column cross-section on the right-hand or downflow side of the system, the velocity of the water, $V_w$, is obtained as explained below:

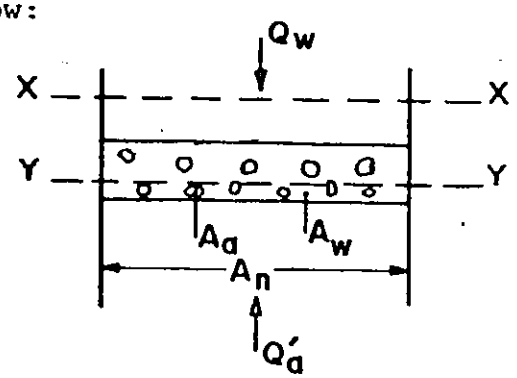


FIG. 12 — CROSS-SECTION OF COLUMN UNIT ELEMENT, SYSTEM III

where, $Q_a'$ = Airflow Rate, corrected for pressure, cfm.

$Q_w$ = Waterflow rate through the column cfs.

$A_a$ = Area of air bubbles present at any time in the cross-section of a column unit element, $ft^2$.

$A_w$ = Area of water present in the cross-section of a column unit element and represents the reduced area through which the water flow, $Q_w$, must pass, $ft^2$.

At Section x - x:

The nominal water velocity is defined as

$$V_n = Q_{w/A_n} \downarrow$$

and is given in ft/sec.

At Section Y - Y:

The velocity of the water in the air-water mixture, $V_w$, in ft/sec., can be found from the relation,

$$V_w = Q_{w/A_w} \downarrow \text{ , and } > V_n$$

The total bubble velocity, $V_T$, in ft/sec., is obtained from the following equation,

$$V_T = \frac{Q_a'}{A_a \times 60} \uparrow$$

Since $A_n = A_a + A_w$

Therefore, $$\frac{Q_w}{V_n} = \frac{Q_a'}{V_T \times 60} + \frac{Q_w}{V_w}$$

or $$\frac{Q_w}{V_w} = \left(A_n - \frac{Q_a'}{V_T \times 60}\right)$$

and $$V_w = \frac{Q_w}{\left(A_n - \frac{Q_a'}{V_T \times 60}\right)} \quad \text{..... 34}$$

given in ft/sec.

Also, in this system, on the right-hand side,

$$V_T = V_b - V_w$$

where $V_b$ is the average terminal bubble velocity.

Therefore, $$V_b = V_T + V_w \quad \text{..... 35}$$

Then the average bubble diameter, $d_{ave.}$, in mm, is obtained from the plot of $V_b$ vs. bubble radius (9), (25), (43).

The average bubble contact time for the entire depth, $t_c$, in seconds, now becomes

$$t_c = \frac{y_1}{V_T} + \frac{d_1}{V_T'}$$

where $V_T'$ is the total bubble velocity in the recirculating tank, in ft/sec.

But, $$\frac{y_1}{V_T} = \frac{8 + 0.29}{V_T}$$

and $$\frac{d_1}{V_T'} = \frac{d_1}{V_b - Q_w/\text{surface area of 1/2 upper tank}}$$

$$= \frac{d_1}{V_b - Q_{w/3.10}}$$

Therefore, the contact time of the air bubble, $t_c$, in seconds, becomes,

$$t_c = \left[\frac{8 + 0.29}{V_T} + \frac{d_1}{V_b - Q_{w/3.10}}\right] \quad \ldots\ldots \quad 36$$

(d) System IV - Circulation with Pumping, $V_w > V_b$

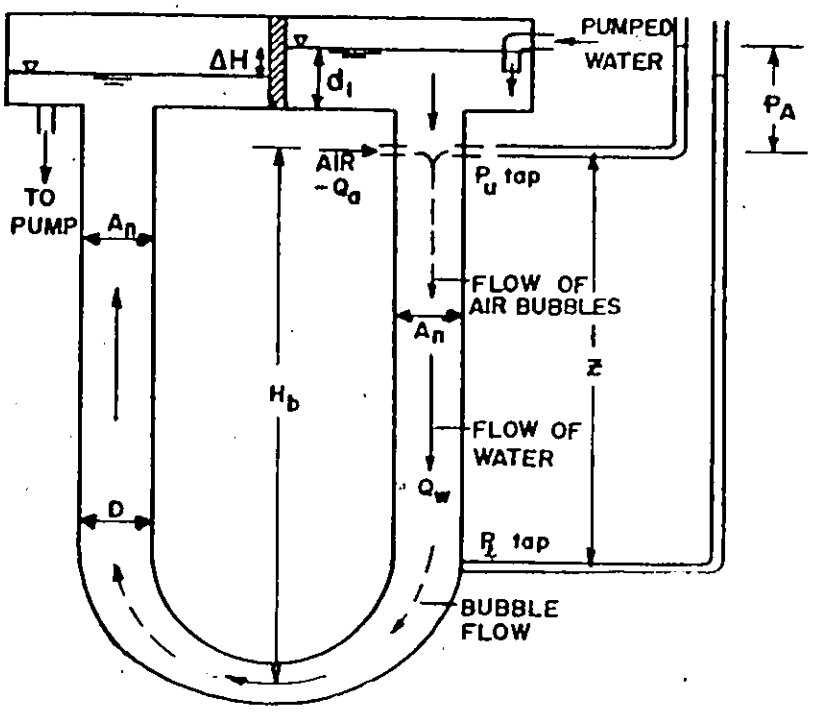


FIG. 13 — DETAILS OF SYSTEM IV

where, $P_A$ = Upper piezometric head, ft.

$H_b$ = Maximum depth of water below the diffuser, ft.

All other variables have been defined in the previous systems.

The inside cross-sectional area of each column, in $ft^2$, is found from

$$A_n = \pi/4 \ (D/12)^2 \quad \ldots\ldots\ldots\ldots\ldots \quad 19$$

The volume of air trapped in the column between the two piezometric taps, in $ft^3$, can be found from

$$V_a = A_n \ (P_u - P_l) \quad \text{..... 33}$$

The pressure-head at mid-depth of distance $Z$ below the diffuser, in ft, is found from $(p_A + Z/2)$, and therefore the airflow rate, corrected for pressure at mid-depth, in cfm, can be determined from

$$Q_a' = \frac{Q_a}{1 + \frac{P_A + Z/2}{34}} \quad \text{..... 37}$$

The average detention time, $t_d$, in seconds, of the air bubble in distance $Z$ on the downflow or right-hand side of the system is determined from the relation,

$$t_d = \frac{V_a}{Q_a} \times 60 \quad \text{..... 26}$$

and the total bubble velocity on the right-hand side, in ft/sec, becomes

$$V_T = Z/t_d \quad \text{..... 27}$$

Therefore, the average contact time for the air bubbles on the right-hand or downflow side, in seconds, can be found from

$$t_{cR} = \frac{H_b}{V_T} \quad \text{..... 38}$$

Further relationships with respect to the air bubbles moving through this system cannot be developed because of the following reasons:

(i) The air bubbles lose their identity and change their characteristics as they flow through the funnel-like bend at the bottom as shown in Figures 6 and 14. This bend induces a great deal of turbulence, creating some separation in the air-water mixture as it flows rapidly through the constriction, especially at higher airflow rates and larger depths. Thus, a single bubble entering this bend is caught up in this turbulence and in some cases, coalesces with other bubbles. At the same time, new and different sized bubbles are created by the turbulence, with an upward, helical pattern of flow movement on the left-hand side of the system. Therefore, even though many small bubbles are present throughout the entire system, on both the left and right-hand sides, the continuity of the system is disrupted to a great extent.

(ii) The graphic plot used for the determination of bubble sizes from their terminal velocities (9), (25), (43), had been obtained, in general, by studying the release of discrete bubbles of different sizes at the bottom of a water column and following their rather direct ascent to the top. The random, helical course followed by the bubbles in this system may question the

Figure 14 - Behaviour of Air Bubble Flow Through the Constriction, System IV

validity and accuracy of any terminal bubble velocities as well as the corresponding bubbble sizes which may be obtained in this system.

Consequently, no further attempt was made to develop the relationships for System IV that were obtained in the other Systems.

## B. LIQUID FILM COEFFICIENT, $K_L$

Equations 13 and 11 have been developed earlier to obtain the oxygen transfer efficiency, $E_o$, and the rate of oxygen transferred, $R_o$. Bewtra and Nicholas (15), (33), further expanded these equations for oxygen transferred in a full-scale, aeration tank, a system comparable to System II of this study. However, these equations can be adapted easily to any of the four systems described in this work. One of their basic equations is

$$R_o = \left[K_f A_f + K_a \frac{305\ Q_a'}{10 d_{ave.}} \frac{H_T}{V_b + V_w} \alpha' \beta\right]\left(C_i - C_L\right) \quad \ldots 39$$

where $R_o$ = Total rate of oxygen transferred, lb/hr.

$K_f$ = Overall gas transfer coefficient during bubble formation, lb/hr per $ft^2$ per mg/l.

$K_a$ = Gas transfer coefficient during ascent, lb/hr per $ft^2$ per mg/l.

$A_f$ = Mean surface area of all bubbles in formation at any instant, $ft^2$.

$Q_a'$ = Airflow rate corresponding to half-depth of diffuser submergence and liquid temperature, cfm.

$H_T$ = Depth of diffuser submergence, ft.

$V_b$ = Terminal velocity of the air bubble during ascent, ft/sec.

$V_w$ = Velocity of the air-liquid mixture, ft/sec.

$d_{ave.}$ = Mean air bubble diameter at mid-depth of submergence, mm.

$\alpha'$ = Effect of air bubble entrainment in the downward moving liquid or carry-over effect, dimensionless.

$\beta$ = Factor relating diameter of each bubble to its volume and surface area, dimensionless.

$C_i$ = Dissolved oxygen saturation concentration at mid-depth and liquid temperature, mg/l.

$C_L$ = Dissolved oxygen concentration of the liquid, mg/l.

For coarse-bubble diffusion, such as in this study, the amount of oxygen transferred during bubble formation is negligible (11).

$$\text{Therefore,} \quad R_o = K_a \frac{305\, Q_a'}{10 d_{ave.}} \frac{H_T}{V_b + V_w} \alpha' \beta \left(C_i - C_L\right) \quad \ldots\ 40$$

Since there was no carry-over effect in any of the four systems, and the $\beta$ factor remains nearly unity in most cases, it is reasonable to assume that $\alpha' \beta = 1$. Also, since the rate of oxygen transferred into water is computed at zero dissolved oxygen concentration, therefore $C_L = 0$. Substituting these values in Equation 40 and also replacing $Q_a'$ with $Q_a\left(\frac{34}{34 + H_s}\right)$, where $H_s$ is the mid-depth pressure head, in feet, the equation is reduced to,

$$R_o = \frac{305 K_a}{10 d_{ave.}} \frac{H_T}{V_b + V_w} C_i Q_a \left(\frac{34}{34 + H_s}\right) \quad \ldots\ 41$$

$$\text{Similarly,} \quad E_o = \frac{R_o}{R_s} \times 100, \ \% \quad \ldots\ 13$$

$$= \frac{R_o}{1.05 Q_a} \times 100$$

$$= \frac{\dfrac{305 K_a}{10 d_{ave.}} \dfrac{H_T}{V_b + V_w} C_i Q_a \left(\dfrac{34}{34 + H_s}\right)}{1.05\, Q_a} \times 100$$

$$= \frac{305 K_a H_T C_i}{10.5 d_{ave.} (V_b + V_w)} \left(\frac{1}{1 + H_s/34}\right) \times 100, \ \% \quad \ldots\ 42$$

Since $K_a$ is the only transfer coefficient found in the above expression and if the gas transfer across the liquid film is considered, then $K_a$ can be replaced with $K_L$.

$$\text{Therefore,} \quad K_L = K_a = \frac{E_o \; 10.5 \; d_{ave.} \left(V_b + V_w\right) \left(1 + H_{s/34}\right)}{100 \; H_T \; C_i \times 305}$$

$$\text{or} \quad K_L = \frac{10.5 \; E_o \; d_{ave.}}{30500 \; C_i} \left(\frac{V_b + V_w}{H_T}\right) \left(1 + \frac{H_s}{34}\right), \text{ ft/sec.}$$

..... 43

In this expression, $E_o$, $V_b$, and $V_w$ are all known from the previous calculations, $C_i$, $H_T$, and $H_s$ are known from the data, and $d_{ave.}$ is known from the calibration plot of bubble terminal velocity vs. bubble radius (9), (25), (43).

In order to adapt Equation 43 to each of the four systems, only the term $\left(\frac{V_b + V_w}{H_T}\right)$ requires consideration, because all other variables remain unchanged. However, $\left(\frac{V_b + V_w}{H_T}\right)$ is actually an expression of 1/contact time of the air bubble, that is, $1/t_c$, in $\text{sec}^{-1}$, and the equations for this variable have already been developed separately for each of Systems I, II, and III. Therefore, by substituting the value $1/t_c$ for $\left(\frac{V_b + V_w}{H_T}\right)$ in Equation 43, the parameter $K_L$ can be determined separately for each system, except for System IV, because of reasons already discussed.

# VII - RESULTS

This study was performed under four different systems as described in the previous chapters, and the computed results of these four systems are presented separately in Tables 1 through 7. The raw experimental data and certain other computed values can be found in Appendix C. The results for transfer efficiencies, unit power efficiencies, Overall Transfer Coefficients, and Liquid-Film Coefficients from Systems I, II, III, and IV, as well as the results for the porous diffusers are plotted in Figures 15 to 43.

In most cases, data and the subsequent computed values produced an accuracy of ±5%. However, when the results were based on several observations and computations, as well as where interpolations and calculations were made from other figures, reproducability of results is considered to be ± 10%. Thus, in this presentation, the values of more important parameters, such as oxygen transfer efficiencies, are considered accurate to within ± 10%.

In these experiments, no attempt was made to hold the water temperature constant. Although it has been shown that the Overall Transfer Coefficient, $K_L a$, increases about 2% for every 1°C rise in temperature (12), (13), (41),

Eckenfelder (13), Downing (44), and Bewtra et al. (42) have proven that for a given airflow rate, the product of $K_L a$ and $C_i$ (at $C_L=0$) in Equation 3 is constant for the temperature range of 10-30°C. This means that, even though $C_i$ decreases with temperature, the $K_L a$ value increases in the same proportion, making dc/dt a constant throughout the above temperature range. The temperatures recorded in this work were well within this range and therefore, no compensation for temperature effect has been made in the results for rates of oxygen absorption and for efficiencies. However, for comparative purposes, the $K_L a$ values are corrected to 20°C, using Equation 18:

$$(K_L a)_T = (K_L a)_{20}\ 1.02^{(T-20)} \quad \text{..... 18}$$

Since no other suitable relation could be found in the literature, the following identical equation was used to correct the $K_L$ values to 20°C:

$$(K_L)_T = (K_L)_{20}\ 1.02^{(T-20)} \quad \text{..... 44}$$

The values of $K_L a$ and $K_L$ have thus been converted from experimental values to the corresponding values at 20°C and are presented for comparison in Table 5.

Another important factor for consideration is the effect of the oxygen probe position on oxygen transfer rate values. As explained in Chapter IV, the apparatus was equipped with two oxygen probes, one on each side of the U-Tube column, so that individual or simultaneous dissolved

oxygen readings could be obtained. Thus, the effect of probe position on the absorption of oxygen into the water could be determined. In his earlier work, however, the author (10) had demonstrated clearly that, regardless of the probe position on the U-Tube, no appreciable difference in oxygen transfer rates was obtained, irrespective of the system, column heights, and airflow rates. Results, as reproduced in Table 8, indicate average differences of less than 4%, well within the reproducability of this experimental work.

As outlined in Chapter VI, an indirect method was used to determine bubble velocities, contact times and bubble sizes. However, in addition, a direct method for some of the experiments was also used. 16 mm movies were taken on TRI-X Reversal movie film, at a rate of 64 frames/sec, and involving three foot column lengths of different systems when in full operation. A split-second digital clock was placed beside the column section and photographed simultaneously. Analysis of the 16 mm movies was performed on a variable-speed, frame per frame analyzer. Results for bubble velocities and mean bubble sizes, wherever possible to obtain, indicated good agreement, within ± 10%, with those values determined by the indirect method.

Table 1 - Computed Results for System I

| 1 | 2 | 3 | 4 | 5 | 6 | 7 | 8 | 9 |
|---|---|---|---|---|---|---|---|---|
| Run No. | $H_T$ (ft) | $Q_a$* (scfm) | $E_o$ (%) | $E_p$ (lb/kwhr) | $K_La$ ($hr^{-1}$) | $t_c$ (sec) | $d_{ave.}$ (mm) | $K_L$ (ft/sec.) |
| 1 | 8.75 | 0.13 | 3.96 | 3.66 | 10.63 | 9.86 | 12.4 | $18.4 \times 10^{-5}$ |
| 2 | " | 0.19 | 3.59 | 3.31 | 14.50 | 7.83 | 21.0 | 37.5 " |
| 3 | " | 0.25 | 3.39 | 3.13 | 18.38 | 7.27 | 25.0 | 45.6 " |
| 4 | " | 0.31 | 3.08 | 2.84 | 20.85 | 7.69 | 22.5 | 35.2 " |
| 5 | " | 0.38 | 2.92 | 2.70 | 23.90 | 7.99 | 21.0 | 30.2 " |
| 6 | 7.75 | 0.12 | 3.31 | 3.42 | 9.80 | 8.06 | 16.0 | 25.3 " |
| 7 | " | 0.18 | 3.00 | 3.10 | 13.38 | 7.29 | 18.6 | 29.5 " |
| 8 | " | 0.25 | 2.93 | 3.03 | 17.50 | 6.89 | 21.3 | 35.1 " |
| 9 | " | 0.31 | 2.84 | 2.93 | 21.40 | 7.21 | 19.7 | 30.4 " |
| 10 | " | 0.37 | 2.76 | 2.85 | 24.90 | 7.28 | 19.7 | 29.2 " |
| 11 | 6.75 | 0.12 | 3.08 | 3.62 | 10.48 | 7.21 | 14.2 | 23.8 " |
| 12 | " | 0.18 | 3.11 | 3.66 | 16.00 | 6.42 | 18.8 | 35.7 " |
| 13 | " | 0.24 | 2.86 | 3.37 | 19.58 | 6.25 | 19.3 | 34.8 " |
| 14 | " | 0.30 | 2.64 | 3.11 | 22.60 | 6.14 | 21.0 | 35.5 " |
| 15 | " | 0.36 | 2.60 | 3.06 | 26.80 | 6.07 | 22.0 | 37.0 " |
| 16 | 5.75 | 0.12 | 2.40 | 3.29 | 9.65 | 6.29 | 14.0 | 20.9 " |
| 17 | " | 0.18 | 2.32 | 3.17 | 13.80 | 5.19 | 19.8 | 35.0 " |
| 18 | " | 0.23 | 2.28 | 3.12 | 18.20 | 5.09 | 22.1 | 39.4 " |
| 19 | " | 0.29 | 2.07 | 2.83 | 20.70 | 4.85 | 24.8 | 42.1 " |
| 20 | " | 0.35 | 2.25 | 3.07 | 27.00 | 5.03 | 22.6 | 40.4 " |

*Flows through a cross-sectional area of $\pi/36$ $ft^2$

Table 1 - Computed Results For System I (continued)

| 1 | 2 | 3 | 4 | 5 | 6 | 7 | 8 | 9 |
|---|---|---|---|---|---|---|---|---|
| 21 | 4.75 | 0.11 | 2.06 | 3.37 | 9.66 | *—— | —— | —— |
| 22 | " | 0.17 | 2.05 | 3.36 | 14.50 | 4.28 | 19.9 | $37.6 \times 10^{-5}$ |
| 23 | " | 0.23 | 1.96 | 3.21 | 18.50 | 3.94 | 25.0 | 49.2 " |
| 24 | " | 0.29 | 2.19 | 3.60 | 25.90 | 3.74 | 28.1 | 65.3 " |
| 25 | " | 0.34 | 1.87 | 3.07 | 26.80 | 3.92 | 25.8 | 48.9 " |
| 26 | 3.75 | 0.11 | 1.42 | 2.93 | 8.28 | —— | —— | —— |
| 27 | " | 0.17 | 1.48 | 3.04 | 13.00 | —— | —— | —— |
| 28 | " | 0.22 | 1.37 | 2.82 | 16.01 | 2.99 | 26.6 | $48.3 \times 10^{-5}$ |
| 29 | " | 0.28 | 1.38 | 2.85 | 20.25 | 2.99 | 27.6 | 50.7 " |
| 30 | " | 0.33 | 1.35 | 2.78 | 23.70 | 2.98 | 28.0 | 50.4 " |
| 31 | 2.75 | 0.11 | 1.19 | 3.31 | 9.38 | —— | —— | —— |
| 32 | " | 0.16 | 1.04 | 2.89 | 12.30 | —— | —— | —— |
| 33 | " | 0.22 | 1.02 | 2.83 | 16.01 | 3.03 | 15.0 | $20.5 \times 10^{-5}$ |
| 34 | " | 0.27 | 1.05 | 2.92 | 20.70 | 2.82 | 16.9 | 25.6 " |
| 35 | " | 0.32 | 0.95 | 2.65 | 22.60 | 2.52 | 21.0 | 32.1 " |
| 36 | 1.75 | 0.11 | 0.78 | 3.37 | 9.10 | —— | —— | —— |
| 37 | " | 0.16 | 0.73 | 3.16 | 12.68 | —— | —— | —— |
| 38 | " | 0.21 | 0.67 | 2.88 | 15.42 | —— | —— | —— |
| 39 | " | 0.26 | 0.65 | 2.80 | 18.75 | —— | —— | —— |
| 40 | " | 0.32 | 0.65 | 2.81 | 22.60 | —— | —— | —— |

*——omitted due to accuracy of $\Delta H_T$, i.e., when $(H_E - H_\Theta) < 0.10$ ft., causing an error of > 10% r w.r.t. least reading of ± 0.01 ft.

Table 2 - Computed Results for System II

| 1 | 2 | 3 | 4 | 5 | 6 | 7 | 8 | 9 | 10 | 11 |
|---|---|---|---|---|---|---|---|---|---|---|
| Run No. | $H_T$ (ft) | $Q_a$ * (scfm) | $E_o$ (%) | $E_p$ (lb/kwhr) | $K_La$ ($hr^{-1}$) | $V_n$ (ft/sec) | $V_T$ (ft/sec) | $t_c$ (sec.) | $d_{ave.}$ (mm) | $K_L$ (ft/sec.) |
| 1 | 9.25 | 0.13 | 4.95 | 4.37 | 1.24 | 0.87 | 2.40 | 3.85 | 36.5 | $17.4 \times 10^{-4}$ |
| 2 | " | 0.19 | 4.17 | 3.69 | 1.59 | 1.03 | 2.66 | 3.48 | 39.0 | 17.6 " |
| 3 | " | 0.25 | 3.93 | 3.49 | 2.00 | 1.17 | 2.81 | 3.29 | 39.0 | 17.6 " |
| 4 | " | 0.32 | 3.58 | 3.18 | 2.28 | 1.31 | 3.01 | 3.07 | 42.4 | 18.8 " |
| 5 | " | 0.38 | 3.16 | 2.82 | 2.41 | 1.41 | 3.16 | 2.92 | 44.0 | 18.0 " |
| 6 | 8.25 | 0.12 | 4.66 | 4.57 | 1.17 | 0.78 | 2.24 | 3.68 | 32.4 | 15.2 " |
| 7 | " | 0.19 | 4.13 | 4.06 | 1.57 | 0.94 | 2.58 | 3.20 | 39.5 | 18.9 " |
| 8 | " | 0.25 | 3.88 | 3.83 | 1.98 | 1.06 | 2.65 | 3.11 | 37.8 | 17.6 " |
| 9 | " | 0.31 | 3.31 | 3.28 | 2.12 | 1.19 | 2.92 | 2.82 | 43.8 | 19.4 " |
| 10 | " | 0.37 | 3.09 | 3.07 | 2.39 | 1.30 | 3.02 | 2.73 | 42.5 | 18.2 " |
| 11 | 7.25 | 0.12 | 4.62 | 5.12 | 1.21 | 0.76 | 2.24 | 3.23 | 32.4 | 17.5 " |
| 12 | " | 0.18 | 3.78 | 4.20 | 1.48 | 0.91 | 2.47 | 2.93 | 37.0 | 18.0 " |
| 13 | " | 0.24 | 3.53 | 3.93 | 1.86 | 1.03 | 2.74 | 2.64 | 43.0 | 21.9 " |
| 14 | " | 0.30 | 3.18 | 3.55 | 2.11 | 1.15 | 2.80 | 2.59 | 39.0 | 18.4 " |
| 15 | " | 0.36 | 3.11 | 3.48 | 2.48 | 1.24 | 2.96 | 2.45 | 42.6 | 20.8 " |
| 16 | 6.25 | 0.12 | 4.44 | 5.65 | 1.15 | 0.71 | 2.03 | 3.07 | 27.8 | 14.9 " |
| 17 | " | 0.18 | 3.61 | 4.61 | 1.42 | 0.85 | 2.35 | 2.66 | 32.6 | 16.6 " |
| 18 | " | 0.24 | 3.41 | 4.37 | 1.80 | 0.96 | 2.54 | 2.46 | 37.5 | 19.6 " |
| 19 | " | 0.30 | 3.12 | 4.01 | 2.07 | 1.06 | 2.54 | 2.46 | 32.4 | 15.6 " |
| 20 | " | 0.35 | 2.99 | 3.86 | 2.38 | 1.14 | 2.65 | 2.36 | 32.2 | 15.6 " |

*Flows through a cross-sectional area of $\pi/36$ $ft^2$

Table 2. Computed Results for System II (continued)

| 1 | 2 | 3 | 4 | 5 | 6 | 7 | 8 | 9 | 10 | 11 |
|---|---|---|---|---|---|---|---|---|---|---|
| 21 | 5.25 | 0.12 | 3.28 | 4.92 | 0.83 | 0.62 | * ——— | ——— | ——— | ——— |
| 22 | " | 0.17 | 3.24 | 4.88 | 1.24 | 0.75 | 2.18 | 2.42 | 31.5 | $15.3 \times 10^{-4}$ |
| 23 | " | 0.23 | 2.97 | 4.48 | 1.52 | 0.83 | 2.47 | 2.13 | 39.0 | 19.8 " |
| 24 | " | 0.29 | 2.65 | 4.02 | 1.70 | 0.96 | 2.50 | 2.10 | 36.2 | 16.6 " |
| 25 | " | 0.34 | 2.67 | 4.05 | 2.07 | 1.03 | 2.67 | 1.97 | 38.5 | 19.2 |
| 26 | 4.25 | 0.11 | 3.11 | 5.71 | 0.79 | 0.49 | ——— | ——— | ——— | ——— |
| 27 | " | 0.17 | 2.94 | 5.42 | 1.14 | 0.61 | ——— | ——— | ——— | ——— |
| 28 | " | 0.23 | 2.66 | 4.91 | 1.38 | 0.71 | 2.37 | 1.79 | 40.0 | $21.6 \times 10^{-4}$ |
| 29 | " | 0.28 | 2.54 | 4.71 | 1.66 | 0.81 | 2.47 | 1.72 | 39.7 | 21.4 " |
| 30 | " | 0.34 | 2.41 | 4.49 | 1.90 | 0.87 | 2.53 | 1.68 | 39.0 | 20.5 " |
| 31 | 3.25 | 0.11 | 2.79 | 6.64 | 0.73 | 0.31 | ——— | ——— | ——— | ——— |
| 32 | " | 0.16 | 2.45 | 5.85 | 0.97 | 0.44 | ——— | ——— | ——— | ——— |
| 33 | " | 0.22 | 2.19 | 5.23 | 1.15 | 0.53 | ——— | ——— | ——— | ——— |
| 34 | " | 0.27 | 2.05 | 4.93 | 1.36 | 0.60 | ——— | ——— | ——— | ——— |
| 35 | " | 0.33 | 1.99 | 4.78 | 1.59 | 0.67 | 2.32 | 1.40 | 38.8 | $20.3 \times 10^{-4}$ |

* ——— omitted due to accuracy of $P_u - P_l$, i.e., when < 0.050 ft, causing an error of > 10% w.r.t. least reading of ± 0.005 ft

Table 3 - Computed Results for System III

| 1 | 2 | 3 | 4 | 5 | 6 | 7 |
|---|---|---|---|---|---|---|
| Run No. | $H_T$ (ft) | $Q_a$ * (scfm) | $Q_w$ * (USGPM) | $E_o$ (%) | $E_p$ (lb/kwhr) | $K_La$ ($hr^{-1}$) |
| 1 | 4.00 | 0.11 | 22.8 | 10.95 | 6.12 | 2.76 |
| 2 | " | 0.17 | " | 8.75 | 5.92 | 3.41 |
| 3 | " | 0.22 | " | 7.70 | 5.98 | 4.11 |
| 4 | " | 0.28 | " | 6.49 | 5.49 | 4.42 |
| 5 | " | 0.33 | " | 5.81 | 5.26 | 4.90 |
| 6 | 4.00 | 0.11 | 10.0 | 3.74 | 5.69 | 0.98 |
| 7 | " | 0.11 | 15.0 | 5.33 | 6.21 | 1.50 |
| 8 | " | 0.22 | 10.0 | 3.23 | 4.91 | 1.86 |
| 9 | " | 0.22 | 15.0 | 4.97 | 5.68 | 2.93 |
| 10 | " | 0.33 | 10.0 | 3.22 | 4.90 | 2.93 |
| 11 | " | 0.33 | 15.0 | 4.13 | 4.99 | 3.83 |
| 12 | 5.00 | 0.11 | 25.2 | 12.61 | 5.51 | 3.17 |
| 13 | " | 0.17 | " | 10.58 | 5.76 | 4.11 |
| 14 | " | 0.23 | " | 8.23 | 5.05 | 4.38 |
| 15 | " | 0.29 | " | 7.97 | 5.30 | 5.45 |
| 16 | " | 0.34 | " | 7.09 | 5.03 | 5.93 |
| 17 | 6.00 | 0.12 | 26.0 | 12.85 | 4.85 | 3.17 |
| 18 | " | 0.18 | " | 9.84 | 4.73 | 3.72 |
| 19 | " | 0.23 | " | 8.40 | 4.54 | 4.34 |
| 20 | " | 0.29 | " | 6.97 | 4.04 | 4.56 |
| 21 | " | 0.35 | " | 6.39 | 3.89 | 5.14 |

*Flows through a cross-sectional area of $\pi/36$ $ft^2$

Table 3 - Computed Results for System III

| 8 | 9 | 10 | 11 | 12 |
|---|---|---|---|---|
| $V_T$ (ft/sec.) | $V_n$ (ft/sec.) | $d_{ave.}$ (mm) | $t_c$ (sec.) | $K_L$ (ft/sec.) |
| 0.22 | 0.58 | 11.0 | 15.94 | $2.42 \times 10^{-4}$ |
| 0.30 | " | 14.2 | 11.91 | 3.44 " |
| 0.36 | " | 17.0 | 10.04 | 4.38 " |
| 0.42 | " | 18.9 | 8.70 | 4.87 " |
| 0.49 | " | 22.1 | 7.55 | 6.03 " |
| 0.91 | 0.26 | 22.1 | 4.28 | 6.41 " |
| 0.54 | 0.38 | 14.0 | 6.94 | 3.82 " |
| 0.79 | 0.26 | 17.6 | 4.95 | 4.19 " |
| 0.46 | 0.38 | 11.2 | 8.15 | 2.55 " |
| 0.74 | 0.26 | 16.9 | 5.32 | 3.92 " |
| 0.53 | 0.38 | 15.2 | 7.18 | 3.42 " |
| 0.26 | 0.64 | 15.2 | 17.44 | 3.55 " |
| 0.36 | " | 18.0 | 12.79 | 4.93 " |
| 0.43 | " | 20.9 | 10.82 | 5.42 " |
| 0.48 | " | 22.8 | 9.77 | 6.53 " |
| 0.53 | " | 25.5 | 8.90 | 7.27 " |
| 0.27 | 0.66 | 16.5 | 20.57 | 3.31 " |
| 0.37 | " | 18.8 | 15.28 | 3.98 " |
| 0.44 | " | 22.5 | 12.89 | 4.93 " |
| 0.50 | " | 25.1 | 11.42 | 5.23 " |
| 0.56 | " | 28.0 | 10.29 | 6.06 " |

Table 3 - Computed Results for System III (continued)

| 1 | 2 | 3 | 4 | 5 | 6 | 7 |
|---|---|---|---|---|---|---|
| 22 | 7.00 | 0.12 | 24.0 | 15.25 | 5.39 | 3.76 |
| 23 | " | 0.18 | " | 12.19 | 5.36 | 4.62 |
| 24 | " | 0.24 | " | 10.16 | 5.06 | 5.28 |
| 25 | " | 0.30 | " | 8.76 | 4.64 | 5.83 |
| 26 | " | 0.36 | " | 7.46 | 4.11 | 6.11 |
| 27 | 8.00 | 0.12 | 23.0 | 14.91 | 5.06 | 3.45 |
| 28 | " | 0.18 | " | 10.49 | 4.36 | 3.76 |
| 29 | " | 0.25 | " | 9.45 | 4.41 | 4.63 |
| 30 | " | 0.31 | " | 8.53 | 4.31 | 5.32 |
| 31 | " | 0.37 | " | 8.43 | 4.47 | 6.45 |
| 32 | 9.00 | 0.13 | 10.0 | 7.16 | 4.83 | 1.69 |
| 33 | " | 0.13 | 15.0 | 14.37 | 7.04 | 3.49 |
| 34 | " | 0.25 | 10.0 | 5.11 | 3.40 | 2.55 |
| 35 | " | 0.25 | 15.0 | 7.57 | 3.96 | 3.86 |
| 36 | " | 0.38 | 10.0 | 4.87 | 3.25 | 3.83 |
| 37 | " | 0.38 | 15.0 | 5.66 | 3.06 | 4.52 |
| 38 | 9.00 | 0.13 | 22.0 | 17.56 | 4.61 | 4.07 |
| 39 | " | 0.19 | " | 11.05 | 3.59 | 3.97 |
| 40 | " | 0.25 | " | 12.42 | 4.65 | 6.08 |
| 41 | " | 0.31 | " | 11.23 | 4.65 | 7.00 |
| 42 | " | 0.38 | " | 9.43 | 4.16 | 7.21 |

Table 3 - Computed Results for System III (continued)

| 8 | 9 | 10 | 11 | 12 |
|---|---|---|---|---|
| 0.25 | 0.61 | 13.0 | 26.23 | $2.45 \times 10^{-4}$ |
| 0.34 | " | 16.9 | 19.51 | 3.53 " |
| 0.41 | " | 19.3 | 16.30 | 4.10 " |
| 0.46 | " | 22.1 | 14.54 | 4.69 " |
| 0.51 | " | 24.0 | 13.28 | 4.86 " |
| 0.25 | 0.59 | 12.4 | 30.29 | 1.89 " |
| 0.33 | " | 16.6 | 23.10 | 2.42 " |
| 0.40 | " | 18.0 | 19.27 | 2.89 " |
| 0.47 | " | 21.0 | 16.20 | 3.70 " |
| 0.53 | " | 24.0 | 14.73 | 4.70 " |
| 0.69 | 0.26 | 15.6 | 12.94 | 2.75 " |
| 0.45 | 0.38 | 10.4 | 19.56 | 2.51 " |
| 0.64 | 0.26 | 12.5 | 14.11 | 1.53 " |
| 0.47 | 0.38 | 12.1 | 18.94 | 1.69 " |
| 0.61 | 0.26 | 12.2 | 14.97 | 1.41 " |
| 0.49 | 0.38 | 14.0 | 18.32 | 1.56 " |
| 0.21 | 0.56 | 10.4 | 40.93 | 1.40 " |
| 0.28 | " | 13.0 | 30.96 | 1.51 " |
| 0.35 | " | 16.7 | 24.98 | 2.76 " |
| 0.42 | " | 18.5 | 20.92 | 3.38 " |
| 0.49 | " | 21.0 | 18.08 | 3.79 " |

Table 4 - Computed Results for System IV

| 1 | 2 | 3 | 4 | 5 | 6 | 7 | 8 | 9 | 10 |
|---|---|---|---|---|---|---|---|---|---|
| Run No. | $H_b$ (ft) | $Q_a$ * (scfm) | $Q_w$ * (USGPM) | $E_o$ ( % ) | $E_P$ (lb/kwhr) | $K_La$ ($hr^{-1}$) | $V_n$ (ft/sec.) | $V_T$ (ft/sec.) | $t_{cR}$ (sec.) |
| 1 | 3.00 | 0.11 | 58.0 | 10.62 | 1.90 | 2.74 | 1.48 | 0.32 | 9.37 |
| 2 | " | 0.16 | 60.0 | 8.89 | 2.04 | 3.56 | 1.53 | 0.35 | 8.48 |
| 3 | " | 0.21 | 62.0 | 7.71 | 2.04 | 4.24 | 1.58 | 0.39 | 7.63 |
| 4 | " | 0.26 | 64.0 | 7.70 | 2.22 | 5.38 | 1.63 | 0.41 | 7.32 |
| 5 | " | 0.32 | 65.0 | 7.36 | 2.33 | 6.28 | 1.66 | 0.42 | 7.20 |
| 6 | 4.00 | 0.11 | 59.0 | 12.78 | 2.12 | 3.38 | 1.51 | 0.37 | 10.95 |
| 7 | " | 0.16 | 61.0 | 10.65 | 2.21 | 4.28 | 1.56 | 0.43 | 9.33 |
| 8 | " | 0.21 | 63.0 | 9.51 | 2.30 | 5.18 | 1.61 | 0.47 | 8.50 |
| 9 | " | 0.26 | 65.0 | 8.91 | 2.38 | 6.14 | 1.66 | 0.51 | 7.87 |
| 10 | " | 0.32 | 66.0 | 8.17 | 2.39 | 6.83 | 1.68 | 0.52 | 7.69 |
| 11 | 5.01 | 0.11 | 62.0 | 13.47 | 1.97 | 3.42 | 1.58 | 0.51 | 9.92 |
| 12 | " | 0.16 | 64.0 | 11.09 | 2.05 | 4.28 | 1.64 | 0.54 | 9.21 |
| 13 | " | 0.21 | 65.0 | 10.14 | 2.24 | 5.32 | 1.66 | 0.61 | 8.17 |
| 14 | " | 0.26 | 66.0 | 9.08 | 2.22 | 6.07 | 1.68 | 0.60 | 8.34 |
| 15 | " | 0.32 | 67.0 | 9.03 | 2.46 | 7.39 | 1.71 | 0.60 | 8.32 |
| 16 | 6.01 | 0.11 | 62.0 | 14.00 | 2.01 | 3.42 | 1.58 | 0.53 | 11.32 |
| 17 | " | 0.16 | 64.0 | 12.83 | 2.30 | 4.76 | 1.64 | 0.57 | 10.55 |
| 18 | " | 0.21 | 65.0 | 11.45 | 2.39 | 5.76 | 1.66 | 0.59 | 10.10 |
| 19 | " | 0.26 | 66.0 | 11.45 | 2.77 | 7.32 | 1.68 | 0.66 | 9.05 |
| 20 | " | 0.32 | 67.0 | 12.08 | 3.18 | 9.38 | 1.71 | 0.66 | 9.15 |

*Flows through a cross-sectional area of $\pi/36$ $ft^2$

Table 4 - Computed Results for System IV (continued)

| 1 | 2 | 3 | 4 | 5 | 6 | 7 | 8 | 9 | 10 |
|---|---|---|---|---|---|---|---|---|---|
| 21 | 6.01 | 0.11 | 69.0 | 16.78 | 1.91 | 4.10 | 1.76 | 0.65 | 9.25 |
| 22 | " | 0.11 | 74.0 | 17.74 | 1.77 | 4.38 | 1.89 | 0.83 | 7.34 |
| 23 | " | 0.21 | 69.0 | 12.45 | 2.42 | 6.25 | 1.76 | 0.71 | 8.46 |
| 24 | " | 0.21 | 74.0 | 14.53 | 2.47 | 7.42 | 1.89 | 0.78 | 7.70 |
| 25 | " | 0.32 | 69.0 | 12.17 | 3.09 | 9.45 | 1.76 | 0.71 | 8.46 |
| 26 | " | 0.32 | 74.0 | 15.74 | 3.49 | 12.42 | 1.89 | 0.70 | 8.58 |
| 27 | 7.01 | 0.11 | 63.0 | 17.32 | 2.34 | 3.97 | 1.60 | 0.56 | 12.41 |
| 28 | " | 0.16 | 65.0 | 14.19 | 2.42 | 5.01 | 1.66 | 0.64 | 11.00 |
| 29 | " | 0.21 | 66.0 | 12.57 | 2.50 | 5.97 | 1.69 | 0.66 | 10.61 |
| 30 | " | 0.26 | 67.0 | 12.11 | 2.70 | 7.28 | 1.71 | 0.71 | 9.94 |
| 31 | " | 0.32 | 68.0 | 13.52 | 3.35 | 9.86 | 1.74 | 0.72 | 9.74 |
| 32 | 8.02 | 0.11 | 63.0 | 18.99 | 2.50 | 4.28 | 1.61 | 0.56 | 14.32 |
| 33 | " | 0.16 | 65.0 | 16.36 | 2.72 | 5.59 | 1.66 | 0.67 | 11.96 |
| 34 | " | 0.21 | 66.0 | 14.97 | 2.90 | 6.90 | 1.68 | 0.73 | 11.00 |
| 35 | " | 0.26 | 68.0 | 14.13 | 3.00 | 8.28 | 1.74 | 0.76 | 10.51 |

Table 5 - Comparison of Computed Results For All Four Systems

| | SYSTEM | | | | |
|---|---|---|---|---|---|
| | I | II | III | IV | |
| Parameter | | | | | Units |
| $E_p$ | 2.65 - 3.65 | 2.81 - 6.65 | 3.88 - 6.10 | 1.90 - 3.35 | lb/kwhr |
| $E_o$ | 0.65 - 3.95 | 1.98 - 4.90 | 5.80 - 17.6 | 7.40 - 19.0 | % |
| $^*K_La_{20}$ | 7.79 - 25.25 | 0.77 - 2.41 | 3.22 - 7.75 | 3.03 - 9.86 | $hr^{-1}$ |
| $^*K_{L_{20}}$ (overall) | $(1.77-6.12)\times10^{-4}$ | $(8.32-21.4)\times10^{-4}$ | $(1.67-7.63)\times10^{-4}$ | ——— | ft/sec. |
| $K_L$ (10 mm bubble) | $1.36 \times 10^{-4}$ | $3.70 \times 10^{-4}$ | $1.70 \times 10^{-4}$ | ——— | ft/sec. |
| $K_L$ (25 mm bubble) | $4.45 \times 10^{-4}$ | $10.8 \times 10^{-4}$ | $5.78 \times 10^{-4}$ | ——— | ft/sec. |
| $t_{cu}$ | 0.87 - 1.10 | 0.40 - 0.42 | 1.77 - 4.31 | 1.79 - 2.40 (downflow side only) | sec/ft |

* $K_La_{20}$ and $K_{L_{20}}$ obtained from Equations 18 and 44 respectively.

Table 6 - Computed Results for Porous Diffusers - System II

| 1 | 2 | 3 | 4 | 5 | 6 |
|---|---|---|---|---|---|
| Run No. | $H_T$ (ft) | $Q_a$ * (scfm) | $E_o$ (%) | $E_p$ (lb/kwhr) | $K_La$ ($hr^{-1}$) |
| 1 | 9.25 | 0.13 | 9.04 | 7.96 | 2.24 |
| 2 | " | 0.25 | 5.92 | 5.28 | 2.97 |
| 3 | " | 0.38 | 5.36 | 4.79 | 4.04 |
| 4 | 6.25 | 0.12 | 7.72 | 9.85 | 1.97 |
| 5 | " | 0.24 | 5.46 | 7.01 | 2.80 |
| 6 | " | 0.35 | 4.75 | 6.13 | 3.66 |
| 7 | 3.25 | 0.11 | 5.22 | 12.45 | 1.38 |
| 8 | " | 0.22 | 4.35 | 10.41 | 2.32 |
| 9 | " | 0.33 | 3.74 | 9.00 | 3.01 |

*Flows through a cross-sectional area of $\pi/36$ $ft^2$

Fisher Scientific Porous Stones

Table 7 - Computed Results for Porous Diffusers - System II

| 1 | 2 | 3 | 4 | 5 | 6 |
|---|---|---|---|---|---|
| Run No. | $H_T$ (ft) | $Q_a$ * (scfm) | $E_o$ (%) | $E_p$ (lb/kwhr) | $K_La$ ($hr^{-1}$) |
| 1 | 9.25 | 0.13 | 8.38 | 7.40 | 2.14 |
| 2 | " | 0.25 | 5.86 | 5.21 | 3.00 |
| 3 | " | 0.38 | 4.57 | 4.08 | 3.52 |
| 4 | 6.25 | 0.12 | 7.65 | 9.76 | 2.00 |
| 5 | " | 0.24 | 5.28 | 6.79 | 2.80 |
| 6 | " | 0.35 | 4.01 | 5.16 | 3.18 |
| 7 | 3.25 | 0.11 | 5.02 | 11.98 | 1.35 |
| 8 | " | 0.22 | 3.57 | 8.54 | 1.93 |
| 9 | " | 0.33 | 2.86 | 6.86 | 2.35 |

*Flows through a cross-sectional area of $\pi/36$ $ft^2$

Norton Company Porous Plates

| SYSTEM AND RUN No. | AIRFLOW RATE (scfm) | OXYGEN TRANSFER RATE - mg/l/hr | | |
|---|---|---|---|---|
| | | PROBE A | PROBE B | % DIFFERENCE |
| II - 24 | 0.10 | 17.55 | 17.38 | 0.97 |
| II - 25 | 0.20 | 29.00 | 32.00 | 9.37 |
| II - 26 | 0.30 | 39.80 | 39.20 | 1.51 |
| II - 27 | 0.40 | 48.20 | 48.20 | 0.00 |
| II - 28 | 0.50 | 54.30 | 54.40 | 0.18 |
| | | | | AVG. = 2.41 |
| III - 29 | 0.10 | 35.90 | 36.10 | 0.55 |
| III - 30 | 0.10 | 40.50 | 40.65 | 0.37 |
| III - 31 | 0.15 | 47.90 | 46.60 | 2.72 |
| III - 32 | 0.15 | 60.40 | 57.70 | 4.47 |
| | | | | AVG. = 2.03 |
| IV - 54 | 0.10 | 49.10 | 46.40 | 5.50 |
| IV - 55 | 0.10 | 45.70 | 44.80 | 1.97 |
| IV - 56 | 0.10 | 44.00 | 42.60 | 3.18 |
| IV - 66 | 0.15 | 56.40 | 53.80 | 4.61 |
| IV - 67 | 0.15 | 57.20 | 53.40 | 6.64 |
| IV - 68 | 0.15 | 58.50 | 58.50 | 0.00 |
| | | | | AVG. = 3.65 |

Table 8 : Comparison of Oxygen Transfer Rates For Different Probe Positions

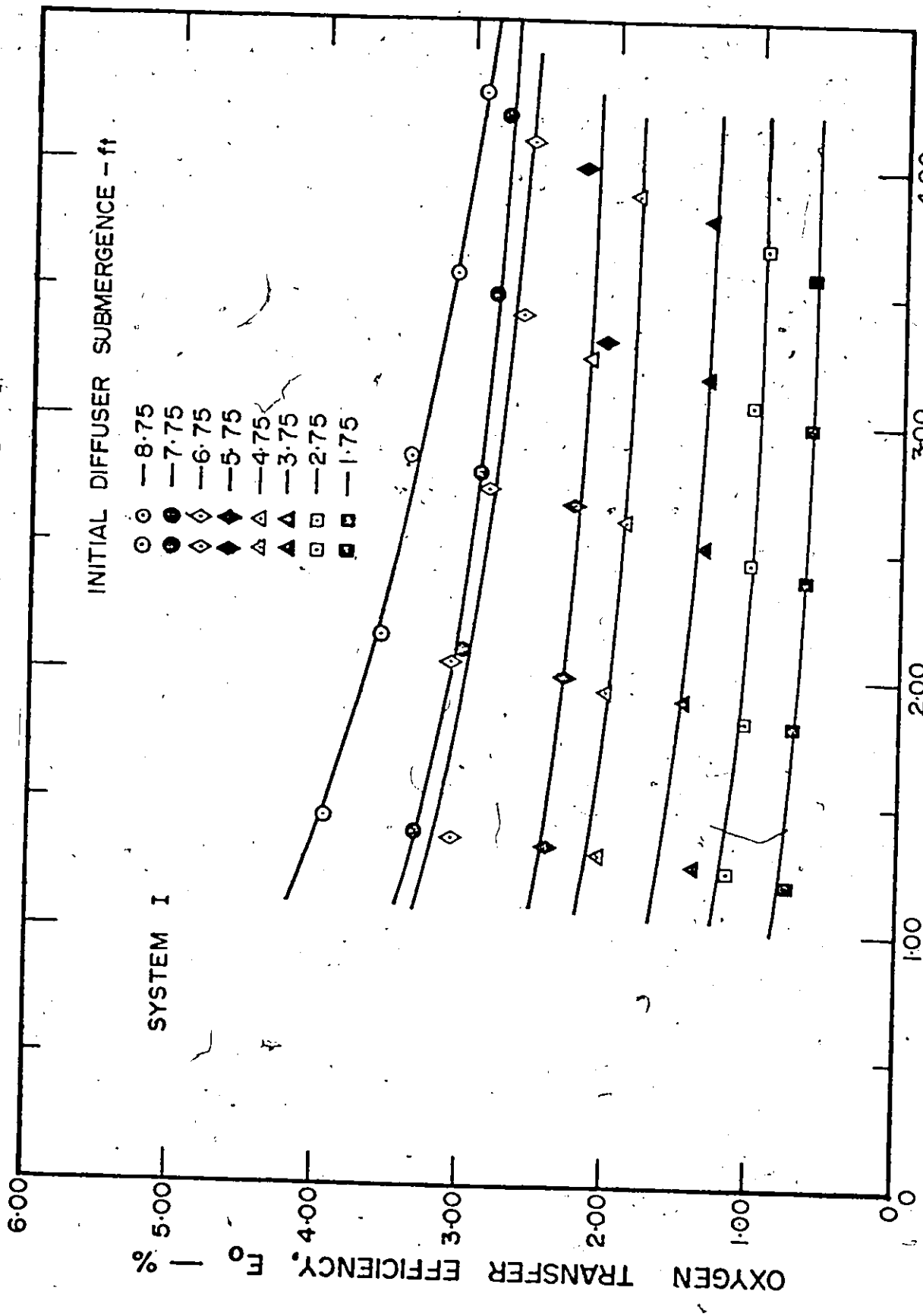


Figure 15 - Effect of Diffuser Submergence and Airflow Rate on Oxygen Transfer Efficiency, System I

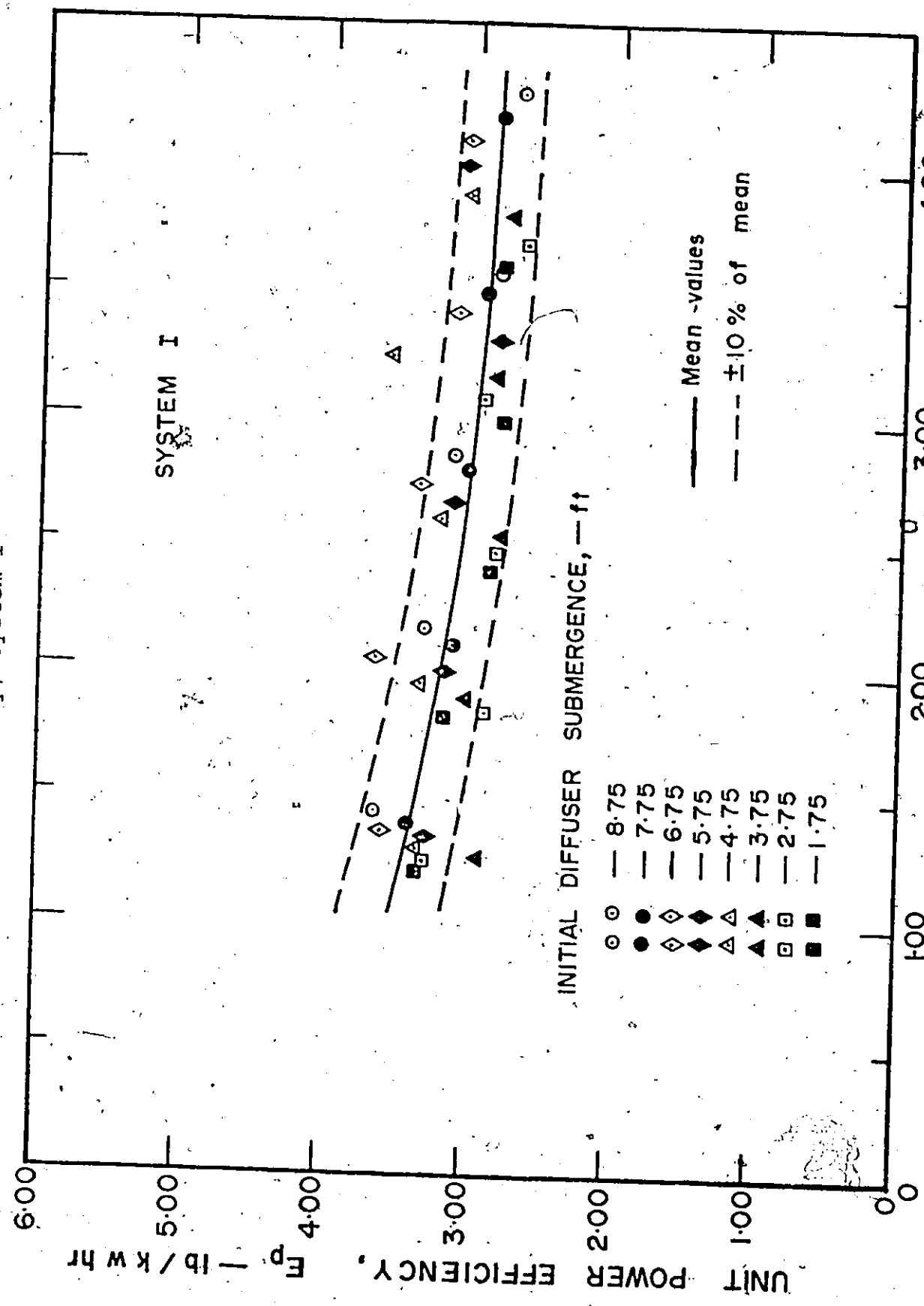


Figure 16 - Effect of Diffuser Submergence and Airflow Rate on Unit Power Efficiency, System I

Figure 17 - Effect of Diffuser Submergence and Airflow Rate on the Overall Transfer Coefficient, System I

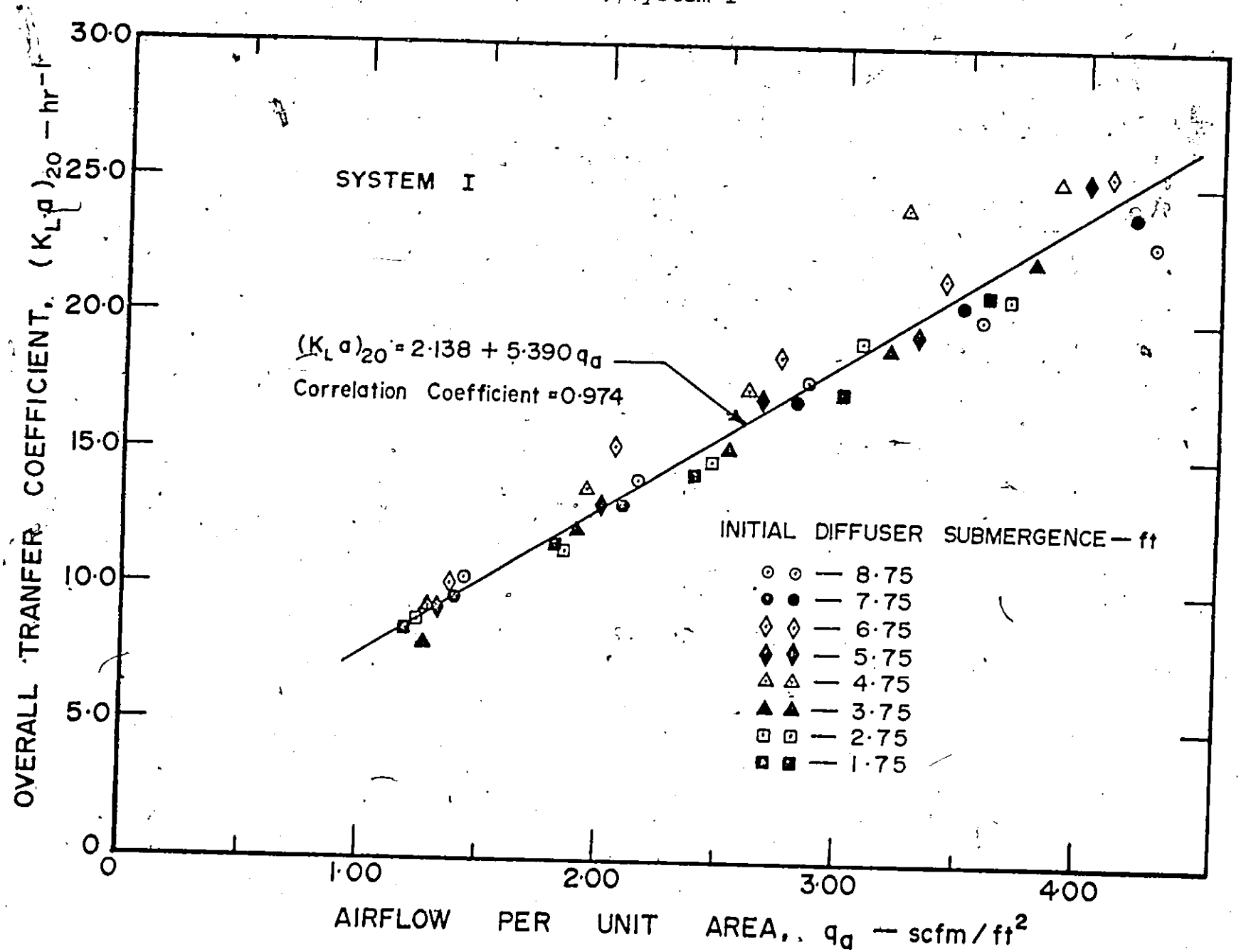

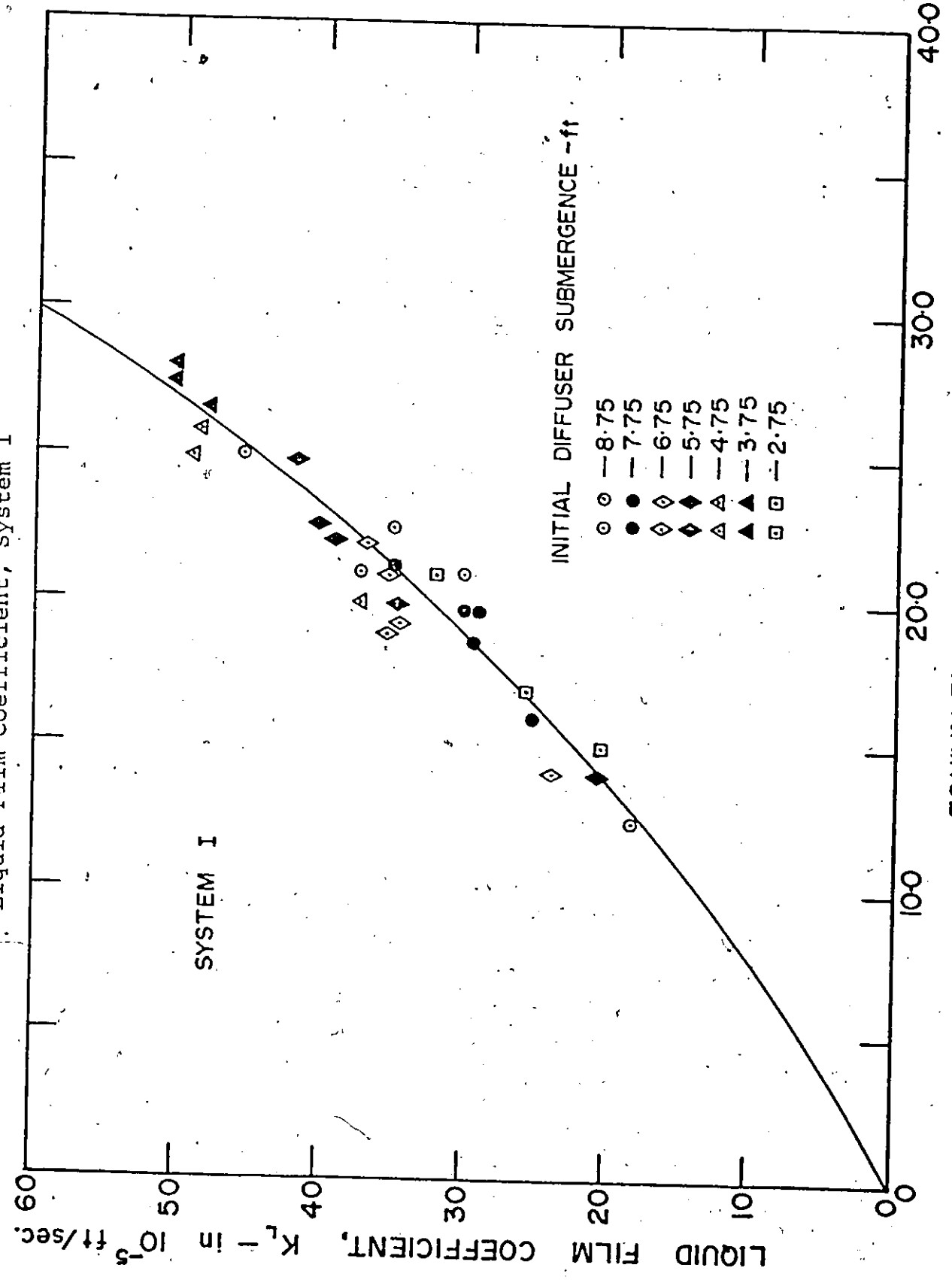


Figure 18 - Effect of Bubble Size and Diffuser Submergence on the Liquid Film Coefficient, System I

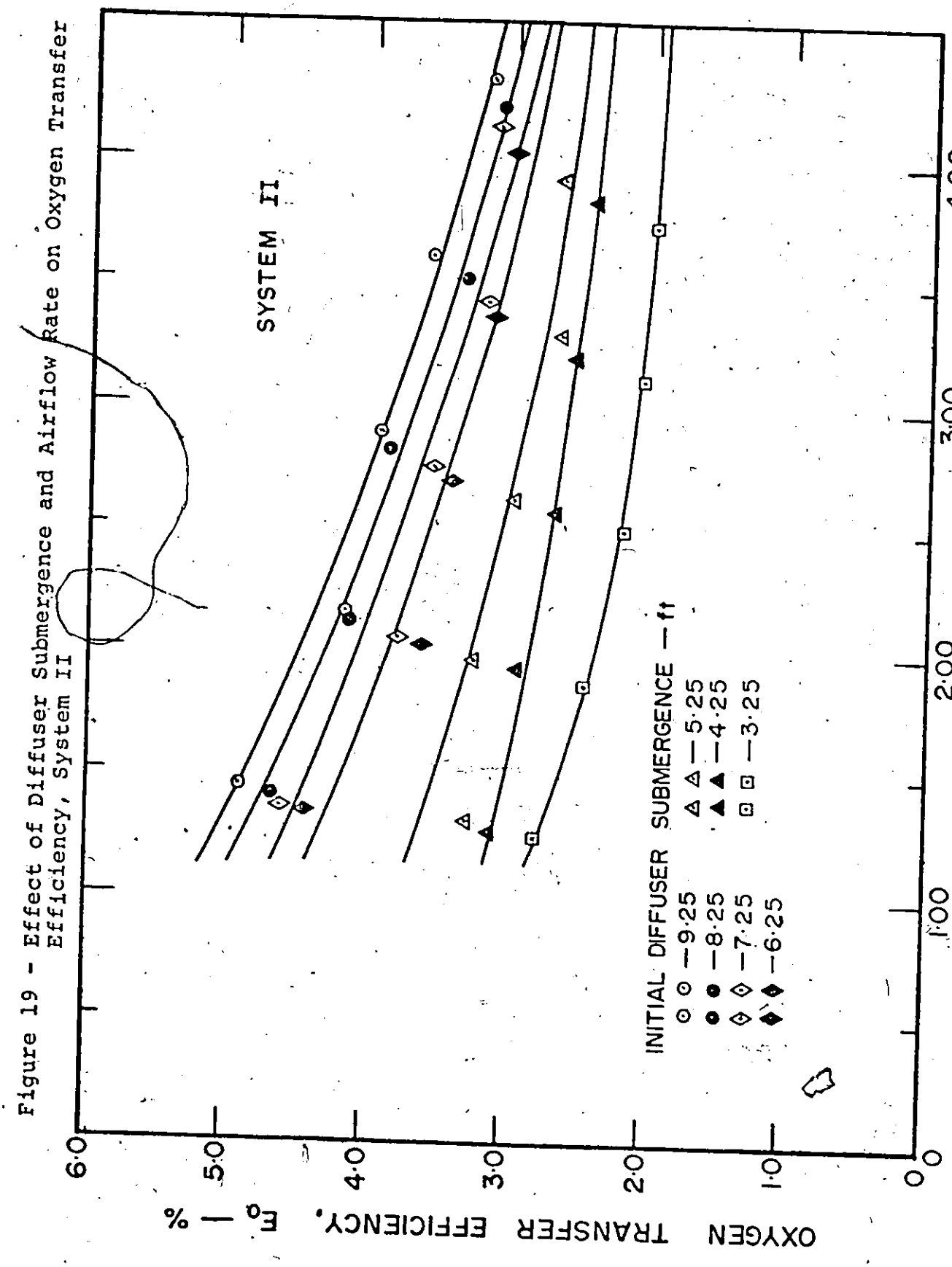


Figure 19 - Effect of Diffuser Submergence and Airflow Rate on Oxygen Transfer Efficiency, System II

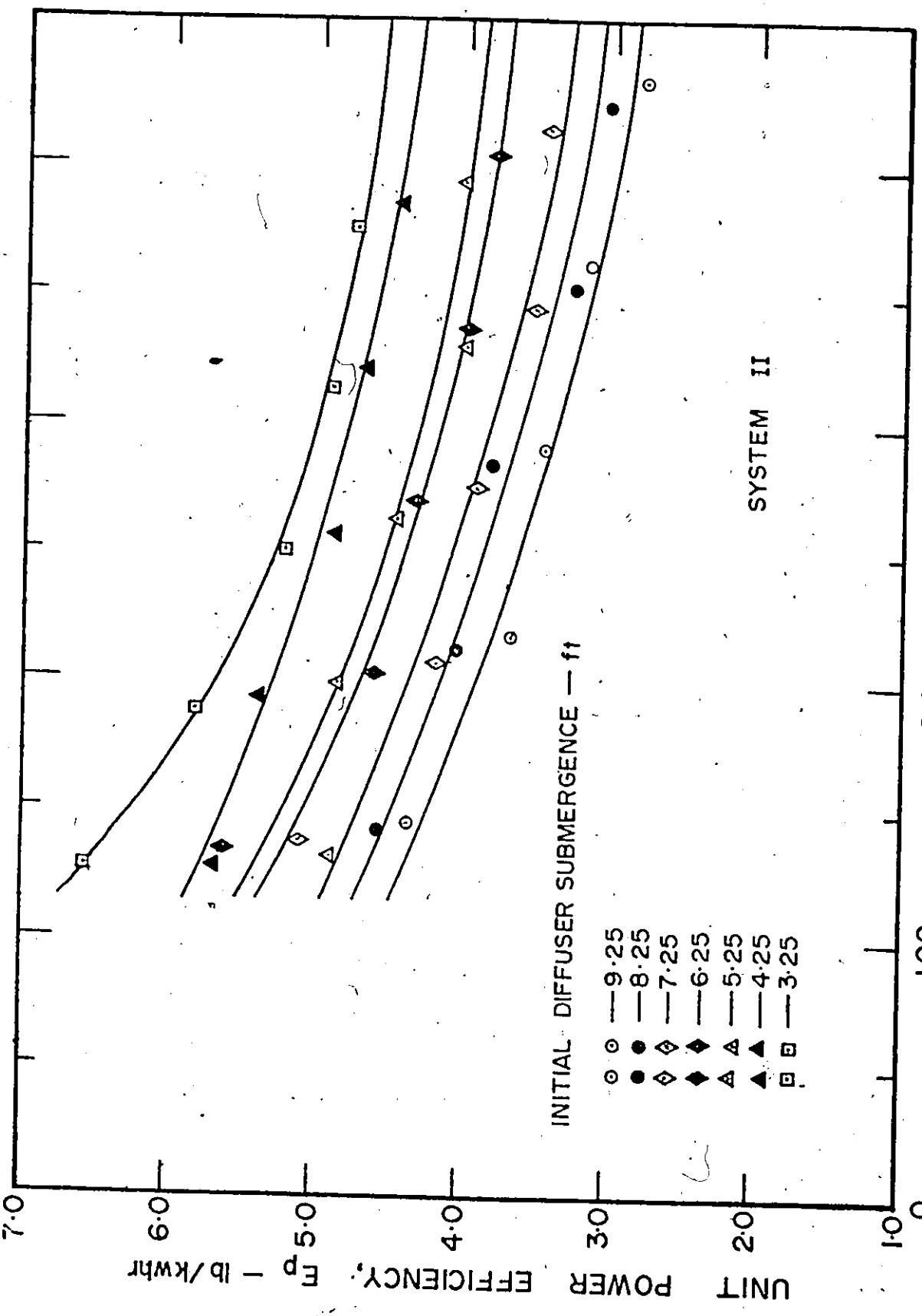


Figure 20 - Effect of Diffuser Submergence and Airflow Rate on Unit Power Efficiency, System II

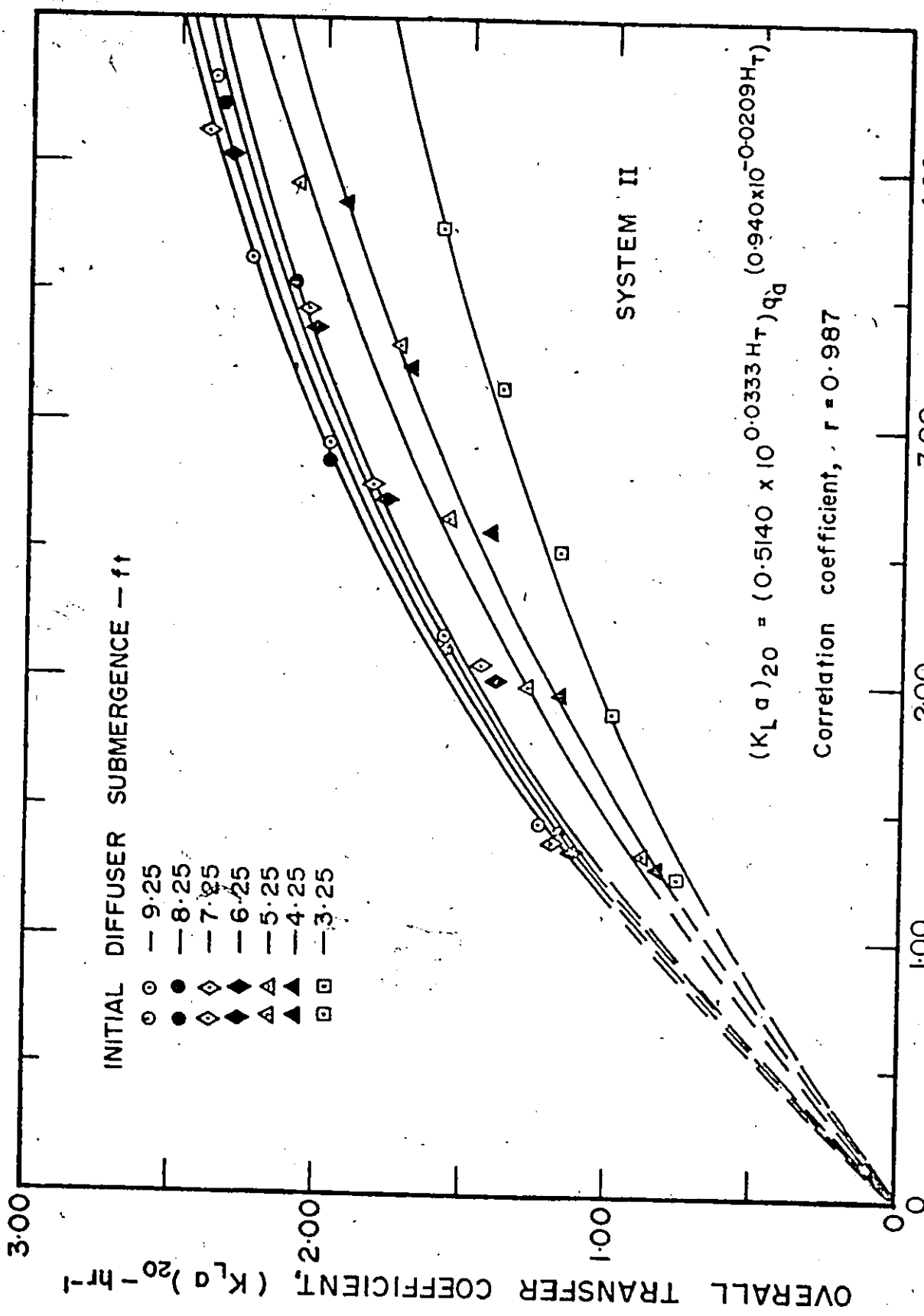


Figure 21 - Effect of Diffuser Submergence and Airflow Rate on the Overall Transfer Coefficient, System II

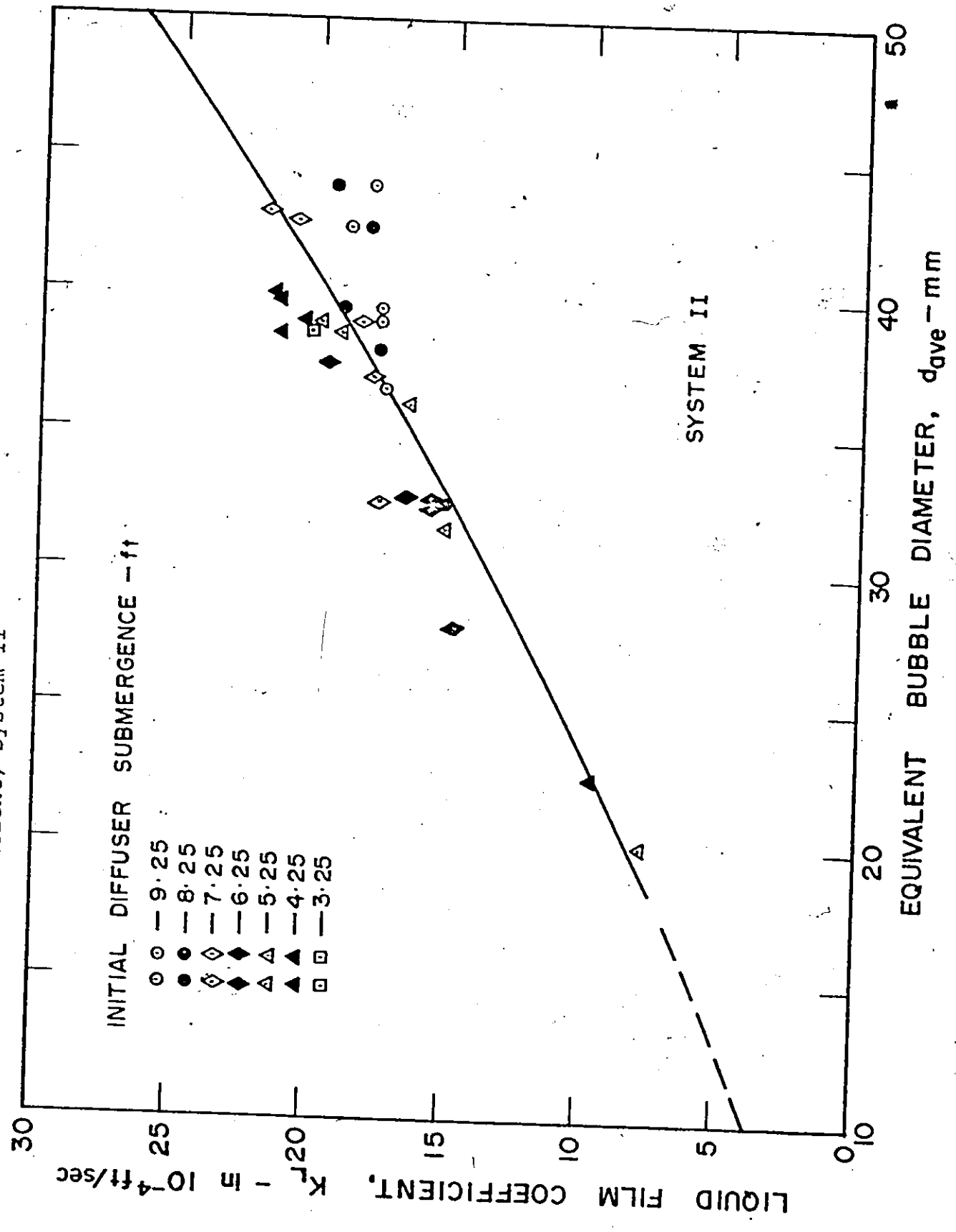


Figure 22 - Effect of Diffuser Submergence and Bubble Size on the Liquid Film Coefficient, System II

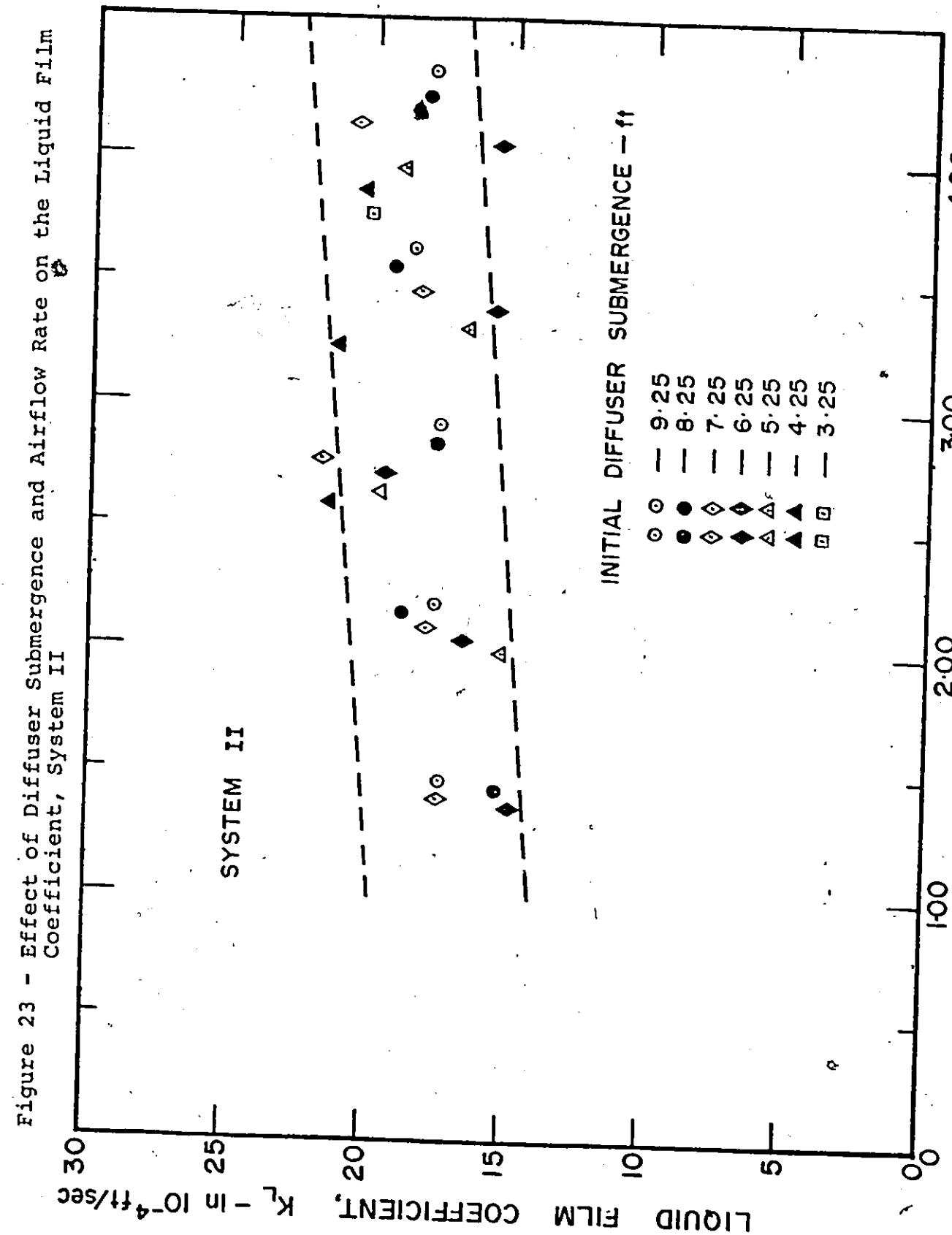


Figure 23 - Effect of Diffuser Submergence and Airflow Rate on the Liquid Film Coefficient, System II

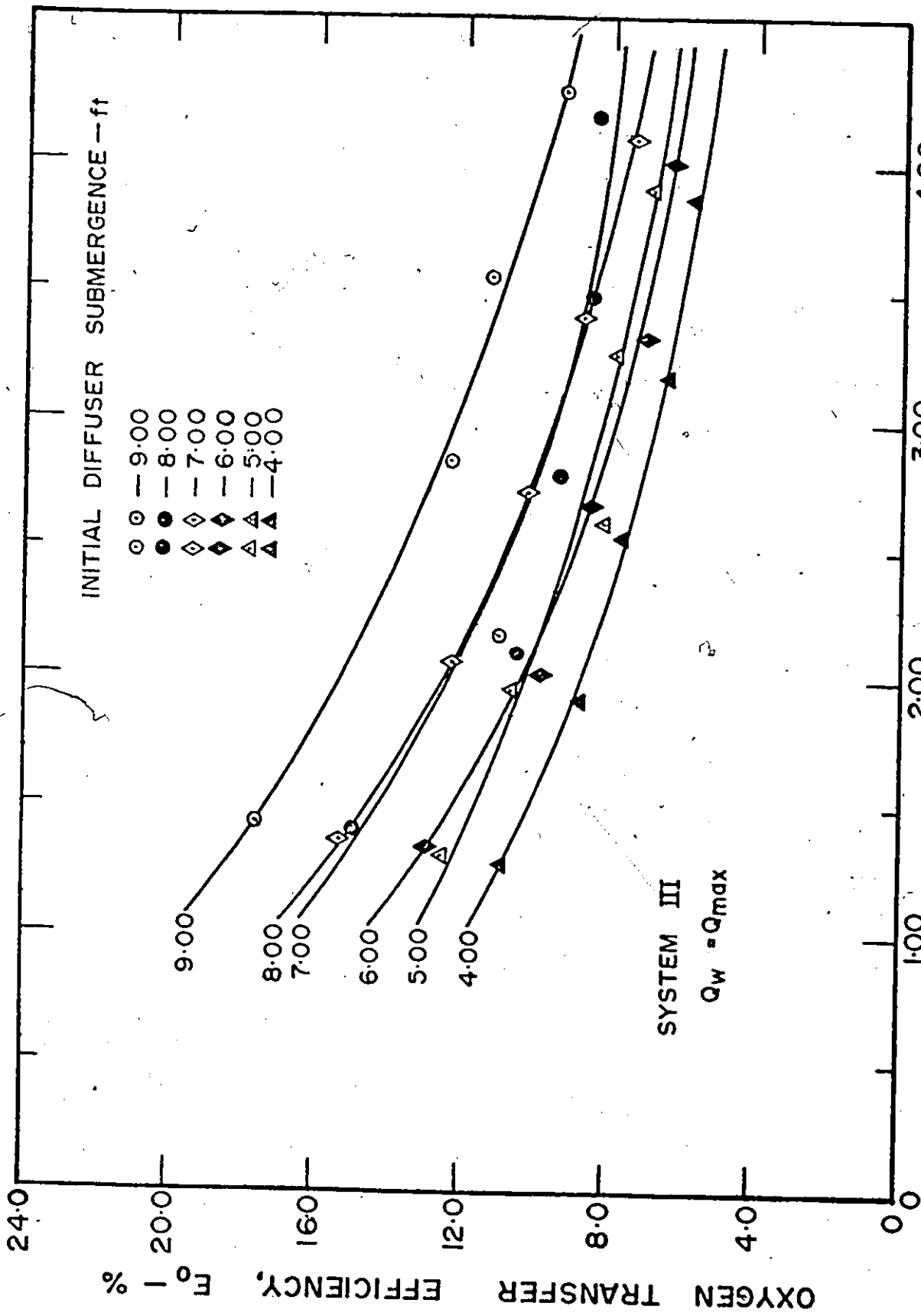


Figure 24 - Effect of Diffuser Submergence and Airflow Rate on Oxygen Transfer Efficiency, System III

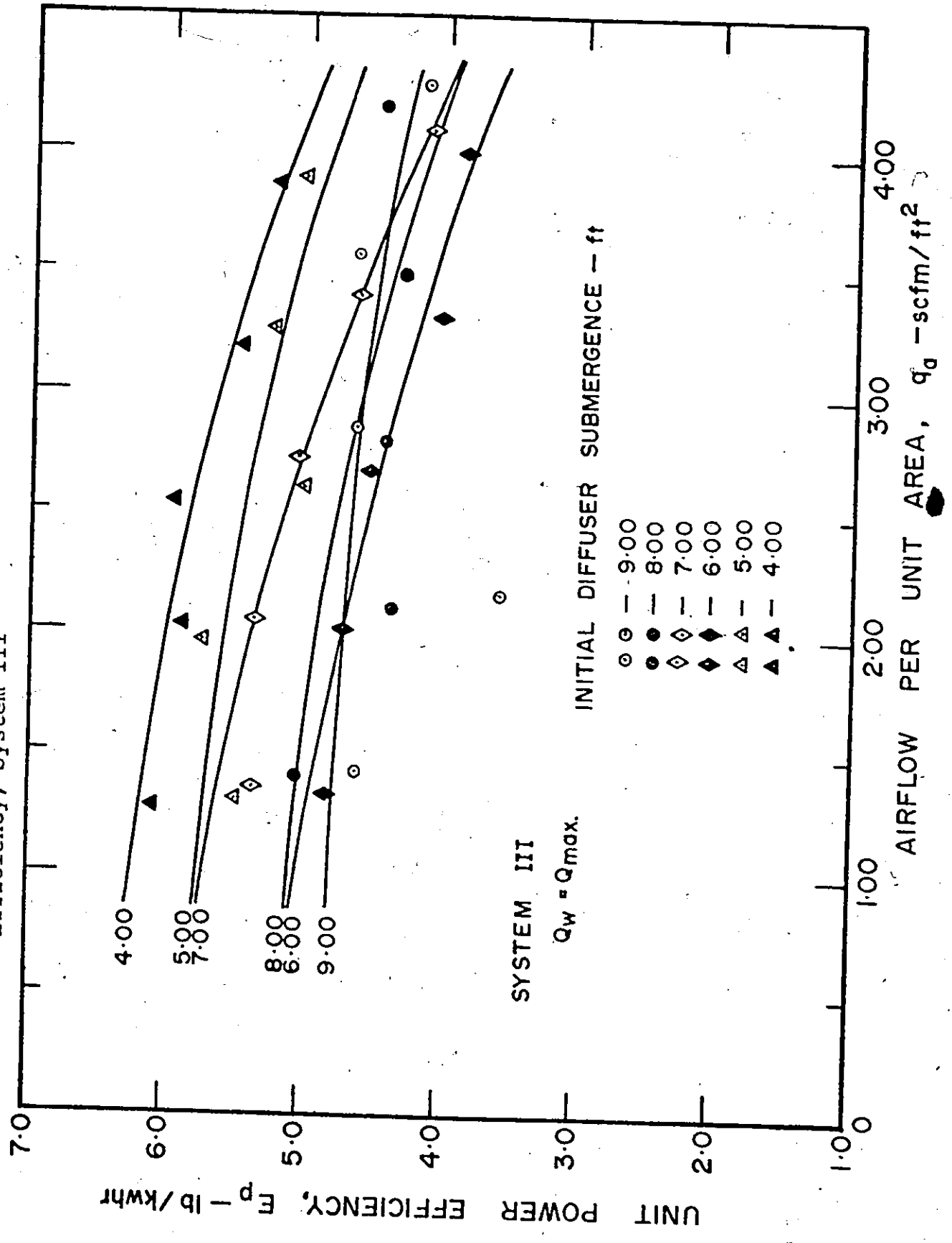


Figure 25 - Effect of Diffuser Submergence and Airflow Rate on Unit Power Efficiency, System III

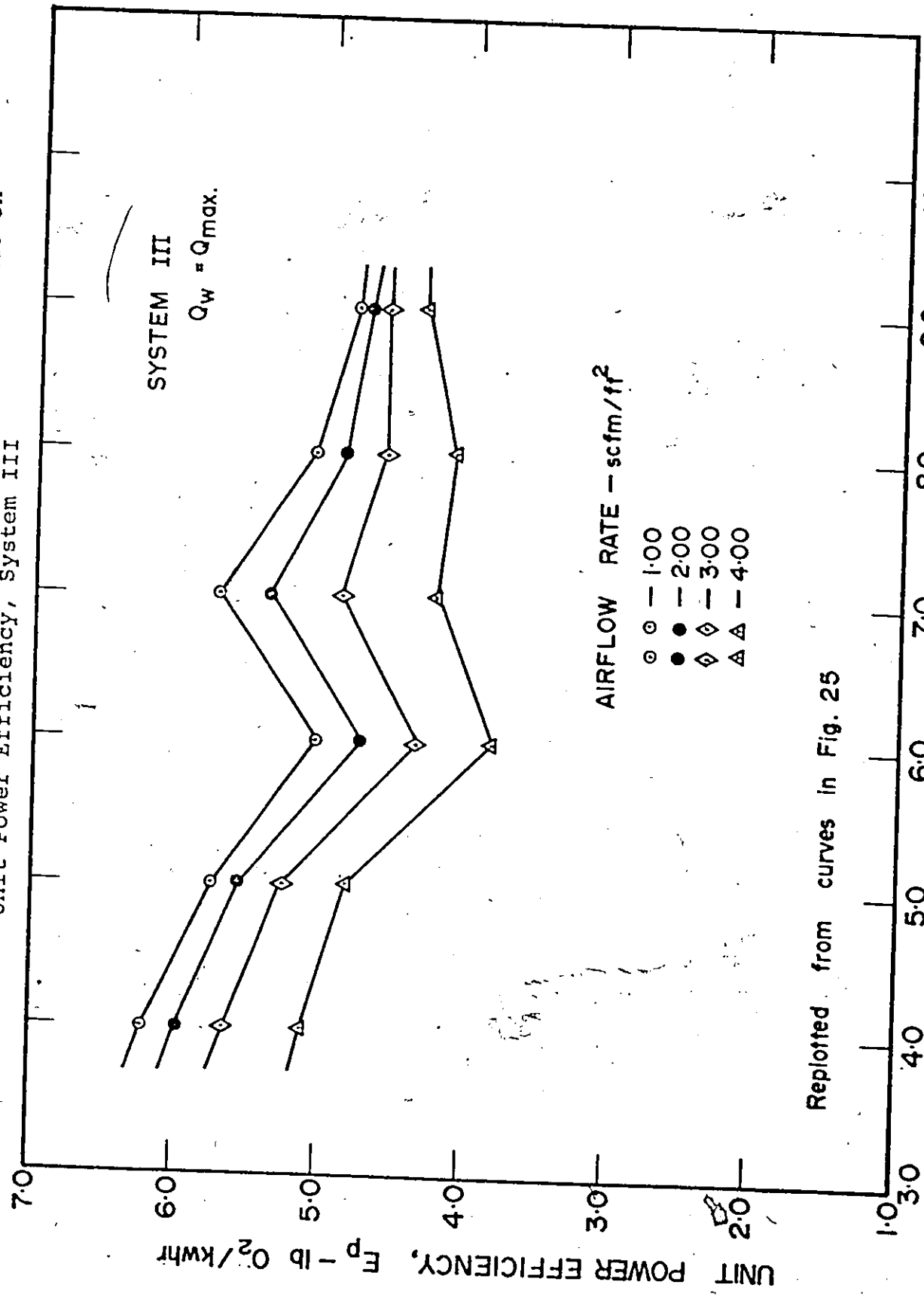


Figure 26 - Effect of Diffuser Submergence and Airflow Rate on Unit Power Efficiency, System III

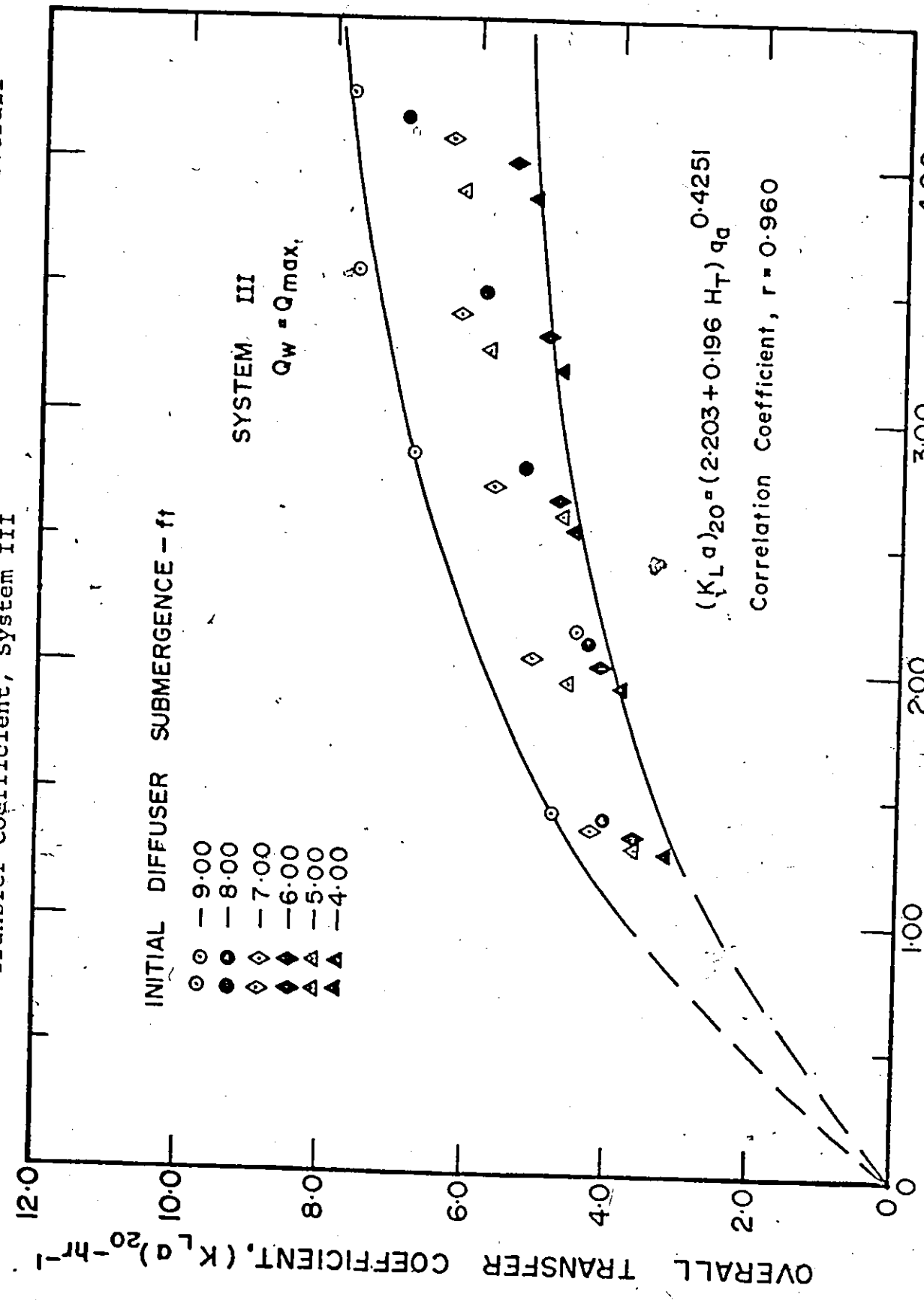


Figure 27 - Effect of Diffuser Submergence and Airflow Rate on the Overall Transfer Coefficient, System III

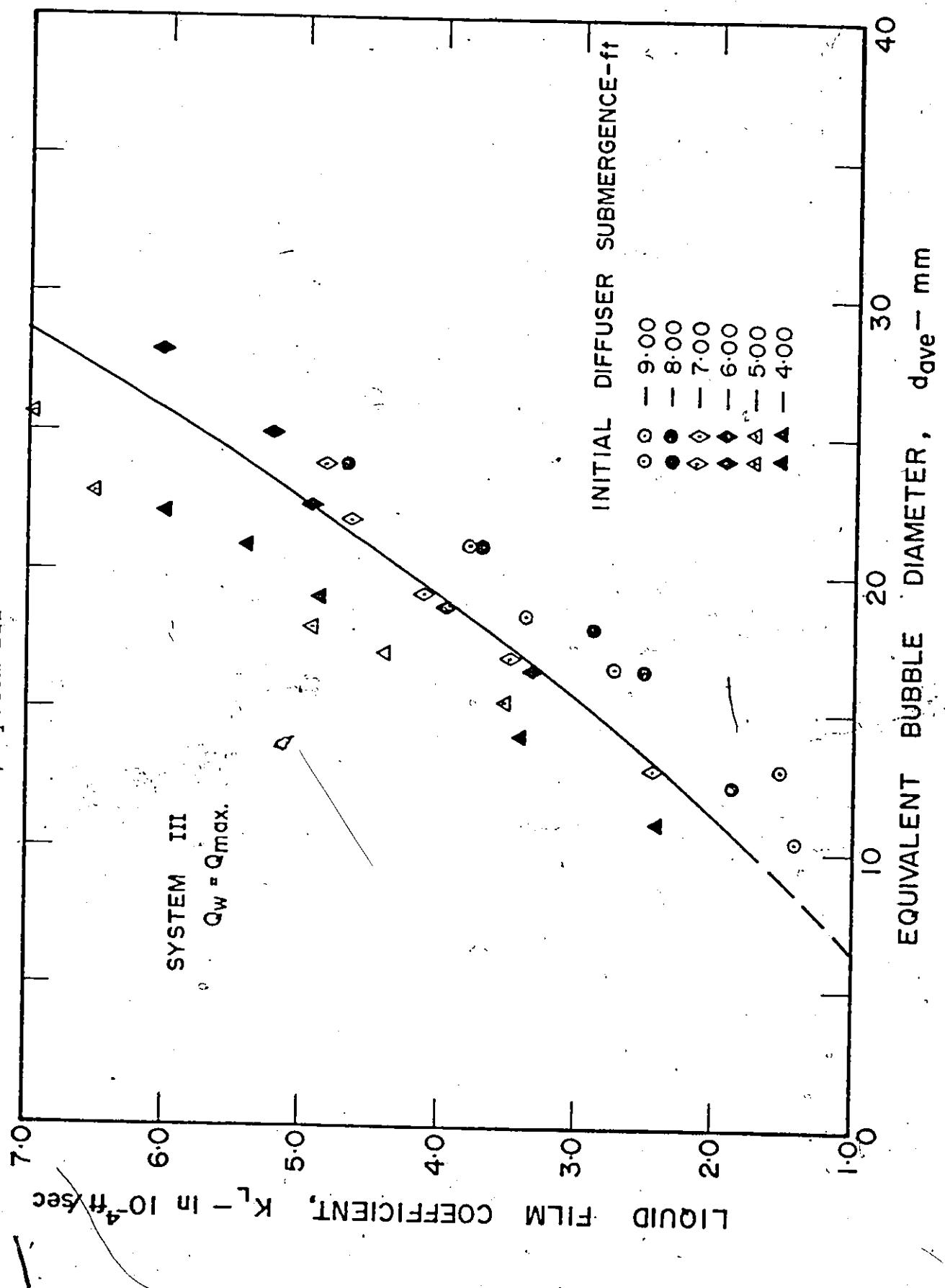


Figure 28 - Effect of Diffuser Submergence and Bubble Size on the Liquid Film Coefficient, System III

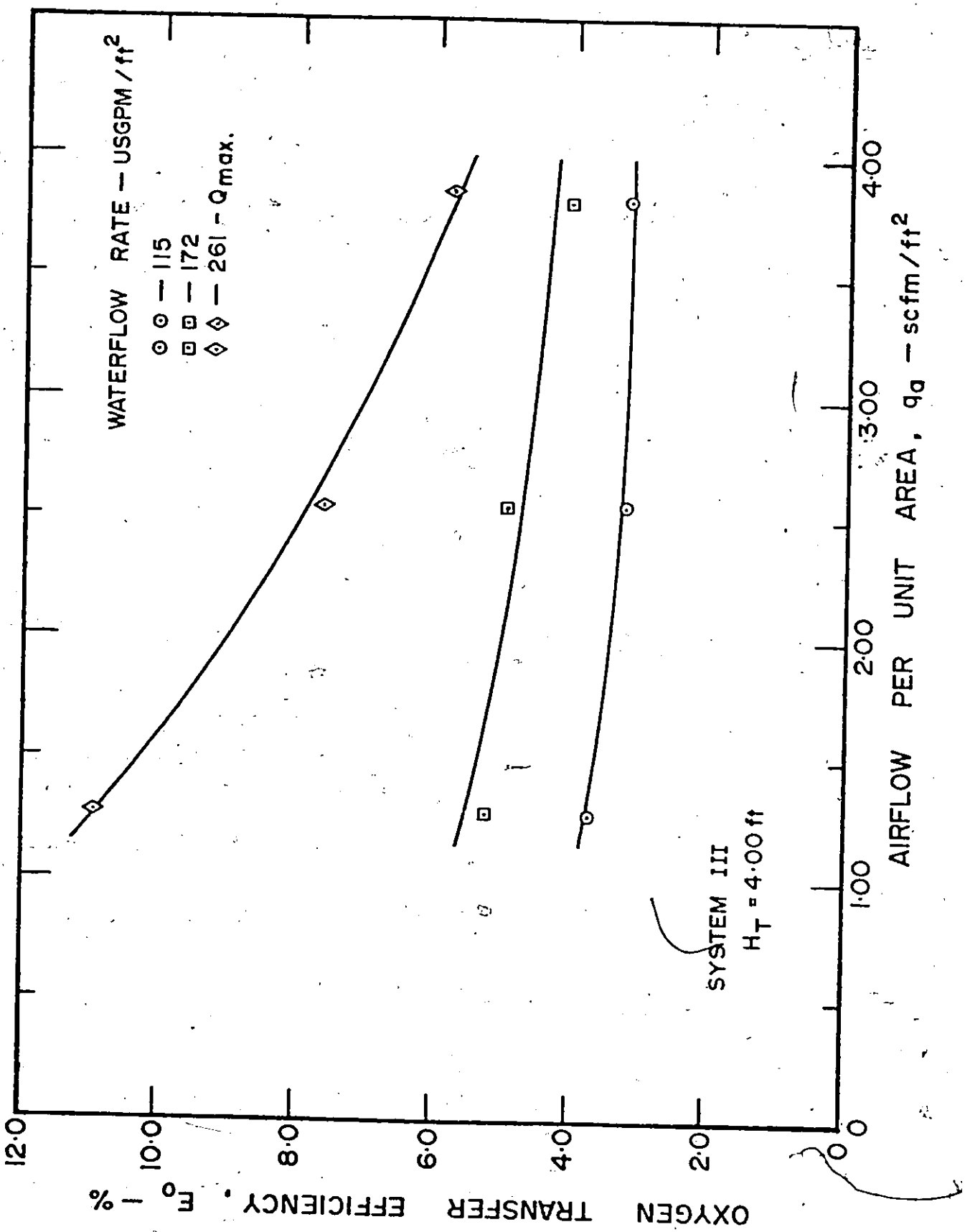


Figure 29 - Effect of Different Operating Conditions on Oxygen Transfer Efficiency, System III

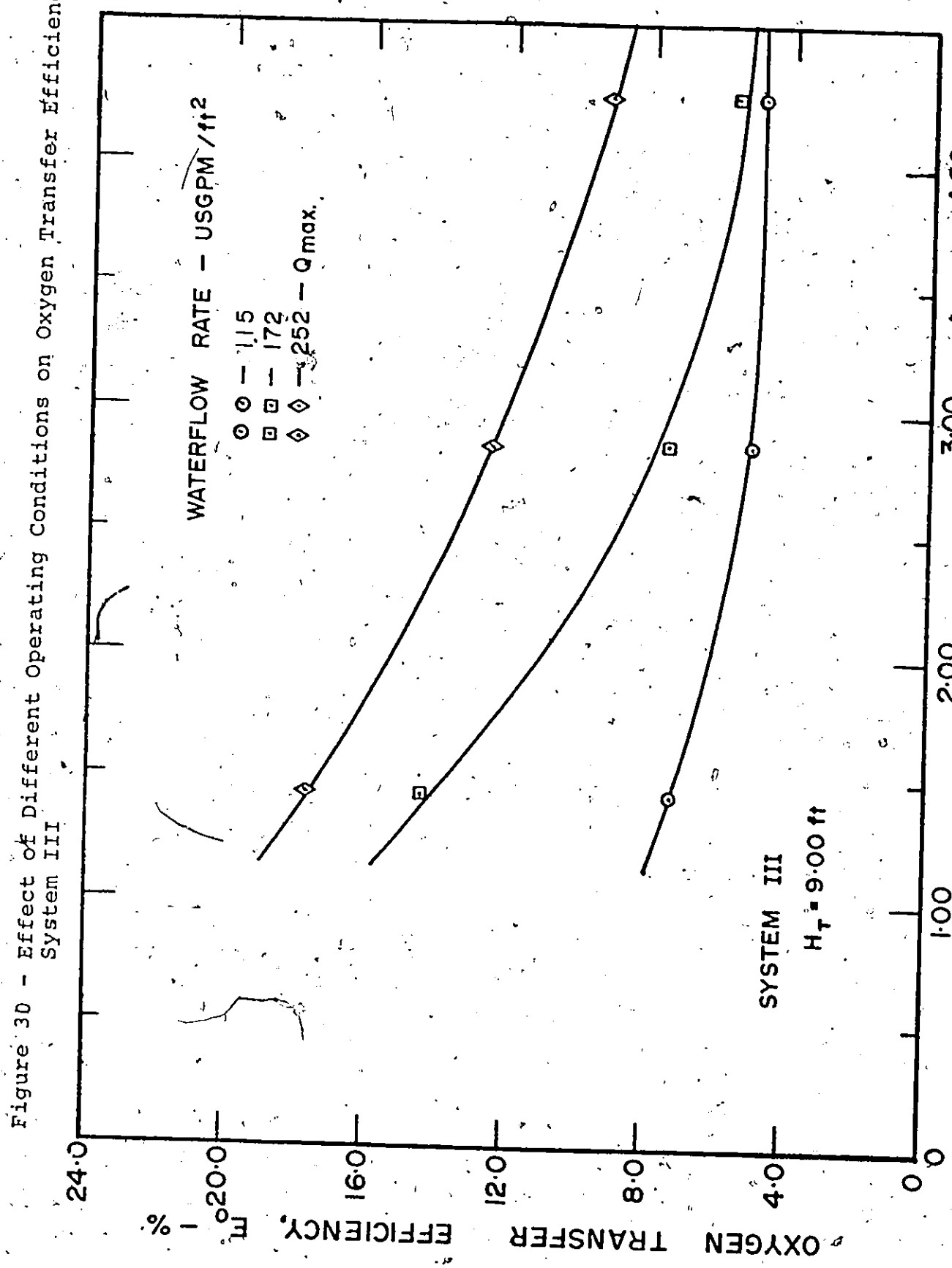


Figure 30 - Effect of Different Operating Conditions on Oxygen Transfer Efficiency, System III

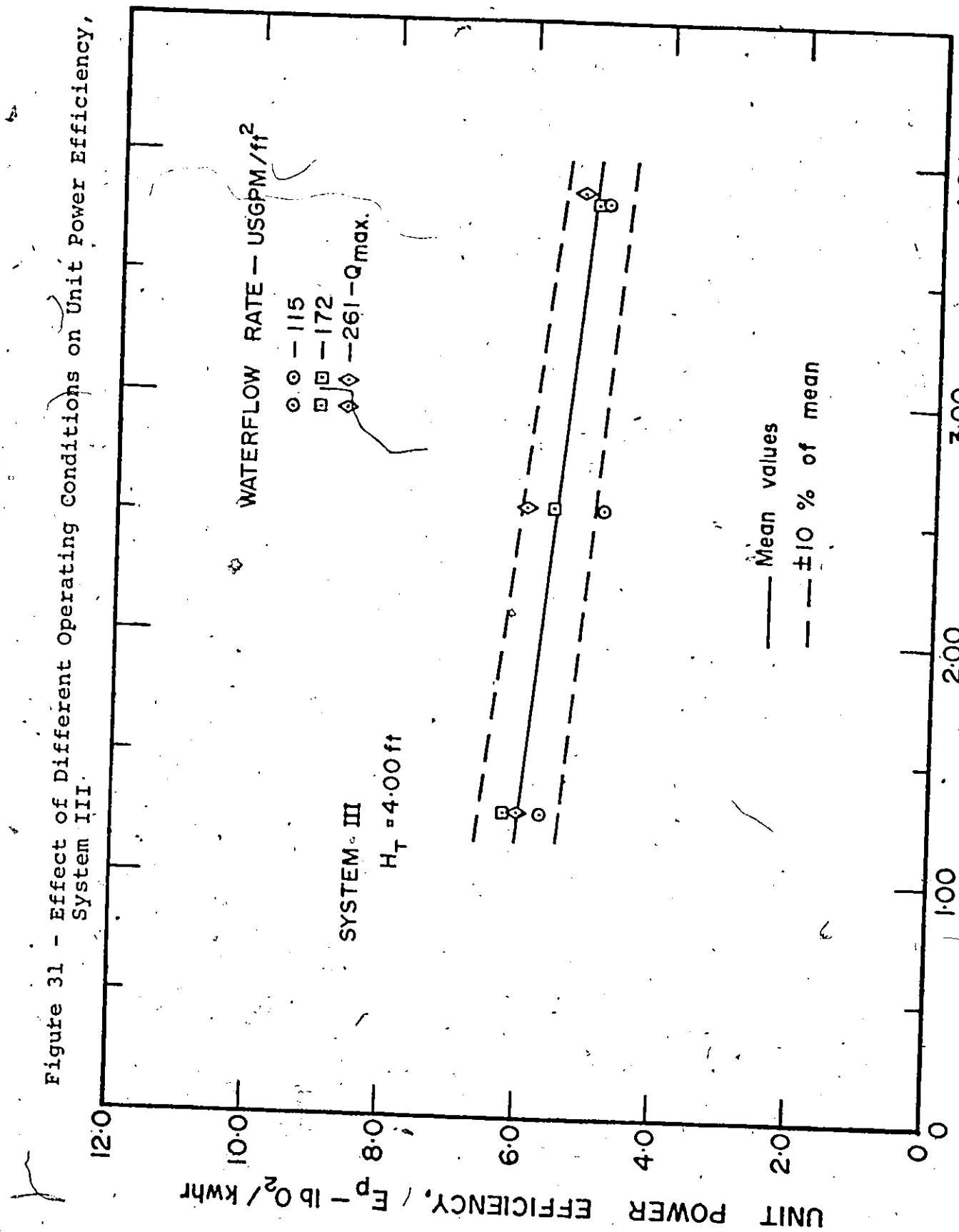


Figure 31 - Effect of Different Operating Conditions on Unit Power Efficiency, System III.

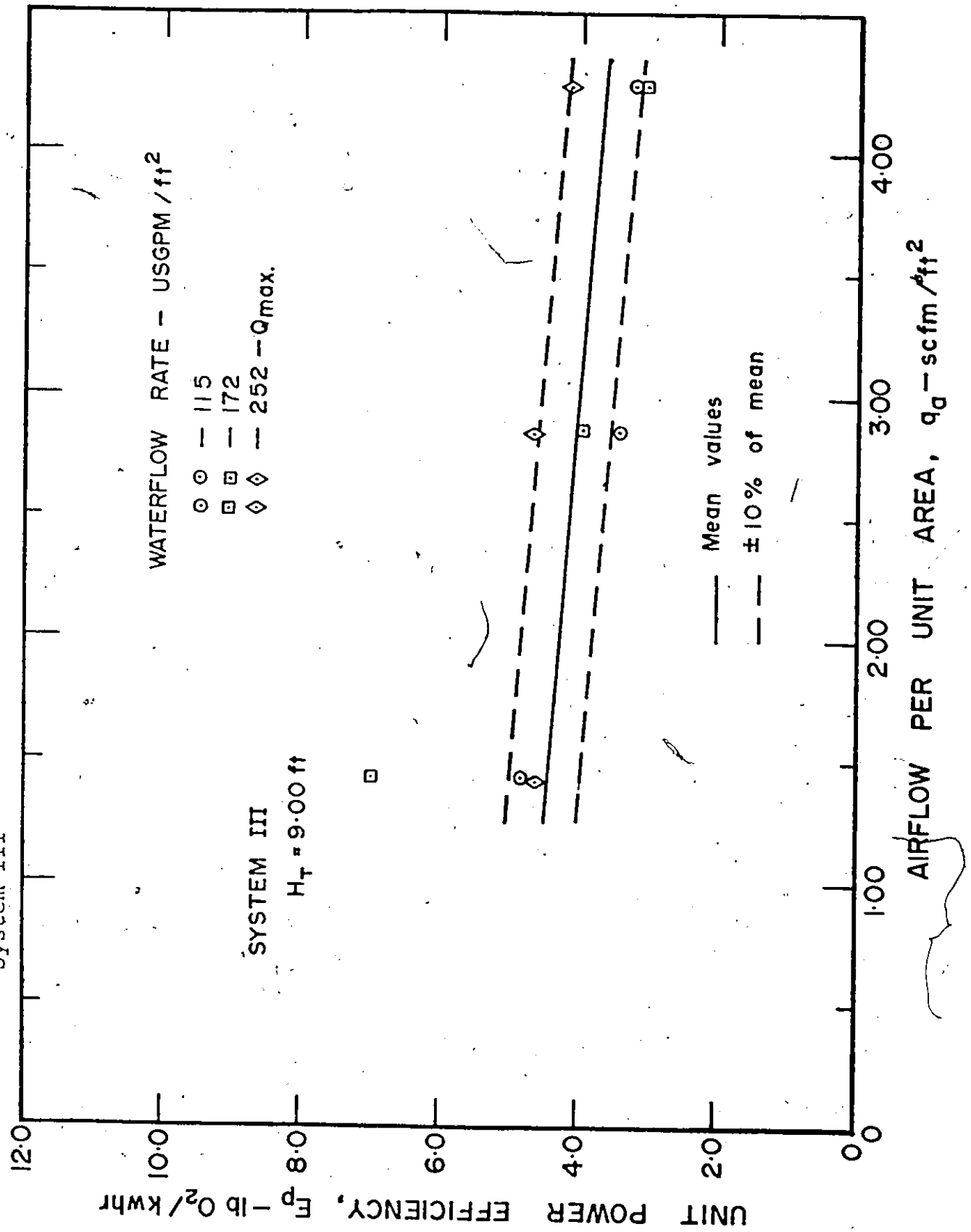


Figure 32 - Effect of Different Operating Conditions on Unit Power Efficiency, System III

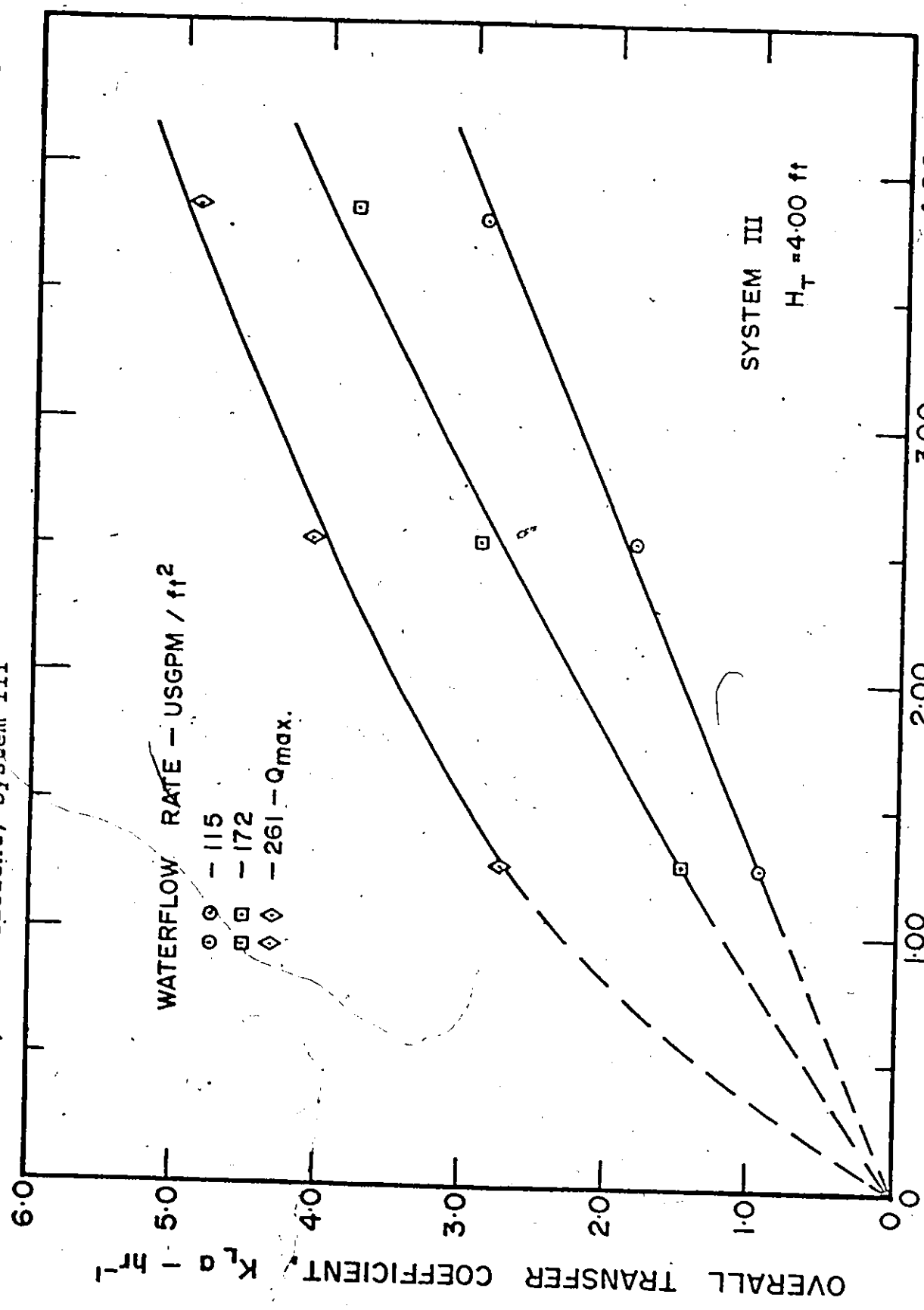


Figure 33 - Effect of Different Operating Conditions on the Overall Transfer Coefficient, System III

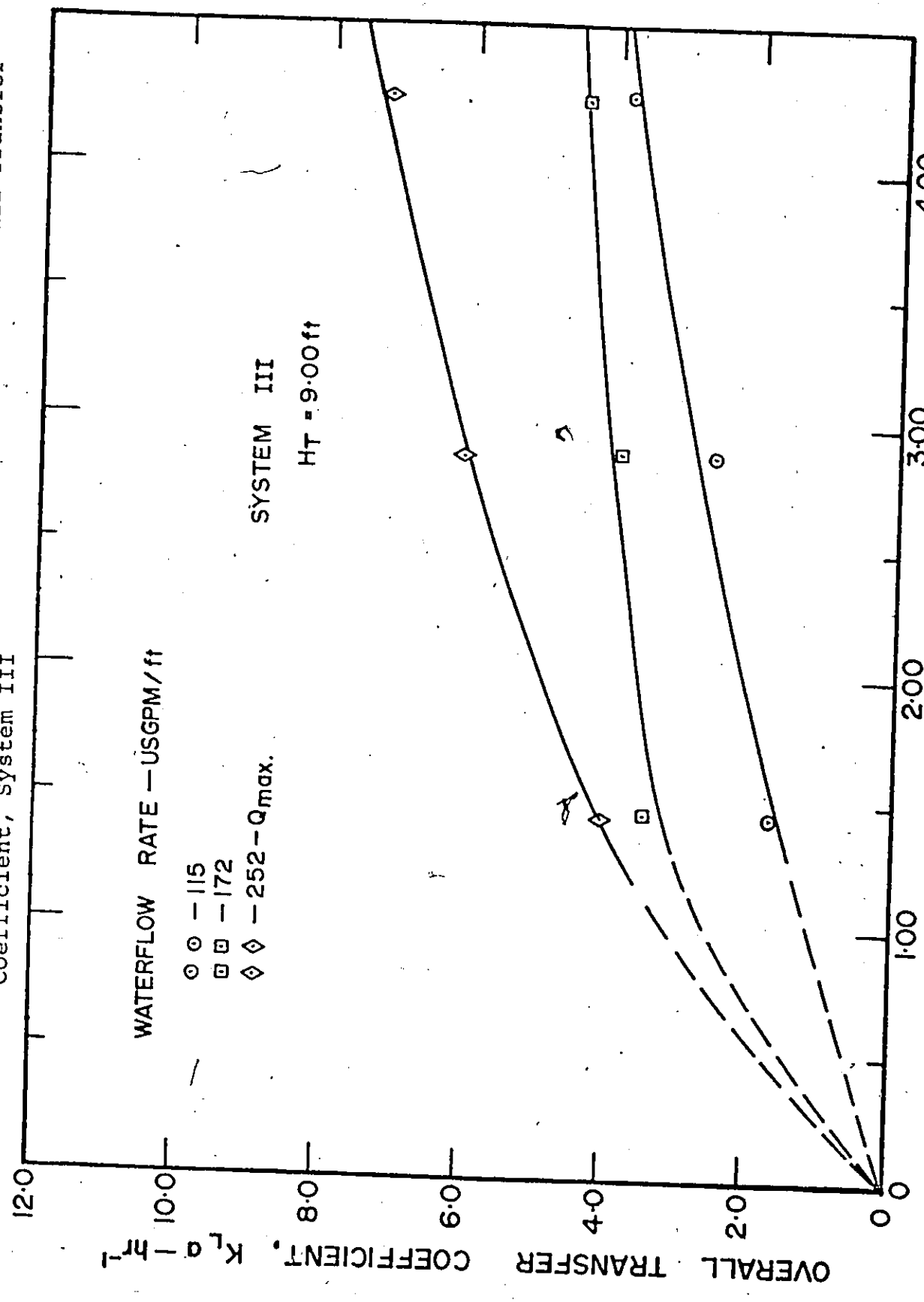


Figure 34 - Effect of Different Operating Conditions on the Overall Transfer Coefficient, System III

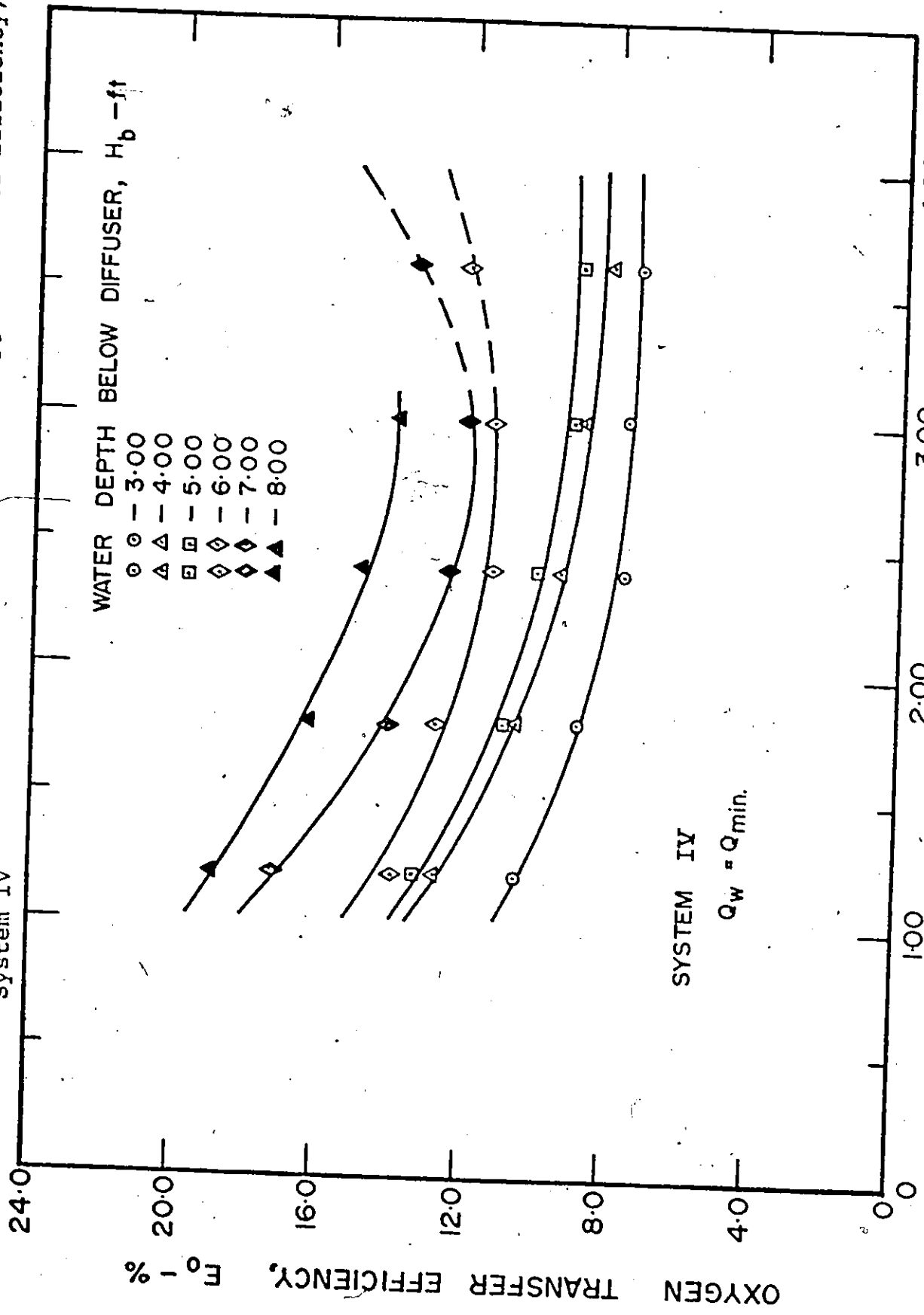


Figure 35 - Effect of Water Depth and Airflow Rate on Oxygen Transfer Efficiency, System IV

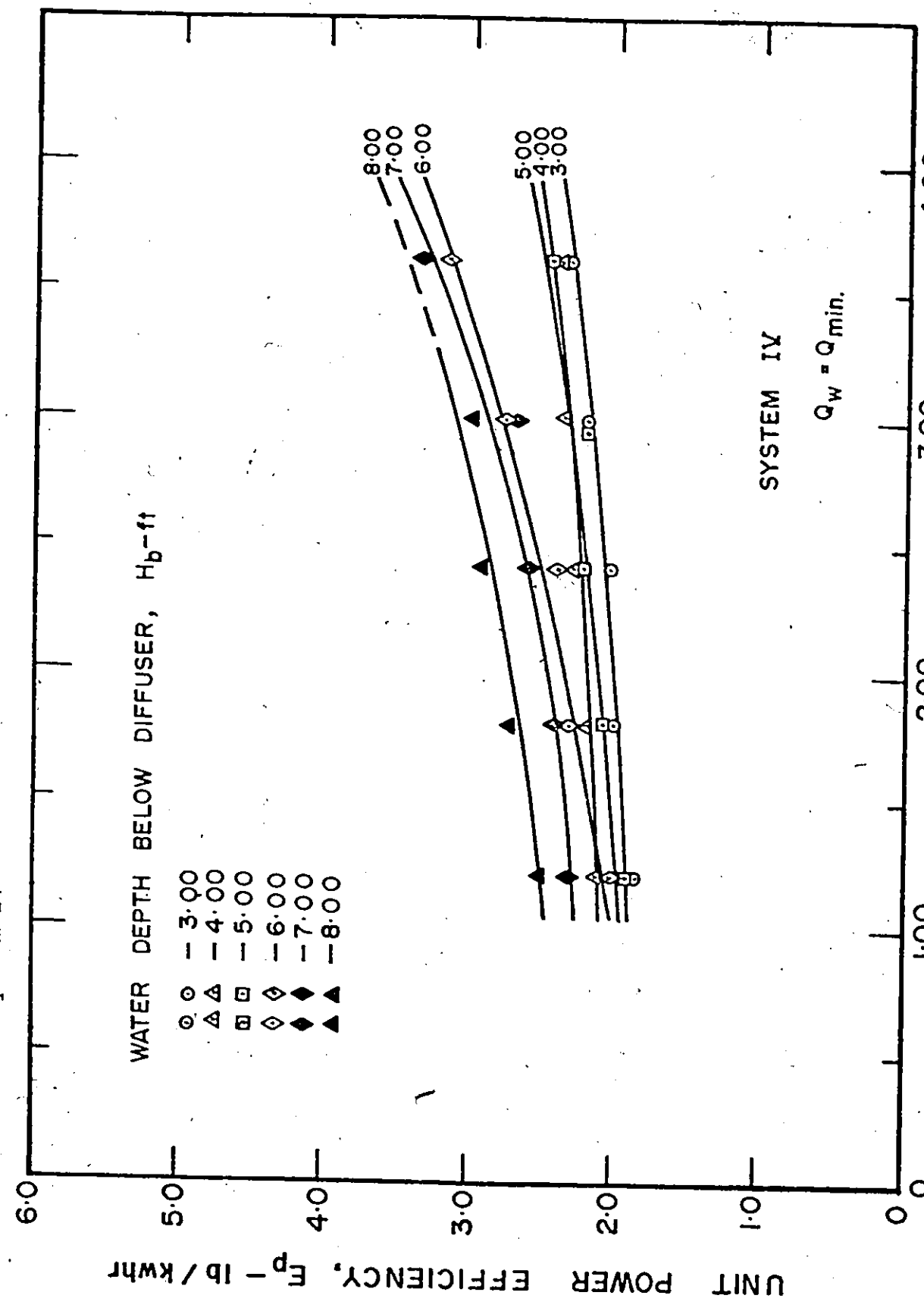


Figure 36 - Effect of Water Depth and Airflow Rate on Unit Power Efficiency, System IV

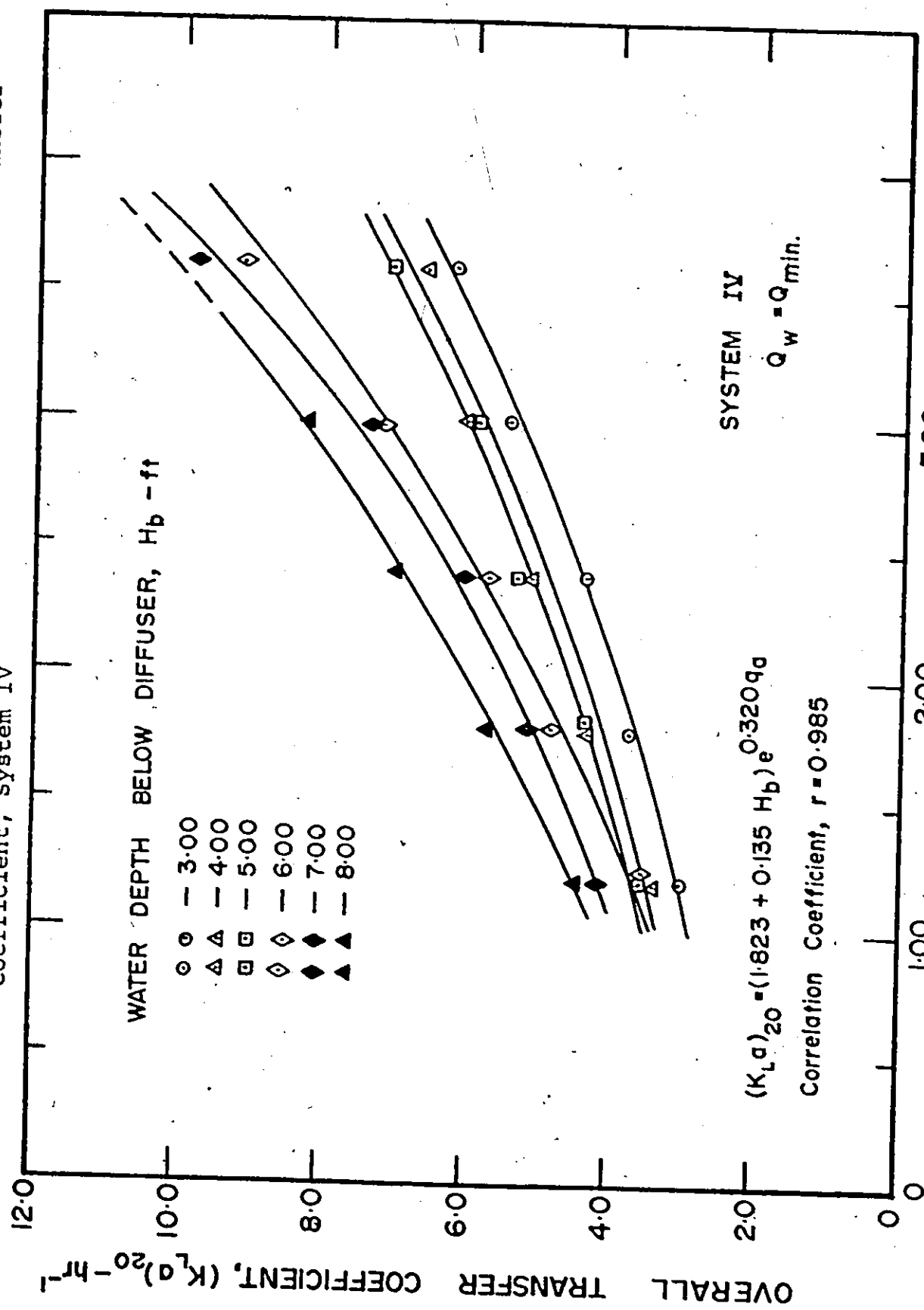


Figure 37 - Effect of Water Depth and Airflow Rate on the Overall Transfer Coefficient, System IV

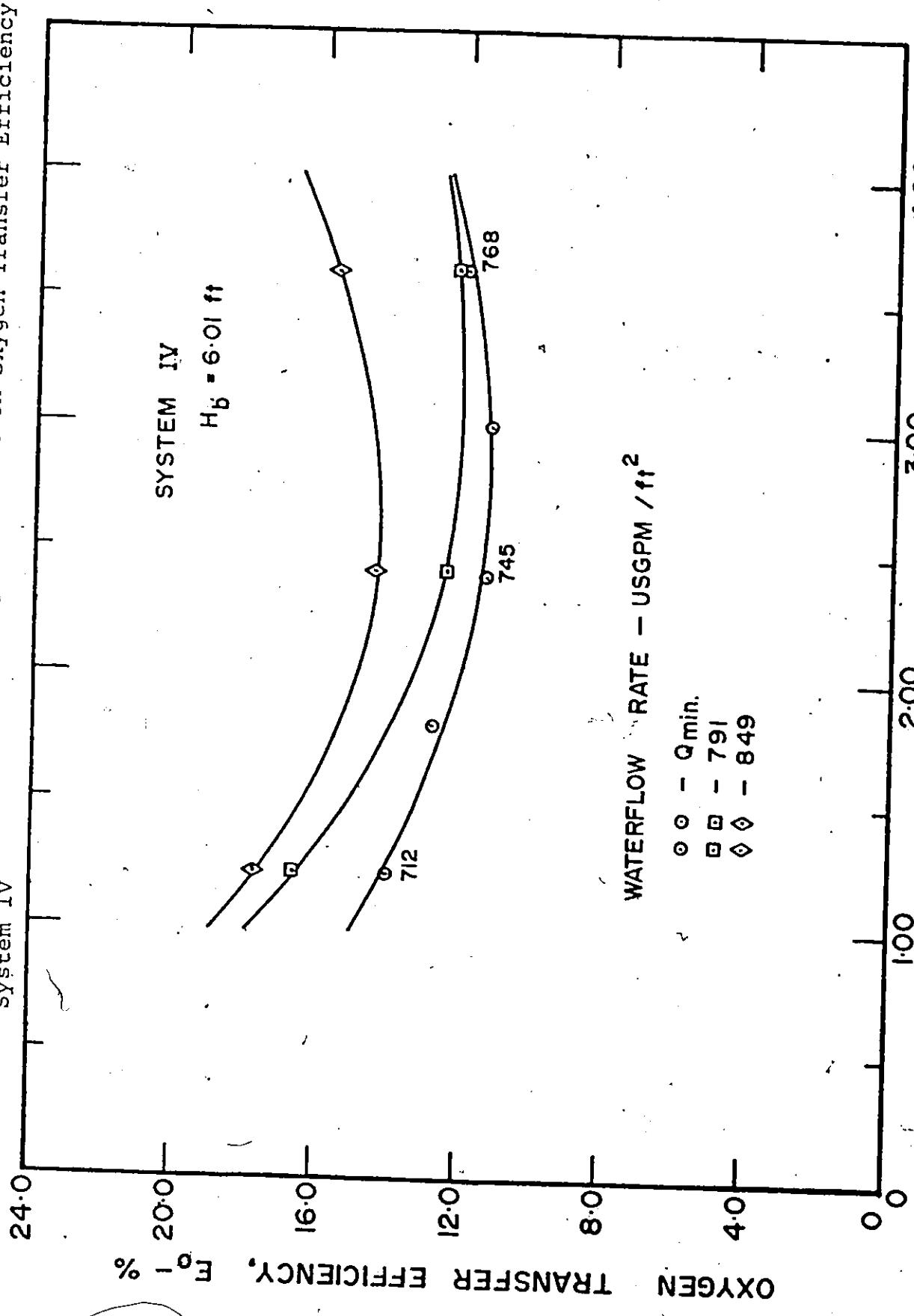


Figure 38 - Effect of Different Operating Conditions on Oxygen Transfer Efficiency, System IV

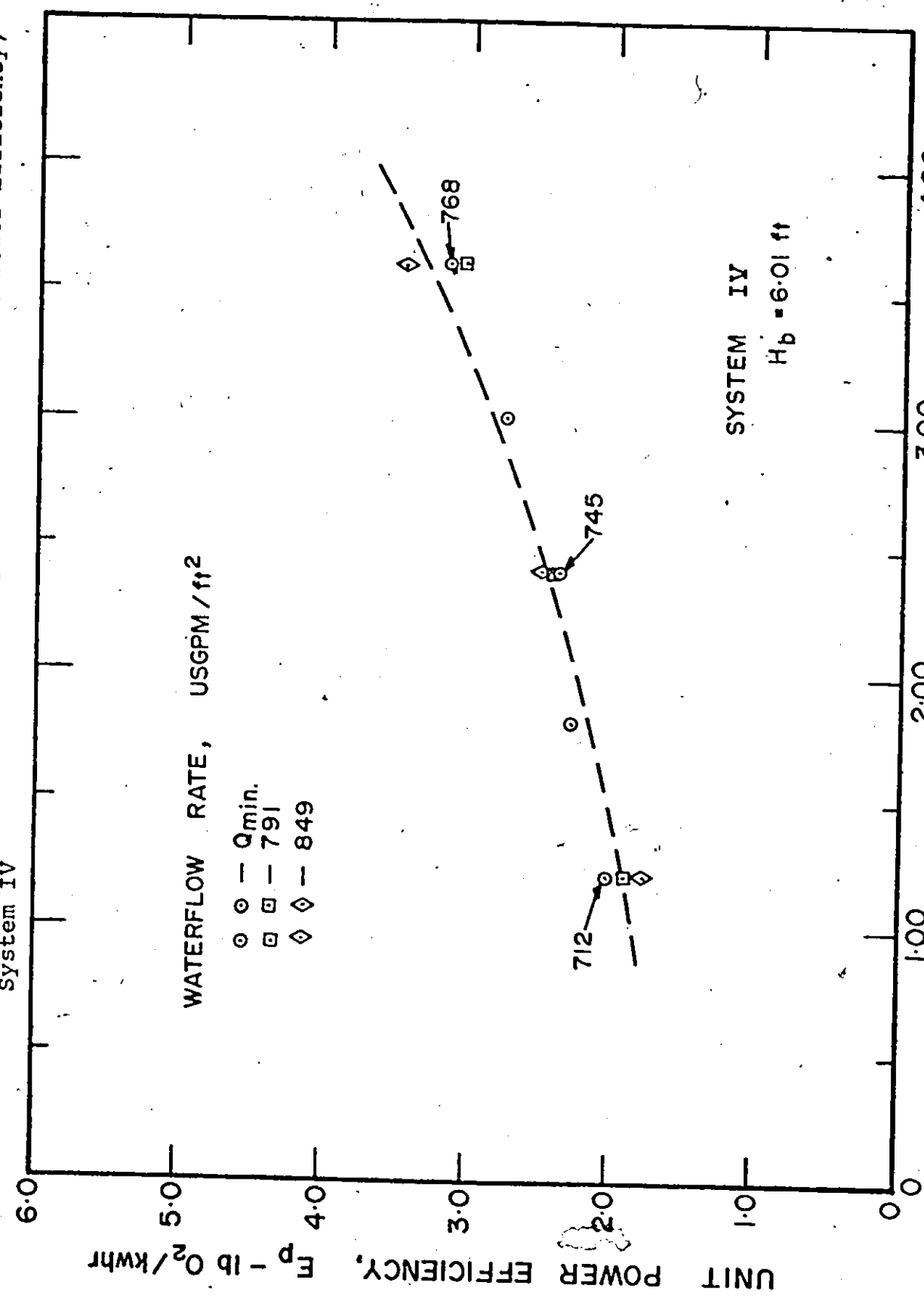


Figure 39 - Effect of Different Operating Conditions on Unit Power Efficiency, System IV

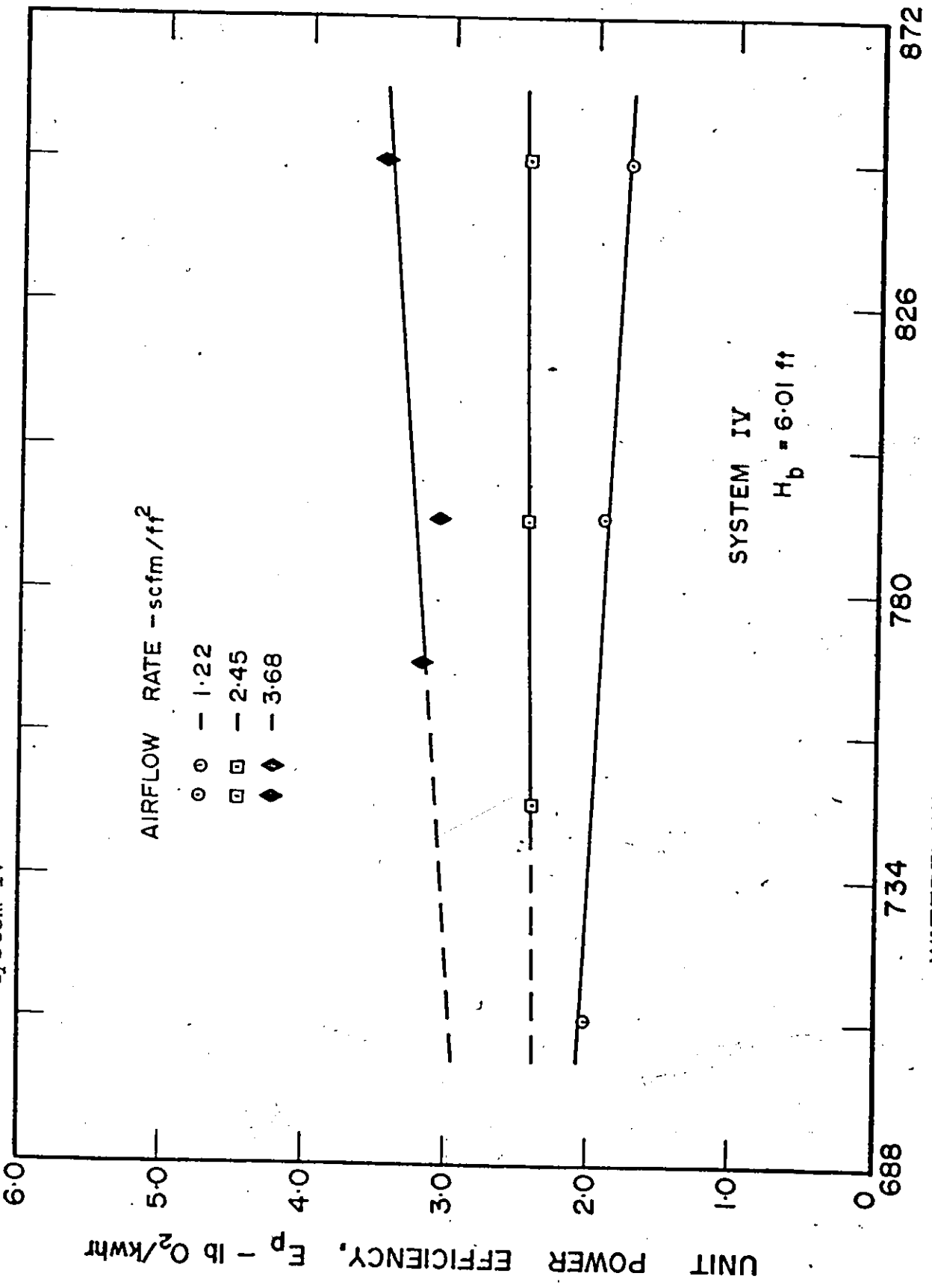


Figure 40 - Effect of Different Operating Conditions on Unit Power Efficiency, System IV

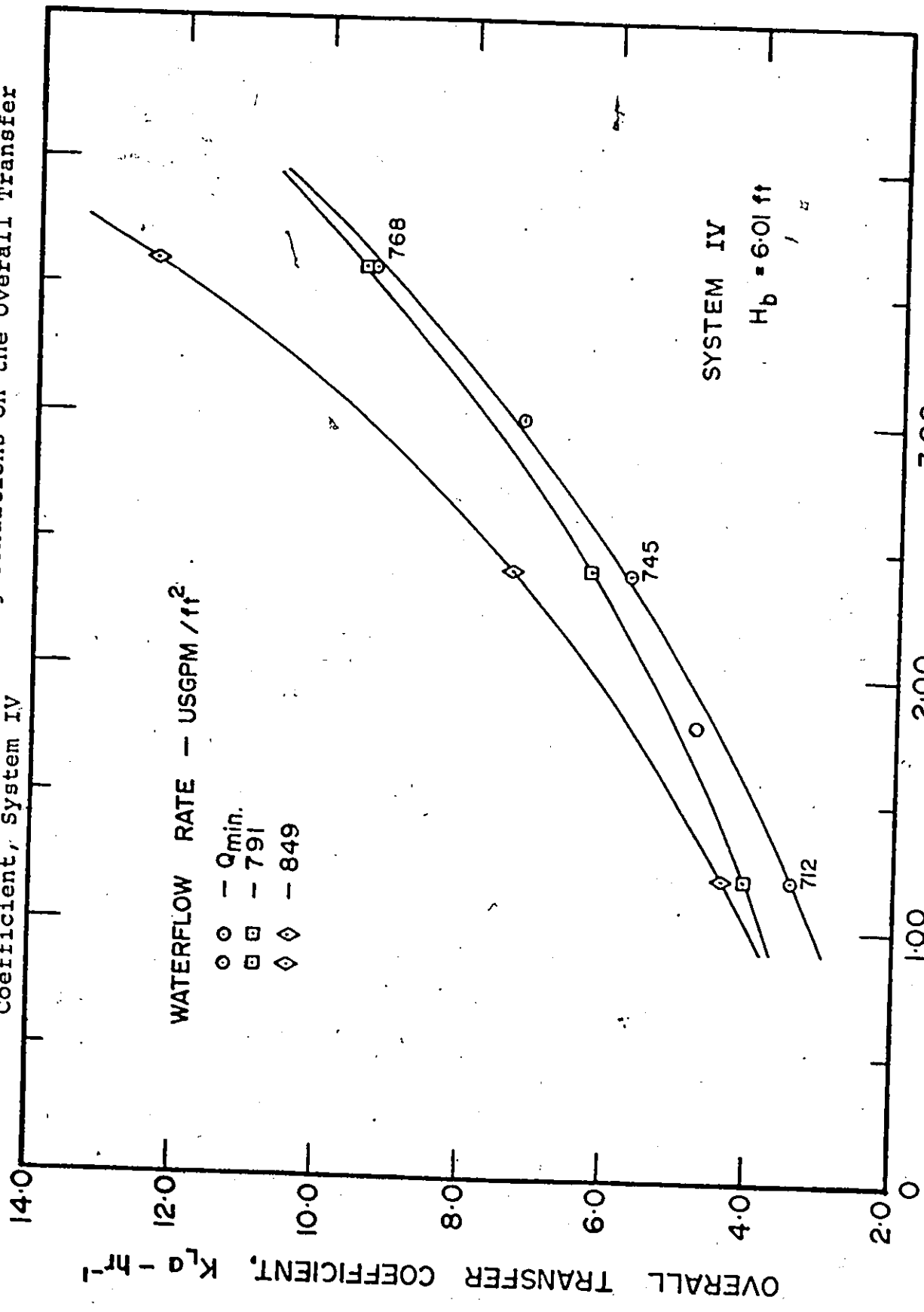


Figure 41 - Effect of Different Operating Conditions on the Overall Transfer Coefficient, System IV

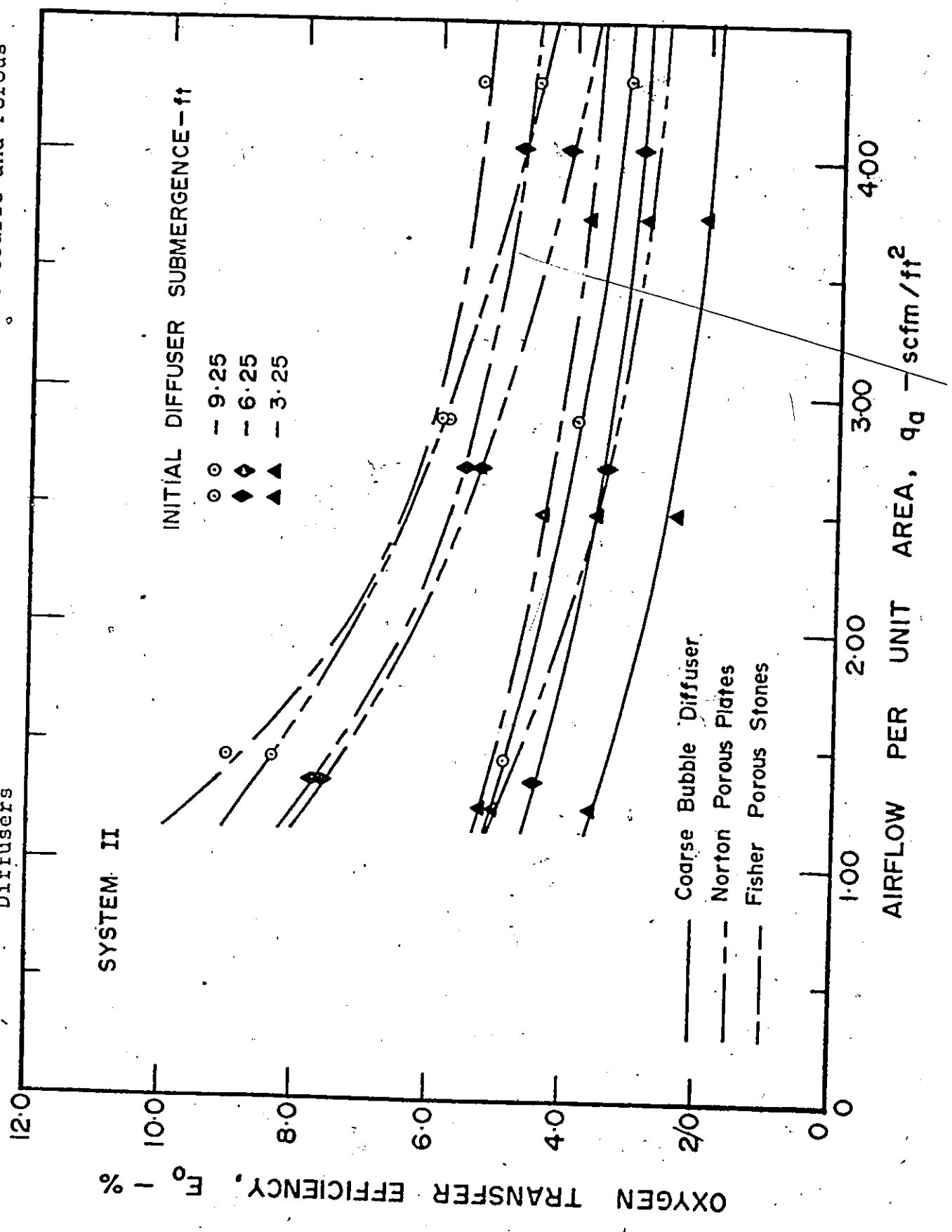


Figure 42 - Comparison of Oxygen Transfer Efficiencies for Coarse and Porous Diffusers

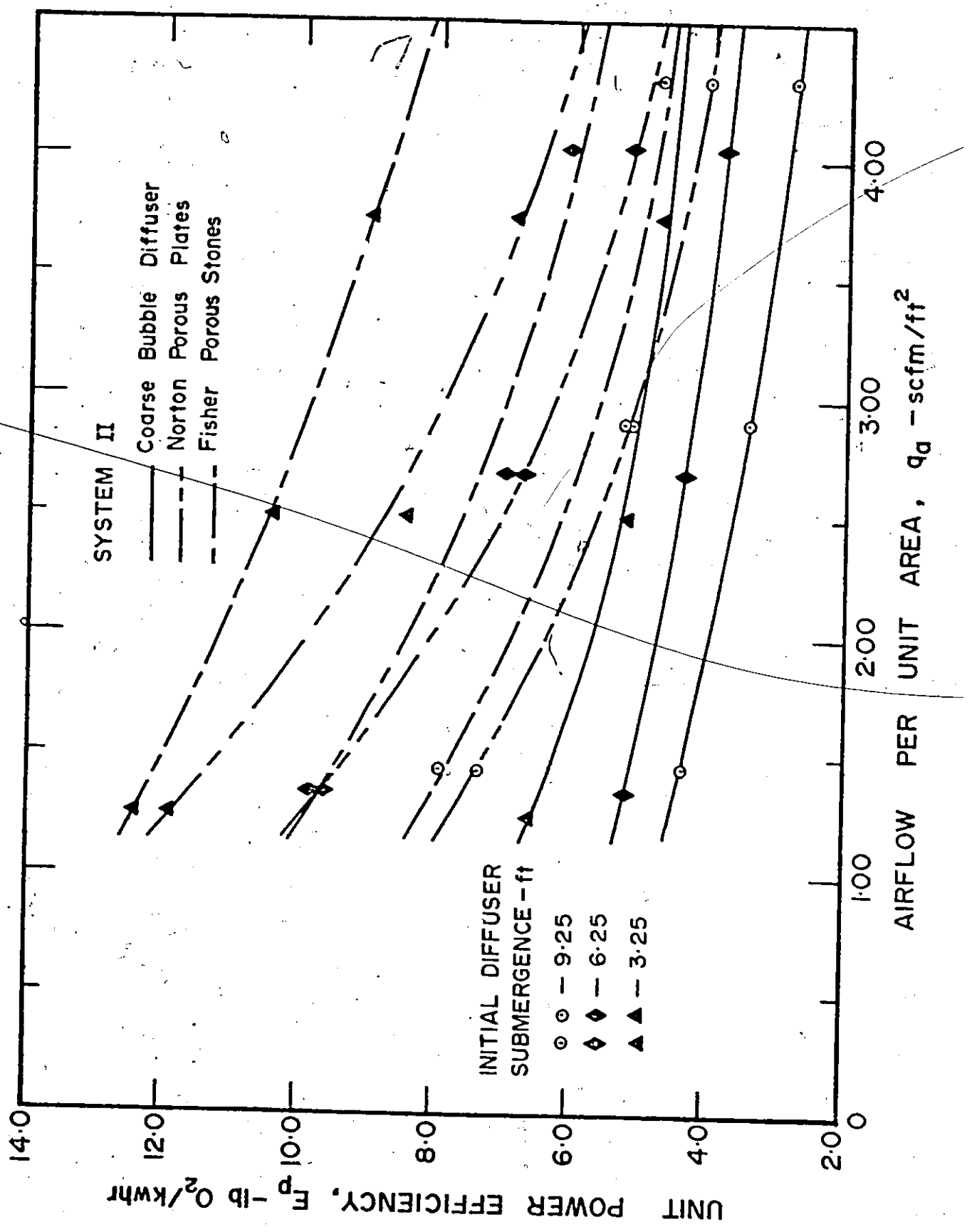


Figure 43 - Comparison of Unit Power Efficiencies for Coarse and Porous Diffusers

# VIII - DISCUSSION

## A. SYSTEM I - Simple Water Column

The operating conditions of this system are described previously in Chapter V and are explained with Figures 8 and 9. The results have been plotted in Figures 15 to 18. In this system, column heights were varied from 2 to 9 feet, in 1 foot increments, while the airflow rates ranged from 0.10 to 0.38 scfm. The waterflow rate remained zero.

It is seen from Figure 15 that the oxygen transfer efficiency, $E_o$, decreases with an increase in the airflow per unit area, $q_a$. The influence of $q_a$ on $E_o$ becomes less significant as the airflow rate is increased. The reason for this behaviour is that when $q_a$ increases, the air bubbles become larger, as is apparent from Figure 44, and this increase in bubble diameter results in less oxygen being transferred due to the reduced ratio of interfacial area to bubble volume. Also, as the air bubbles become larger, their terminal or rising velocities become larger, as reported by Carver (9), and supported by Figure 45. This Figure clearly shows an increase in $V_b$ with $q_a$, with a levelling off at the higher airflow rates and there appears to be no significant effect of diffuser submergence on the terminal bubble velocity.

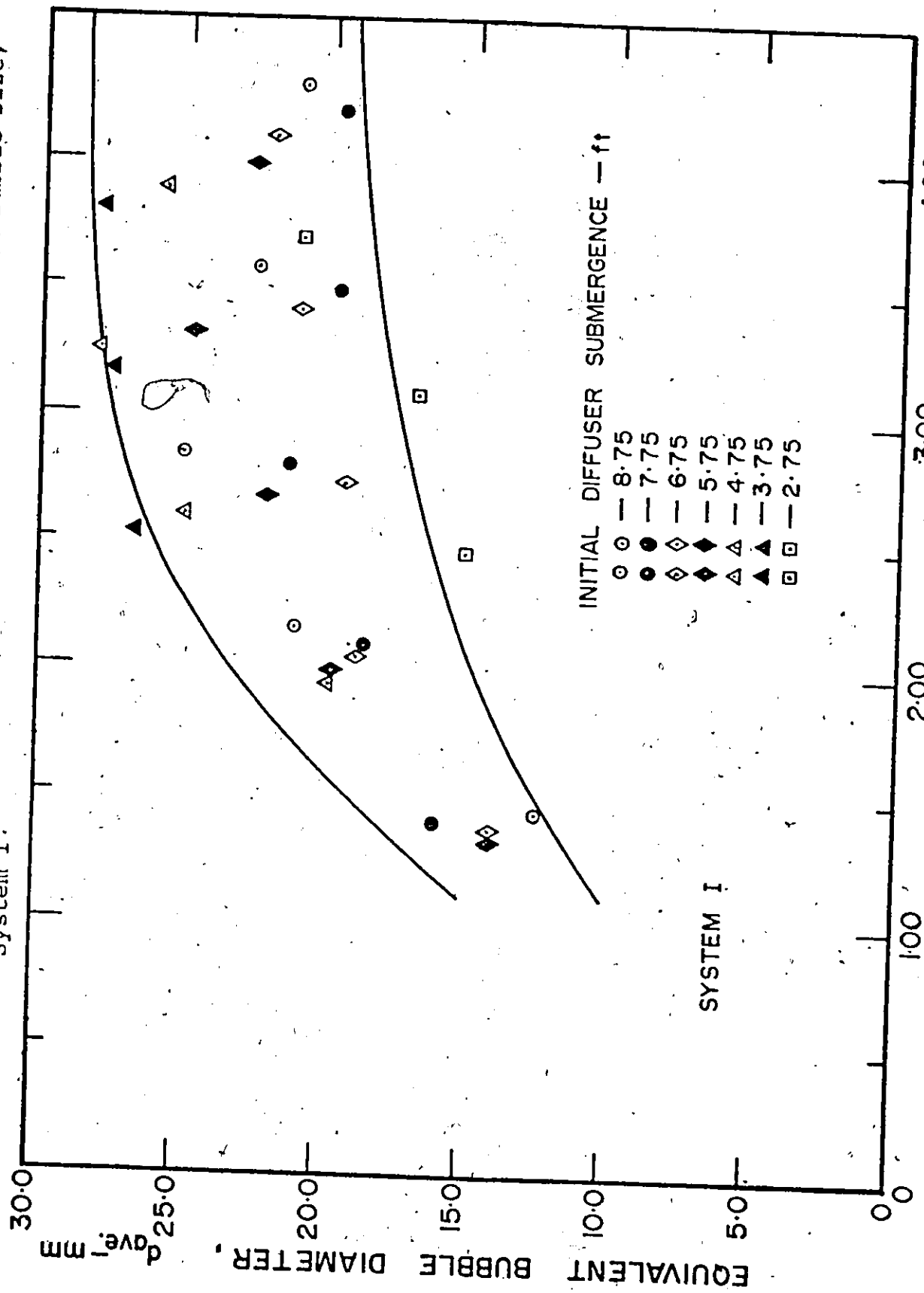


Figure 44 - Effect of Diffuser Submergence and Airflow Rate on Bubble Size, System I.

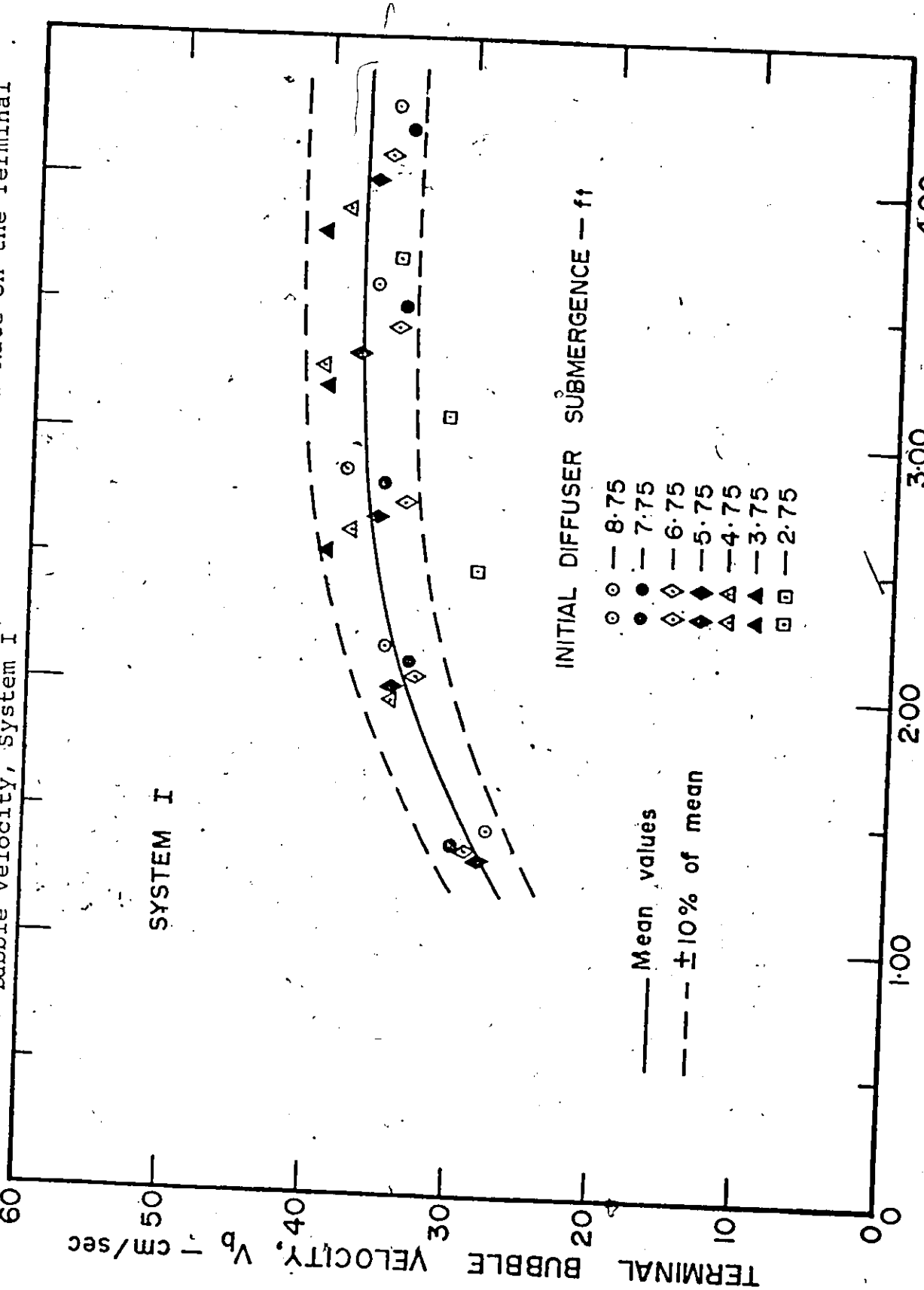


Figure 45 - Effect of Diffuser Submergence and Airflow Rate on the Terminal Bubble Velocity, System I

Equation 23 shows that the contact time of the air bubble is reduced when its terminal velocity increases and the effect of $q_a$ on $t_c$ is shown in Figure 46. It is interesting to note that the pattern of curves in Figures 15 and 46 is quite similar, thus indicating that the bubble contact time is a very important variable in oxygen absorption efficiency.

Figure 15 also shows that the efficiency, $E_o$, decreases with a decrease in diffuser submergence, for a given airflow rate. This again can be explained by the increase in bubble contact time, $t_c$, with an increase in diffuser submergence, as shown in Figure 46. This increase in contact time is due to an increase in distance travelled as well as due to a decrease in bubble size and consequently the terminal velocity of the bubble. Also, with greater submergence comes an increase in the solubility of oxygen, $C_i$, and subsequently an increase in the oxygen deficit or driving force, $(C_i-C_L)$. All these factors contribute to an increase in oxygen transfer efficiency with increased diffuser submergence.

Figure 16 shows the relationship between $q_a$, and the unit power efficiency, $E_p$, for various depths of diffuser submergence. It can be seen that as $q_a$ increases, there is a slight decrease in $E_p$, regardless of the diffuser submergence. Here again, as the airflow rate is increased, for a particular diffuser submergence, there is an increase in air bubble size and consequently, the contact time, $t_c$, is reduced. In addition to this, an increase in $q_a$ means a corresponding

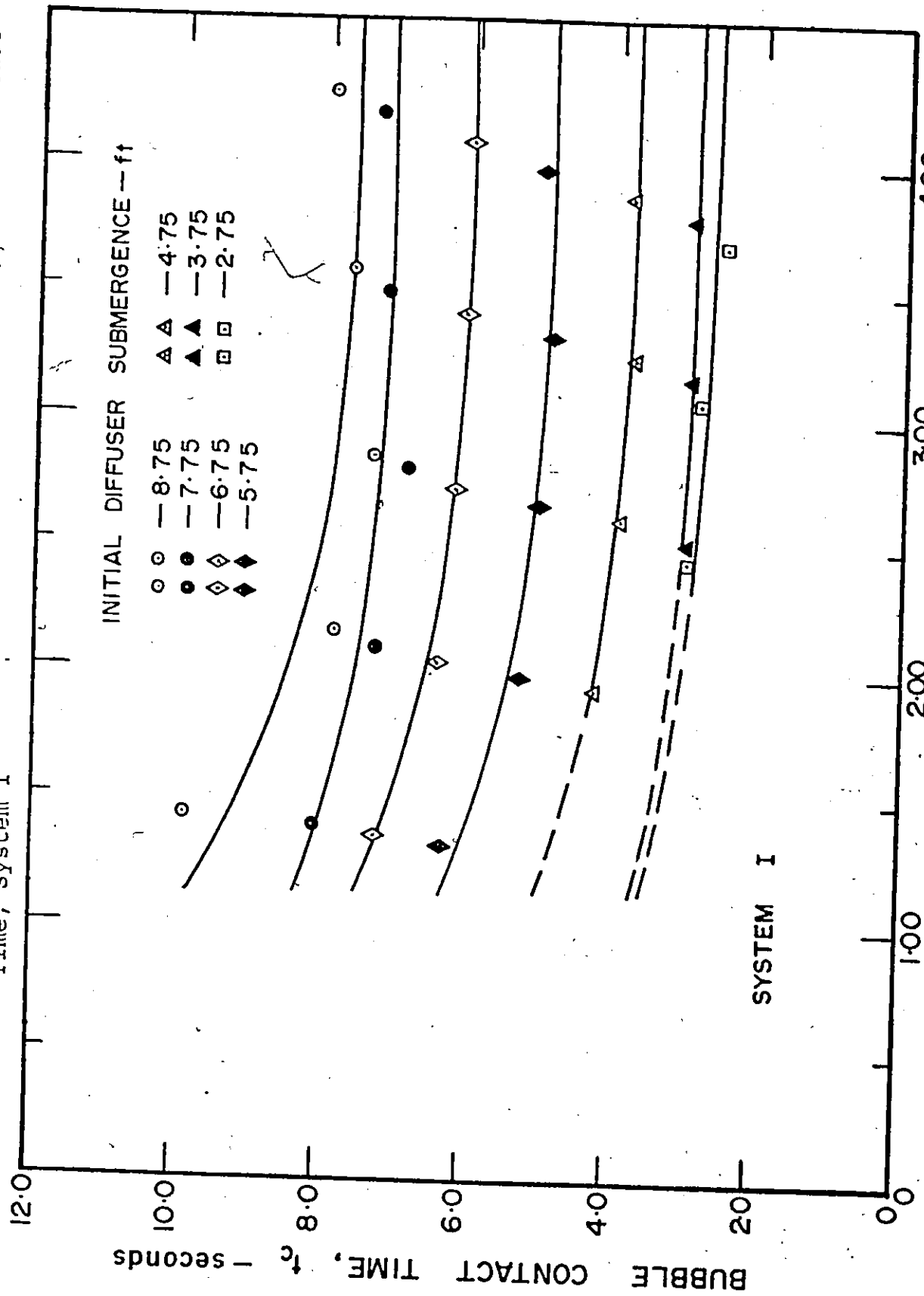


Figure 46 - Effect of Diffuser Submergence and Airflow Rate on Bubble Contact Time, System I

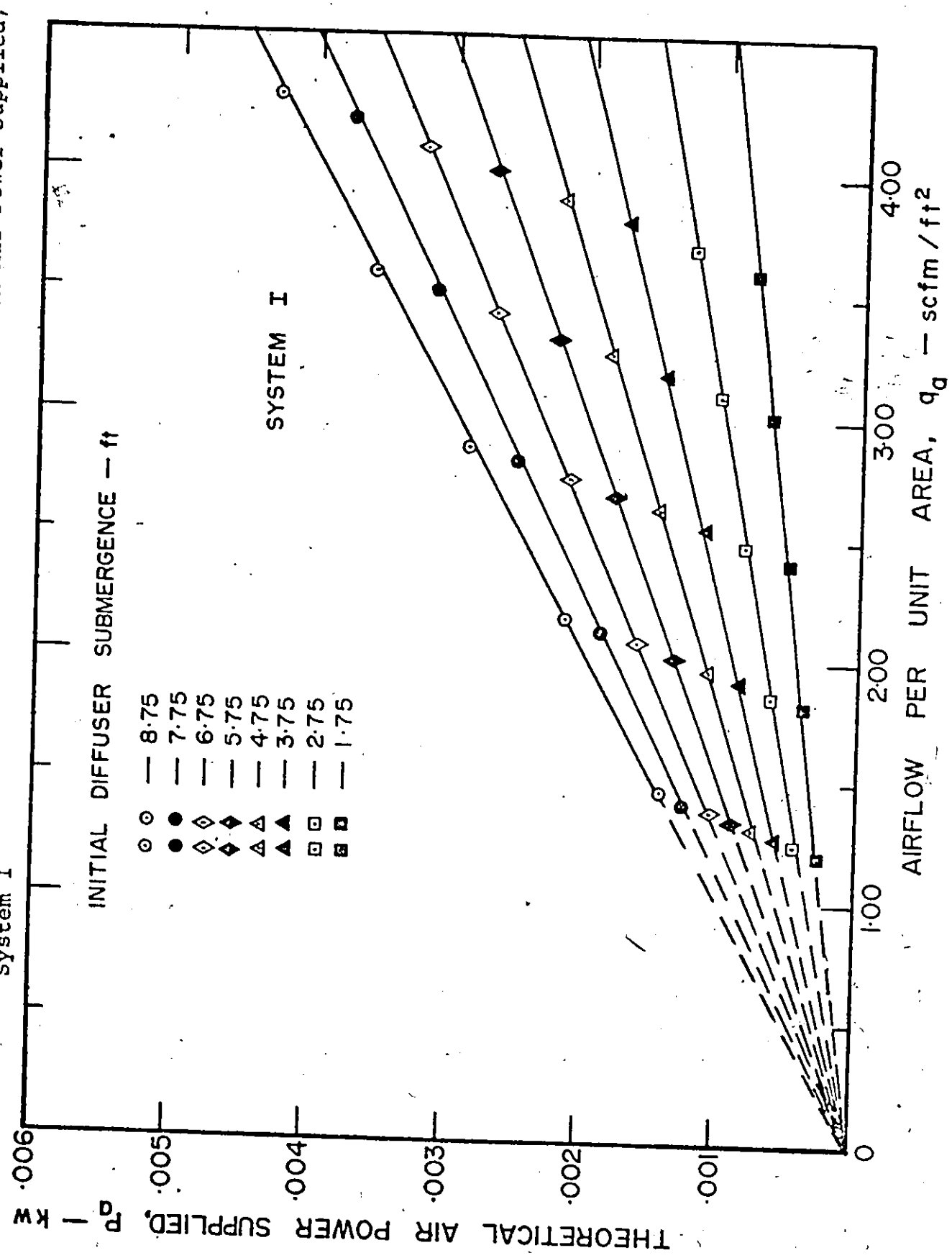


Figure 47 - Effect of Diffuser Submergence and Airflow Rate on Air Power Supplied, System I

increase in the air power supplied to the system, as shown in Figure 47. Thus, these two factors offset any benefits achieved in oxygen transfer directly from the increased airflow rates and the overall effect is a slight decrease in $E_p$.

However, at any given value of $q_a$, there appears to be no significant effect of diffuser submergence on $E_p$, with most of the values falling within the ±10% limits of the mean values. This can be explained by examining Figures 46 and 47. According to Figure 46, increased bubble contact times are associated with greater depths; however, Figure 47 shows that, for any given airflow rate, as the diffuser submergence is increased, the air power supplied also increases proportionally. The overall effect of these opposing factors is a rather constant value of $E_p$. The air power, $P_a$, is a function of airflow rate and diffuser submergence and was calculated from Equation 15.

Figure 17 shows the relationship of the Overall Transfer Coefficient, $(K_La)_{20}$, to the unit airflow rate, $q_a$, for various values of diffuser submergence. Although independent of submergence depth, $(K_La)_{20}$ increases linearly with $q_a$. The reason for this behaviour is the increase in total number of air bubbles available inside the column due to an increase in $q_a$; that is, when more air is supplied to the system, more bubbles, with an increased total interfacial area, are available for the transfer of oxygen to the surrounding liquid. $(K_La)_{20}$, as a function of $q_a$, can be

expressed by the following linear relationship,

$$(K_L a)_{20} = 2.138 + 5.390\ q_a \quad \ldots\ldots\ldots\ldots \quad 45$$

with a Correlation Coefficient, r, of 0.974 (45).

Figure 18 gives the relationship between the Liquid Film Coefficient, $K_L$, and the equivalent bubble diameter, $d_{ave.}$, for different diffuser submergences. A similar, curvilinear nature of the plot was also observed by Carver (9) and Barnhart (43), among others. Although there appears to be no significant effect of the diffuser submergence on $K_L$, an increase in bubble size definitely increases the value of $K_L$. This can be explained by the fact that larger air bubbles have larger terminal velocities, thus causing larger shear forces at the bubble boundary or air-water interface. This increase in shear force is considered to be responsible for the rapid renewal of the liquid film, thereby resulting in an increase in $K_L$ for the larger air bubbles. $(K_L)_{20}$ values of $1.77 \times 10^{-4}$ to $6.12 \times 10^{-4}$ ft/sec. or 19.4 to 67.1 cm/hr over a bubble size range of 12.4 to 28.1 mm diameter have been obtained in this system. Scouller and Watson (6), using a 2.4 mm diameter air bubble rising through water, determined an average $K_L$ of 140 cm/hr. Similarly, Ippen et al. (5) reported values of $K_L$ between 110 and 200 cm/hr, while Barnhart (43) obtained $K_L$ values of 112 to 170 cm/hr, with the bubble sizes smaller than those in this study. The lower $K_L$ values reported in this system might be explained by the fact that a large mass of

air bubbles were present in the column of water, as compared to individual or multiple bubbles used by the other investigators. In a mass of confined bubbles, the liquid between them becomes saturated with dissolved oxygen more rapidly and this reduces the concentration gradient across the liquid film. Thus, the higher concentration of dissolved oxygen in the liquid in the wakes of the ascending bubbles is responsible for increased resistance to lateral diffusion of oxygen into the water and a reduced $K_L$ value is obtained. In the case of a single bubble rising through a column of water, there is no such reduction in lateral diffusion of oxygen and higher velocity gradients are expected to exist.

## B. SYSTEM II - Circulation Without Pumping

The operating conditions of System II are described previously in Chapter V and are explained with Figures 8 and 10. The results have been plotted in Figures 19 to 23. In this system, column heights varied from 2 to 8 feet, in 1 foot intervals, while the airflow rates ranged from 0.11 to 0.38 scfm. There was no pumping of water but circulation of water did occur through the closed-loop. In this system, both air and water move co-currently and the bubbles are rising under the influence of two velocities, the water velocity and their own terminal velocity. The water velocities, as measured by the pitot-tube in this system, are designated as the average nominal water velocities, $V_n$, and are plotted in Figure 48.

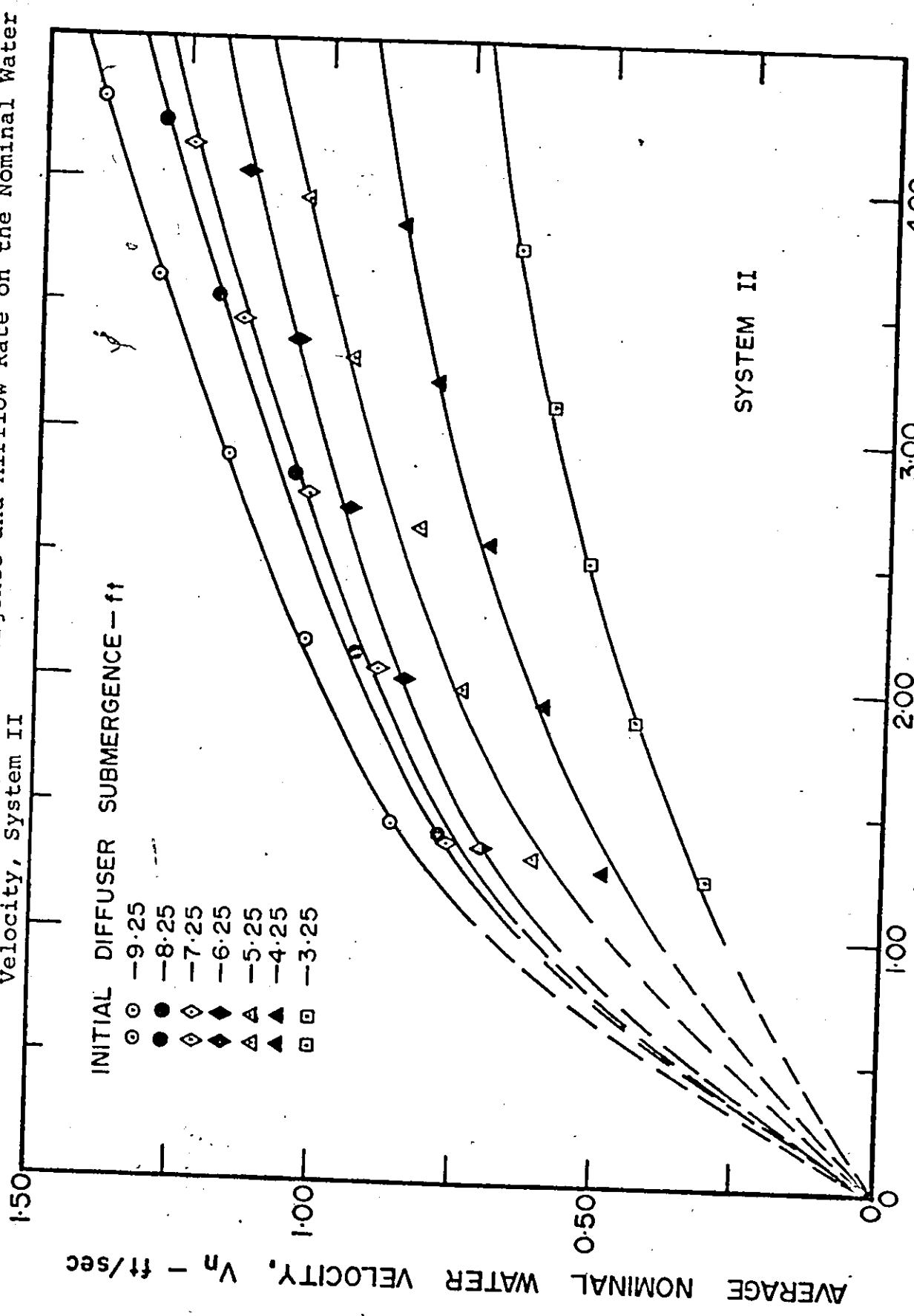


Figure 48 - Effect of Diffuser Submergence and Airflow Rate on the Nominal Water Velocity, System II

The relationship between the unit airflow rate, diffuser submergence and the oxygen transfer efficiency can be seen in Figure 19. If the diffuser submergence is held constant and the unit airflow rate, $q_a$, is increased, there is a decrease in the oxygen transfer efficiency, $E_o$. The influence of $q_a$ on $E_o$ becomes less significant as the airflow is increased. In this System, again, the reason for this behaviour is an increase in air bubble size with an increase in $q_a$, thereby reducing the ratio of the interfacial area to bubble volume and also increasing the bubble terminal velocity. The combined effect of these two factors is the reduction in the amount of oxygen transferred. The increase in bubble diameter, $d_{ave.}$, with increase in $q_a$ is evident from Figure 49, and the resulting larger terminal velocities are shown in Figure 50. This Figure clearly shows an increase in $V_b$ with $q_a$, with a levelling off effect at the higher airflow rates, and there appears to be no significant effect of diffuser submergence on this velocity.

It can be seen from Figure 48 that $V_n$ also increases with an increase in $q_a$ for any particular diffuser submergence. Thus, the total bubble velocity, $V_T$, which is the vectorial sum of the average terminal velocity of the air bubble and the average water velocity on the diffuser side of the system, also increases with an increase in $q_a$ and it is confirmed by Figure 51. In this Figure, even though there is indication that the total bubble velocity, $V_T$, increases with an increase in diffuser submergence for any

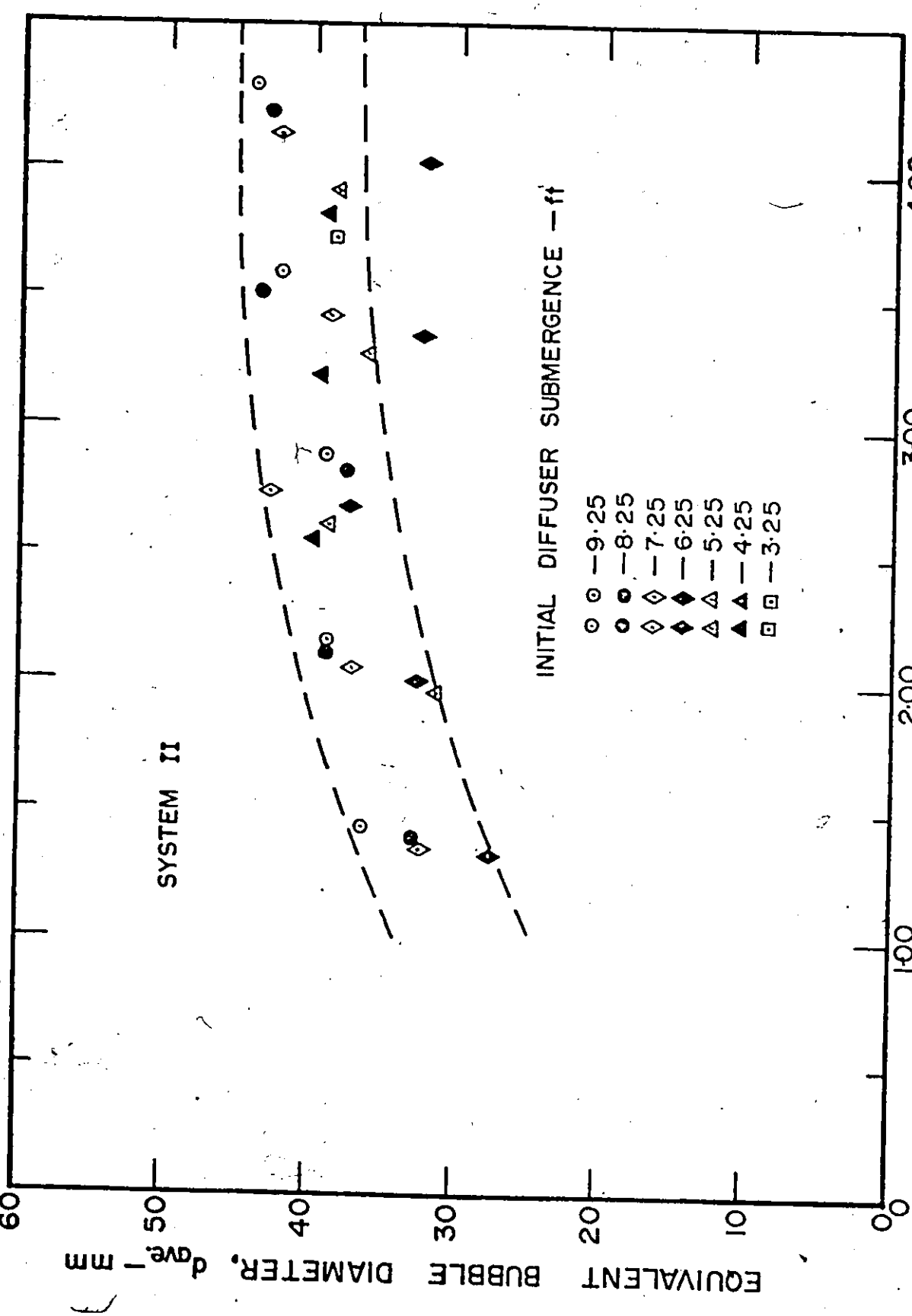


Figure 49 - Effect of Diffuser Submergence and Airflow Rate on Bubble Size, System II

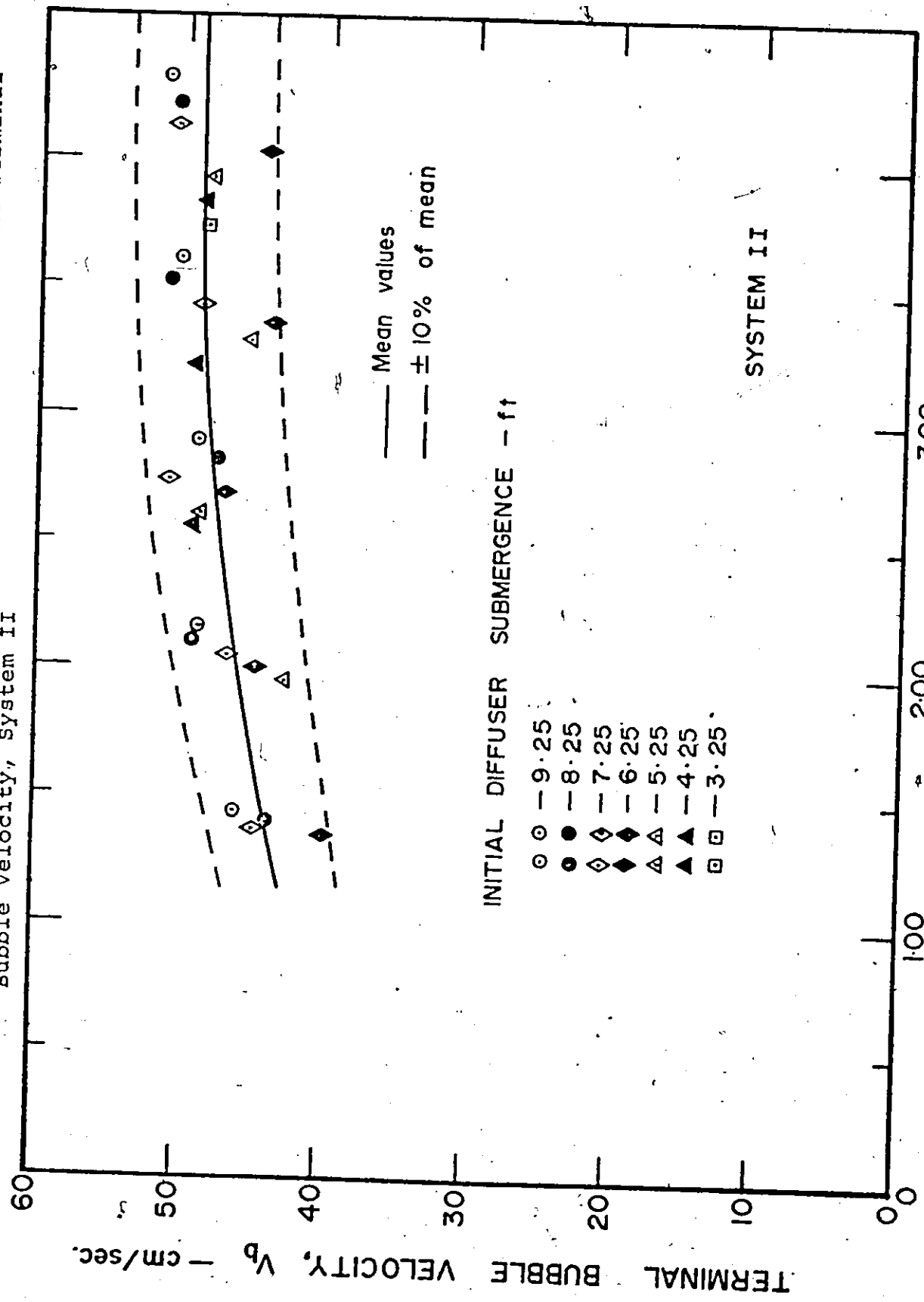


Figure 50 - Effect of Diffuser Submergence and Airflow Rate on the Terminal Bubble Velocity, System II

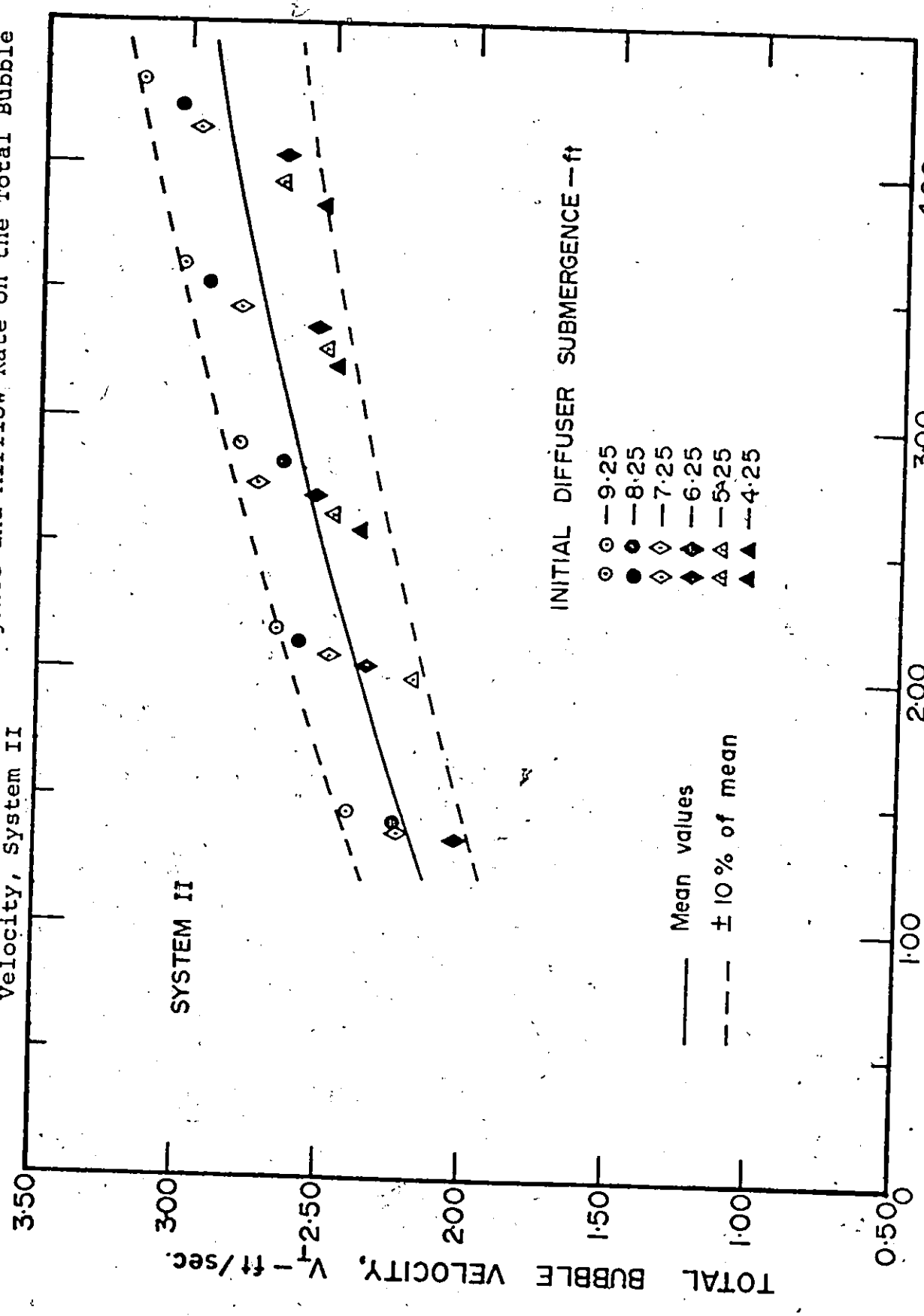


Figure 51 - Effect of Diffuser Submergence and Airflow Rate on the Total Bubble Velocity, System II

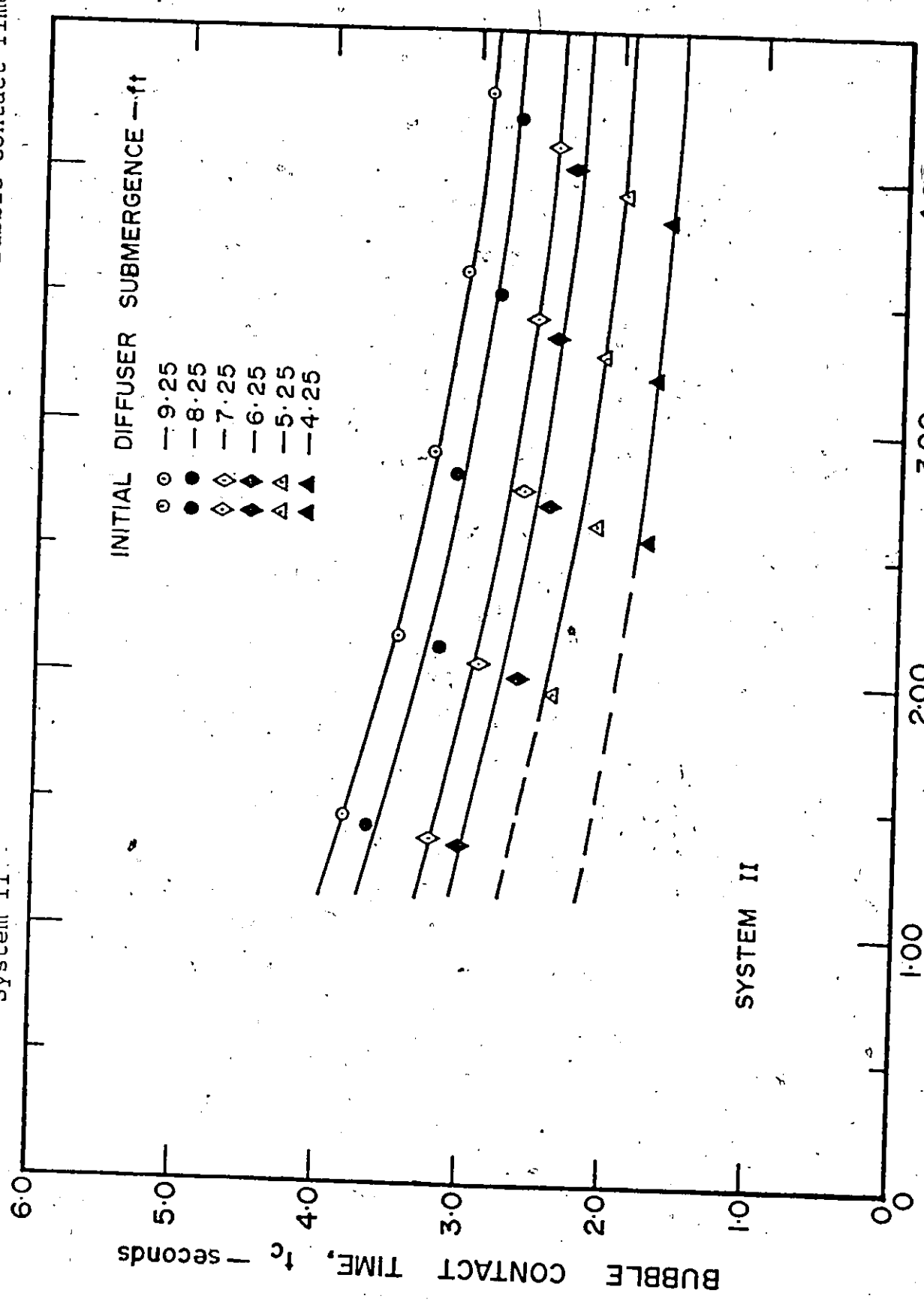


Figure 52 - Effect of Diffuser Submergence and Airflow Rate on Bubble Contact Time, System II

given airflow rate, most of the $V_T$ values fall within ±10% of an average value. Consequently, as the airflow increases, the combination of larger bubble sizes and increased velocities results in a reduction in the contact time of the air bubbles, $t_c$, and subsequently a decrease in $E_o$, as is expected from Equation 42. The effect of $q_a$ on $t_c$ can be seen in Figure 52. It is interesting to note that the pattern of curves in Figures 19 and 52 is quite similar, thus indicating again that the contact time is a very important variable in the oxygen absorption efficiency.

In Figure 19, it can also be seen that, when $q_a$ is held constant, there is an increase in $E_o$ as the diffuser submergence is increased. The nominal bubble velocity, $V_n$, increases with an increase in submergence as is seen from Figure 48, while the bubble terminal velocity decreases slightly due to a decrease in bubble size. The overall effect is a slight increase in $V_T$ with diffuser submergence for any given airflow rate, as is illustrated in Figure 51. On the other hand, there is an increase in contact time of the bubbles with an increase in submergence, as is apparent from Equation 28. The combined effect of increased bubble velocities and the increase in distance travelled by the air bubbles is an increase in contact time, $t_c$, with an increase in diffuser submergence, as shown in Figure 52, and thus the transfer efficiency shows an increase in value. Also, with greater submergence, there is an increase in the solubility of oxygen $C_i$ and thus an increase in the

driving force $(C_i - C_L)$. This also contributes to an increase in oxygen transfer efficiency.

Figure 20 shows the relationship between the unit airflow rate, diffuser submergence, and the unit power efficiency, $E_p$. It is observed from this Figure that $E_p$ decreases both with an increase in airflow rate and an increase in diffuser submergence. The decrease in $E_p$ with increased $q_a$ can be related, once again, to the increased bubble diameters and increased velocities, and consequently, reduced contact times of the air bubbles, when $q_a$ is increased. This is supported by the plots in Figures 49, 51 and 52. In addition, the air power supplied, $P_a$, or power input to the system, is increased when $q_a$ increases, as is shown in Figure 53. Therefore, for a given submergence, the amount of oxygen transferred per unit power input to the system is reduced when $q_a$ is increased. However, contrary to expectations, the values for $E_p$ dropped when the diffuser submergence was increased and the airflow rate held constant. The reason for this behaviour is that, although there is an increase in the bubble-travel distance with an increase in submergence depth, there is also a corresponding increase in circulating and bubble velocities with depth, as shown in Figures 48 and 51. Consequently, there is virtually no change in the contact time of the air bubble per unit distance, or unit contact time, $t_{cu}$, despite the increase in submergence. This can be seen from the values reported in Table 5. At the same time,

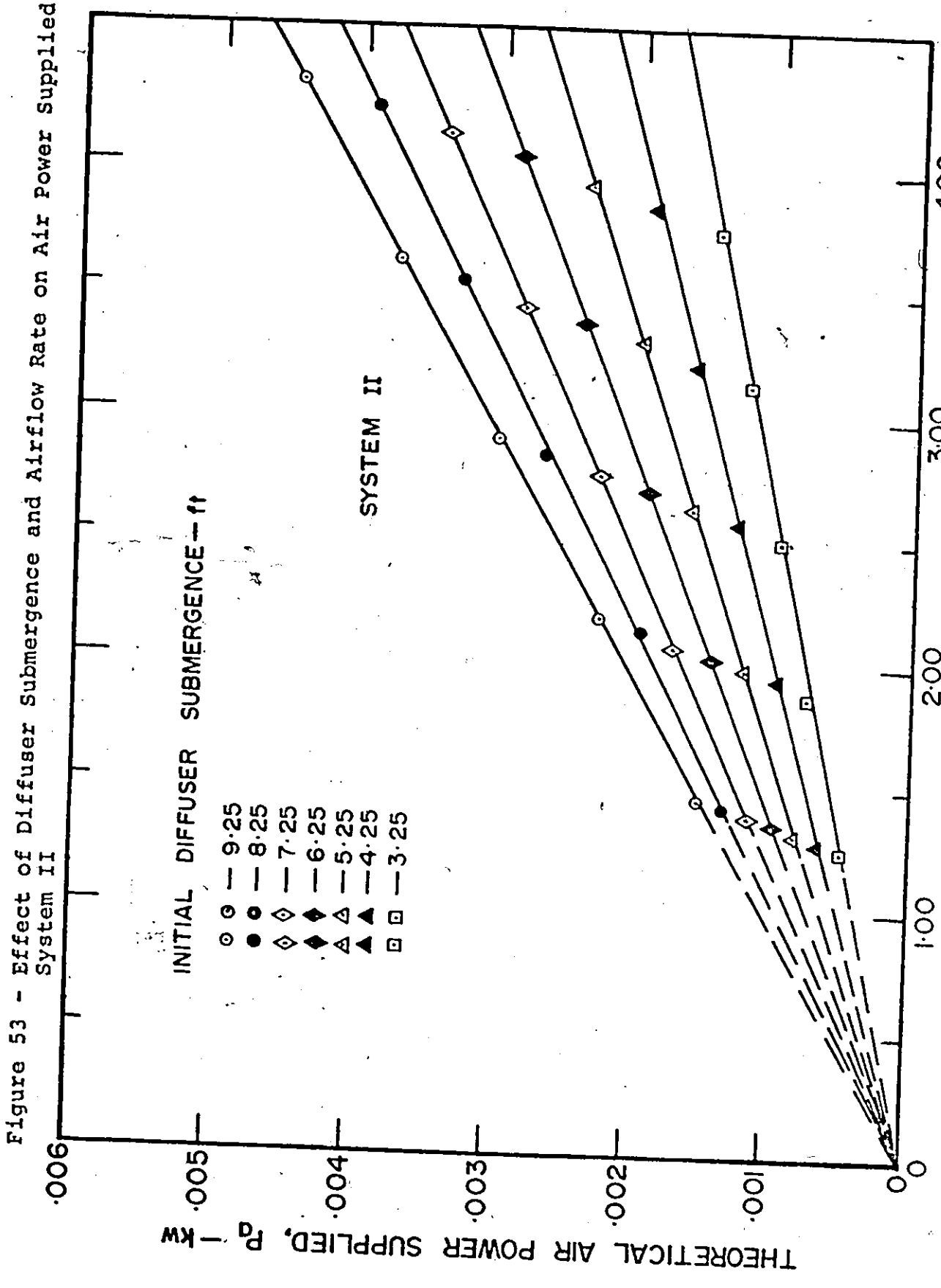


Figure 53 - Effect of Diffuser Submergence and Airflow Rate on Air Power Supplied, System II

there is an increase in air power supplied, $P_a$, with an increase in diffuser submergence, as seen from Figure 53. Therefore, the unit power efficiency, $E_p$, decreases with an increase in submergence depth. A close examination of Figures 52 and 53 shows that, over the range of airflows tested, the air power has increased on an average, by 2.33 times, in changing the diffuser submergence from 4.25 ft to 9.25 ft, whereas the total contact time of the air bubble, $t_c$, shows a corresponding average increase of only 1.75 times over the same conditions.

Figure 21 shows the change in the Overall Transfer Coefficient, $(K_La)_{20}$, with the airflow rate and the diffuser submergence. In this system, $(K_La)_{20}$ shows an increase in value both when the unit airflow rate, $q_a$, is increased and when the diffuser submergence is increased. As in System I, a higher airflow rate means an increase in the number of air bubbles in the system, with a subsequent increase in the total interfacial area and the amount of oxygen transferred to the liquid. With $q_a$ remaining constant and submergence depth increasing, the simultaneous effect of increased contact time, $t_c$, as well as a larger deficit or driving force, $(C_i-C_L)$, results in more oxygen transfer, despite the adverse effect of increased circulating and air bubble velocities with increased diffuser submergence. Thus, $(K_La)_{20}$ shows an increase both with airflow rate and with submergence depth, and the relationship between them is given by the following equation with a Correlation Coefficient,

r = 0.987:

$$(K_L a)_{20} = A\, q_a^{B} \quad \text{..... 46}$$

where $A = (0.5140 \times 10^{0.0333H_T})$

$B = (0.940 \times 10^{-0.0209H_T})$

Eckenfelder (31) also had observed an increase in $K_L a$ with airflow rate and depth, while working with coarse-bubble spargers and an experimental, conventional aeration tank. Since System II represents a cross-section of a typical spiral-flow tank, there appears to be good agreement between these data and the observations made by Eckenfelder.

The effects of bubble size, airflow rate, and diffuser submergence on the Liquid Film Coefficient, $K_L$, are shown in Figures 22 and 23. Like in System I, there is an increase in $K_L$ with an increase in the equivalent bubble diameter, $d_{ave.}$. Again, this is attributed to the larger boundary shears and rapid renewal of the liquid film exhibited by the larger air bubbles. The values of $K_L$ increase with increased values of $q_a$ since the bubble sizes are observed to increase with $q_a$ (see figure 49). Figure 23 shows the general trend of increasing $K_L$ values with an increase in the unit airflow rate. From both Figures 22 and 23, it is apparent that there is no discernible effect of diffuser submergence on $K_L$. $(K_L)_{20}$ values of $8.32 \times 10^{-4}$ to $21.4 \times 10^{-4}$ ft/sec. or 91.3 to 235 cm/hr, with the

bubble size ranging between 20 and 44 mm in diameter, have been obtained in this system. Both parameters, $K_L$ and bubble size, in System II are larger in value than the values reported for System I. The $(K_L)_{20}$ values obtained in System II are comparable to those obtained by several other authors (5), (6), (43) and quoted earlier in this chapter; however, the bubble sizes are much larger than those reported in any previous work.

## C. SYSTEM III - Circulation With Pumping, $V_w \leq V_b$

The operating conditions of System III are given in Chapter V and are explained with Figures 8 and 11. The results have been plotted in Figures 24 to 34. In this system, column heights varied from 3 to 8 feet, in 1 foot intervals, while the airflow rates ranged from 0.11 to 0.38 scfm. The water was pumped against the movement of air bubbles, thus creating counter-current air-water flow conditions. The pumping rate was controlled such that the average velocity of the water, $V_w$, was 'equal to' or 'less than' the velocity of the rising air bubbles, i.e., $V_w \leq V_b$ This waterflow rate, $Q_w$, was responsible for slowing down the upward movement of the air bubbles. The maximum rate at which the water could be circulated without disturbing the stability of the system has been designated as $Q_{max}$. Since the water was pumped through the closed-hoop, head differential across the central partition in the recirculating

tank was obtained. This head differential was almost completely due to the bulking effect of the air present in the air-water mixture and not due to friction. For an example, in a typical run, the total differential head, $\Delta H$, was 0.730 ft. But when the air was shut off, the head loss due to friction, etc., was reduced to 0.021 feet and this represents less than 3% of the total differential head. Therefore, frictional resistance contributed very little to the total pumping head required to circulate water in the closed-loop of this system.

Figure 24 shows the relationship between the oxygen transfer efficiency, $E_o$, the unit airflow rate, $q_a$, and the initial diffuser submergence. Similar to the previous two systems, $E_o$ decreases as $q_a$ is increased for any particular submergence. The reasons for this behaviour once again are attributed to the increase in bubble size with an increase in airflow rate. This increase in bubble size results in the reduction in the ratio of interfacial area to bubble volume and the increase in terminal velocity of the bubble, consequently increasing the total bubble velocity as well. This increase in total bubble velocity, in turn, leads to a reduction in the contact time of the air bubbles and subsequently a decrease in $E_o$. This explanation is supported by the plots in Figures 54, 55, 56, and 57, showing the effect of $q_a$ on $d_{ave.}$, $V_b$, $V_T$, and $t_c$. It is interesting to note from Figures 24 and 57 that the influence of airflow rate on contact time shows a pattern similar to its effect

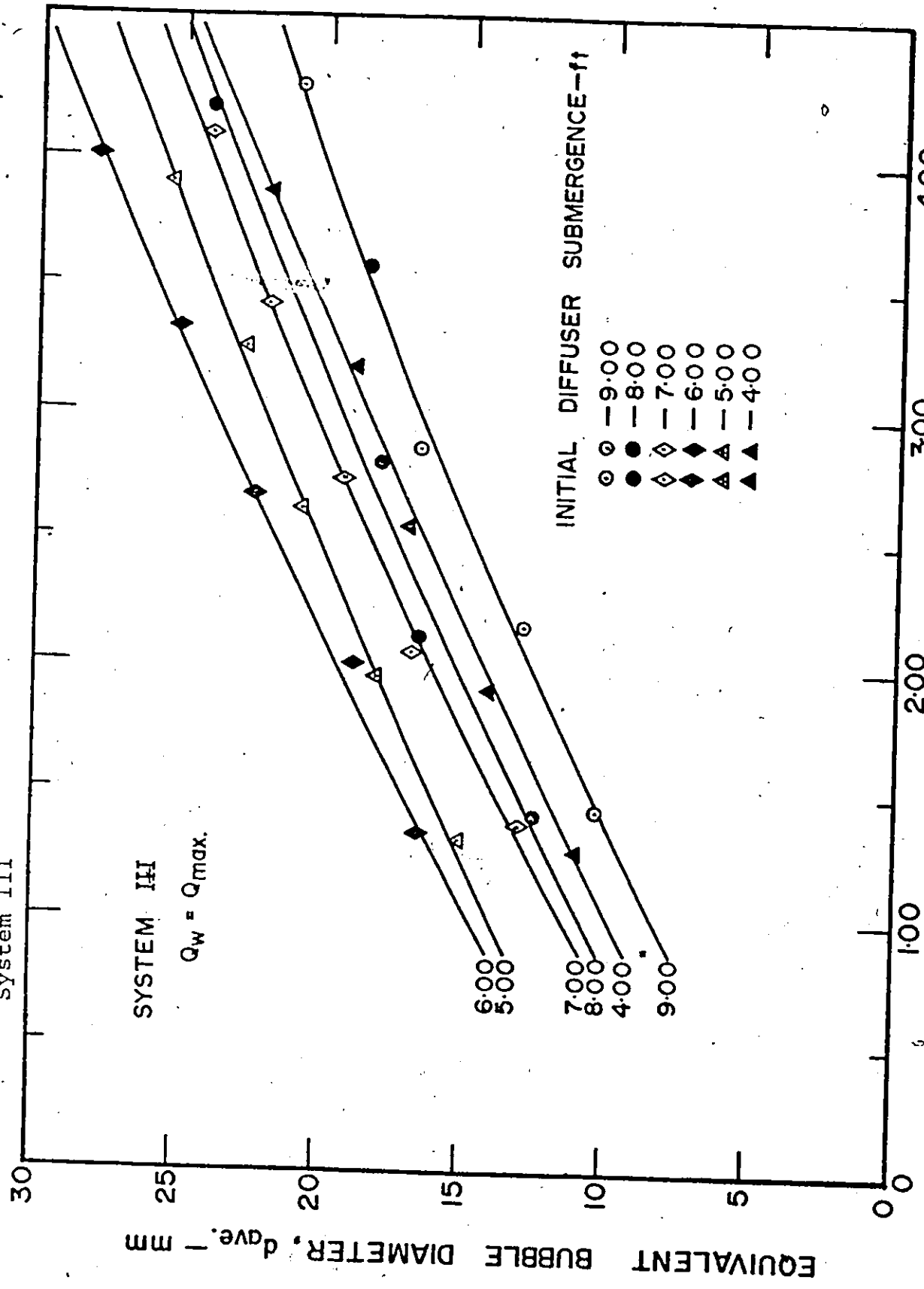


Figure 54 - Effect of Diffuser Submergence and Airflow Rate on Bubble Size, System III

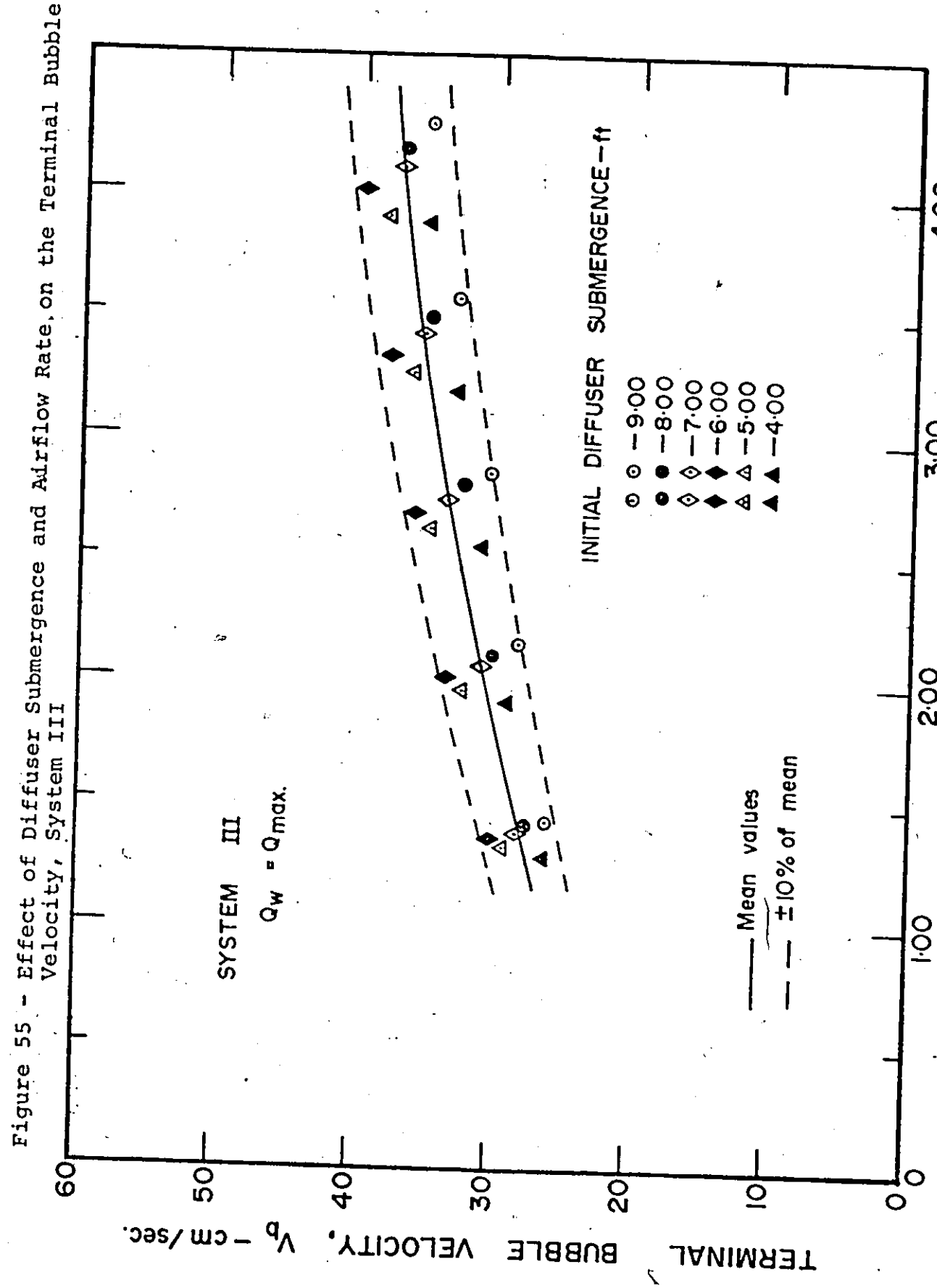


Figure 55 - Effect of Diffuser Submergence and Airflow Rate on the Terminal Bubble Velocity, System III

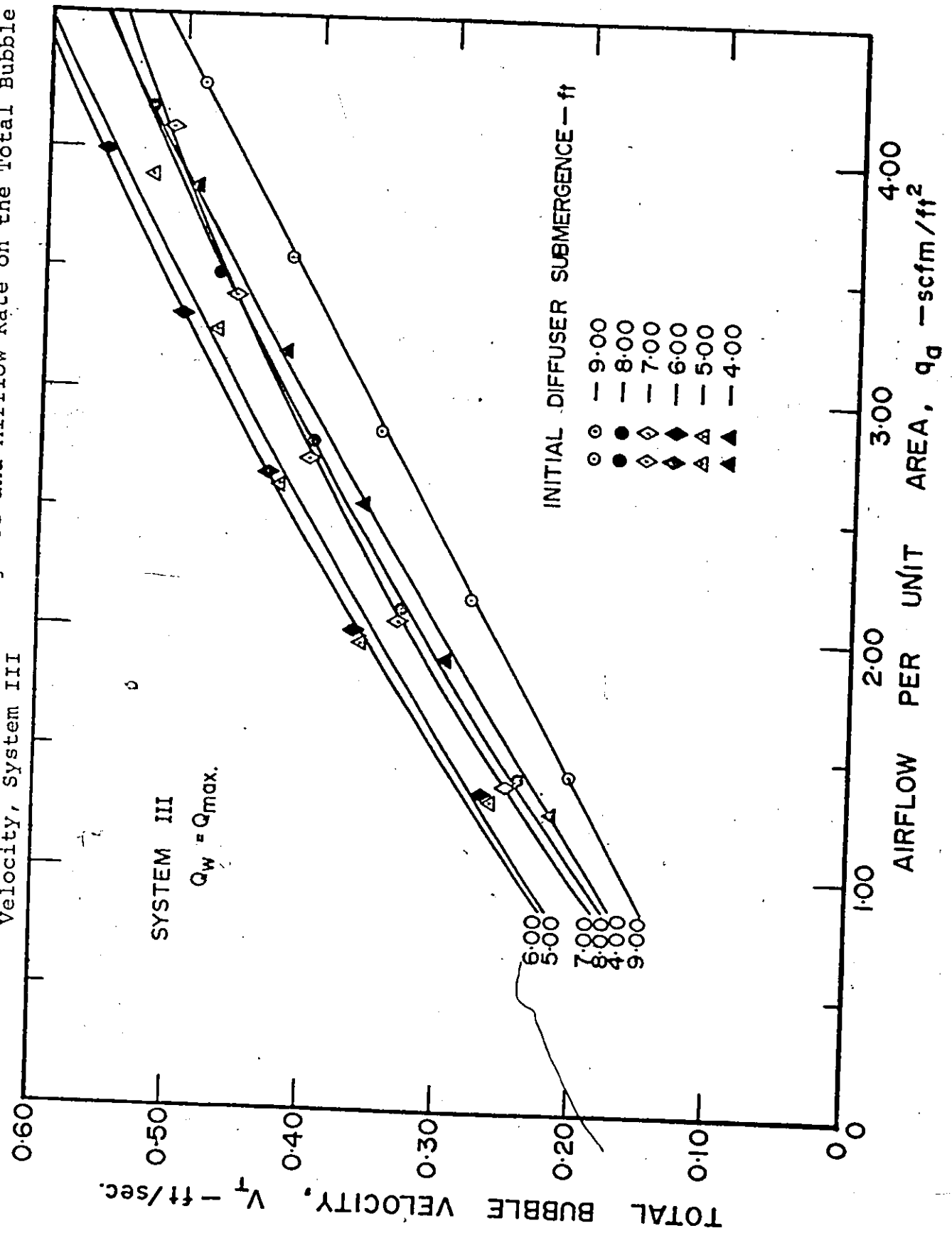


Figure 56 - Effect of Diffuser Submergence and Airflow Rate on the Total Bubble Velocity, System III

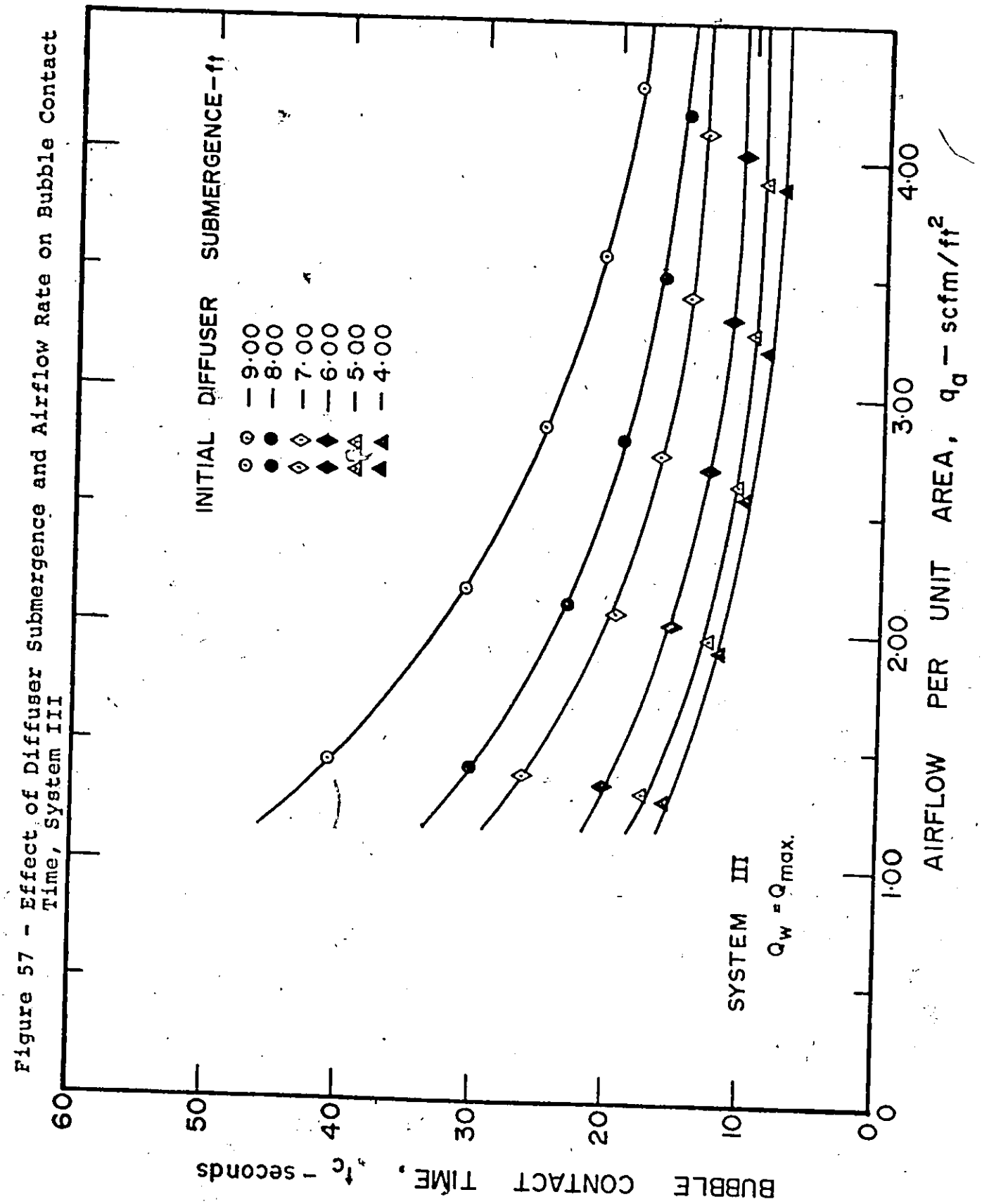


Figure 57 - Effect of Diffuser Submergence and Airflow Rate on Bubble Contact Time, System III

on $E_o$. Thus, the contact time again is an important variable in this System.

It can also be seen in Figure 24 that $E_o$ increases with diffuser submergence for any particular airflow rate. This is a direct result of the increase in contact time of the slow moving bubbles as the depth is increased, as is evident from Figure 57. This influence is more significant at the low airflow rates than at the higher ones since much larger air bubbles are formed at the high air flows, regardless of depth, and they rise faster through the water. Thus, the increase in contact time, and subsequently the increase in $E_o$, is not as large at the high airflow rates as at the low air flows and therefore, the result is the tapering effect observed in Figures 24 and 57. In addition to the contact time, the deficit or driving force, $(C_i - C_L)$, also increases with depth and thus more oxygen is transferred.

Figures 25 and 26 show the effects of airflow rate and diffuser submergence on the unit power efficiency, $E_p$. It is noticed that, as the unit airflow rate, $q_a$, is increased and the submergence remains constant, $E_p$ decreases in value. There are several reasons for this observation in System III. One reason is the decrease in bubble contact time, $t_c$, with airflow rate, as illustrated in Figure 57. Also, in this system, $E_p$ is a function of both the air power supplied, $P_a$, and the input water power, $P_w$. When the airflow is increased, the bulk volume of the system is increased, with a subsequent rise in $\Delta H$. This, in turn,

causes $P_w$ to increase, as shown in Figure 58. At the same time, $P_a$ increases proportionally with the increase in $q_a$, as illustrated in Figure 59. Therefore, the combined increase in power input plus the decrease in bubble contact time mentioned above, offsets any increase in oxygen transferred with an increase in air flow and therefore $E_p$ decreases.

Figure 26 also indicates that, for any airflow rate, increasing the diffuser submergence results in a decrease in $E_p$. However, this decrease in $E_p$ seems to occur in two stages, with the 6 foot submergence depth as the separating point. It is interesting to note from Figure 60 in this system, that the highest waterflow rate occurs at the 6 foot submergence depth. This is believed to be due to the fact that the bubble sizes are the largest at this particular depth, as shown in Figure 61. As a result of the largest bubble sizes, both terminal and total bubble velocities are also highest at this 6 foot depth, as shown in Figures 55 and 62. Consequently, the greatest flow rate of water is needed at this depth to counteract the velocity of the air bubbles and to maintain equilibrium conditions. This point is illustrated by the previous Figure 60 and further supported by Figures 63 and 64. Although the values for the average water velocity, $V_w$, appear to lie within ±10% of the mean values, still there is a definite indication of the pattern of change. It is interesting to observe that

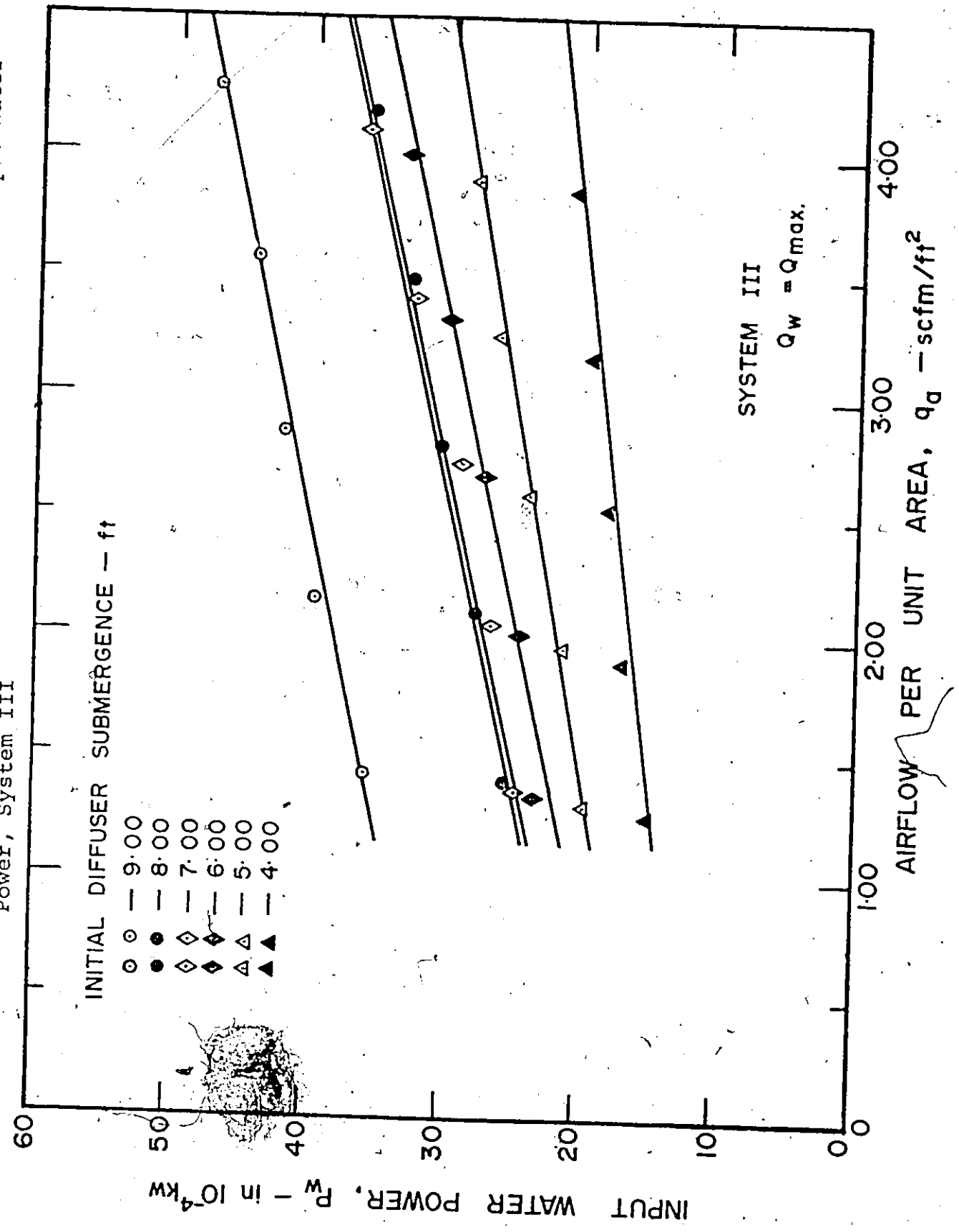


Figure 58 - Effect of Diffuser Submergence and Airflow Rate on Input Water Power, System III

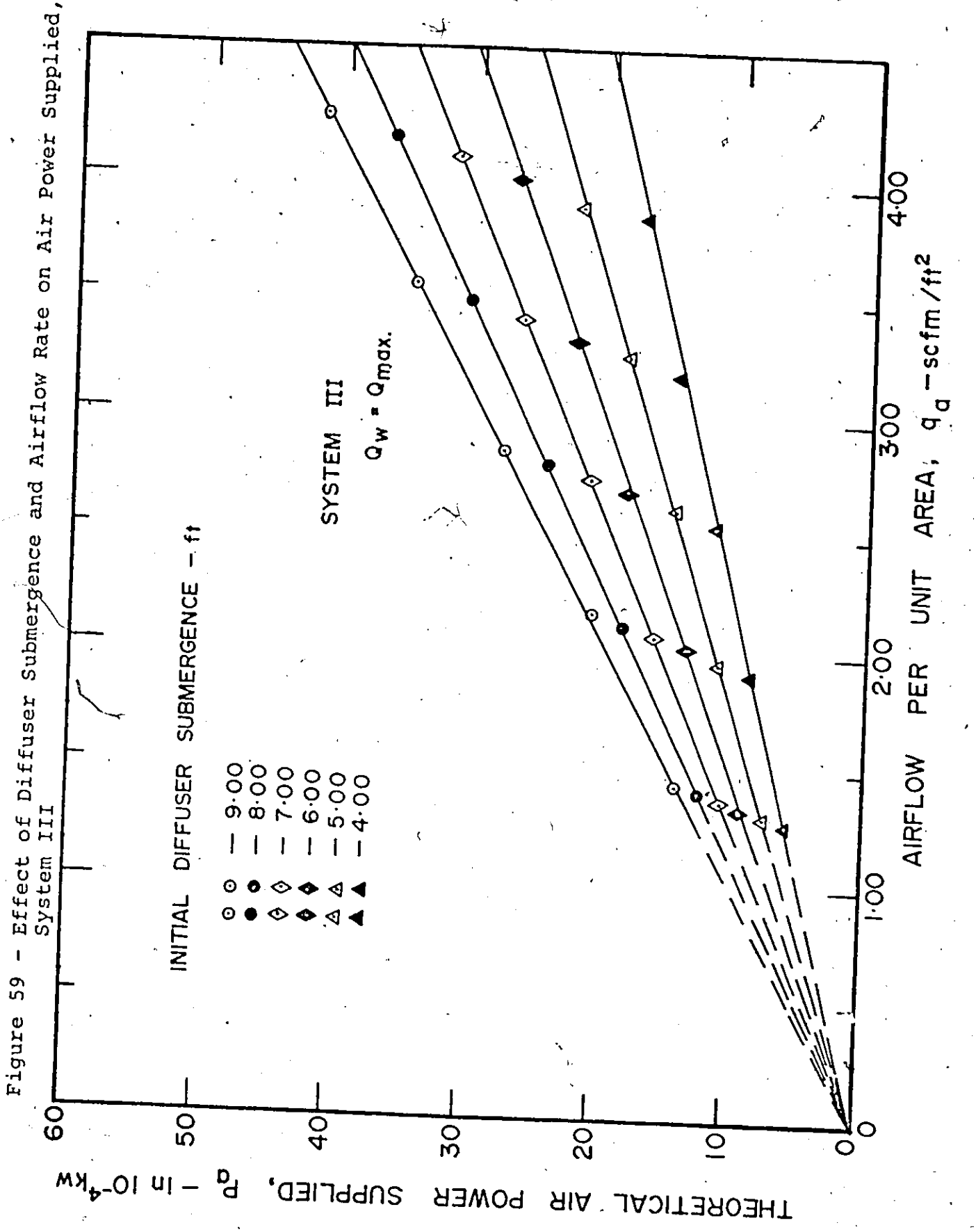


Figure 59 - Effect of Diffuser Submergence and Airflow Rate on Air Power Supplied, System III

Figure 60 - Effect of Diffuser Submergence and Airflow Rate on the Nominal Water Velocity, System III

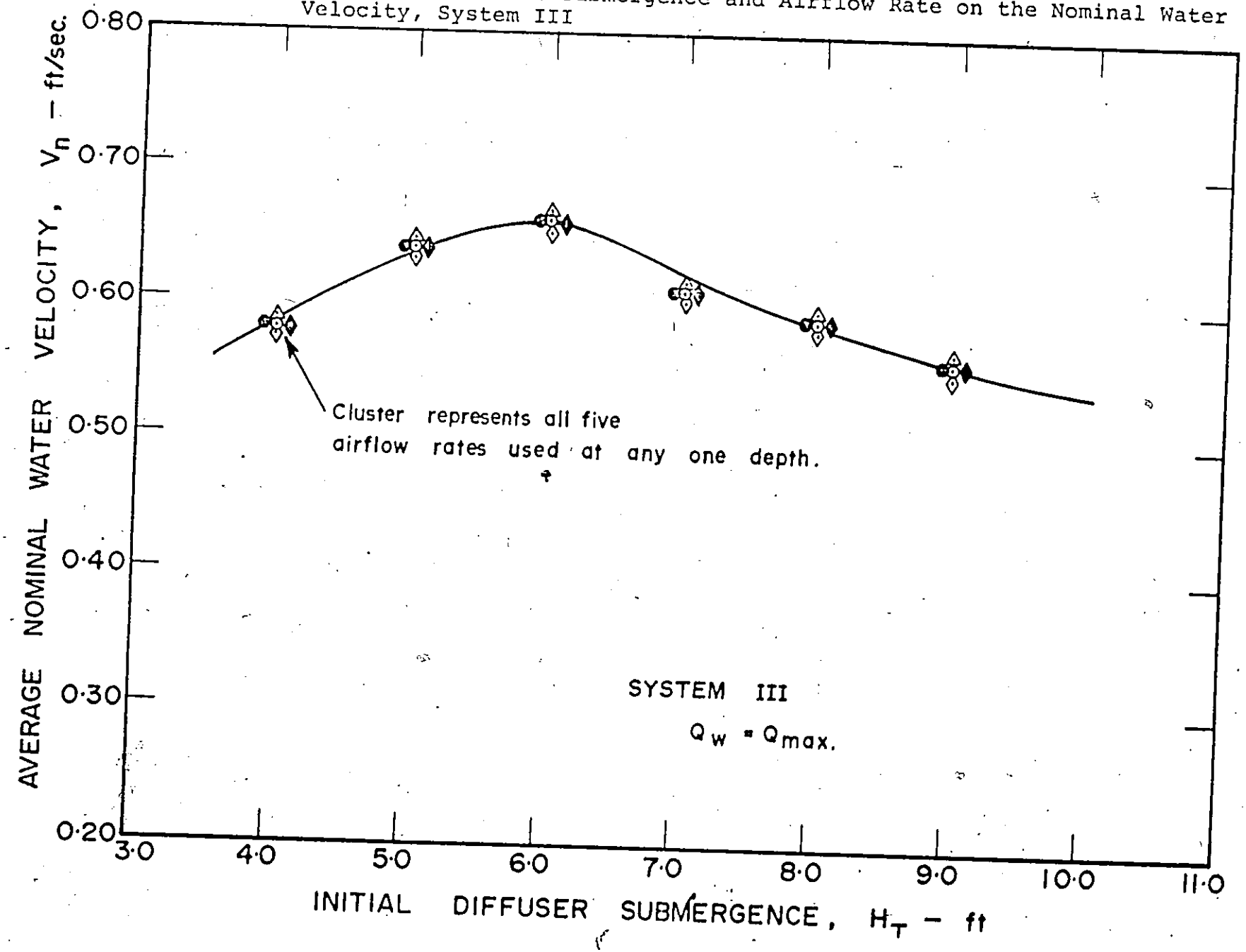

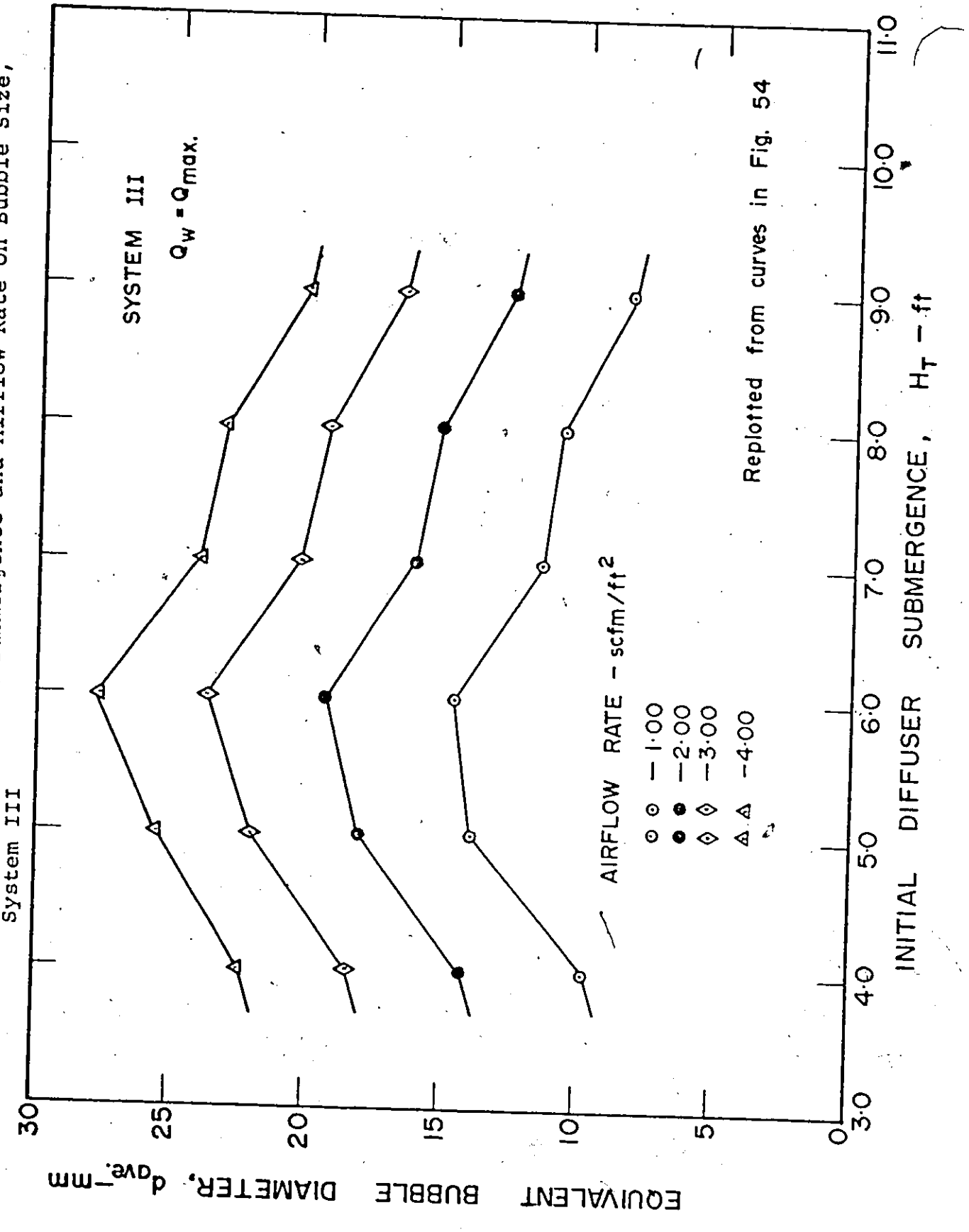


Figure 61 - Effect of Diffuser Submergence and Airflow Rate on Bubble Size, System III

Figure 62 - Effect of Diffuser Submergence and Airflow Rate on the Total Bubble Velocity, System III

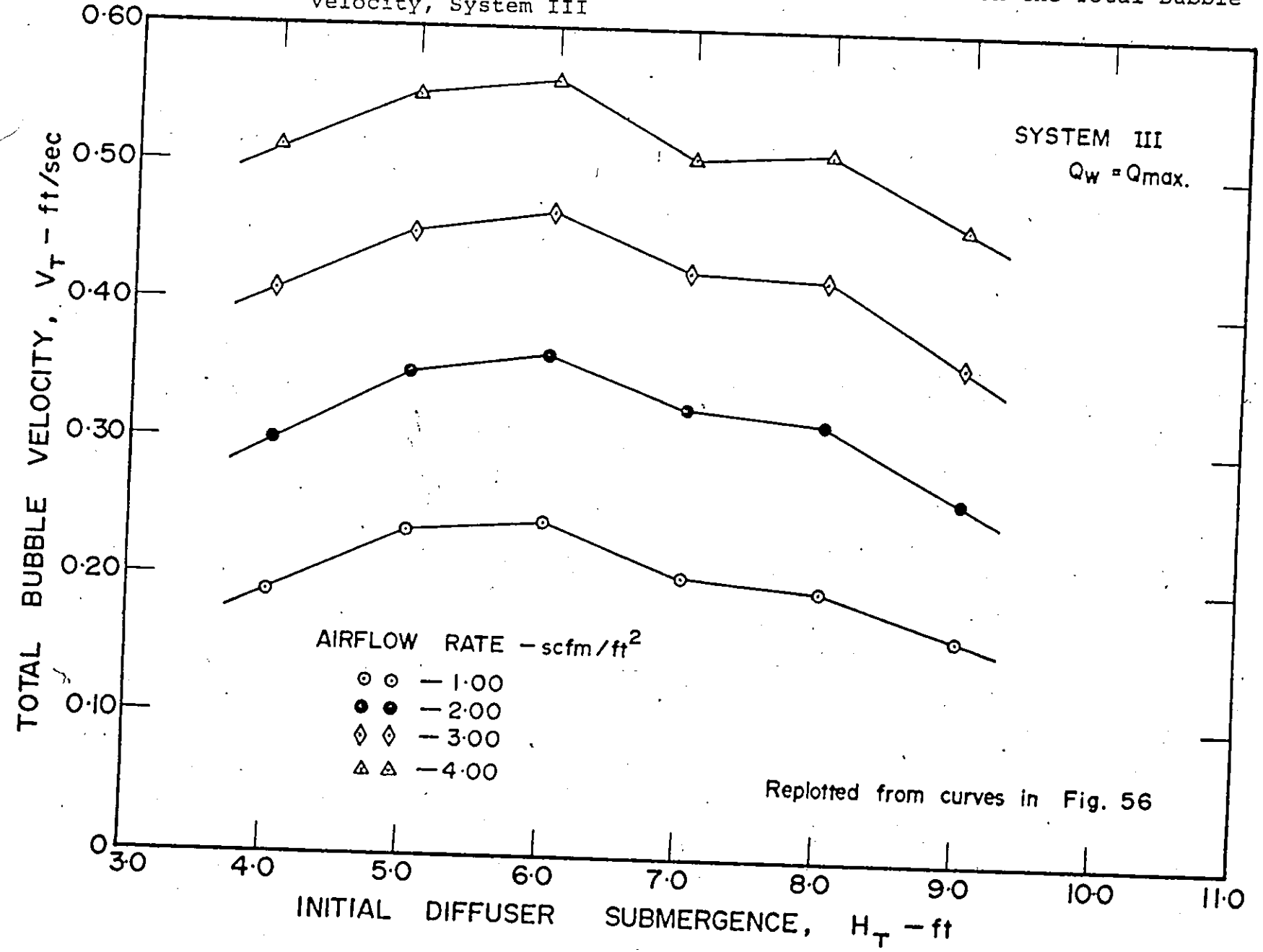

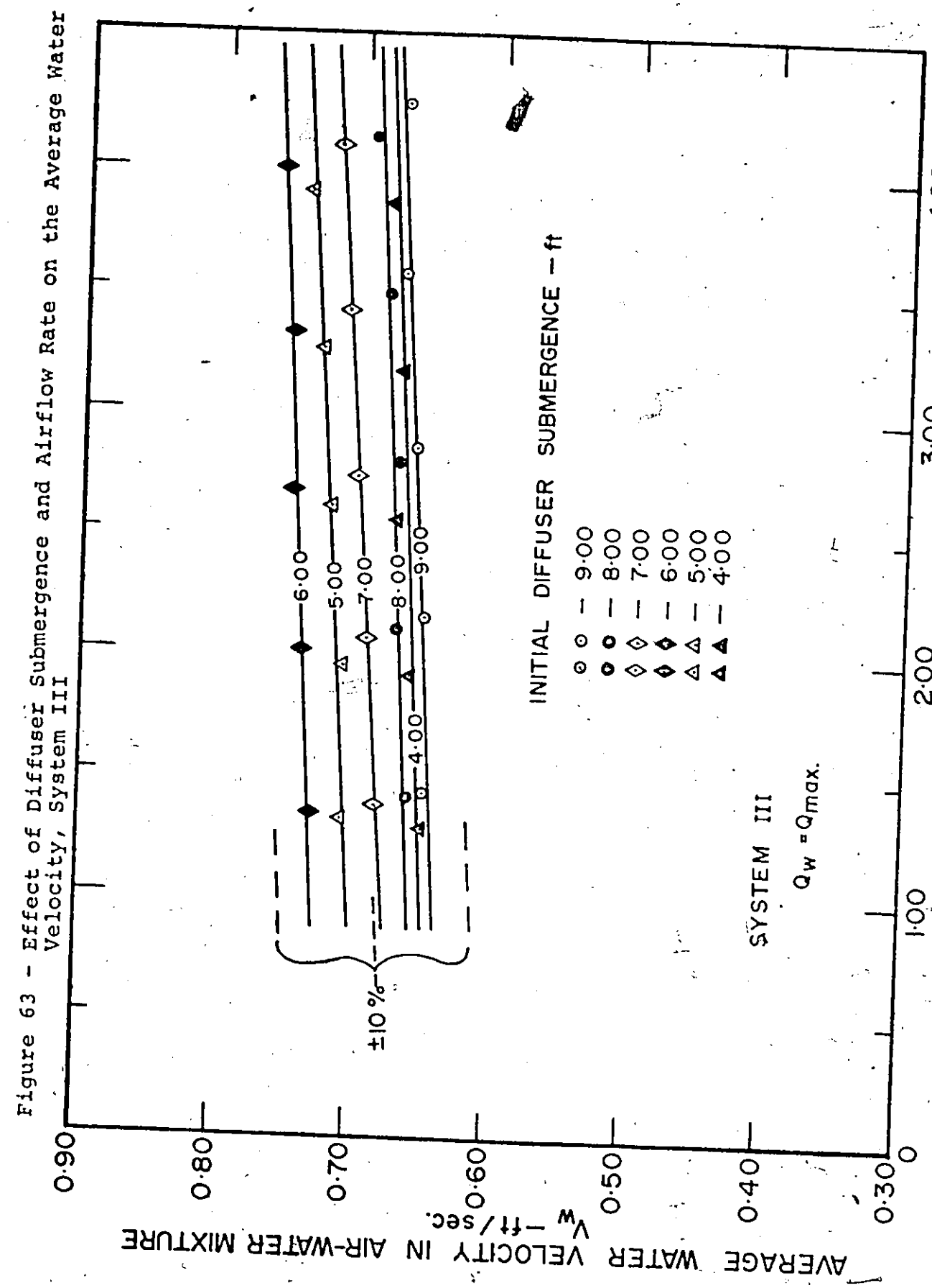


Figure 63 - Effect of Diffuser Submergence and Airflow Rate on the Average Water Velocity, System III

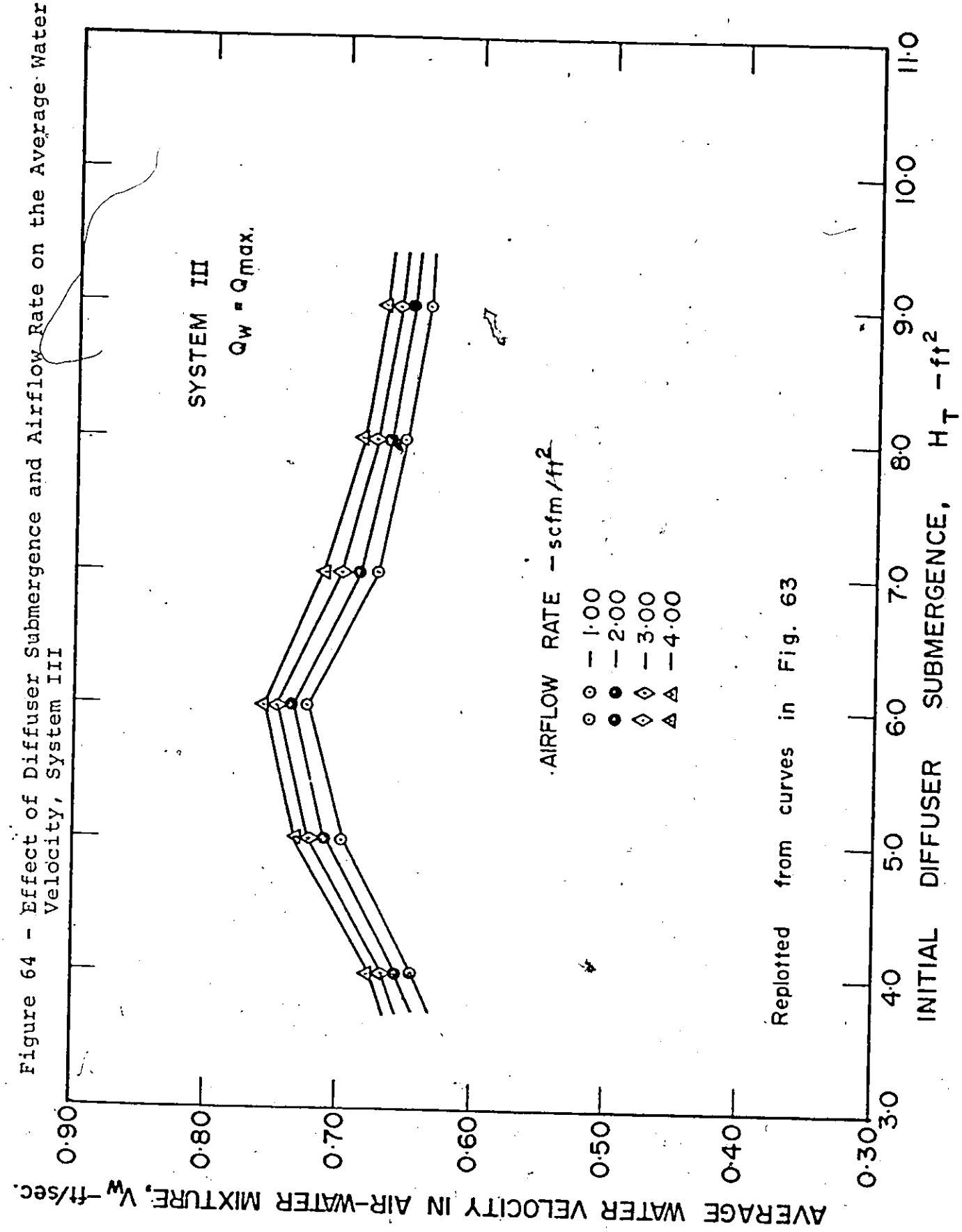


Figure 64 - Effect of Diffuser Submergence and Airflow Rate on the Average Water Velocity, System III

$Q_{max}$, varies with the submergence but is independent of airflow rates.

Figure 57 shows that the bubble contact time increases with an increase in submergence depth. At the same time, however, increasing the water depth increases both the air power, $P_a$, and the water power, $P_w$, as shown in Figures 58 and 59, with the result that $E_p$ decreases with an increase in submergence depth. When the diffuser submergence increases from 6.00 ft to 7.00 ft, the waterflow rate drops, as shown in Figure 60, thereby reducing the increase in water power, while simultaneously benefitting from the increase in contact time with depth. The overall effect is an increase in $E_p$ or temporary recovery, as observed in Figure 26. However, as the submergence is increased further, $E_p$ values begin to drop again, because of the reasons mentioned earlier. Another important factor influencing $E_p$ at higher depths is the driving force, $(C_i - C_L)$. Because of high oxygen transfer efficiencies, $E_o$, at higher depths (8 - 18%), the partial pressure of oxygen inside the air bubbles is dropped, with the result that the concentration gradient or driving force, $(C_i - C_L)$, is reduced. Therefore, there is less oxygen transferred to the liquid.

The Overall Transfer Coefficient, $(K_La)_{20}$, as a function of the unit airflow rate and diffuser submergence, is given in Figure 27. Like in System II, $(K_La)_{20}$ shows an increase in value, both as the unit airflow rate, $q_a$, is increased, and as the diffuser submergence is increased,

although the latter observation is not as pronounced as in the previous system. This can be explained by the difficulty in keeping System III stabilized, with continuous counter-current, air-water flow. The everchanging nature of equilibrium conditions in this system makes the correlation of data to be the most difficult of all the four systems. The increase in $(K_L a)_{20}$ with an increase in $q_a$ is again attributed to the additional supply of oxygen and increased number of air bubbles present for that transfer to occur; while the increase in $(K_L a)_{20}$ with depth is explained by the increase in bubble contact time, $t_c$, (Figure 57), and a larger deficit or driving force, $(C_i - C_L)$, existing at higher water depths. A relationship for $(K_L a)_{20}$ is given by the following equation with a Correlation Coefficient, r, of 0.960:

$$(K_L a)_{20} = (2.203 + 0.196\ H_T) q_a^{0.4251} \quad \ldots\ldots\ 47$$

Figure 28 gives the relationship between the Liquid Film Coefficient, $K_L$, the bubble size and the diffuser submergence. As expected, $K_L$ increases with bubble diameter, $d_{ave.}$, because of the larger boundary shear and larger concentration gradients across the liquid film associated with the bigger air bubbles. As observed in the previous two systems, there is an increasing, curvilinear relationship between $K_L$ and $q_a$, and this is in agreement with other studies found in the literature (9), (43). No appreciable

effect of diffuser submergence on $K_L$ is observed, although there are indications from Figure 28 that $K_L$ might vary inversely with depth. This phenomenon has been observed by several authors (9), (12), (15), (31), (43) in studies conducted with fine bubble or porous diffusers. The explanation given is that higher oxygen transfer takes place during bubble formation and burst because of the continual replenishment of the air-water interface and subsequent high surface renewal rate. Also, the oxygen deficit during bubble formation is higher than the average oxygen deficit during ascent. When the bubble reaches its terminal velocity, the transfer rate becomes constant as it rises through the liquid. Therefore, the average value for $K_L$ over the entire height of the water column, decreases with increasing column height. Although System III still is a coarse-bubble system, the bubble sizes (10-28 mm) are smaller than in the previous two systems, especially in comparison to System II. This results from the shearing action of the downward flowing water as it passes over the diffuser openings. Therefore, near the diffuser, fine bubble conditions, with respect to oxygen transfer rates, might prevail momentarily and the values for $K_L$ would thus be higher at the lower water depths due to the reasons explained earlier. In this system, $(K_L)_{20}$ values of $1.67 \times 10^{-4}$ to $7.63 \times 10^{-4}$ ft/sec. or 18.3 to 83.8 cm/hr have been obtained and these are comparable to System I.

Several experiments were conducted to determine the

effect of reducing the waterflow rate below $Q_{max.}$ while keeping $q_a$ constant. Two different initial diffuser submergence depths, 4.00 and 9.00 feet, and two different waterflow rates, $q_w$, of 115 and 172 USGPM/ft$^2$ were employed. The results are plotted in Figures 29 to 34. It is clearly seen from Figures 65 and 66 that the reduction in waterflow rate reduces the water power input to the system. The change in $K_La$ with changes in waterflow and airflow rates is shown in Figures 33 and 34. As expected, there is a reduction in $K_La$ values due to the reduced shear at the bubble interface, as well as the decreased bubble contact time at lower waterflow rates. In other words, as the downward water velocity is reduced, the total or resultant bubble velocity upward, $(V_b-V_w)$, is increased and subsequently the contact time is decreased. This results in a reduction in oxygen transfer.

The effects of reducing the waterflow rate on the oxygen transfer efficiency, $E_o$, are plotted in Figures 29 and 30. Like in the case of $K_La$, the reduction in downward water velocity, due to the reduced flow rate, allows the air bubbles to rise much quicker through the column, thereby reducing the contact time. Consequently, less oxygen is transferred to the water and the value of $E_o$ decreases as compared to values at $Q_{max.}$. This effect is more pronounced at lower airflow rates because of the small number of bubbles present in the system. Earlier work by the author (10) also confirms the above observations.

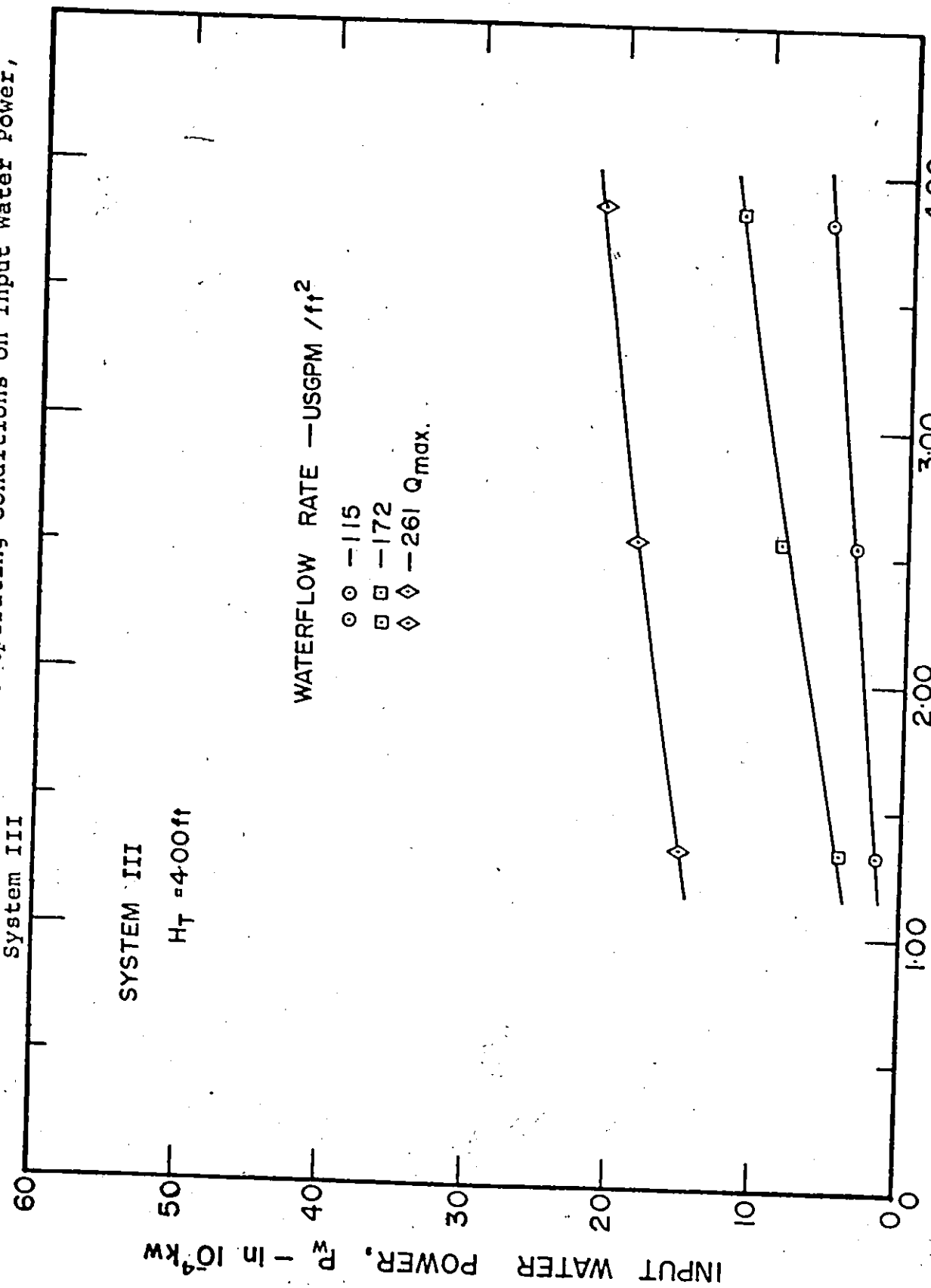


Figure 65 - Effect of Different Operating Conditions on Input Water Power, System III

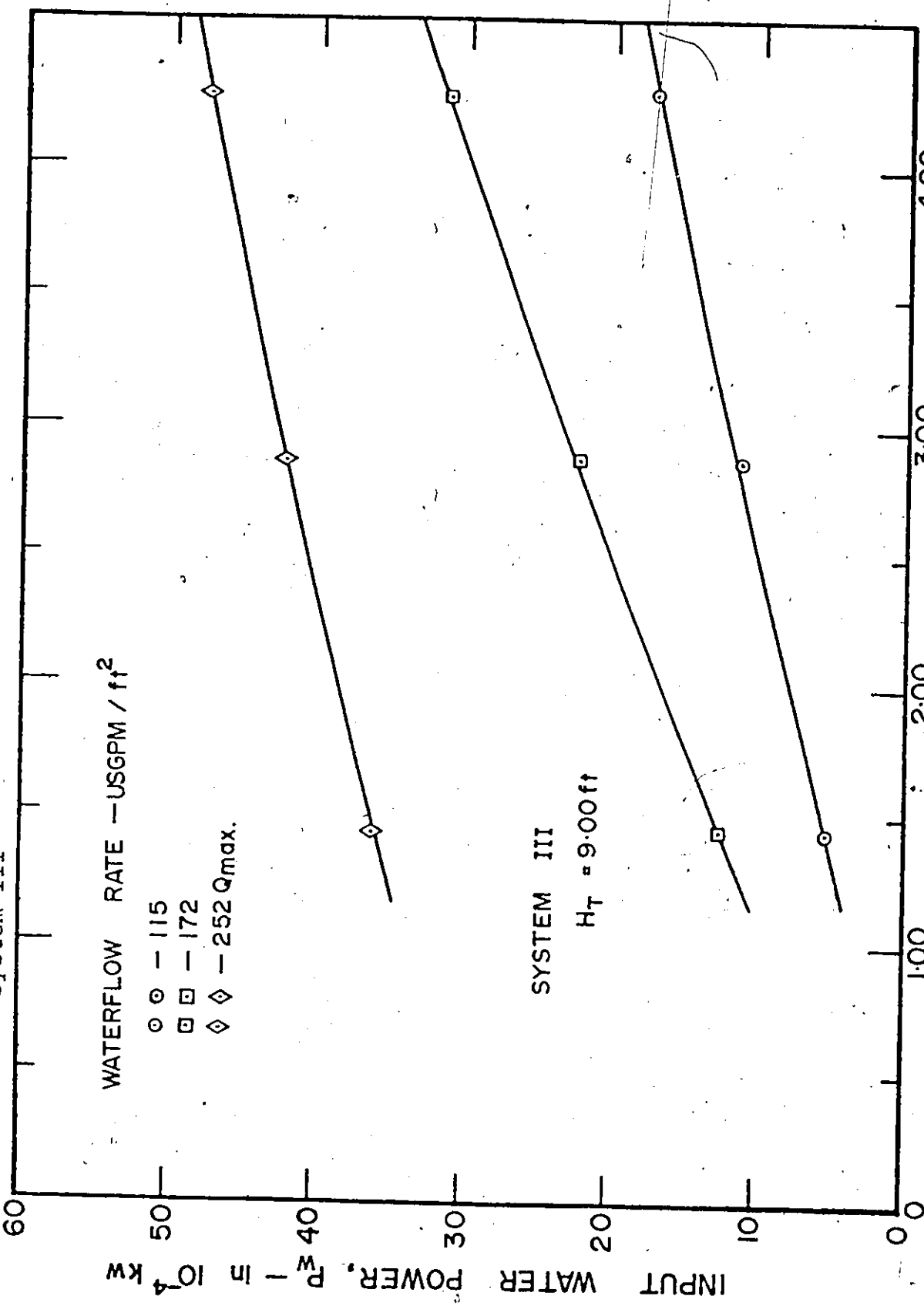


Figure 66 - Effect of Different Operating Conditions on Input Water Power, System III

Figures 31 and 32 show the effect of reducing the waterflow rate, below $Q_{max.}$, on the unit power efficiency, $E_p$. Within ±10% of the mean value, there appears to be no significant change in the value of $E_p$ at any particular airflow rate, regardless of the waterflow rate. This also was observed in earlier work by the author (10). In other words, reducing $q_w$ will reduce the amount of oxygen transferred, as explained earlier, but at the same time, the input water power is reduced. These two factors are compensating in character and $E_p$ remains relatively constant. Therefore, this suggests that, in System III, increasing the waterflow rate will substantially increase the value of $E_o$, in terms of per cent oxygen transferred/oxygen supplied; however, this action will not significantly change the value of $E_p$, or the amount of oxygen transferred/power input, because of the additional power being put into the system. This fact must be considered in estimating the operating costs, if System III were to be applied in full-scale operation of an aeration tank in a treatment plant.

## D. SYSTEM IV - Circulation With Pumping, $V_w > V_b$

The operating conditions for this system are presented in Chapter V and are explained with Figures 8 and 13. The results are plotted in Figures 35 to 41. In System IV, column heights varied from 2 to 7 feet, in 1 foot intervals, while airflow rates ranged from 0.10 to 0.32 scfm. Two

important differences existed in this system as compared to the others. First, the coarse-bubble diffuser was located near the top of the aeration column, just below the recirculating tank, and second, the water was pumped against the air bubble flow such that co-current, air-water flow conditions existed. In order to achieve this, the average velocity of the water was kept just greater than the terminal bubble velocity on the diffuser side of the system, i.e., $V_w > V_b$. The waterflow rate required to create these conditions has been designated $Q_{min}$. With $Q_w \geq Q_{min}$, the air bubbles traversed the entire length of the U-Tube, i.e., downward on one side and upward on the other side, under co-current flow conditions. This system is similar in principle to the U-Tube concept presented by Bruijn (16) and Speece (17), described earlier. Since water was pumped through the closed loop, head differentials, $\Delta H$, required across the central partition in the recirculating tank, were recorded. In this system also, the head differential was almost entirely due to the bulking effect of the air-water mixture and not due to the friction. Since the air bubbles moved in a downward direction, starting near the top of the column, the diffuser submergence relative to the change in column height, could no longer be used as a comparative parameter. Instead, the depth of water below the diffuser, $H_b$, was considered to be more appropriate. The physical significance of $H_b$ is shown in Figure 13. As noted previously in Chapter VI, the flow conditions of the air-water mixture could not be analysed

nor the parameters computed for that side of ths system in which air and water flowed co-currently upward. However, it is assumed in the discussion of results that the flow conditions existing on this side apply equally to all heights and airflows. For the purpose of comparison, analyses are made employing observations and results from the downflow or right-side only.

It can be seen from Figure 35 that, if the unit airflow rate, $q_a$, is held constant and the depth of water below the diffuser, $H_b$, is increased, the oxygen transfer efficiency, $E_o$, shows an increase in value. This can be attributed to the fact that increasing the water depth also increases the total contact time of the air bubbles, as seen in Figure 67. In this Figure, only the contact time on the downflow side, $t_{cR}$, is given, for reasons already mentioned in Chapter VI. Also, as the bubbles move downward, the hydrostatic head around them increases, thereby reducing their size. Likewise, the dissolved oxygen deficit is increased due to an increase in the saturation concentration. In addition, the natural buoyant force of the air bubble, in the direction opposite to their direction of movement, causes a great deal of turbulence at the bubble surface, resulting in a high rate of surface renewal. All of these factors result in more oxygen being transferred for the same rate of air supply and therefore, $E_o$ increases with depth. Speece (17) had obtained similar results with his U-Tube apparatus and his explanation was on the same lines

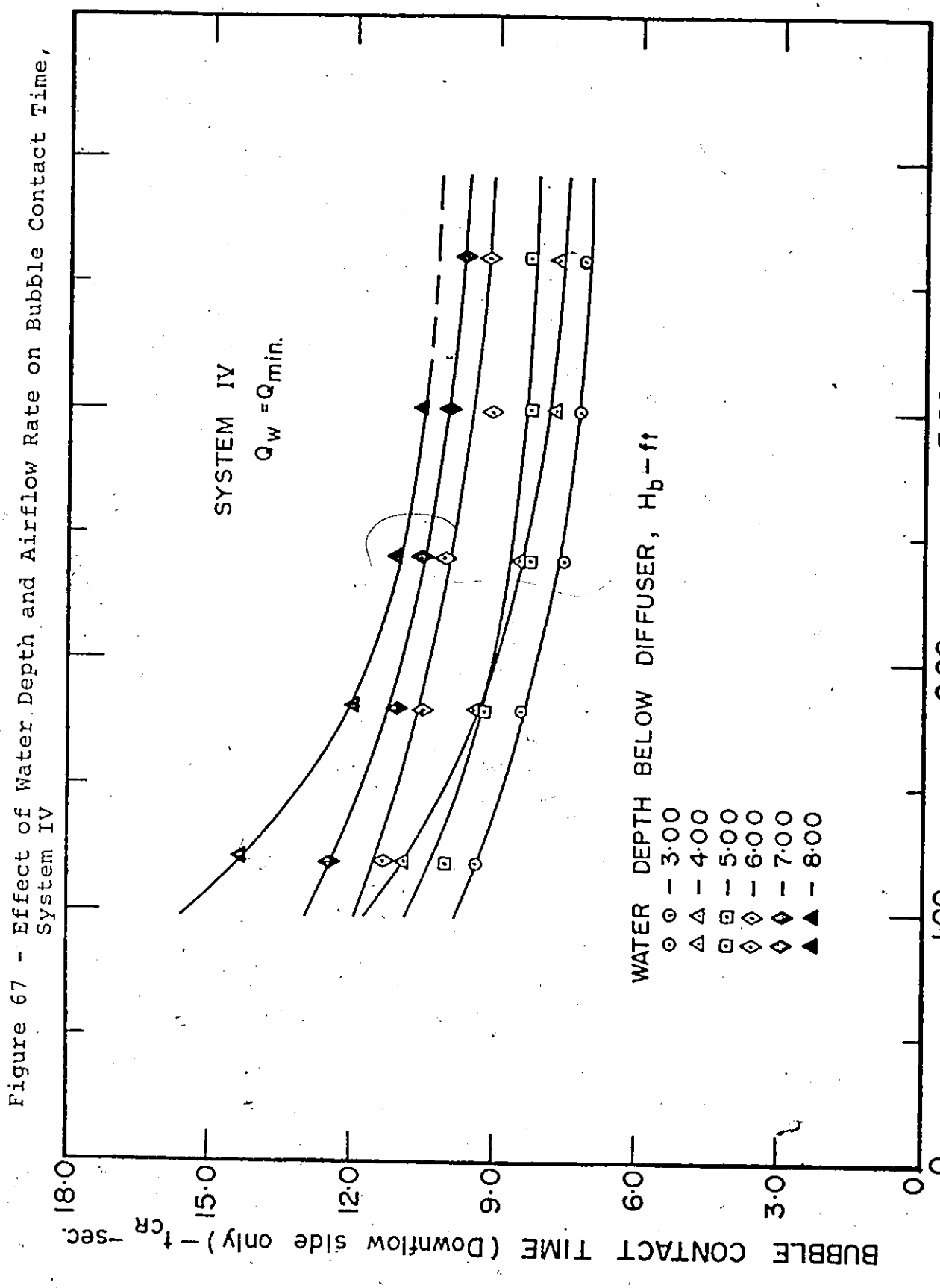


Figure 67 - Effect of Water Depth and Airflow Rate on Bubble Contact Time, System IV

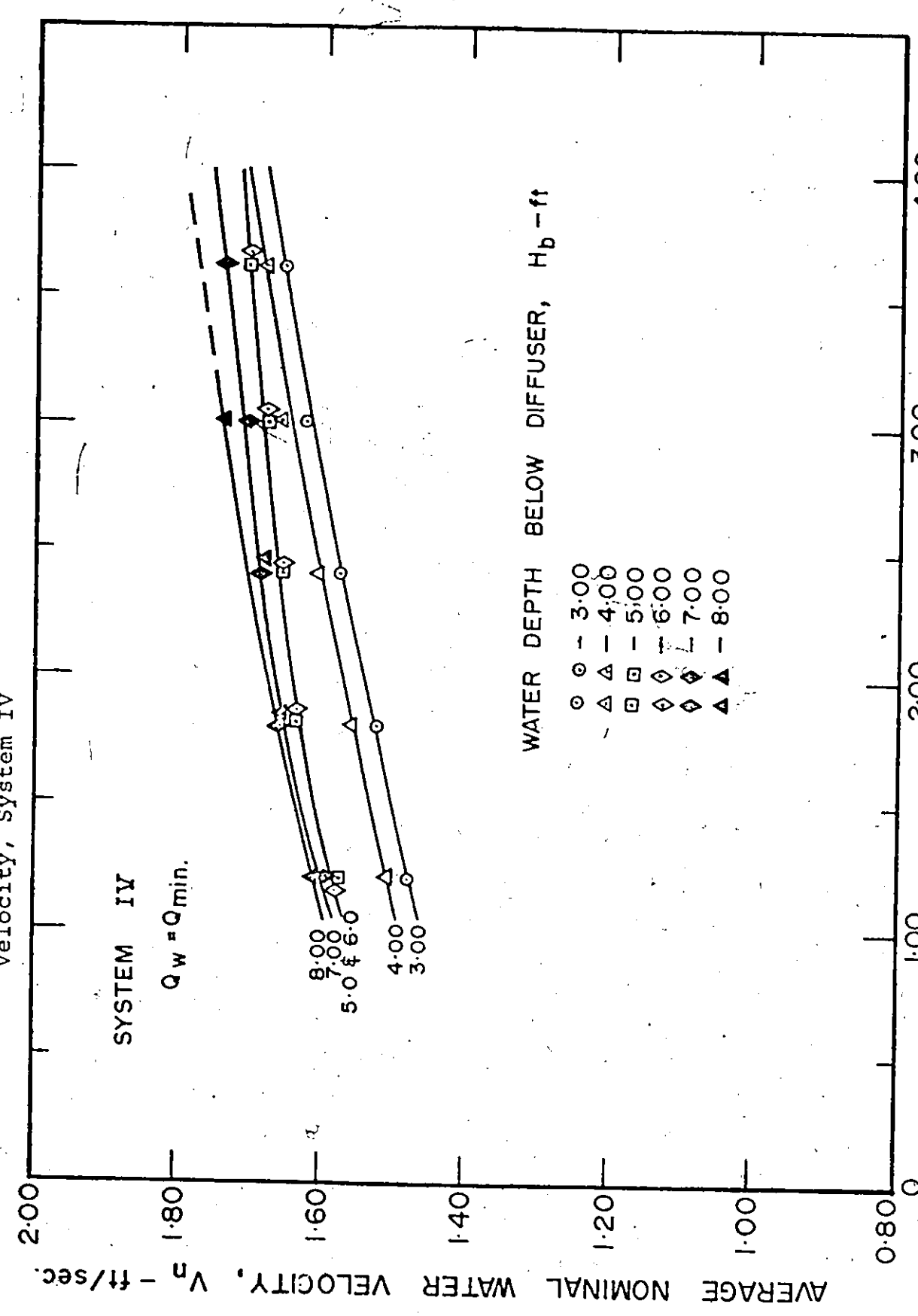


Figure 68 - Effect of Water Depth and Airflow Rate on the Nominal Water Velocity, System IV

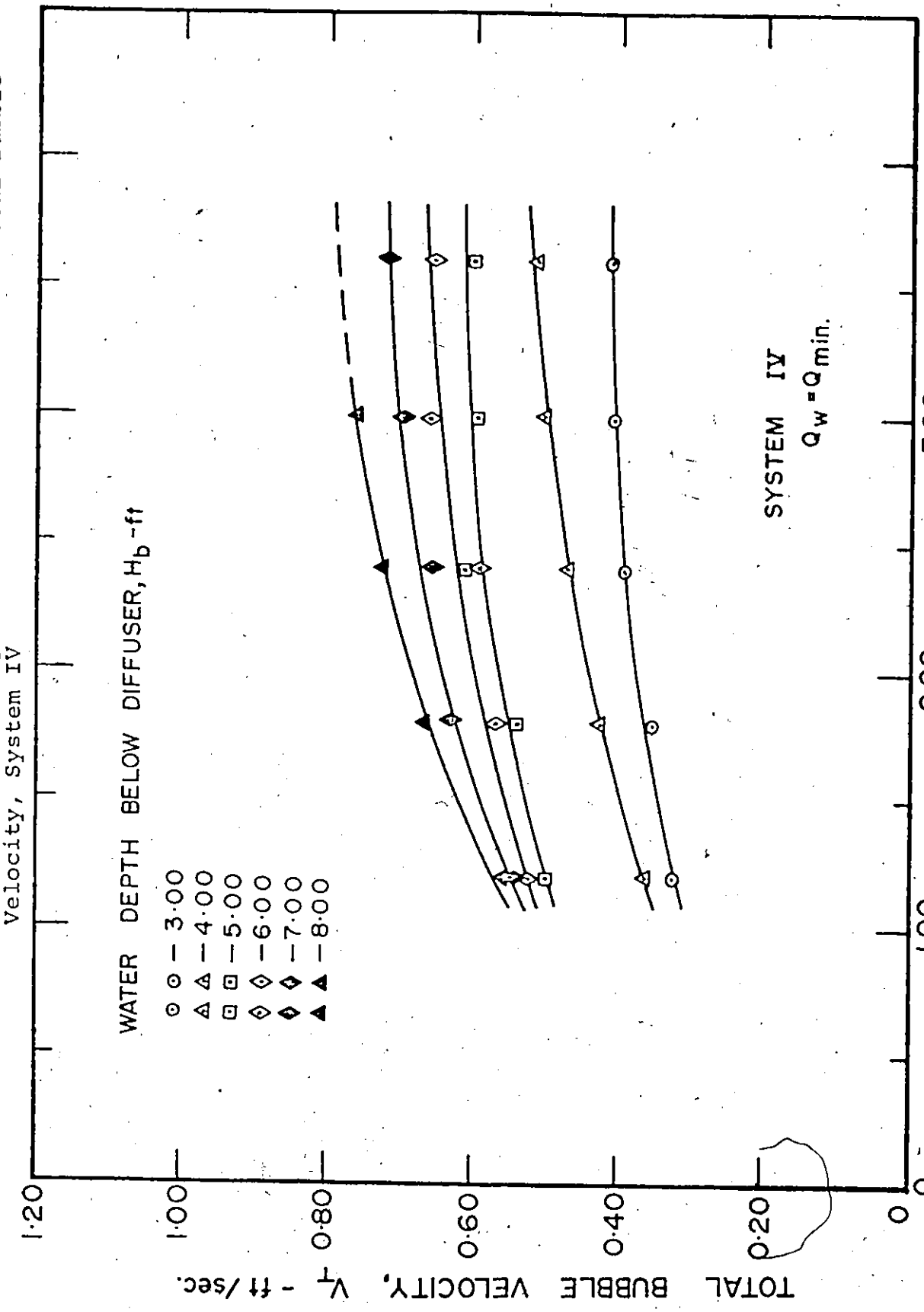


Figure 69 - Effect of Water Depth and Airflow Rate on the Total Bubble Velocity, System IV

as given above. It can be noticed in Figures 35 and 67 that the point representing the highest airflow rate and the largest depth is missing. This could not be obtained due to the physical limitations in the equipment. However, it is expected that this point would follow the trends observed in the graphs.

Figure 35 also indicates that, for any value of $H_b$, increasing the unit airflow rate, $q_a$, decreases the value of $E_o$, except at higher airflows and larger water depths. In this system also, the size of the bubbles emanating from the diffuser increases as $q_a$ is increased. However, within 1/2 to 1 foot below the diffuser, the larger air bubbles were seen to break into much smaller bubbles due to turbulence and increasing hydrostatic pressure. This observation was made both visually and with movies. Consequently, these smaller bubbles had less resistance to the increasing waterflow rates, given by the nominal water velocity, $V_n$, in Figure 68, and moved faster downward through the system. The resultant increase in total downward bubble velocity, $V_T$, with increasing $q_a$, as shown in Figure 69, resulted in the subsequent decrease in contact time as observed in Figure 67. Therefore, despite the advantages associated with smaller bubbles, the bubble contact time per unit distance of travel, $t_{cu}$, in this system decreases in value and consequently, $E_o$ decreases as $q_a$ is increased. The sudden increase in $E_o$ at the higher airflow rates, for $H_b$ equal to 6, 7, and 8 feet,

is believed to be a result of the high turbulence observed at these operating conditions. In other words, the combination of higher airflow, higher water flow (as given in Figure 68), and large water depth produces such strong turbulence in the system, that surface renewal rates are substantially increased with a subsequent increase in the amount of oxygen transferred. Consequently, the transfer efficiency, $E_o$, actually increases rather than decreases as observed at lower airflow rates and smaller water depths.

Figure 36 shows the relationship between the unit power efficiency, $E_p$, and the unit airflow rate, $q_a$, for various depths of water below the diffuser, $H_b$. It can be seen that $E_p$ increases both with increasing airflow rate and with increasing water depth. The explanation lies in the fact that, in System IV, power requirements for air injection are low because the air is diffused at very shallow depths. As such, air power supplied, $P_a$, becomes very small compared to the input water power, $P_w$, as is evident from Figures 70 and 71. Therefore, the increase in total power input ($P_a+P_w$), because of increasing $q_a$ or $H_b$, is primarily due to a change in $P_w$ which does not increase as rapidly as does $q_a$ or $H_b$. At the same time, by increasing $q_a$, the ratio of interfacial area to bubble volume is increased due to the formation of smaller bubbles, and also, more oxygen is supplied to the system. By increasing $H_b$, the contact time of the air bubble is increased, as shown in Figure 67. Consequently, more oxygen is transferred to the

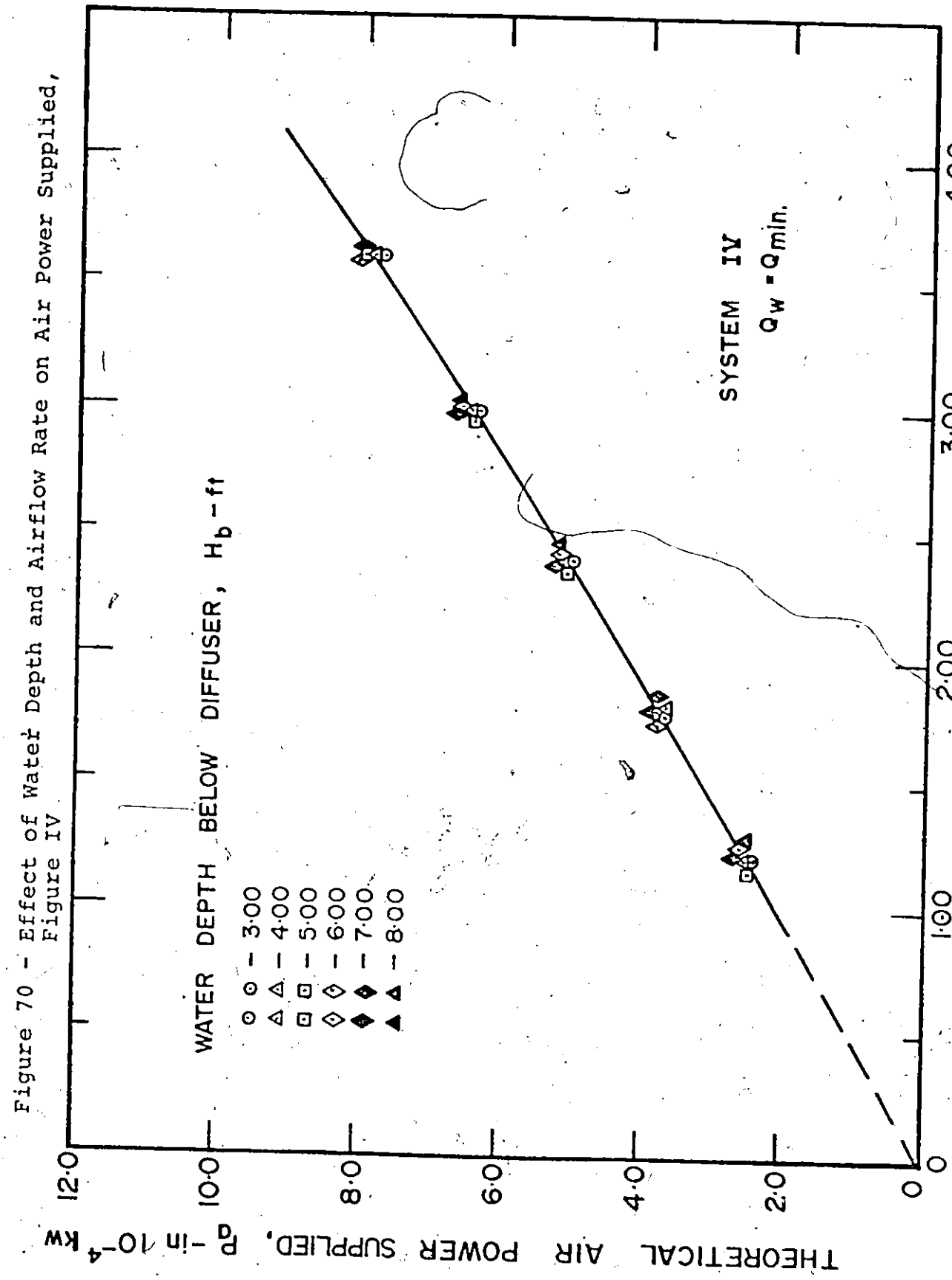


Figure 70 - Effect of Water Depth and Airflow Rate on Air Power Supplied, Figure IV

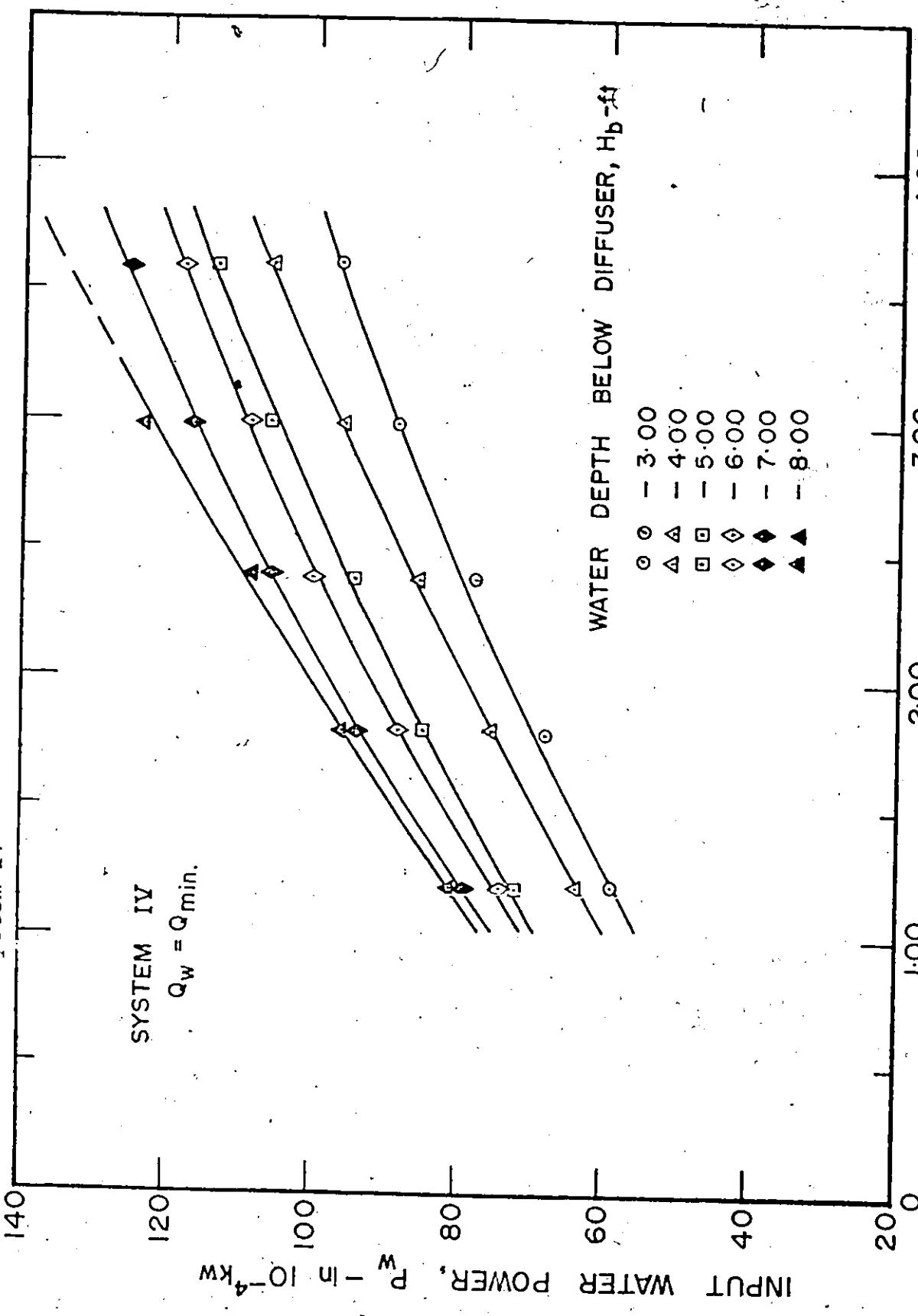


Figure 71 - Effect of Water Depth and Airflow Rate on Input Water Power, System IV

liquid, with the percentage increase apparently being more than the corresponding percentage increase in the power input. This results in $E_p$ increasing with both air flow and depth of water below the diffuser.

It is interesting to note from Figure 70 that, while $P_a$ increases proportionally with the airflow rate, increasing the depth of water below the diffuser, while maintaining a constant airflow rate, shows little change in $P_a$. This insignificant change in $P_a$ is due to the fact that the submergence of the diffuser showed little change when the depth of the water below the diffuser was changed from 3 to 8 feet. Since air power is a function of airflow rate and diffuser submergence and since both are relatively constant, $P_a$ also remains constant.

The Overall Transfer Coefficient, $(K_La)_{20}$, as a function of water depth and airflow rate, is given in Figure 37. $(K_La)_{20}$ increases both with an increase in $q_a$ and $H_b$. The plots demonstrate an upward curvilinear tendency, in contrast to the downward or levelling off trend in $(K_La)_{20}$ for the previous systems. Again, the increase in $(K_La)_{20}$ with an increase in $q_a$ is attributed to the additional supply of oxygen transfer, while the increase in $(K_La)_{20}$ due to an increase in $H_b$ is due to the larger total contact time of the air bubbles (Figure 67) as well as increased concentration gradients. The curvilinear upward trend in Figure 37 is probably due to the increase in turbulence as $q_a$ increases, which results in higher surface renewal rates and more oxygen

transferred to the liquid. Once again, this rise is more rapid and noticeable at the larger water depths of $H_b$ equal to 6, 7, and 8 feet, for reasons already discussed. A relationship for $(K_La)_{20}$ is given by the following equation,

$$(K_La)_{20} = (1.823 + 0.135\ H_b)e^{0.320q_a} \quad \ldots\ldots\ 48$$

with a Correlation Coefficient, r, of 0.985.

In System IV, several experiments were conducted to determine the effect of increasing the waterflow rate above $Q_{min.}$, while keeping $q_a$ constant. These additional tests were performed at $H_b$ equal to 6 feet, and unit waterflow rates of $Q_{min.}$, 791 and 849 USGPM/ft$^2$. The results are presented in Figures 38 to 41. As expected, increasing the waterflow rate, for a given airflow rate, increased the value of the Overall Transfer Coefficient, $K_La$, as shown in Figure 41. This is attributed to the increased turbulence and subsequent greater surface renewal rates of the air bubbles when the waterflow rate is increased. The same reasons can be given to account for the increase in oxygen transfer efficiency, $E_o$, with increased waterflow rates, shown in Figure 38. Even though bubble contact times, in this co-current flow, become reduced due to the increased water velocity at higher waterflow rates, the greater turbulence generated under this condition increases the rate of renewal of the bubble surface, with the result that much more oxygen is transferred for the same rate of oxygen

supply. This increase in rate of oxygen transfer more than compensates for the reduction in contact time, with the result that $E_o$ increases in value. The same pattern of increase in $E_o$ at higher airflow rates is obtained with the increased waterflow rates as with $Q_{min.}$ shown in Figure 35. The greater turbulence as explained earlier, is responsible for this increase.

The effect of increasing the unit waterflow rate, $q_w$, on the unit power efficiency, $E_p$, can be observed in Figures 39 and 40. Results indicate that $E_p$ changes very little, regardless of the waterflow rate. Any increase in the amount of oxygen transferred due to the greater turbulence generated by the higher waterflow rates is offset by the decrease in bubble contact time and increase in water power supplied. As a result, $E_p$ undergoes a very small change in value. However, from Figure 40, it appears advantageous to use higher airflow rates with higher water flows and larger water depths. This recommendation for the operating conditions in System IV is further supported by the results presented in Figures 35, 36, 38, and 39.

## E. COMPARISON OF THE FOUR SYSTEMS

A general comparison of the results of all four systems, in terms of important parameters, is given in Table 5. Although $K_L$, $K_La$, and $t_{cu}$ provide basic information on the characteristics of each system, still the most important

parameters for comparison of these four systems are $E_o$ and $E_p$, the oxygen transfer efficiency and the unit power efficiency, respectively. As mentioned earlier, the contact time of air bubbles with water could be computed only for the downflow side in System IV.

From the Table, it is evident that System III is the most efficient of the aeration systems studied in this work, both in terms of $E_o$ and $E_p$. It shows very high values for both $E_o$ and $E_p$. In comparison, System IV shows equally high $E_o$ values but possesses much lower $E_p$ values, while System II has equally high $E_p$ values but lower $E_o$ values. System I gives lower results for both the parameters.

The improved performance under System III of aeration is attributed to the increased contact time between the air bubbles and water during counter-current flow of air and water (Figure 72 shows air bubble flow pattern in column section, System III). Results for the unit contact time, $t_{cu}$, shown in Table 5, support this reasoning. The $t_{cu}$ values of 1.77 - 4.31 sec/ft of aeration depth for System III are much higher than in any of the remaining three systems. In System IV, $t_{cu}$ was computed for the downflow side only; however, it is expected that $t_{cu}$ values on the upflow side would be much lower due to the swifter co-current flow conditions on that side of the system. Although System I shows a higher contact time as compared to System II, the efficiency values for this System are lower. The reasons for this trend are reflected in the relatively lower $K_L$

Figure 72 - Bubble Flow Pattern In Column Section, System III

values for the same bubble diameter obtained in System I as compared to System II.

It must also be remembered that the pumping of water in Systems III and IV adds considerable water power to the total power input values used in the determination of $E_p$ values. This is especially true for System IV where water power is very large in comparison to the air power supplied. In Systems I and II, no such water power is supplied. Therefore, under favourable conditions, such as availability of natural head in wastewater flow to replace the pumping head used in this study, Systems III and IV would show even higher $E_p$ values. A complete elimination of this high water power input in System IV may prove this system equally or even more efficient than System III.

Results for the Overall Transfer Coefficient, $K_La$, and the Liquid Film Coefficient, $K_L$, corrected to 20°C, are also compared for all systems in Table 5. As indicated, System I produced the highest $(K_La)_{20}$ values with System II the lowest. This suggests that the greatest overall turbulence is found in System I where rising bubbles create a great deal of local eddy currents and highly turbulent conditions. System II gave the highest results for $(K_L)_{20}$ although values could not be obtained for System IV. Even though many factors influence $K_L$, perhaps bubble size has the greatest single effect and in System II, the largest air bubbles were observed. From the comparison of $K_L$ values for 10 mm and 25 mm bubbles in Systems I, II, and III, it

can be seen that, with the effect of bubble size eliminated, System II still shows the highest $K_L$ values for both the bubble sizes compared. This suggests that there are other factors also significantly influencing $K_L$. One such factor might be the circulating velocities in the systems; System II had the highest circulating velocities and this could account for the higher $K_L$ values obtained. Eckenfelder (12) also has commented that, the higher the circulating velocities, the larger the values for the Liquid Film Coefficient, $K_L$.

## F. POROUS DIFFUSERS

The experiments performed using porous diffusers in System II has already been outlined in Chapter V. Computed results are presented in Tables 6 and 7, while raw data are tabulated in Appendix C. Comparison of the aeration efficiencies, using porous diffusers, with those of the coarse-bubble diffuser is presented in Tables 9 and 10 and are plotted in Figures 42 and 43.

As expected, the generation of much smaller bubbles (< 5 mm for Fisher porous stones and < 10 mm for Norton porous plates) by both types of porous diffusers resulted in increased aeration efficiencies, both in terms of the oxygen transfer efficiency, $E_o$, and the unit power efficiency, $E_p$. This improvement occurred at every unit airflow rate and diffuser submergence tested, and is attributed to the increased

Table 9 - Comparison of Aeration Diffuser Efficiencies in System ~~II~~ - $E_o$

| | $H_T$ = 9.25 ft. | | | Units |
|---|---|---|---|---|
| | Airflow Rates ⟶ | 1.46 | 2.91 | 4.36 | scfm/ft$^2$ |
| $E_o$ | Coarse Bubble Diffuser | 4.85 | 3.85 | 3.20 | % |
| | % Increase* | — | — | — | |
| $E_o$ | Fisher Porous Stones | 9.00 | 5.90 | 5.35 | % |
| | % Increase* | 85.6 | 53.2 | 67.2 | |
| $E_o$ | Norton Porous Plates | 8.38 | 5.90 | 4.55 | % |
| | % Increase* | 72.8 | 53.2 | 42.2 | |

*Relative to Coarse Bubble Diffusers

Table 9 (continued)

| | $H_T$ = 6.25 ft. | | | Units |
|---|---|---|---|---|
| | Airflow Rates ⟶ | 1.35 | 2.70 | 4.06 | scfm/ft$^2$ |
| $E_o$ | Coarse Bubble Diffuser | 4.40 | 3.40 | 2.95 | % |
| | % Increase* | — | — | — | |
| $E_o$ | Fisher Porous Stones | 7.70 | 5.50 | 4.75 | % |
| | % Increase* | 75.0 | 61.8 | 61.0 | |
| $E_o$ | Norton Porous Plates | 7.65 | 5.30 | 4.00 | % |
| | % Increase* | 73.8 | 55.8 | 35.6 | |

*Relative to Coarse Bubble Diffusers

Table 9 (continued)

| | $H_T$ = 3.25 ft. | | | Units |
|---|---|---|---|---|
| | Airflow Rates ⟶ | 1.25 | 2.51 | 3.76 | scfm/ft$^2$ |
| $E_o$ | Coarse Bubble Diffuser* | 3.60 | 2.35 | 2.00 | % |
| | % Increase | — | — | — | |
| $E_o$ | Fisher Porous Stones* | 5.20 | 4.35 | 3.75 | % |
| | % Increase | 44.4 | 85.2 | 87.5 | |
| $E_o$ | Norton Porous Plates* | 5.00 | 3.55 | 2.85 | % |
| | % Increase | 38.9 | 51.1 | 42.5 | |

*Relative to Coarse Bubble Diffusers

Table 10 - Comparison of Aeration Diffuser Efficiencies in System II - $E_p$

| | $H_T$ = 9.25 ft. | | | Units |
|---|---|---|---|---|
| | Airflow Rates → | 1.46 | 2.91 | 4.36 | scfm/ft$^2$ |
| $E_p$ | Coarse Bubble Diffuser | 4.38 | 3.49 | 2.81 | lb/kwhr |
| | % Increase* | — | — | — | |
| $E_p$ | Fisher Porous Stones | 7.96 | 5.28 | 4.79 | lb/kwhr |
| | % Increase* | 81.8 | 51.2 | 70.5 | |
| $E_p$ | Norton Porous Plates | 7.40 | 5.21 | 4.08 | lb/kwhr |
| | % Increase* | 68.9 | 49.3 | 45.2 | |

*Relative to Coarse Bubble Diffusers

Table 10 (Continued)

| | $H_T$ = 6.25 ft. | | | Units |
|---|---|---|---|---|
| | Airflow Rates → | 1.35 | 2.70 | 4.06 | $scfm/ft^2$ |
| $E_p$ | Coarse Bubble Diffuser | 5.22 | 4.36 | 3.83 | lb/kwhr |
| | % Increase* | — | — | — | |
| $E_p$ | Fisher Porous Stones | 9.85 | 7.01 | 6.13 | lb/kwhr |
| | % Increase* | 88.6 | 60.8 | 60.0 | |
| $E_p$ | Norton Porous Plates | 9.76 | 6.79 | 5.16 | lb/kwhr |
| | % Increase* | 86.8 | 55.7 | 34.7 | |

*Relative to Coarse Bubble Diffusers

Table 10 (continued)

| | $H_T$ = 3.25 ft. | | | Units |
|---|---|---|---|---|
| | Airflow Rates ⟶ | 1.25 | 2.51 | 3.76 | scfm/ft$^2$ |
| $E_p$ | Coarse Bubble Diffuser | 6.65 | 5.25 | 4.78 | lb/kwhr |
| | % Increase* | — | — | — | |
| $E_p$ | Fisher Porous Stones | 12.45 | 10.41 | 9.00 | lb/kwhr |
| | % Increase* | 87.2 | 98.3 | 88.3 | |
| $E_p$ | Norton Porous Plates | 11.98 | 8.54 | 6.86 | lb/kwhr |
| | % Increase* | 80.2 | 62.6 | 43.5 | |

*Relative to Coarse Bubble Diffusers

contact time and larger interfacial area to bubble volume ratio obtained with the use of smaller bubbles. Results from Tables 9 and 10 indicate as much as 88% increase in $E_o$ values and 98% increase in $E_p$ values, relative to efficiencies obtained with the coarse-bubble diffuser and reported earlier. Efficiencies were somewhat higher using the Fisher porous stones than with the other type of porous diffusers, probably because a difference in porosity resulted in smaller bubbles being generated by the Fisher stone.

# IX - CONCLUSIONS

Based on the results of this experimental work, using coarse-bubble diffusers and the four systems of aeration, the following conclusions can be drawn:

A. SYSTEM I - Simple Water Column

1. The oxygen transfer efficiency, $E_o$, decreases with an increase in airflow rate and a decrease in diffuser submergence.

2. The unit power efficiency, $E_p$, decreases slightly when the airflow rate is increased. There appears to be no significant change in $E_p$ when diffuser submergence is varied.

3. The Overall Transfer Coefficient, $K_La$, corrected to 20°C, increases linearly with an increase in airflow rate, but is independent of diffuser submergence. The relationship can be expressed by the equation,

$$(K_La)_{20} = 2.138 + 5.390\ q_a$$

4. The Liquid Film Coefficient, $K_L$, increases with an increase in air bubble size but appears to be unaffected by diffuser submergence.

SYSTEM II - Circulation Without Pumping

1. The oxygen transfer efficiency, $E_o$, decreases with an increase in air flow and a decrease in diffuser submergence.

2. The unit power efficiency, $E_p$, decreases both with an increase in airflow rate and an increase in diffuser submergence.

3. The Overall Transfer Coefficient, $K_La$, corrected to 20°C, increases both when the airflow rate is increased and when the diffuser submergence is increased. The relationship can be expressed by the equation:

$$(K_La)_{20} = A\, q_a^{\,B}$$

where, $A = (0.5140 \times 10^{0.0333H_T})$

$B = (0.940 \times 10^{-0.0209H_T})$

4. The Liquid Film Coefficient, $K_L$, increases with an increase in air bubble size but there

appears to be no significant effect of diffuser submergence on $K_L$.

## SYSTEM III - Circulation With Pumping, $V_w \leq V_b$

1. The oxygen transfer efficiency, $E_o$, decreases as the airflow rate is increased and the diffuser submergence is decreased.

2. The unit power efficiency, $E_p$, decreases with an increase in air flow and an increase in diffuser submergence.

3. The Overall Transfer Coefficient, $K_La$, corrected to 20°C, increases with an increase in airflow rate and an increase in diffuser submergence, although the latter effect is not as pronounced as in the previous system. The relationship can be expressed by the equation:

$$(K_La)_{20} = (2.203 + 0.196\ H_T)q_a^{0.4251}$$

4. The Liquid Film Coefficient, $K_L$, increases as the bubble size increases but no appreciable effect of diffuser submergence is observed. However, there are indications that $K_L$ might vary inversely with depth.

5. A reduction in the waterflow rate below maximum in this System reduces the oxygen transfer efficiency, $E_o$, due to a reduction in bubble contact time, but has no significant effect on the unit power efficiency, $E_p$. Although reducing the waterflow rate results in less oxygen being transferred, there is a corresponding drop in input water power and therefore $E_p$ shows little change.

SYSTEM IV - Circulation with Pumping, $V_w > V_b$

1. The oxygen transfer efficiency, $E_o$, increases as the depth of water below the diffuser increases and decreases when the airflow rate is increased, except at very high air flows and large depths, when it shows an increase in value. This increase in $E_o$ is due to the turbulence generated by these flow conditions.

2. The unit power efficiency, $E_p$, increases with both an increase in airflow rate and an increase in depth of water below the diffuser.

3. The Overall Transfer Coefficient, corrected to 20°C, increases both with an increase in air flow and an increase in water depth below the diffuser. The relationship is given by the

equation:

$$(K_L a)_{20} = (1.823 + 0.135\ H_b)e^{0.320 q_a}$$

4. Increasing the waterflow rate beyond the minimum value in this system increases $E_o$, due to the greater turbulence generated, but has little effect on the unit power efficiency, $E_p$. Any increase in oxygen transfer due to turbulence is offset by the increase in water power supplied and decreased bubble contact time and therefore $E_p$ shows little change in value

B. GENERAL

1. The bubble diameter and the contact time between air bubbles and water are important parameters influencing the aeration efficiencies. Both the bubble diameter and the contact time are dependent on the operating conditions such as airflow rate, diffuser submergence and waterflow rate.

2. Optimization of oxygen transfer in this investigation, on a basis of the aeration systems studied, was achieved in System III where countercurrent flow of air and water was maintained. The higher values of both oxygen transfer efficiency, $E_o$, and unit power efficiency, $E_p$,

obtained in this System have been shown to result from the increased contact time between the air bubbles and water during counter-current flow conditions.

3. Both in Systems III and IV, the pumping of water adds considerable water power to the total power input values used in evaluating $E_p$. However, under favourable conditions, such as availability of natural head in wastewater flow, to replace the pumping head, Systems III and IV would produce even higher values of $E_p$. A complete elimination of the high water power input in System IV might prove this system equally or more efficient than System III.

4. Aeration efficiencies were much higher when fine-bubble producing porous diffusers were used instead of the coarse-bubble diffuser. This expected improvement is attributed to the increased contact time and larger ratio of interfacial area to bubble volume obtained with the smaller bubbles.

5. Although results for certain portions of the experiments are reproducable within ±5%, the overall reproducability of results in this study is considered to be ±10%.

# X - APPENDICES

# APPENDIX A

## NOMENCLATURE

| | | |
|---|---|---|
| $A$ | = | Interfacial or absorbing area of bubble surface, $ft.^2$ |
| $A_a$ | = | Area of air bubbles present at any time in the cross-section of a column unit element, $ft.^2$ |
| $A_f$ | = | Mean surface area of all bubbles in formation at any instant, $ft.^2$ |
| $A_n$ | = | Inside cross-sectional or confining area normal to flow of water in the aeration column, $ft.^2$ |
| $A_w$ | = | Area of water present in the cross-section of a column unit element and represents the reduced cross-sectional area through which the water flow, $Q_w$, must pass, $ft.^2$ |
| $C_i$ | = | Equilibrium concentration of oxygen at the phase interface, mg/l. Assumed to be equal to the saturation value at mid-depth over diffuser. |
| $C_L$ | = | Concentration of oxygen in the liquid at time t, mg/l. |
| $C_L'$ | = | Reading of oxygen concentration in the liquid at time t from the recorder plot, mg/l. |
| $(C_i-C_L)$ | = | Oxygen saturation deficit in the liquid, mg/l. |
| $C_o$ | = | Initial concentration of oxygen in the liquid, mg/l. |

$C_s$ = Solubility of oxygen in water at a specific temperature and at a total pressure of 760 mm mercury, mg/l.

$D$ = Inside diameter of the plexiglass columns, inches.

$E_o$ = $\frac{R_o}{R_s} \times 100$ = Aeration efficiency, %.

$E_p$ = $R_o/P_a+P_w$ = Aeration efficiency in terms of rate of oxygen transferred per unit power input, lb/kwhr.

$H_b$ = Maximum depth of water below diffuser, System IV, ft.

$H_E$ = Expanded water depth above diffuser in System I, ft.

$H_s$ = Water pressure at mid-depth of vertical travel of air bubble from the outlet, ft.

$H_T$ = Initial submergence of the air diffuser, ft.

$H_T'$ = True water pressure head or diffuser submergence, ft.

$\Delta H$ = Differential water head in the recirculating tank, ft.

$\Delta H_T$ = Change in water depth in System I due to presence of air in the column = $H_E-H_T$, ft.

$K_a$ = Gas transfer coefficient during bubble ascent, lb/hr/ft$^2$ per mg/l.

$K_f$ = Gas transfer coefficient during bubble formation, lb/hr/ft$^2$ per mg/l.

$K_L$ = Liquid diffusion coefficient, lb. oxygen per hour per ft$^2$ per unit concentration difference in mg/l, i.e., lb/hr/ft$^2$ per mg/l. Also defined as the Liquid Film Coefficient, ft/sec.

$K_L a$ = Overall gas transfer coefficient, $hr^{-1}$

$P$ = Barometric pressure, mm Hg.

$P_a$ = Theoretical power required to compress the air, kw.

$P_l$ = Piezometric reading for the lower tap after air is introduced, ft.

$P_u$ = Piezometric reading for the upper tap after air is introduced, ft.

$P_w$ = Water power supplied to the system, kw.

$Q_a$ = Rate of airflow into the water at S.T.P. conditions, scfm.

$Q_a'$ = Rate of airflow into the water at mid-pressure head of vertical air bubble travel, cfm.

$Q_w$ = Waterflow rate through the system, USGPM or cfm.

$Q_{max.}$ = Waterflow rate in System III, just large enough to permit counter-current, air-water flow conditions to exist, USGPM.

$Q_{min.}$ = Waterflow rate in System IV, just small enough to permit co-current, air-water flow conditions to exist, USGPM.

$R_o$ = Total rate of oxygen transferred in water, lb/hr.

$R_s$ = Rate of oxygen supplied to the water, lb/hr.

$V_a$ = Volume of trapped air between piezometric taps, $ft.^3$

$V_b$ = Terminal velocity of rise of an air bubble in stationary water, ft/sec. or cm/sec.

$V_n$ = $Q_w/A_n$ = Nominal water velocity in aeration column, ft/sec.

$V_{p_{ave.}}$ = Average water velocity as measured by the pitot tube, ft/sec.

$V_T$ = Total air bubble velocity, ft/sec.

$V_T'$ = Total air bubble velocity in the recirculating tank on the diffuser side of System III, ft/sec.

$V_w$ = Average water velocity in an air-water stream, ft/sec.

$\Delta V$ = Change in volume of fluid due to trapped air, System I, $ft.^3$

W = Weight of water in the aeration system, lb.

$d_1$ = Water depth in the recirculating tank on the diffuser side of Systems III and IV, ft.

$d_{ave.}$ = Average air bubble diameter, mm.

dc/dt = Rate of change of dissolved oxygen concentration in the liquid, mg/l/hr.

$h_1$ = Lower piezometric head, Systems II and III, ft.

$\Delta h$ = $P_u - P_1$ = Piezometric differential, ft.

p = Pressure of saturated water vapour at the temperature of the water, mm Hg.

$P_A$ = Upper piezometric head, System IV, ft.

$q_a$ = Qa/An = Airflow rate per unit cross-sectional area of column, $scfm/ft.^2$

$q_w$ = Qw/An = Waterflow rate per unit cross-sectional area of column, $USGPM/ft^2$ or $cfm/ft.^2$

r = Correlation Coefficient, dimensionless.

t = Time readings from recorder chart for dissolved oxygen concentration, minutes.

$t_c$ = Average air bubble contact time, sec.

$t_{cR}$ = Average bubble contact time on the downflow side of System IV, sec.

$t_{cu}$ = Unit contact time of the air bubble, i.e., the bubble contact time per unit travelling distance, sec./ft.

$t_d$ = Average detention time of the air bubble between piezometric taps, sec.

$y_1$ = Distance from the diffuser to tank bottom, System III, ft.

$z$ = Distance between piezometric taps, ft.

$\alpha'$ = Effect of air bubble entrainment in the downward moving liquid or carry-over effect, dimensionless.

$\beta$ = Factor relating diameter of each bubble to its volume and surface area, dimensionless.

$\phi$ = Calibration constant for the oxygen probe, dimensionless.

APPENDIX B

Table 11 - Data for a Typical Run, System IV - No. 28

Probe Constant $\phi$ = 0.907

Chart Speed (mm/min.) = 5

$t = \frac{\text{Hor. Dist. on Chart}}{\text{Chart Speed}}$ = minutes

DATE = June 1, 1972

WATER TEMPERATURE = 17.8 °C

$C_S$ = 9.55 mg/l

$H_S$ = 5.01 ft

SLOPE = 2.18 $hr^{-1}$. (From Figure 74)

W = 429 lb

$H_T'$ = 1.76 ft

$\Delta H$ = 0.760 ft

PRESSURE - CORRECTED AIRFLOW RATE;

$Q_a$ = 0.16 scfm

RATE OF WATERFLOW, $Q_w$ = 65 USGPM
= 65 x 0.1336 cfm
= 8.68 cfm

From Figure 73 -Recorder Plot

| Time - t (min.) | $C_L = (C_L'/\phi)$ (mg/l) | $\frac{C_i}{C_i - C_L}$ |
|---|---|---|
| 0 | 0.81 | 1.080 |
| 1.0 | 0.85 | 1.085 |
| 2.0 | 0.93 | 1.090 |
| 3.0 | 1.13 | 1.120 |
| 4.0 | 1.58 | 1.170 |
| 5.0 | 2.09 | 1.236 |
| 6.0 | 2.79 | 1.340 |
| 7.0 | 3.41 | 1.450 |
| 8.0 | 4.09 | 1.595 |
| 9.0 | 4.68 | 1.750 |
| 10.0 | 5.26 | 1.925 |

APPENDIX B (continued)

Typical Calculations for Run No. 28, System IV

$Q_a = 0.16$ scfm

$q_a = \frac{0.16}{\pi/36} = 1.83$ scfm/ft$^2$

$Q_w = 65$ USGPM

$$C_i = C_s\left(1 + \frac{H_s}{34}\right)$$

$$= 9.55\left(1 + \frac{5.01}{34}\right)$$

$$= 9.55\ (1.147)$$

$$= 10.95 \text{ mg/l}$$

$$\frac{dc}{dt} = \text{SLOPE} \times 2.30 \times C_i$$

$$= 2.18 \times 2.30 \times 10.95$$

$$= 54.85 \text{ mg/l/hr}$$

$$R_o = \frac{dc}{dt} \times W \times 10^{-6}$$

$$= 54.85 \times 429 \times 10^{-6}$$

$$= 2.36 \times 10^{-2} \text{ lb/hr}$$

$$R_s = 1.05\ Q_a$$

$$= 1.05 \times 0.16$$

$$= 0.168 \text{ lb/hr}$$

$$P_a = 0.168\ Q_a\left[\left(\frac{H_T + 34}{34}\right)^{0.286} - 1\right]$$

$$= 0.168 \times 0.16\left[\left(\frac{1.76 + 34}{34}\right)^{0.286} - 1\right]$$

$$= 0.0269\left[(1.0518)^{0.286} - 1\right]$$

$$= 3.85 \times 10^{-4} \text{ kw}$$

$$P_w = 1.885 \times 10^{-4} \cdot Q_w \cdot \Delta H$$

$$= 1.885 \times 10^{-4} \times 65 \times 0.760$$

$$= 93.30 \times 10^{-4} \text{ kw}$$

$$E_p = \frac{R_o}{P_a + P_w}$$

$$= \frac{2.36 \times 10^{-2}}{3.85 \times 10^{-4} + 93.30 \times 10^{-4}}$$

$$= 2.42 \text{ lb/kwhr}$$

$$E_o = \frac{R_o}{R_s} \times 100$$

$$= \frac{2.36 \times 10^{-2}}{0.168} \times 100$$

$$= 14.05\%$$

$$K_L a = \text{SLOPE} \times 2.30$$

$$= 2.18 \times 2.30$$

$$= 5.01 \text{ hr}^{-1}$$

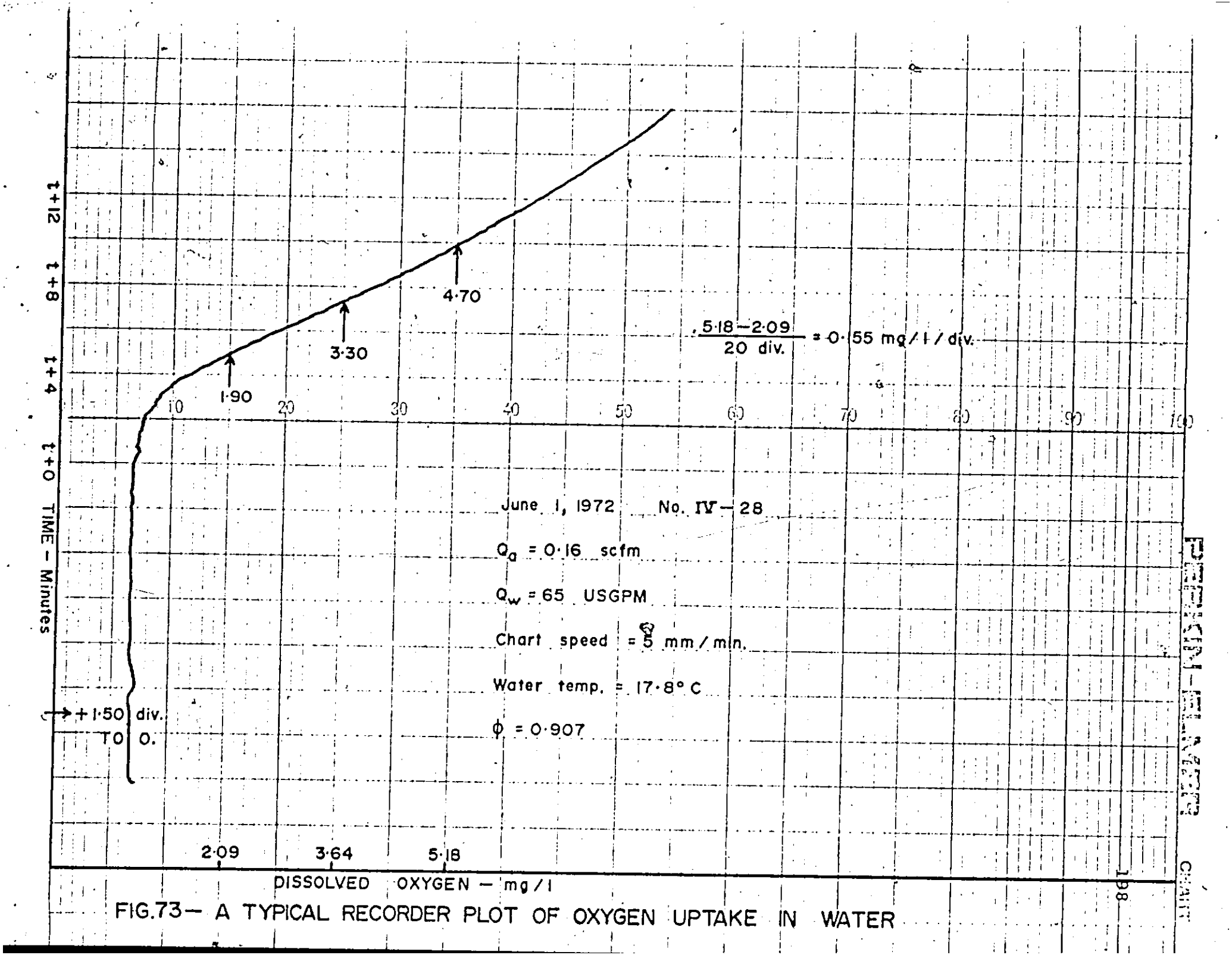


FIG.73– A TYPICAL RECORDER PLOT OF OXYGEN UPTAKE IN WATER

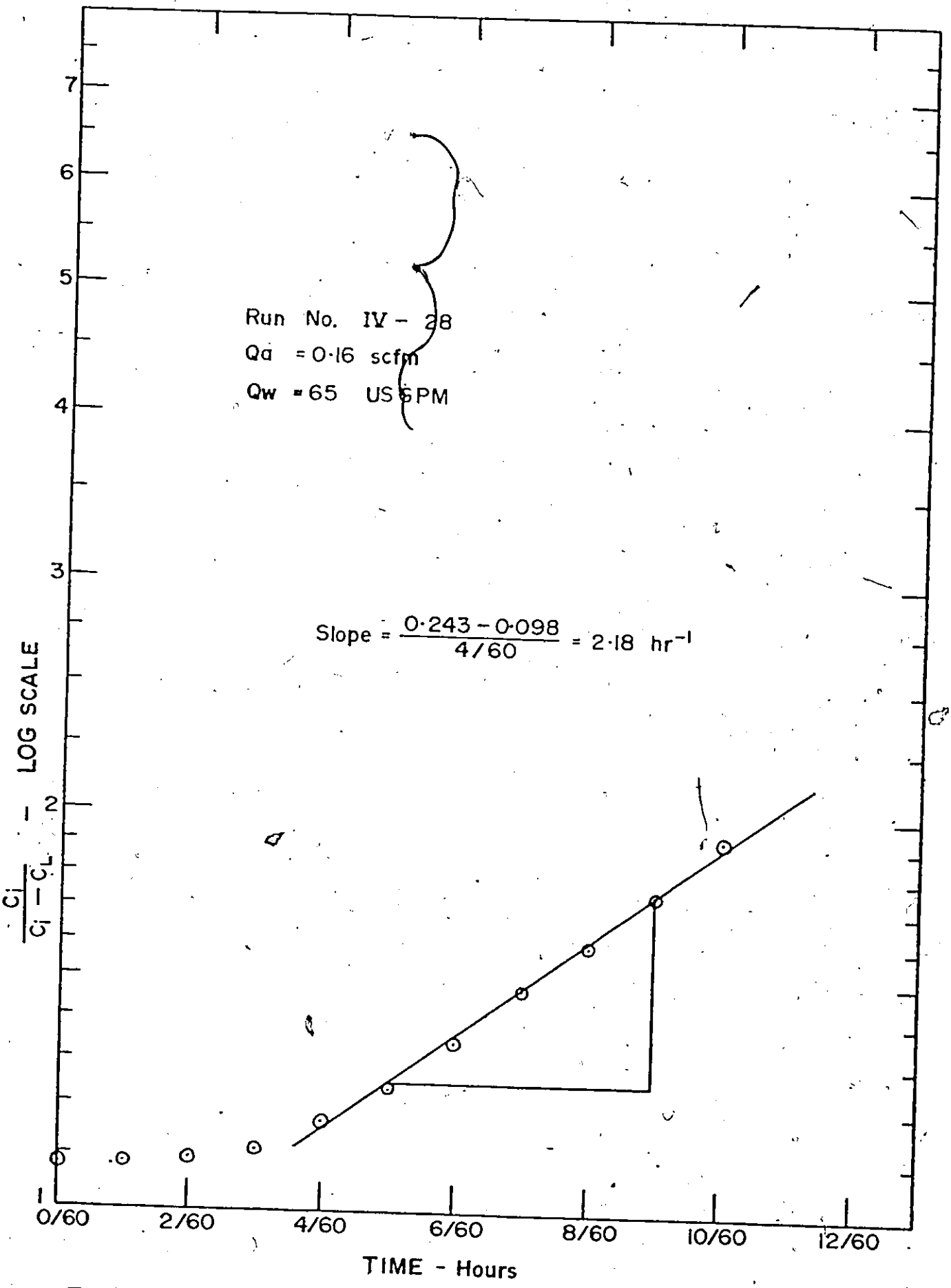


FIG. 74 – SEMI-LOG PLOT OF DATA FOR COMPUTATION OF OXYGEN UPTAKE RATE

Appendix C....Table 12 - Data for System I

| 1 | 2 | 3 | 4 | 5 | 6 | 7 | 8 | 9 | 10 | 11 |
|---|---|---|---|---|---|---|---|---|---|---|
| Run No. | T (°C) | $H_s$ (ft) | $C_s$ (mg/l) | Slope ($hr^{-1}$) | W (lb) | $R_o$ (lb/hr) | $P_a$ (kw) | $H_E$ (ft) | *Qa (scfm) | $V_b$ (cm/sec) |
| 1 | 21.5 | 4.38 | 8.90 | 4.62 | 49.0 | $5.23 \times 10^{-3}$ | .00143 | 8.96 | 0.11 | 27.7 |
| 2 | 21.8 | " | 8.85 | 6.30 | " | 7.10 " | .00214 | 9.00 | 0.17 | 35.1 |
| 3 | 21.9 | " | 8.82 | 7.98 | " | 8.96 " | .00286 | 9.06 | 0.22 | 38.0 |
| 4 | 22.1 | " | 8.79 | 9.06 | " | 10.15 " | .00357 | 9.16 | 0.28 | 36.3 |
| 5 | 22.3 | " | 8.77 | 10.38 | " | 11.58 " | .00429 | 9.26 | 0.33 | 35.4 |
| 6 | 21.1 | 3.88 | 8.98 | 4.26 | 43.6 | 4.27 " | .00125 | 7.92 | 0.11 | 30.0 |
| 7 | 21.3 | " | 8.94 | 5.82 | " | 5.81 " | .00187 | 7.98 | 0.17 | 33.4 |
| 8 | 21.6 | " | 8.88 | 7.62 | " | 7.56 " | .00250 | 8.04 | 0.22 | 35.6 |
| 9 | 21.9 | " | 8.82 | 9.30 | " | 9.15 " | .00312 | 8.13 | 0.28 | 34.4 |
| 10 | 22.1 | " | 8.79 | 10.86 | " | 10.67 " | .00374 | 8.21 | 0.33 | 34.4 |
| 11 | 22.2 | 3.38 | 8.79 | 4.56 | 38.2 | 3.87 " | .00107 | 6.90 | 0.11 | 29.2 |
| 12 | 22.4 | " | 8.76 | 6.96 | " | 5.88 " | .00161 | 6.95 | 0.16 | 33.0 |
| 13 | 22.3 | " | 8.77 | 8.52 | " | 7.21 " | .00214 | 7.01 | 0.22 | 34.2 |
| 14 | 22.5 | " | 8.76 | 9.84 | " | 8.32 " | .00268 | 7.07 | 0.27 | 35.1 |
| 15 | 22.5 | " | 8.76 | 11.66 | " | 9.83 " | .00321 | 7.13 | 0.33 | 35.8 |
| 16 | 22.9 | 2.88 | 8.72 | 4.20 | 32.7 | 2.95 " | .00090 | 5.88 | 0.11 | 28.5 |
| 17 | 23.0 | " | 8.70 | 6.00 | " | 4.27 " | .00135 | 5.91 | 0.16 | 34.7 |
| 18 | 23.2 | " | 8.67 | 7.92 | " | 5.60 " | .00180 | 5.96 | 0.22 | 35.7 |
| 19 | 23.3 | " | 8.65 | 9.00 | " | 6.35 " | .00224 | 6.00 | 0.27 | 37.7 |
| 20 | 23.4 | " | 8.63 | 11.76 | " | 8.28 " | .00269 | 6.06 | 0.33 | 36.8 |

*Flows through a cross-sectional area of $\pi/36$ $ft^2$

Table 12 - Data for System I (continued)

| 1 | 2 | 3 | 4 | 5 | 6 | 7 | 8 | 9 | 10 | 11 |
|---|---|---|---|---|---|---|---|---|---|---|
| 21 | 22.7 | 2.38 | 8.73 | 4.20 | 27.2 | $2.46 \times 10^{-3}$ | .00073 | 4.84 | 0.11 | * —— |
| 22 | 22.8 | " | 8.72 | 6.30 | " | 3.68 " | .00109 | 4.88 | 0.16 | 34.8 |
| 23 | 23.0 | " | 8.70 | 8.04 | " | 4.68 " | .00146 | 4.91 | 0.21 | 38.0 |
| 24 | 23.2 | " | 8.67 | 11.28 | " | 6.56 " | .00182 | 4.94 | 0.27 | 40.3 |
| 25 | 23.3 | " | 8.65 | 11.64 | " | 6.73 " | .00219 | 4.99 | 0.32 | 38.8 |
| 26 | 23.1 | 1.88 | 8.69 | 3.60 | 21.8 | 1.66 " | .00057 | 3.81 | 0.11 | —— |
| 27 | 23.2 | " | 8.66 | 5.64 | " | 2.58 " | .00085 | 3.84 | 0.16 | —— |
| 28 | 23.2 | " | 8.66 | 6.96 | " | 3.19 " | .00113 | 3.87 | 0.21 | 39.4 |
| 29 | 23.3 | " | 8.65 | 8.80 | " | 4.03 " | .00142 | 3.90 | 0.26 | 39.8 |
| 30 | 23.3 | " | 8.65 | 10.32 | " | 4.72 " | .00170 | 3.93 | 0.32 | 40.2 |
| 31 | 24.0 | 1.38 | 8.50 | 4.08 | 16.3 | 1.35 " | .00041 | 2.81 | 0.10 | —— |
| 32 | 24.1 | " | 8.49 | 5.34 | " | 1.77 " | .00061 | 2.83 | 0.16 | —— |
| 33 | 24.1 | " | 8.49 | 6.96 | " | 2.31 " | .00082 | 2.87 | 0.21 | 28.9 |
| 34 | 24.1 | " | 8.49 | 9.00 | " | 2.98 " | .00102 | 2.89 | 0.26 | 31.3 |
| 35 | 24.2 | " | 8.48 | 9.84 | " | 3.25 " | .00123 | 2.90 | 0.32 | 35.1 |
| 36 | 24.0 | 0.88 | 8.50 | 3.96 | 10.9 | 0.86 " | .00026 | 1.80 | 0.10 | —— |
| 37 | 24.0 | " | 8.50 | 5.52 | " | 1.21 " | .00038 | 1.81 | 0.15 | —— |
| 38 | 24.0 | " | 8.50 | 6.72 | " | 1.47 " | .00051 | 1.82 | 0.21 | —— |
| 39 | 24.0 | " | 8.50 | 8.16 | " | 1.79 " | .00064 | 1.83 | 0.26 | —— |
| 40 | 24.0 | " | 8.50 | 9.84 | " | 2.15 " | .00077 | 1.84 | 0.31 | —— |

* —— omitted due to accuracy of $\Delta H_T$, i.e., when $(H_E - H_T) < 0.10$ ft, causing an error of > 10% w.r.t. least reading of ± 0.01 ft

Table 13 - Data for System II

| 1 | 2 | 3 | 4 | 5 | 6 | 7 | 8 |
|---|---|---|---|---|---|---|---|
| Run No. | T (°C) | $H_S$ (ft) | $C_S$ (mg/l) | Slope ($hr^{-1}$) | W (lb) | $R_o$ (lb/hr) | $P_a$ (kw) |
| 1 | 19.8 | 4.59 | 9.24 | 0.54 | 506 | $6.60 \times 10^{-3}$ | 0.00151 |
| 2 | 20.4 | 4.58 | 9.13 | 0.69 | " | 8.33 " | 0.00223 |
| 3 | 20.5 | 4.56 | 9.10 | 0.87 | " | 10.46 " | 0.00300 |
| 4 | 20.5 | 4.55 | 9.10 | 0.99 | " | 11.90 " | 0.00374 |
| 5 | 20.5 | 4.55 | 9.10 | 1.05 | " | 12.60 " | 0.00447 |
| 6 | 19.4 | 4.10 | 9.33 | 0.51 | 495 | 6.07 " | 0.00133 |
| 7 | 19.6 | 4.08 | 9.28 | 0.68 | " | 8.06 " | 0.00198 |
| 8 | 19.9 | 4.07 | 9.22 | 0.86 | " | 10.10 " | 0.00264 |
| 9 | 20.2 | 4.06 | 9.16 | 0.92 | " | 10.77 " | 0.00329 |
| 10 | 20.5 | 4.05 | 9.10 | 1.04 | " | 12.07 " | 0.00393 |
| 11 | 20.4 | 3.60 | 9.12 | 0.53 | 484 | 5.88 " | 0.00115 |
| 12 | 20.6 | 3.59 | 9.08 | 0.65 | " | 7.21 " | 0.00172 |
| 13 | 20.9 | 3.58 | 9.02 | 0.81 | " | 8.97 " | 0.00228 |
| 14 | 21.2 | 3.57 | 8.96 | 0.92 | " | 10.09 " | 0.00284 |
| 15 | 21.4 | 3.56 | 8.92 | 1.08 | " | 11.85 " | 0.00340 |
| 16 | 19.8 | 3.10 | 9.24 | 0.50 | 474 | 5.51 " | 0.00097 |
| 17 | 20.2 | 3.09 | 9.16 | 0.62 | " | 6.71 " | 0.00145 |
| 18 | 20.4 | 3.08 | 9.12 | 0.78 | " | 8.45 " | 0.00193 |
| 19 | 20.7 | 3.07 | 9.06 | 0.90 | " | 9.66 " | 0.00241 |
| 20 | 20.9 | 3.06 | 9.02 | 1.04 | " | 11.10 " | 0.00288 |

Table 13 - Data for System II

| 9 | 10 | 11 | 12 | 13 | 14 | 15 | 16 |
|---|---|---|---|---|---|---|---|
| $P_u - P_l$ (ft) | $h_l$ (ft) | s (ft) | Qa'* (scfm) | $t_d$ (sec) | $V_{Pave}$ (=$V_n$) (ft/sec) | $V_w$ (ft/sec.) | $V_b$ (cm/sec.) |
| 0.070 | 9.18 | 8.00 | 0.11 | 3.33 | 0.87 | 0.89 | 46.1 |
| 0.095 | 9.15 | " | 0.17 | 3.00 | 1.03 | 1.06 | 48.8 |
| 0.120 | 9.13 | " | 0.22 | 2.85 | 1.17 | 1.21 | 48.8 |
| 0.140 | 9.10 | " | 0.28 | 2.66 | 1.31 | 1.36 | 50.3 |
| 0.160 | 9.08 | " | 0.33 | 2.53 | 1.41 | 1.47 | 51.5 |
| 0.065 | 8.18 | 7.00 | 0.11 | 3.12 | 0.78 | 0.80 | 43.9 |
| 0.085 | 8.16 | " | 0.16 | 2.72 | 0.94 | 0.97 | 49.1 |
| 0.110 | 8.14 | " | 0.22 | 2.64 | 1.06 | 1.10 | 47.3 |
| 0.125 | 8.12 | " | 0.27 | 2.40 | 1.19 | 1.24 | 51.2 |
| 0.145 | 8.10 | " | 0.33 | 2.32 | 1.30 | 1.36 | 50.6 |
| 0.055 | 7.20 | 5.99 | 0.11 | 2.67 | 0.76 | 0.78 | 44.6 |
| 0.075 | 7.18 | " | 0.16 | 2.43 | 0.91 | 0.94 | 46.7 |
| 0.090 | 7.16 | " | 0.22 | 2.18 | 1.03 | 1.07 | 50.9 |
| 0.110 | 7.14 | " | 0.27 | 2.14 | 1.15 | 1.20 | 48.8 |
| 0.125 | 7.12 | " | 0.32 | 2.02 | 1.24 | 1.30 | 50.7 |
| 0.050 | 6.20 | 4.99 | 0.11 | 2.45 | 0.71 | 0.73 | 39.7 |
| 0.065 | 6.18 | " | 0.16 | 2.13 | 0.85 | 0.88 | 44.9 |
| 0.080 | 6.17 | " | 0.21 | 1.96 | 0.96 | 1.00 | 47.0 |
| 0.100 | 6.15 | " | 0.27 | 1.96 | 1.06 | 1.11 | 43.9 |
| 0.115 | 6.13 | " | 0.32 | 1.88 | 1.14 | 1.20 | 44.3 |

*Flows through a cross-sectional area of $\pi/36$ $ft^2$

Table 13 - Data for System II (continued)

| 1 | 2 | 3 | 4 | 5 | 6 | 7 | 8 |
|---|---|---|---|---|---|---|---|
| 21 | 17.4 | 2.61 | 9.62 | 0.36 | 463 | $3.97 \times 10^{-3}$ | 0.00081 |
| 22 | 17.8 | 2.60 | 9.54 | 0.54 | " | 5.88 " | 0.00120 |
| 23 | 18.2 | 2.59 | 9.49 | 0.66 | " | 7.18 " | 0.00160 |
| 24 | 18.5 | 2.58 | 9.45 | 0.74 | " | 8.02 " | 0.00199 |
| 25 | 18.8 | 2.58 | 9.42 | 0.90 | " | 9.67 " | 0.00239 |
| 26 | 17.3 | 2.11 | 9.64 | 0.35 | 452 | 3.67 " | 0.00064 |
| 27 | 17.8 | 2.11 | 9.54 | 0.50 | " | 5.21 " | 0.00096 |
| 28 | 18.3 | 2.10 | 9.47 | 0.60 | " | 6.28 " | 0.00128 |
| 29 | 18.7 | 2.09 | 9.44 | 0.72 | " | 7.49 " | 0.00159 |
| 30 | 19.0 | 2.09 | 9.40 | 0.83 | " | 8.54 " | 0.00190 |
| 31 | 17.6 | 1.62 | 9.58 | 0.32 | 411 | 3.21 " | 0.00048 |
| 32 | 18.2 | 1.61 | 9.49 | 0.42 | " | 4.23 " | 0.00072 |
| 33 | 18.5 | 1.61 | 9.45 | 0.50 | " | 5.03 " | 0.00096 |
| 34 | 19.0 | 1.60 | 9.40 | 0.59 | " | 5.90 " | 0.00120 |
| 35 | 19.3 | 1.60 | 9.34 | 0.69 | " | 6.84 " | 0.00143 |

Table 13 - Data for System II (continued)

| 9 | 10 | 11 | 12 | 13 | 14 | 15 | 16 |
|---|---|---|---|---|---|---|---|
| 0.045 | 5.21 | 398 | 0.11 | *—— | 0.62 | 0.64 | —— |
| 0.055 | 5.20 | " | 0.16 | 1.82 | 0.75 | 0.78 | 42.7 |
| 0.065 | 5.18 | " | 0.21 | 1.61 | 0.83 | 0.87 | 48.8 |
| 0.080 | 5.17 | " | 0.26 | 1.59 | 0.96 | 1.01 | 45.5 |
| 0.090 | 5.15 | " | 0.32 | 1.49 | 1.03 | 1.09 | 48.2 |
| 0.035 | 4.22 | 298 | 0.10 | —— | 0.49 | 0.51 | —— |
| 0.040 | 4.21 | " | 0.16 | —— | 0.61 | 0.64 | —— |
| 0.050 | 4.20 | " | 0.21 | 1.26 | 0.71 | 0.75 | 49.4 |
| 0.060 | 4.19 | " | 0.26 | 1.21 | 0.81 | 0.86 | 49.1 |
| 0.070 | 4.17 | " | 0.31 | 1.18 | 0.87 | 0.93 | 48.8 |
| 0.020 | 3.23 | 197 | 0.10 | —— | 0.31 | 0.33 | —— |
| 0.025 | 3.22 | " | 0.15 | —— | 0.44 | 0.47 | —— |
| 0.035 | 3.21 | " | 0.21 | —— | 0.53 | 0.57 | —— |
| 0.045 | 3.20 | " | 0.26 | —— | 0.60 | 0.65 | —— |
| 0.050 | 3.19 | " | 0.31 | 0.85 | 0.67 | 0.73 | 48.5 |

*——omitted due to accuracy of $(P_u - P_l)$, i.e., when < 0.050 ft, causing an error of > 10% w.r.t. least reading of ± 0.005 ft

Table 14 - Data for System III

| 1 | 2 | 3 | 4 | 5 | 6 | 7 | 8 | 9 | 10 |
|---|---|---|---|---|---|---|---|---|---|
| Run No. | T (°C) | $H_S$ (ft) | $C_S$ (mg/l) | Slope ($hr^{-1}$) | W (lb) | $R_o$ (lb/hr) | $P_a$ (kw) | $\Delta H$ (ft) | $P_w$ (kw) |
| 1 | 12.1 | 1.93 | 10.78 | 1.20 | 406 | $1.28 \times 10^{-2}$ | .000584 | 0.350 | .001506 |
| 2 | 13.6 | 1.93 | 10.48 | 1.49 | " | 1.54 " | .000874 | 0.400 | .001718 |
| 3 | 14.8 | 1.92 | 10.24 | 1.79 | " | 1.80 " | .001162 | 0.430 | .001848 |
| 4 | 16.0 | 1.92 | 10.00 | 1.92 | " | 1.90 " | .001451 | 0.465 | .001998 |
| 5 | 17.1 | 1.92 | 9.68 | 2.13 | " | 2.04 " | .001741 | 0.495 | .002130 |
| 6 | 14.1 | 1.99 | 10.38 | 0.43 | " | $4.39 \times 10^{-3}$ | .000602 | 0.090 | .000170 |
| 7 | 17.0 | 1.97 | 9.70 | 0.65 | " | 6.25 " | .000598 | 0.145 | .000409 |
| 8 | 18.7 | 1.96 | 9.43 | 0.81 | " | 7.56 " | .001190 | 0.185 | .000349 |
| 9 | 19.9 | 1.93 | 9.22 | 1.28 | " | 11.62 " | .001170 | 0.310 | .000876 |
| 10 | 21.2 | 1.94 | 8.97 | 1.28 | " | 11.30 " | .001761 | 0.290 | .000547 |
| 11 | 21.9 | 1.91 | 8.82 | 1.67 | " | 14.46 " | .001736 | 0.410 | .001160 |
| 12 | 12.7 | 2.43 | 10.66 | 1.38 | 417 | $1.51 \times 10^{-2}$ | .000749 | 0.420 | .001996 |
| 13 | 14.1 | 2.43 | 10.38 | 1.79 | " | 1.91 " | .001121 | 0.460 | .002185 |
| 14 | 15.5 | 2.42 | 10.10 | 1.91 | " | 1.98 " | .001489 | 0.510 | .002425 |
| 15 | 16.6 | 2.41 | 9.82 | 2.37 | " | 2.39 " | .001853 | 0.560 | .002660 |
| 16 | 17.5 | 2.40 | 9.60 | 2.58 | " | 2.55 " | .002217 | 0.600 | .002850 |
| 17 | 12.4 | 2.91 | 10.72 | 1.38 | 428 | 1.58 " | .000911 | 0.480 | .002350 |
| 18 | 13.6 | 2.90 | 10.48 | 1.62 | " | 1.82 " | .001361 | 0.505 | .002475 |
| 19 | 14.8 | 2.90 | 10.24 | 1.89 | " | 2.07 " | .001809 | 0.560 | .002740 |
| 20 | 15.7 | 2.89 | 10.06 | 1.98 | " | 2.14 " | .002255 | 0.620 | .003040 |
| 21 | 16.5 | 2.88 | 9.85 | 2.24 | " | 2.36 " | .002701 | 0.685 | .003360 |

Table 14 -Data for System III

| 11 | 12 | 13 | 14 | 15 | 16 | 17 | 18 | 19 | 20 |
|---|---|---|---|---|---|---|---|---|---|
| $P_u - P_l$ (ft) | $h_l$ (ft) | s (ft) | *Qa (scfm) | $t_d$ (sec.) | $V_w$ (ft/sec.) | $V_b$ (cm/sec) | $Y_l$ (ft) | $d_l$ (ft) | $V_T$ (ft/sec.) |
| 0.270 | 3.86 | 2.98 | 0.10 | 13.55 | 0.65 | 26.5 | 3.27 | 0.925 | 0.85 |
| 0.295 | 3.85 | " | 0.16 | 9.88 | 0.66 | 29.3 | " | 0.950 | 0.94 |
| 0.325 | 3.84 | " | 0.21 | 8.18 | 0.67 | 31.4 | " | 0.965 | 1.01 |
| 0.350 | 3.84 | " | 0.26 | 7.03 | 0.67 | 33.2 | " | 0.985 | 1.07 |
| 0.360 | 3.84 | " | 0.31 | 6.03 | 0.68 | 35.7 | " | 1.000 | 1.15 |
| 0.065 | 3.97 | " | 0.10 | 3.27 | 0.26 | 35.7 | " | 0.795 | 1.16 |
| 0.110 | 3.95 | " | 0.10 | 5.54 | 0.40 | 28.6 | " | 0.830 | 0.93 |
| 0.150 | 3.93 | " | 0.21 | 3.77 | 0.27 | 32.3 | " | 0.850 | 1.05 |
| 0.255 | 3.87 | " | 0.21 | 6.43 | 0.42 | 26.9 | " | 0.910 | 0.87 |
| 0.240 | 3.88 | " | 0.31 | 4.02 | 0.28 | 31.1 | " | 0.905 | 1.01 |
| 0.340 | 3.83 | " | 0.31 | 5.67 | 0.44 | 29.6 | " | 0.960 | 0.96 |
| 0.305 | 4.87 | 3.98 | 0.11 | 15.14 | 0.71 | 29.6 | 4.27 | 0.970 | 0.95 |
| 0.330 | 4.86 | " | 0.16 | 10.93 | 0.71 | 32.6 | " | 0.985 | 1.05 |
| 0.375 | 4.84 | " | 0.21 | 9.31 | 0.72 | 35.1 | " | 1.010 | 1.13 |
| 0.420 | 4.82 | " | 0.26 | 8.35 | 0.73 | 36.9 | " | 1.035 | 1.19 |
| 0.455 | 4.81 | " | 0.32 | 7.53 | 0.74 | 38.7 | " | 1.060 | 1.25 |
| 0.375 | 5.83 | 4.99 | 0.11 | 18.39 | 0.73 | 30.5 | 5.28 | 0.995 | 0.98 |
| 0.415 | 5.81 | " | 0.16 | 13.57 | 0.74 | 33.9 | " | 1.010 | 1.09 |
| 0.465 | 5.79 | " | 0.21 | 11.42 | 0.75 | 36.3 | " | 1.045 | 1.17 |
| 0.505 | 5.78 | " | 0.27 | 9.90 | 0.75 | 38.1 | " | 1.070 | 1.23 |
| 0.545 | 5.77 | " | 0.32 | 8.90 | 0.76 | 40.3 | " | 1.100 | 1.30 |

*Flows through a cross-sectional area of $\pi/36$ ft$^2$

Table 14 - Data for System III (continued)

| 1 | 2 | 3 | 4 | 5 | 6 | 7 | 8 | 9 | 10 |
|---|---|---|---|---|---|---|---|---|---|
| 22 | 12.9 | 3.38 | 10.62 | 1.64 | 438 | $1.92 \times 10^{-2}$ | .001071 | 0.550 | .002490 |
| 23 | 14.4 | 3.37 | 10.32 | 2.01 | " | 2.30 " | .001600 | 0.595 | .002690 |
| 24 | 15.7 | 3.35 | 10.06 | 2.30 | " | 2.56 " | .002125 | 0.645 | .002920 |
| 25 | 16.7 | 3.34 | 9.79 | 2.54 | " | 2.75 " | .002645 | 0.725 | .003280 |
| 26 | 17.7 | 3.33 | 9.56 | 2.66 | " | 2.81 " | .003164 | 0.810 | .003665 |
| 27 | 10.9 | 3.84 | 11.12 | 1.50 | 450 | 1.92 " | .001236 | 0.590 | .002555 |
| 28 | 12.3 | 3.83 | 10.74 | 1.64 | " | 2.03 " | .001847 | 0.645 | .002795 |
| 29 | 13.5 | 3.82 | 10.50 | 2.01 | " | 2.43 " | .002455 | 0.705 | .003060 |
| 30 | 14.6 | 3.81 | 10.28 | 2.31 | " | 2.74 " | .003061 | 0.760 | .003290 |
| 31 | 15.8 | 3.80 | 10.04 | 2.81 | " | 3.25 " | .003663 | 0.830 | .003600 |
| 32 | 12.0 | 4.44 | 10.80 | 0.74 | 461 | $9.48 \times 10^{-3}$ | .001455 | 0.270 | .000509 |
| 33 | 13.7 | 4.41 | 10.46 | 1.52 | " | $1.90 \times 10^{-2}$ | .001443 | 0.445 | .001257 |
| 34 | 15.2 | 4.37 | 10.16 | 1.11 | " | 1.35 " | .002856 | 0.590 | .001112 |
| 35 | 16.2 | 4.32 | 9.94 | 1.68 | " | 2.00 " | .002821 | 0.785 | .002220 |
| 36 | 17.2 | 4.29 | 9.66 | 1.67 | " | 1.92 " | .004199 | 0.905 | .001705 |
| 37 | 18.0 | 4.25 | 9.50 | 1.97 | " | 2.23 " | .004152 | 1.110 | .003140 |
| 38 | 11.5 | 4.30 | 10.95 | 1.77 | " | 2.31 " | .001402 | 0.870 | .003610 |
| 39 | 13.0 | 4.29 | 10.60 | 1.73 | " | 2.18 " | .002097 | 0.960 | .003980 |
| 40 | 14.2 | 4.28 | 10.36 | 2.64 | " | 3.27 " | .002790 | 1.020 | .004230 |
| 41 | 15.3 | 4.28 | 10.14 | 3.05 | " | 3.69 " | .003483 | 1.075 | .004460 |
| 42 | 16.3 | 4.27 | 9.92 | 3.14 | " | 3.72 " | .004174 | 1.145 | .004750 |

Table 14 - Data for System III (continued)

| 11 | 12 | 13 | 14 | 15 | 16 | 17 | 18 | 19 | 20 |
|---|---|---|---|---|---|---|---|---|---|
| 0.490 | 6.76 | 5.99 | 0.11 | 23.74 | 0.68 | 28.4 | 6.28 | 1.025 | 0.91 |
| 0.550 | 6.73 | " | 0.16 | 17.79 | 0.69 | 31.4 | " | 1.055 | 1.01 |
| 0.610 | 6.71 | " | 0.22 | 14.79 | 0.70 | 33.9 | " | 1.085 | 1.09 |
| 0.670 | 6.68 | " | 0.27 | 12.98 | 0.71 | 35.7 | " | 1.125 | 1.15 |
| 0.725 | 6.66 | " | 0.32 | 11.71 | 0.72 | 37.5 | " | 1.165 | 1.21 |
| 0.595 | 7.69 | 7.00 | 0.11 | 28.52 | 0.66 | 27.7 | 7.29 | 1.055 | 0.89 |
| 0.660 | 7.66 | " | 0.16 | 21.10 | 0.67 | 30.5 | " | 1.080 | 0.98 |
| 0.725 | 7.64 | " | 0.22 | 17.37 | 0.67 | 32.6 | " | 1.115 | 1.05 |
| 0.770 | 7.62 | " | 0.27 | 14.75 | 0.68 | 35.2 | " | 1.140 | 1.14 |
| 0.830 | 7.60 | " | 0.33 | 13.28 | 0.69 | 37.2 | " | 1.175 | 1.20 |
| 0.245 | 8.89 | 8.00 | 0.11 | 11.61 | 0.27 | 29.3 | 8.29 | 0.890 | 0.95 |
| 0.375 | 8.82 | " | 0.11 | 17.79 | 0.41 | 26.2 | " | 0.980 | 0.85 |
| 0.530 | 8.74 | " | 0.22 | 12.59 | 0.28 | 28.0 | " | 1.055 | 0.91 |
| 0.715 | 8.65 | " | 0.22 | 16.94 | 0.43 | 27.4 | " | 1.155 | 0.89 |
| 0.835 | 8.59 | " | 0.33 | 13.19 | 0.29 | 27.4 | " | 1.215 | 0.89 |
| 1.035 | 8.50 | " | 0.33 | 16.36 | 0.46 | 29.0 | " | 1.320 | 0.94 |
| 0.820 | 8.60 | " | 0.11 | 38.87 | 0.65 | 26.2 | " | 1.200 | 0.84 |
| 0.895 | 8.58 | " | 0.17 | 28.30 | 0.65 | 28.4 | " | 1.240 | 0.91 |
| 0.960 | 8.56 | " | 0.22 | 22.78 | 0.66 | 30.8 | " | 1.270 | 0.99 |
| 1.000 | 8.55 | " | 0.28 | 18.98 | 0.67 | 33.3 | " | 1.300 | 1.07 |
| 1.035 | 8.54 | " | 0.33 | 16.36 | 0.67 | 35.4 | " | 1.335 | 1.14 |

Table 15 - Data for System IV

| 1 | 2 | 3 | 4 | 5 | 6 | 7 | 8 |
|---|---|---|---|---|---|---|---|
| Run No. | T (°C) | $H_s$ (ft) | $C_s$ (mg/l) | Slope ($hr^{-1}$) | W (lb) | $R_o$ (lb/hr) | $H_T$ (ft) |
| 1 | 14.9 | 3.00 | 10.22 | 1.19 | 385 | $1.17 \times 10^{-2}$ | 1.67 |
| 2 | 16.5 | 3.00 | 9.85 | 1.55 | " | 1.47 " | 1.70 |
| 3 | 17.7 | 3.01 | 9.56 | 1.85 | " | 1.70 " | 1.72 |
| 4 | 18.8 | 3.01 | 9.43 | 2.34 | " | 2.13 " | 1.75 |
| 5 | 19.7 | 3.01 | 9.26 | 2.73 | " | 2.44 " | 1.77 |
| 6 | 17.8 | 3.51 | 9.54 | 1.47 | 396 | 1.41 " | 1.69 |
| 7 | 18.8 | 3.51 | 9.42 | 1.86 | " | 1.76 " | 1.72 |
| 8 | 19.6 | 3.50 | 9.29 | 2.25 | " | 2.10 " | 1.74 |
| 9 | 20.2 | 3.51 | 9.16 | 2.67 | " | 2.46 " | 1.76 |
| 10 | 20.7 | 3.51 | 9.07 | 2.97 | " | 2.71 " | 1.79 |
| 11 | 17.7 | 4.01 | 9.56 | 1.49 | 407 | 1.49 " | 1.70 |
| 12 | 18.8 | 4.01 | 9.43 | 1.86 | " | 1.84 " | 1.73 |
| 13 | 19.6 | 4.01 | 9.28 | 2.31 | " | 2.24 " | 1.76 |
| 14 | 20.6 | 4.01 | 9.08 | 2.64 | " | 2.51 " | 1.79 |
| 15 | 21.5 | 4.01 | 8.90 | 3.21 | " | 3.00 " | 1.82 |
| 16 | 17.9 | 4.51 | 9.52 | 1.49 | 418 | 1.54 " | 1.70 |
| 17 | 18.9 | 4.51 | 9.41 | 2.07 | " | 2.13 " | 1.75 |
| 18 | 19.7 | 4.51 | 9.26 | 2.51 | " | 2.53 " | 1.79 |
| 19 | 20.4 | 4.51 | 9.13 | 3.18 | " | 3.17 " | 1.81 |
| 20 | 20.9 | 4.51 | 9.02 | 4.08 | " | 4.01 " | 1.84 |

Table 15 - Data for System IV

| 9 | 10 | 11 | 12 | 13 | 14 | 15 | 16 |
|---|---|---|---|---|---|---|---|
| $P_a$ (kw) | $\Delta H$ (ft) | $P_w$ (Kw) | $P_u - P_l$ (ft) | $P_A$ (ft) | z (ft) | * $Q_a'$ (scfm) | $t_{dR}$ (sec.) |
| 0.000243 | 0.504 | 0.005910 | 0.110 | 1.67 | 1.90 | 0.10 | 5.91 |
| 0.000371 | 0.605 | 0.006850 | 0.150 | 1.70 | " | 0.15 | 5.37 |
| 0.000502 | 0.670 | 0.007840 | 0.180 | 1.72 | " | 0.20 | 4.84 |
| 0.000637 | 0.740 | 0.008920 | 0.215 | 1.75 | " | 0.24 | 4.63 |
| 0.000775 | 0.790 | 0.009680 | 0.255 | 1.77 | " | 0.29 | 4.56 |
| 0.000246 | 0.575 | 0.006400 | 0.145 | 1.69 | 2.88 | 0.10 | 7.89 |
| 0.000375 | 0.660 | 0.007590 | 0.185 | 1.72 | " | 0.14 | 6.72 |
| 0.000508 | 0.725 | 0.008620 | 0.225 | 1.74 | " | 0.19 | 6.12 |
| 0.000642 | 0.790 | 0.009680 | 0.260 | 1.76 | " | 0.24 | 5.67 |
| 0.000782 | 0.850 | 0.010560 | 0.305 | 1.79 | " | 0.29 | 5.53 |
| 0.000247 | 0.625 | 0.007310 | 0.140 | 1.70 | 3.90 | 0.10 | 7.72 |
| 0.000379 | 0.710 | 0.008570 | 0.195 | 1.73 | " | 0.14 | 7.17 |
| 0.000512 | 0.775 | 0.009500 | 0.230 | 1.76 | " | 0.19 | 6.36 |
| 0.000654 | 0.855 | 0.010630 | 0.295 | 1.79 | " | 0.24 | 6.50 |
| 0.000796 | 0.900 | 0.011360 | 0.350 | 1.82 | " | 0.29 | 6.47 |
| 0.000248 | 0.635 | 0.007430 | 0.165 | 1.70 | 4.90 | 0.09 | 9.23 |
| 0.000382 | 0.735 | 0.008850 | 0.230 | 1.75 | " | 0.14 | 8.59 |
| 0.000521 | 0.820 | 0.010050 | 0.295 | 1.79 | " | 0.19 | 8.24 |
| 0.000659 | 0.865 | 0.010750 | 0.330 | 1.81 | " | 0.23 | 7.38 |
| 0.000805 | 0.935 | 0.011810 | 0.400 | 1.84 | " | 0.28 | 7.46 |

*Flows through a cross-sectional area of $\pi/36$ ft$^2$

Table 15 - Data for System IV (continued)

| 1 | 2 | 3 | 4 | 5 | 6 | 7 | 8 |
|---|---|---|---|---|---|---|---|
| 21 | 17.8 | 4.51 | 9.54 | 1.79 | 418 | $1.85 \times 10^{-2}$ | 1.72 |
| 22 | 18.8 | 4.51 | 9.42 | 1.91 | " | 1.96 " | 1.73 |
| 23 | 19.6 | 4.51 | 9.29 | 2.72 | " | 2.75 " | 1.77 |
| 24 | 20.3 | 4.51 | 9.14 | 3.23 | " | 3.21 " | 1.78 |
| 25 | 21.0 | 4.51 | 9.00 | 4.11 | " | 4.04 " | 1.83 |
| 26 | 21.6 | 4.51 | 8.88 | 5.40 | " | 5.23 " | 1.86 |
| 27 | 16.8 | 5.01 | 9.76 | 1.73 | 429 | 1.91 " | 1.72 |
| 28 | 17.8 | 5.01 | 9.55 | 2.18 | " | 2.36 " | 1.76 |
| 29 | 18.6 | 5.01 | 9.45 | 2.60 | " | 2.78 " | 1.80 |
| 30 | 19.3 | 5.02 | 9.34 | 3.17 | " | 3.35 " | 1.83 |
| 31 | 19.9 | 5.02 | 9.22 | 4.29 | " | 4.49 " | 1.86 |
| 32 | 17.6 | 5.51 | 9.58 | 1.86 | 440 | 2.10 " | 1.72 |
| 33 | 18.4 | 5.51 | 9.46 | 2.43 | " | 2.71 " | 1.76 |
| 34 | 19.2 | 5.51 | 9.36 | 3.00 | " | 3.31 " | 1.79 |
| 35 | 19.9 | 5.51 | 9.22 | 3.60 | " | 3.91 " | 1.83 |

Table 15 - Data for System IV (continued)

| 9 | 10 | 11 | 12 | 13 | 14 | 15 | 16 |
|---|---|---|---|---|---|---|---|
| 0.000251 | 0.725 | 0.009430 | 0.135 | 1.72 | 4.90 | 0.09 | 7.54 |
| 0.000252 | 0.775 | 0.010810 | 0.105 | 1.73 | " | 0.09 | 5.87 |
| 0.000515 | 0.835 | 0.010870 | 0.245 | 1.77 | " | 0.19 | 6.86 |
| 0.000520 | 0.895 | 0.012480 | 0.225 | 1.78 | " | 0.19 | 6.28 |
| 0.000802 | 0.945 | 0.012290 | 0.370 | 1.83 | " | 0.28 | 6.88 |
| 0.000814 | 1.015 | 0.014160 | 0.375 | 1.86 | " | 0.28 | 6.99 |
| 0.000250 | 0.665 | 0.007910 | 0.185 | 1.72 | 5.90 | 0.09 | 10.46 |
| 0.000384 | 0.760 | 0.009330 | 0.245 | 1.76 | " | 0.14 | 9.27 |
| 0.000524 | 0.850 | 0.010580 | 0.315 | 1.80 | " | 0.19 | 8.93 |
| 0.000667 | 0.930 | 0.011750 | 0.370 | 1.83 | " | 0.23 | 8.36 |
| 0.000814 | 0.980 | 0.012570 | 0.435 | 1.86 | " | 0.28 | 8.20 |
| 0.000251 | 0.685 | 0.008130 | 0.215 | 1.72 | 6.90 | 0.09 | 12.34 |
| 0.000384 | 0.780 | 0.009570 | 0.270 | 1.76 | " | 0.14 | 10.31 |
| 0.000523 | 0.875 | 0.010880 | 0.330 | 1.79 | " | 0.18 | 9.47 |
| 0.000669 | 0.965 | 0.012360 | 0.395 | 1.83 | " | 0.23 | 9.05 |

Table 16 Data for Porous Diffusers - System II

| 1 | 2 | 3 | 4 | 5 | 6 | 7 | 8 |
|---|---|---|---|---|---|---|---|
| Run No. | T (°C) | $H_s$ (ft) | $C_s$ (mg/l) | SLOPE ($hr^{-1}$) | W (lb) | $R_o$ (lb/hr) | $P_a$ (kw) |
| 1 | 19.3 | 4.59 | 9.34 | 0.98 | 506 | $1.20 \times 10^{-2}$ | 0.00151 |
| 2 | 19.5 | 4.56 | 9.30 | 1.29 | " | 1.58 " | 0.00300 |
| 3 | 19.7 | 4.53 | 9.26 | 1.76 | " | 2.14 " | 0.00447 |
| 4 | 18.9 | 3.10 | 9.41 | 0.86 | 474 | $9.57 \times 10^{-3}$ | 0.00097 |
| 5 | 19.1 | 3.08 | 9.38 | 1.22 | " | 13.52 " | 0.00193 |
| 6 | 19.3 | 3.06 | 9.35 | 1.59 | " | 17.68 " | 0.00288 |
| 7 | 19.1 | 1.61 | 9.38 | 0.60 | 441 | $5.98 \times 10^{-3}$ | 0.00048 |
| 8 | 19.4 | 1.60 | 9.33 | 1.01 | " | 9.96 " | 0.0096 |
| 9 | 19.6 | 1.59 | 9.29 | 1.31 | " | 12.88 " | 0.00143 |

Fisher Scientific Porous Stones

Table 17 - Data for Porous Diffusers - System II

| 1 | 2 | 3 | 4 | 5 | 6 | 7 | 8 |
|---|---|---|---|---|---|---|---|
| Run No. | T (°C) | $H_s$ (ft) | $C_s$ (mg/l) | SLOPE ($hr^{-1}$) | W (lb) | $R_o$ (lb/hr) | $P_a$ (kw) |
| 1 | 20.4 | 4.59 | 9.12 | 0.93 | 506 | $1.12 \times 10^{-2}$ | 0.00151 |
| 2 | 20.7 | 4.57 | 9.07 | 1.31 | " | 1.56 " | 0.00300 |
| 3 | 20.9 | 4.54 | 9.03 | 1.53 | " | 1.82 " | 0.00447 |
| 4 | 20.3 | 3.10 | 9.15 | 0.87 | 474 | $9.48 \times 10^{-3}$ | 0.00097 |
| 5 | 20.5 | 3.08 | 9.11 | 1.22 | " | 13.18 " | 0.00194 |
| 6 | 20.6 | 3.07 | 9.08 | 1.38 | " | 14.90 " | 0.00289 |
| 7 | 19.8 | 1.61 | 9.24 | 0.59 | 441 | $5.75 \times 10^{-3}$ | 0.00048 |
| 8 | 20.2 | 1.60 | 9.17 | 0.84 | " | 8.20 " | 0.00096 |
| 9/ | 20.4 | 1.60 | 9.12 | 1.02 | " | 9.88 " | 0.00144 |

Norton Company Porous Plates

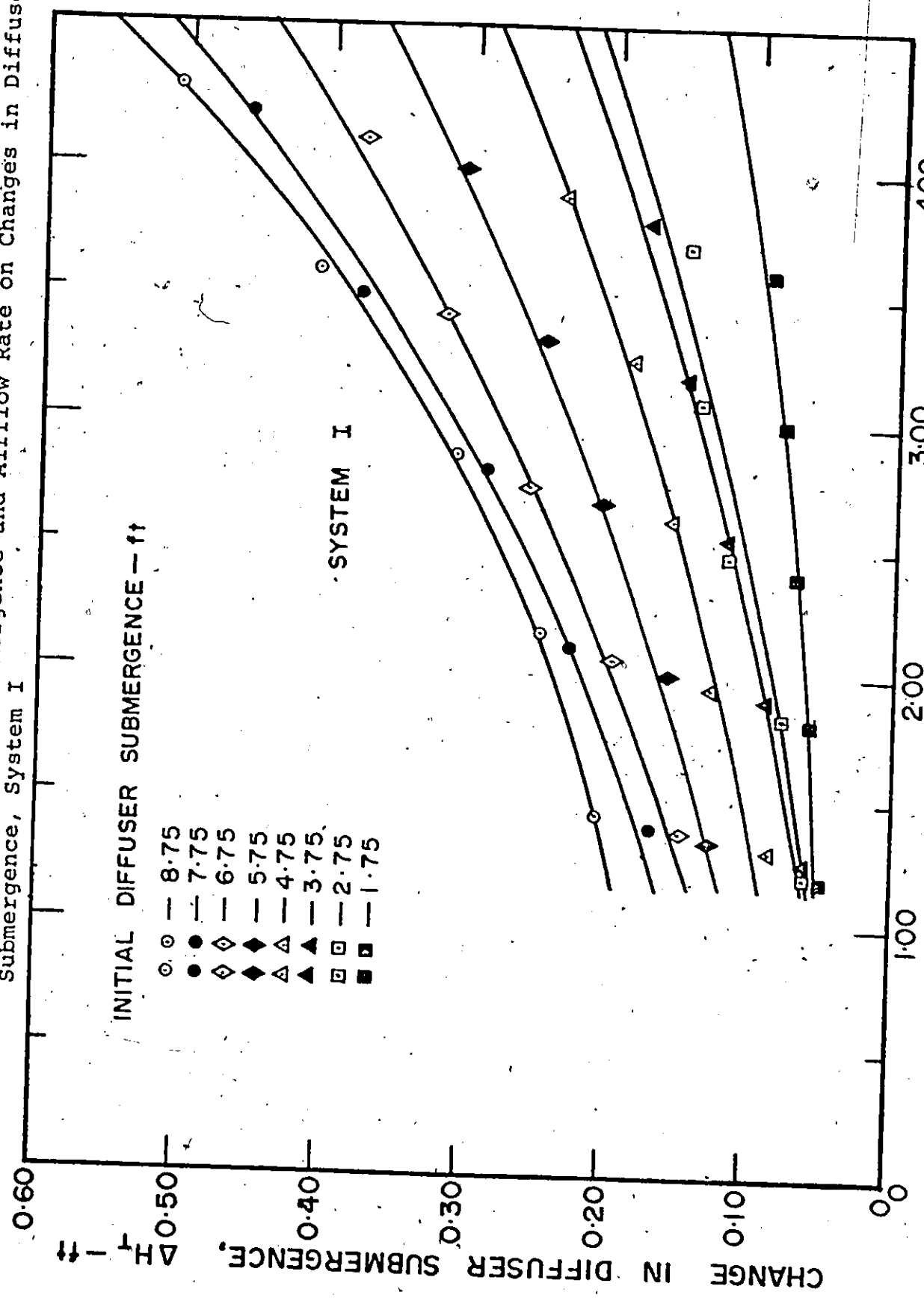


Figure 75 - Effect of Diffuser Submergence and Airflow Rate on Changes in Diffuser Submergence, System I

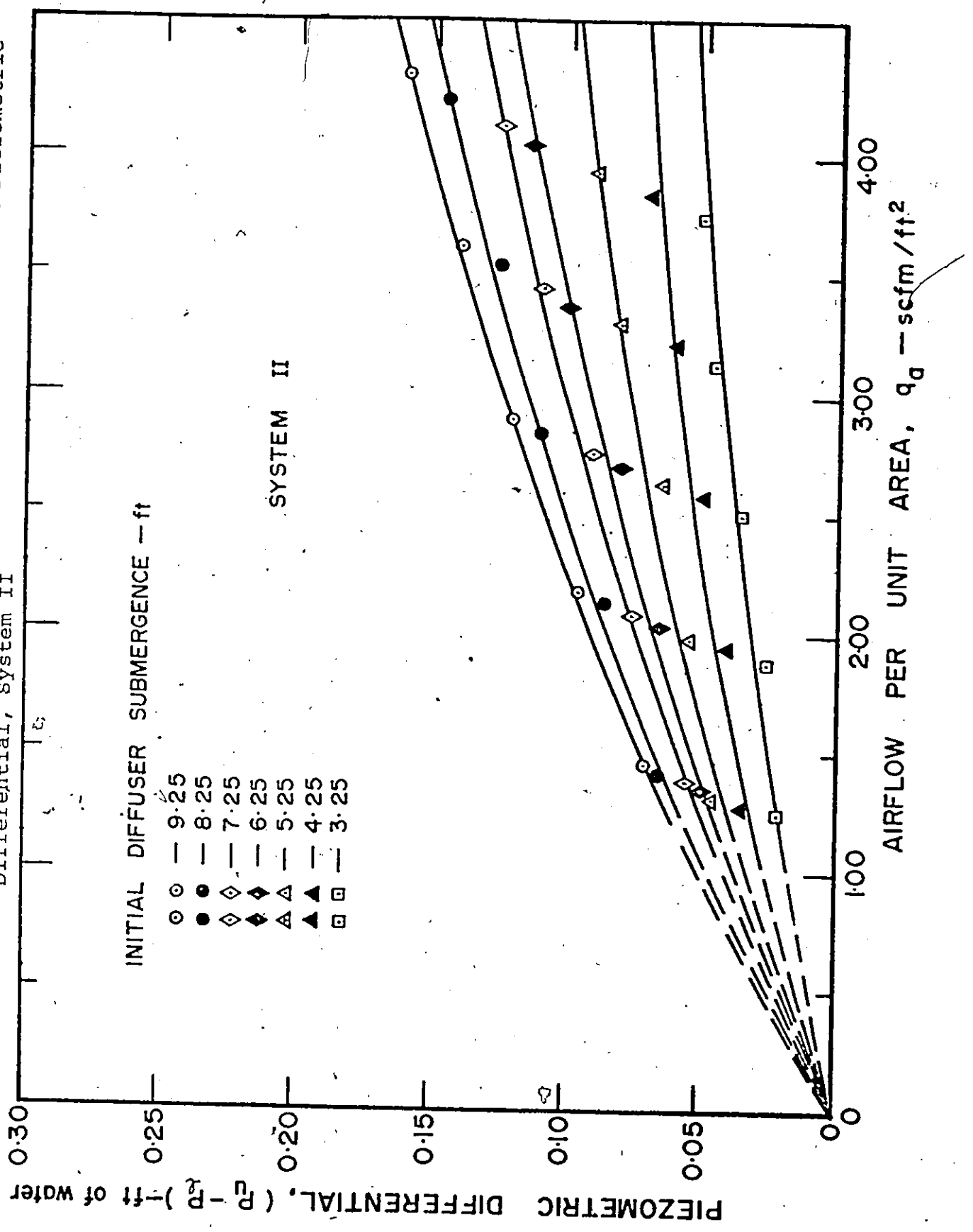


Figure 76 - Effect of Diffuser Submergence and Airflow Rate on Piezometric Differential, System II

Figure 77 - Effect of Diffuser Submergence and Airflow Rate on Piezometric Differential, System III

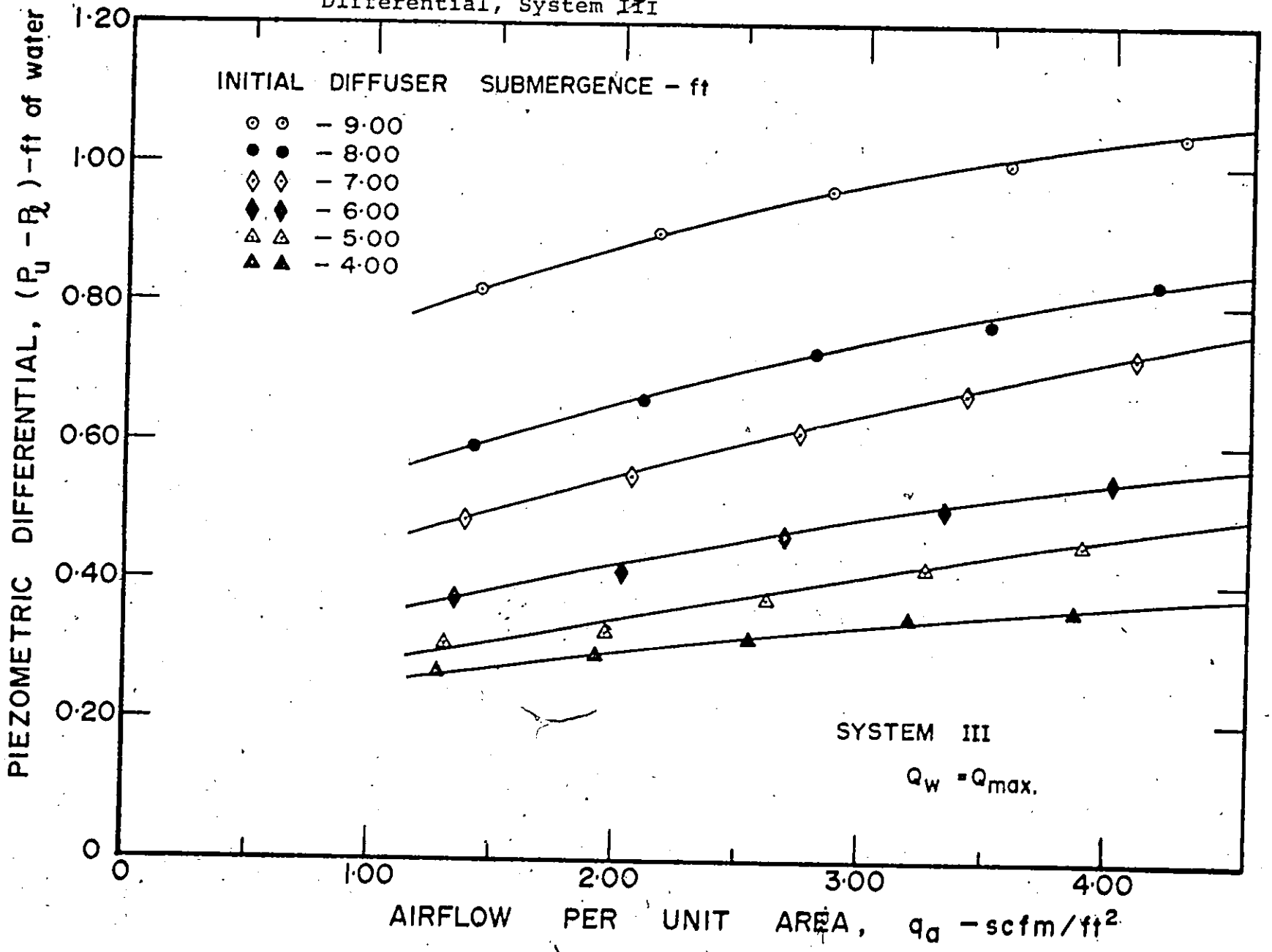

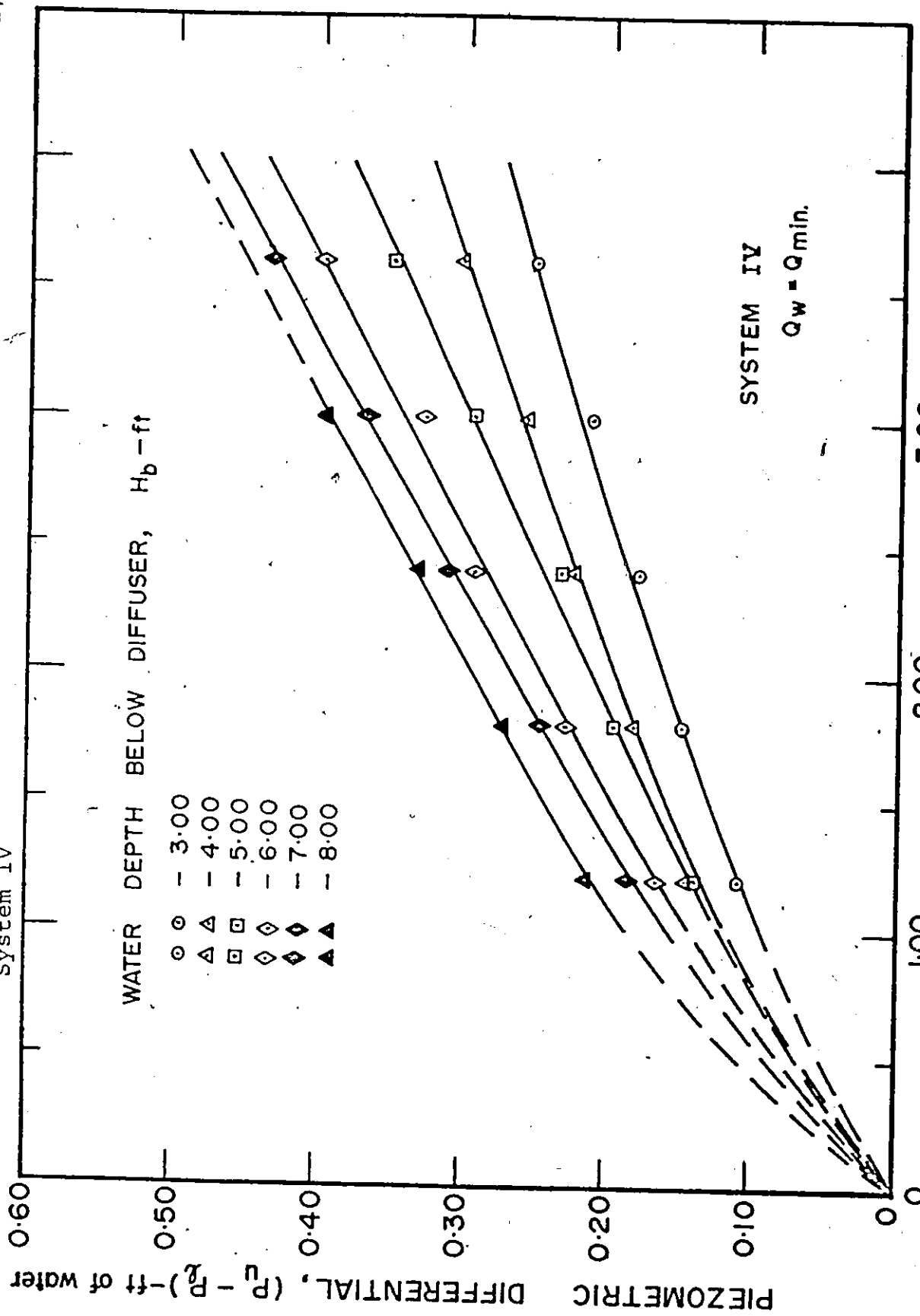


Figure 78 - Effect of Water Depth and Airflow Rate on Piezometric Differential, System IV

# APPENDIX D

## APPLICATION OF THE FOUR SYSTEMS OF AERATION TO CONVENTIONAL AERATION TANKS

### System I

Whenever the rate of oxygen demand of the biological mass is very high, the diffusers can be spread over the entire bottom of the aeration tank. The spacing of the diffusers in both directions should be such that no circulatory motion of the mixed liquor occurs except near the diffuser level, in order to keep the floc in suspension.

### System II

This system is identical to the conventional aeration tanks and no changes will be required except for the control of airflow rate and diffuser location, in order to meet the oxygen demand of the biological mass.

### System III

For the operation of this system, it is necessary that a waterflow rate in the downward direction be as high as possible but not exceed the terminal velocity of the air bubble. This is particularly true if there is sufficient

natural head available in the flow of wastewater.

From the studies with coarse-bubble diffusers, it is observed that a waterflow rate in the range of 250 USGPM/ft$^2$ is required. This is a very high rate of water flow and cannot be adapted economically to the entire aeration tank. However, near the entrance of the tank, soon after mixing the wastewater with the return sludge, when the rate of oxygen demand is highest, a reduced section in the inlet chamber can be provided, in several steps if necessary, in order to obtain the maximum amount of oxygen transfer. The outlet chamber does not necessarily have the same cross-section as that for the inlet chamber, but it should be larger to allow the floc to slow down but not settle out. This chamber will provide sufficient contact time to utilize the oxygen transferred in the inlet chamber. For the remaining part of the aeration tank, the conventional method of air diffusion can be used to keep the floc in suspension. Although experimentation has been performed for a diffuser submergence of only 4 to 9 feet, results indicate that other depths can also be used. The values of differential head $\Delta H$, needed for design, are given in Appendix C.

System IV

This system will be similar to System III in operation, except that the diffusers will be located near the surface and the rate of water flow will be much higher, in the range of 750 USGPM/ft$^2$. This higher rate would mean even a smaller

area of cross-section for the wastewater inlet chamber. However, the outlet chamber does not have to be a reduced section because air leaving in that section will be able to create circulation patterns similar to that present in conventional systems. The outlet chamber can be designed for a capacity to provide enough contact time for utilizing the oxygen transferred in both the inlet and outlet chambers.

The above arrangements can be provided in several steps near the entrance, depending upon the available head and the rate of oxygen demand. For the remaining part of the aeration tank, the conventional methods of air diffusion can be used to keep the floc in suspension. If sufficient natural head is available in the flow of wastewater so that its' pumping can be eliminated, then the power requirements are reduced considerably because of the location of diffusers near the surface, and this system will become very economical. Again, although experiments have been conducted with water depth below the diffuser up to only 8 feet, results indicate that larger depths can be used. Design values of differential head, $\Delta H$, are provided in Appendix C.

# XI - REFERENCES


1. Rich, L. G., "Unit Processes of Sanitary Engineering". p. 38, John Wiley and Sons, N.Y., 1963.

2. Fair, G. M., Geyer, J. C., and Okun, D. A., "Water and Wastewater Engineering". Vol. 2, p.p. 35-15 to 35-20, John Wiley and Sons, N.Y., 1968.

3. Clark, J. W., Viessman, W., Jr., and Hammer, M. J., "Water Supply and Pollution Control". 2nd Edition, p. 514. International Textbook Company, Penn., 1971.

4. Lewis, W. K., and Whitman, W. G., "Principles of Gas Absorption." Industrial and Engineering Chemistry, Vol. 16, December, 1924.

5. Ippen, A. T., Campbell, L. G., and Carver, C. E., Jr., "The Determination of Oxygen Absorption in Aeration Processes." Massachusetts Institute of Technology Hydrodynamics Lab. Tech. Rept. No. 7, May, 1952.

6. Eckenfelder, W. W., Jr., and O'Connor, D. J., "Biological Waste Treatment". pp. 76-114, Pergamon Press Ltd., New York, 1961.

7. Dobbins, W. E., "The Nature of the Oxygen Transfer Coefficient in Aeration Systems". Biological Treatment of Sewage and Industrial Wastes, Vol. 1, pp.141-148, Reinhold Publishing Co., N.Y., 1955.

8. Dobbins, W. E., "Mechanism of Gas Absorption By Turbulent Liquids". Proceedings of the International Conference on Advances in Water Pollution Research, Vol. 2, pp. 61-96, London, 1962.

9. Carver, C. E. Jr., "Absorption of Oxygen in Bubble Aeration" Biological Treatment of Sewage and Industrial Wastes, Vol. 1, pp. 149-171, Reinhold Publishing Co., New York, 1955.

10. Mavinic, D. S., "Oxygen Transfer During Counter - and Co-Current Air-Water Flow in Diffused Aeration System". Master's Thesis, University of Windsor, Windsor, Ontario, October, 1970.

11. Bewtra, J. K., "Effect of Diffuser Arrangement on Oxygen Absorption in Aeration Tanks". Doctoral Dissertation, University of Iowa, Iowa City, February, 1962.

12. Eckenfelder, W. W., Jr., "Factors Affecting the Aeration Efficiency of Sewage and Industrial Wastes". Sewage and Industrial Wastes, Vol. 31, No. 1, pp. 60-69, January, 1959.

13. Eckenfelder, W. W., Jr., "Aeration Efficiency and Design. I. Measurement of Oxygen Transfer Efficiency". Sewage and Industrial Wastes, Vol. 24, No. 10, pp. 1227-1228, October, 1952.

14. Morgan, P. F., and Bewtra, J. K., "Diffused Air Oxygen Transfer Efficiencies". Paper Presented at Conference on Biological Waste Treatment, Manhattan College, pp. 2-11, April, 1960.

15. Bewtra, J. K., and Nicholas, W. R., Oxygenation from Diffused Air in Aeration Tanks". Journal Water Pollution Control Federation, Vol. 36, No. 10, pp. 1196-1223, October, 1964.

16. Bruijn, J., and Tuinzaad, H., "The Relationship Between Depth of U-Tubes and the Aeration Process". Journal American Water Works Association, pp. 879-883, July, 1958.

17. Speece, R. E., Adams, J. L., and Woolridge, C. B., "U-Tube Aeration Operating Characteristics". Journal of the Sanitary Engineering Division, Proceedings of the American Society of Civil Engineers, pp. 563-573, June, 1969.

18. Speece, R. E., "Aeration of Oxygen - Deficient Impoundment Releases". Paper Presented at the Fifth International Water Pollution Research Conference, San Francisco, pp. 29/5 - 29/7, July-August, 1970.

19. Speece, R. E., "Hypolimnion Aeration". Journal American Water Works Association, Vol. 63, No. 1, pp. 6-9, January, 1971.

20. Thackston, E. L., and Speece, R. E., "Review of Supplemental Reaeration of Flowing Streams". Journal Water Pollution Control Federation, Vol. 38, No. 10, pp. 1614-1622, October, 1966.

21. McKeown, J. J., Gove, G. W., and Benedict, A. H., "Field Studies of Artificial Aeration Using a Downflow Tube Contractor". Paper Presented at the Twenty-fifth Annual Purdue Industrial Waste Conference, p. 5, May, 1970.

22. Process Design Manual for Upgrading Existing Wastewater Treatment Plants, Environmental Protection Agency, Washington, D.C., pp. 5-33, 8-7, 8, October, 1971.

23. King, H. R., "Mechanics of Oxygen Absorption in Spiral Flow Aeration Tanks, I. Derivation of Formulas". Sewage and Industrial Wastes, Vol. 27, No. 8, pp. 895-908, August, 1955.

24. Lamb, M., Discussion of the paper "Mechanisms of Gas Absorption by Turbulent Liquids" by W. E. Dobbins, Proceedings of the International Conference on Advances in Water Pollution Research, Vol. 2, pp. 61-96, London, 1962.

25. Pasveer, A., "Considerations on the Efficiency of the Aeration Process". Journal of the Air and Water Pollution Institute, Pergamon Press, Vol. 10, pp. 477-493, London, 1966.

26. Pasveer, A., and Sweeris, S., "A New Development in Diffused Air Aeration". Journal of the Water Pollution Control Federation, Vol. 37, No. 9, pp. 1267-1273, September, 1965.

27. Speece, R. E., "Downflow Bubble Contact Aeration". Journal of the Sanitary Engineering Division, Proceedings of the American Society of Civil Engineers, Vol. 97, pp. 433-440, August, 1971.

28. Pasveer, A., "Research on Activated Sludge. VI. Oxygenation of Water with Air Bubbles". Sewage and Industrial Wastes, Vol. 27, No. 10, pp. 1131-1146, October, 1955.

29. Scouller, W. D., and Nixon, J., "The Solution of Oxygen from Air Bubbles". Journal Institute of Sewage Purification, Paper No. 8, 1934.

30. Morgan, P. F., and Bewtra, J. K., "Air Diffuser Efficiencies," Journal Water Pollution Control Federation, Vol. 32, No. 10, pp. 1047-1058, October, 1960.

31. Eckenfelder, W. W., Jr., "Absorption of Oxygen From Air Bubbles in Water". Journal of the Sanitary Engineering Division, Proceedings of the American Society of Civil Engineers, pp. 89-97, July, 1959.

32. King, H. R., "Mechanics of Oxygen Absorption in Spiral Flow Aeration Tanks. II. Experimental Work". Sewage and Industrial Wastes, Vol. 27, No. 9, p. 1013, September, 1955.

33. Bewtra, J. K., "Oxygen Absorption in Aeration Tanks from Diffused Air". Unpublished Abstract, University of Iowa, Iowa City, pp. 1-4, April, 1962.

34. Pasveer, A., "Research on Activated Sludge. VII. Efficiency of the Diffused Air System". Sewage and Industrial Wastes, Vol. 28, No. 1, p. 28, January, 1956.

35. Mavinic, D. S., and Bewtra, J. K., "Oxygen Transfer Efficiency in Counter - and Co-Current Air-Water Flow." Proceedings of the Sixth Canadian Symposium on Water Pollution Research, Vol. 6, pp. 229-248, Toronto, February, 1971.

36. Barthelemew, W. H., Karow, E. O., and Sfat, M. R., "Oxygen Transfer and Agitation in Submerged Fermentation". Industrial Engineering Chemistry, Vol. 42, p. 1801, 1950.

37. Standard Methods for the Examination of Water and Wastewater, Twelfth Edition, APHA, AWWA, and WPCF, New York, March, 1966.

38. Perry, J. H., "Chemical Engineers' Handbook". McGraw-Hill Book Co., Fourth Edition, New York, 1963.

39. Morris, H. M., "Applied Hydraulics in Engineering". p. 234, The Roland Press Co., New York, 1963.

40. Albertson, M. L., Barton, J. R., and Simons, D. B., "Fluid Mechanics for Engineers". p. 517, Prentice-Hall, N.J., 1960.

41. Streeter, H. W., Wright, C. T., and Kehr, R. W., "An Experimental Study of Atmospheric Reaeration Under Stream Flow Conditions". Sewage Works Journal, Vol. 8, No. 2, p. 282, March, 1936.

42. Bewtra, J. K., Nicholas, W. R., and Polkowski, L. B., "Effect of Temperature on Oxygen Transfer in Water". Water Research, Vol. 4, No. 1, pp. 115-122, January, 1970.

43. Barnhart, E. L., "Transfer of Oxygen in Aqueous Solutions". Journal of the Sanitary Engineering Division, Proceedings of the American Society of Civil Engineers, pp. 648-659, June, 1969.

44. Downing, A. L., "Aeration in the Activated Sludge Process". Journal of the Institution of Public Health Engineers, April, 1960.

45. Neville, A. M., and Kennedy, J. B., "Basic Statistical Methods for Engineers and Scientists". International Textbook Company, Penn., 1966.

# VITA AUCTORIS

Donald S. Mavinic was born in Detroit, Michigan, U.S.A., on April 3, 1946. From 1952 to 1959 he completed his primary education in Windsor at Gordon McGregor and King George Public Schools. From 1960 to 1965, he completed his secondary education at Walkerville Collegiate Institute, also in Windsor. In the fall of 1965, he enrolled at the University of Windsor in the Faculty of Applied Science with the financial help of a University of Windsor Entrance Bursary and Chrysler Canada Scholarship. In May, 1969, he graduated from the University of Windsor with a Bachelor of Applied Science Degree in Civil Engineering.

In September, 1969, he was awarded an NRC Bursary and enrolled in the Faculty of Graduate Studies at the same University, obtaining his Master of Applied Science Degree in Civil Engineering in October, 1970. Immediately, he enrolled in a Ph.D. program at the same University, having been awarded an NRC Scholarship for the next three years of study.